

**EVALUATION OF STEEL I-SECTION BEAM AND BEAM-COLUMN
BRACING REQUIREMENTS BY TEST SIMULATION**

A Thesis
Presented to
The Academic Faculty

by

Ajinkya M. Lokhande

In Partial Fulfillment
of the Requirements for the Degree
Master of Science in Civil Engineering in the
School of Civil and Environmental Engineering

Georgia Institute of Technology
December, 2014

COPYRIGHT © AJINKYA M. LOKHANDE 2014

**EVALUATION OF STEEL I-SECTION BEAM AND BEAM-COLUMN
BRACING REQUIREMENTS BY TEST SIMULATION**

Approved by:

Dr. Donald W. White, Advisor
School of Civil and Environmental Engineering
Georgia Institute of Technology

Dr. Abdul-Hamid Zureick
School of Civil and Environmental Engineering
Georgia Institute of Technology

Dr. David W. Scott
School of Civil and Environmental Engineering
Georgia Institute of Technology

Date Approved: 4th December, 2014

[To my family, for all their love and support]

ACKNOWLEDGEMENTS

I wish to express my deepest gratitude for the guidance provided by my advisor, Dr. Donald White. I am deeply indebted to him for the tremendous amount of time and effort he has dedicated to mentoring this thesis work. His love for research in structural engineering is most admirable, and he is truly an inspiration for me.

I also wish to thank the rest of my committee members Dr. Abdul-Hamid Zureick and Dr. David Scott. Their comments and suggestions have been very helpful.

Special thanks to all my fellow students- Evan P. Prado, Lakshmi Subramanian, Thanh Van Nguyen and Oguzhan Togay for their help and support.

TABLE OF CONTENTS

	Page
ACKNOWLEDGEMENTS	iv
LIST OF TABLES	viii
LIST OF FIGURES	x
SUMMARY	xix
<u>CHAPTER</u>	
1 INTRODUCTION	1
1.1 Problem Statement and Objectives	1
1.2 Research Methods Employed in this Work	5
1.3 Organization	9
2 OVERALL STUDY DESIGN	10
2.1 Study Constants	10
2.2 Overview of Study Variables and Problem Naming Convention	11
2.2.1 Member Type	12
2.2.2 Type of Loading	13
2.2.3 Bracing Type and Number of Intermediate Braces	15
2.2.4 Unbraced Length	16
2.2.5 Bracing Stiffness Ratios for Combined Lateral and Torsional Bracing	17
2.3 Example Naming	23
3 FINITE ELEMENT PROCEDURES	25
3.1 General Modelling Considerations	25
3.2 Modelling of Braces	28

3.3	Material Properties	29
3.4	Residual Stresses	30
3.5	Benchmark Studies	31
3.5.1	Beam Benchmark Study	32
3.5.2	Column Benchmark Study	34
3.6	Geometric Imperfections in Beams	37
3.7	Geometric Imperfections in Beam-Columns	39
3.7.1	Beam-column members with point (nodal) lateral or shear panel (relative) lateral bracing	40
3.7.2	Beam-column members with combined bracing	42
4	BEAMS SUBJECTED TO MOMENT GRADIENT LOADING	45
4.1	Overview	45
4.2	Detailed Study Design	45
4.3	Rigidly-Braced Strengths	48
4.4	Results	50
4.4.1	Beams with Moment Gradient 1 Loading	53
4.4.2	Beams with Moment Gradient 2 Loading	62
5	BEAMS WITH TOP FLANGE LOADING	70
5.1	Overview	70
5.2	Detailed Study Design	70
5.3	Results	71
6	BEAM-COLUMNS SUBJECTED TO AXIAL LOAD AND UNIFORM BENDING MOMENT	78
6.1	Overview	78
6.2	Detailed Study Design	78

6.3 Results	82
6.3.1 Beam-Columns with Lateral Bracing only	82
6.3.2 Beam-Columns with Combined Lateral and Torsional Bracing	106
7 BEAM-COLUMNS SUBJECTED TO AXIAL LOAD AND MOMENT	
GRADIENT LOADING	145
7.1 Overview	145
7.2 Detailed Study Design	145
7.3 Results	149
7.3.1 Beam-Columns with Moment Gradient 1 Loading	149
7.3.2 Beam-Columns with Moment Gradient 2 Loading	183
8 SUMMARY OF RECOMMENDATIONS	197
 APPENDIX A: Knuckle curves and brace force versus brace stiffness plots corresponding to interaction plots in Chapters 4 and 5	 202
REFERENCES	240

LIST OF TABLES

	Page
Table 1.1: Bracing graphics key	3
Table 2.1: Naming convention for cases studied in this research	12
Table 2.2: Torsional to Lateral Bracing stiffness interaction ratios (TLBSRs) for beams subjected to positive bending	17
Table 2.3: Torsional to Lateral Bracing stiffness interaction ratios (TLBSRs) for beams subjected to negative bending	20
Table 4.1: Comparison of rigidly-braced strengths for beams with Moment Gradient 1 loading and $n=1$	48
Table 4.2: Comparison of rigidly-braced strengths for beams with Moment Gradient 1 loading and $n=2$	49
Table 4.3: Comparison of rigidly-braced strengths for beams with Moment Gradient 2 loading and $n=1$	49
Table 4.4: Comparison of simulation results in Figs. 4.1 through 4.3 with AISC predicted full ideal bracing stiffness	59
Table 4.5: Comparison of simulation results in Figs. 4.7 and 4.8 with AISC predicted full ideal bracing stiffness	66
Table 5.1: Comparison of simulation results in Figs. 5.1 and 5.2 with AISC predicted ideal full bracing stiffness	75
Table 6.1: Comparison of simulation results in Figs. 6.1 through 6.3 and Figs. 6.7 through 6.9 with Eq. 6-3	103
Table 6.2: Comparison of simulation results in Figs. 6.4 through 6.6 and Figs. 6.10 through 6.12 with Eq. 6-5	105
Table 6.3: Comparison of simulation results in Figs. 6.13 through 6.20 with Eq. 6-7	140
Table 6.4: Comparison of simulation results in Figs. 6.13 through 6.20 with Eq. 6-8	142
Table 7.1: Comparison of simulation results in Figs. 7.1 through 7.4 with Eq. 6-3	154
Table 7.2: Comparison of simulation results in Figs. 7.5 through 7.12 with Eq. 6-7	180
Table 7.3: Comparison of simulation results in Figs. 7.5 through 7.12 with Eq. 6-8	182

Table 7.4: Comparison of simulation results in Figs. 7.13 through 7.14 with Eq. 6-3	186
Table 7.5: Comparison of simulation results in Figs. 7.15 through 7.18 with Eq. 6-7	195
Table 7.6: Comparison of simulation results in Figs. 7.15 through 7.18 with Eq. 6-8	196

LIST OF FIGURES

	Page
Fig. 1.1: Point (Nodal) lateral bracing with $n = 1$	3
Fig. 1.2: Shear panel (relative) lateral bracing with $n = 2$	3
Fig. 1.3: Point torsional bracing with $n = 1$	3
Fig. 1.4: Point torsional and point (nodal) lateral bracing in combination with $n = 1$	4
Fig. 1.5: Point torsional and shear panel (relative) lateral bracing in combination with $n = 2$	4
Fig. 1.6: Example maximum strength knuckle curve	7
Fig. 1.7: Example brace force versus brace stiffness curve	7
Fig. 1.8: Example bracing stiffness interaction plot for combined bracing cases with lateral bracing on the compression flange	8
Fig. 1.9: Example bracing stiffness interaction plot for combined bracing cases with lateral bracing on the tension flange	9
Fig. 2.1: Cross section dimensions of W21X44	10
Fig. 2.2: Moment Gradient 1 (MG1)	13
Fig. 2.3: Moment Gradient 2 (MG2)	13
Fig. 2.4: Moment Gradient 3 (MG3)	13
Fig. 2.5: Load at centroid	14
Fig. 2.6: Top flange loading	15
Fig. 2.7: Torsional to lateral bracing stiffness interaction ratios (TLBSRs) for beams subjected to positive bending	19
Fig. 2.8: Torsional to lateral bracing stiffness interaction ratios (TLBSRs) for beams subjected to negative bending	21
Fig. 2.9: Naming convention example- B_MG2pt_NB_n1_Lb5	24
Fig. 3.1: Load application- Axial load and moment	26
Fig. 3.2: Representative finite element model	27

Fig. 3.3: Steel stress-strain curve assumed in the structural analysis	29
Fig. 3.4: Lehigh residual stress pattern (Galambos and Ketter, 1959)	31
Fig. 3.5: Results of beam benchmark study with uniform bending	32
Fig. 3.6: Results of beam benchmark study with Moment Gradient 2 loading	34
Fig. 3.7: Geometry of the column considered for the benchmark study	35
Fig. 3.8: Results of the column benchmark study without local buckling imperfections	35
Fig. 3.9: Results of the column benchmark study considering local buckling imperfections	36
Fig. 3.10: Imperfection pattern for beams subjected to single-curvature bending and containing one intermediate brace point	38
Fig. 3.11: Imperfection pattern for beams subjected to single-curvature bending and containing two intermediate brace points	39
Fig. 3.12: Imperfection pattern for beam-columns with lateral bracing only, bracing only on the flange in flexural compression, and one intermediate brace point	41
Fig. 3.13: Imperfection pattern for beam-columns with lateral bracing only, bracing only on the flange in flexural compression, and two intermediate brace points	41
Fig. 3.14: Imperfection pattern in members with a single lateral brace only on the top flange, shown for three different effective flange force ratios	42
Fig. 3.15: Imperfection pattern for beam-columns with combined lateral and torsional bracing and one intermediate brace point	43
Fig. 3.16: Imperfection pattern for beam-columns with combined lateral and torsional bracing and two intermediate brace points	43
Fig. 4.1: Knuckle curves and brace force vs. brace stiffness plots for point (nodal) lateral bracing cases with $n = 1$ and Moment Gradient 1 loading	54
Fig. 4.2: Knuckle curves and brace force vs. brace stiffness plots for shear panel (relative) lateral bracing cases with $n = 2$ and Moment Gradient 1 loading	55
Fig. 4.3: Knuckle curves and brace force vs. brace stiffness plots for point torsional bracing cases with $n = 1$ and Moment Gradient 1 loading	56

Fig. 4.4: Point (nodal) lateral and point torsional bracing stiffness interactions for Moment Gradient 1 loading and $n = 1$	57
Fig. 4.5: Shear panel (relative) lateral and point torsional bracing stiffness interactions for Moment Gradient 1 loading and $n = 2$	58
Fig. 4.6: Plot of brace force versus applied load for B_MG1p_RB_n2_Lb5 with $\beta = 2\beta_{iF.AISC}$	60
Fig. 4.7: Knuckle curves and brace force vs. brace stiffness plots for point (nodal) lateral bracing cases with $n = 1$, Moment Gradient 2, centroidal loading	63
Fig. 4.8: Knuckle curves and brace force vs. brace stiffness plots for torsional bracing cases with $n = 1$, Moment Gradient 2, centroidal loading	64
Fig. 4.9: Point (nodal) lateral and point torsional bracing stiffness interactions for Moment Gradient 2, centroidal loading and $n = 1$	65
Fig. 4.10: Plot of brace force versus applied load for B_MG2pc_TB_n1_Lb5 with $\beta = 80$ kip/in.	67
Fig. 5.1: Knuckle curves and brace force vs. brace stiffness plots for point (nodal) lateral bracing cases with $n = 1$, Moment Gradient 2, top flange loading	72
Fig. 5.2: Knuckle curves and brace force vs. brace stiffness plots for torsional bracing cases with $n = 1$, Moment Gradient 2, top flange loading	73
Fig. 5.3: Point (nodal) lateral and point torsional bracing stiffness interactions for Moment Gradient 2, top flange loading and $n = 1$	74
Fig. 5.4: Plot of brace force versus applied load for B_MG2pt_TB_n1_Lb5 with $\beta = 2\beta_{iF.AISC}$.	76
Fig. 6.1: Knuckle curves and brace force vs. brace stiffness plots for point (nodal) lateral bracing cases with $n = 1$ and constant axial load and uniform bending with effective flange force ratio $(P_{ft}/P_{fc}) \leq 0$, $L_b = 5$ ft	84
Fig. 6.2: Knuckle curves and brace force vs. brace stiffness plots for point (nodal) lateral bracing cases with $n = 1$ and constant axial load and uniform bending with effective flange force ratio $(P_{ft}/P_{fc}) \leq 0$, $L_b = 10$ ft	86
Fig. 6.3: Knuckle curves and brace force vs. brace stiffness plots for point (nodal) lateral bracing cases with $n = 1$ and constant axial load and uniform bending with effective flange force ratio $(P_{ft}/P_{fc}) \leq 0$, $L_b = 15$ ft	88
Fig. 6.4: Knuckle curves and brace force vs. brace stiffness plots for point (nodal)	

lateral bracing cases with $n = 1$ and constant axial load and uniform bending with effective flange force ratio $(P_{ft}/P_{fc}) > 0$, $L_b = 5\text{ft}$	90
Fig. 6.5: Knuckle curves and brace force vs. brace stiffness plots for point (nodal) lateral bracing cases with $n = 1$ and constant axial load and uniform bending with effective flange force ratio $(P_{ft}/P_{fc}) > 0$, $L_b = 10\text{ft}$	91
Fig. 6.6: Knuckle curves and brace force vs. brace stiffness plots for point (nodal) lateral bracing cases with $n = 1$ and constant axial load and uniform bending with effective flange force ratio $(P_{ft}/P_{fc}) > 0$, $L_b = 15\text{ft}$	92
Fig. 6.7: Knuckle curves and brace force vs. brace stiffness plots for shear panel (relative) lateral bracing cases with $n = 2$ and constant axial load and uniform bending with effective flange force ratio $(P_{ft}/P_{fc}) \leq 0$, $L_b = 5\text{ft}$	93
Fig. 6.8: Knuckle curves and brace force vs. brace stiffness plots for shear panel (relative) lateral bracing cases with $n = 2$ and constant axial load and uniform bending with effective flange force ratio $(P_{ft}/P_{fc}) \leq 0$, $L_b = 10\text{ft}$	95
Fig. 6.9: Knuckle curves and brace force vs. brace stiffness plots for shear panel (relative) lateral bracing cases with $n = 2$ and constant axial load and uniform bending with effective flange force ratio $(P_{ft}/P_{fc}) \leq 0$, $L_b = 15\text{ft}$	97
Fig. 6.10: Knuckle curves and brace force vs. brace stiffness plots for shear panel (relative) lateral bracing cases with $n = 2$ and constant axial load and uniform bending with effective flange force ratio $(P_{ft}/P_{fc}) > 0$, $L_b = 5\text{ft}$	99
Fig. 6.11: Knuckle curves and brace force vs. brace stiffness plots for shear panel (relative) lateral bracing cases with $n = 2$ and constant axial load and uniform bending with effective flange force ratio $(P_{ft}/P_{fc}) > 0$, $L_b = 10\text{ft}$	100
Fig. 6.12: Knuckle curves and brace force vs. brace stiffness plots for shear panel (relative) lateral bracing cases with $n = 2$ and constant axial load and uniform bending with effective flange force ratio $(P_{ft}/P_{fc}) > 0$, $L_b = 15\text{ft}$	101
Fig. 6.13: Knuckle curves and brace force vs. brace stiffness plots for combined point (nodal) lateral and torsional bracing cases with $n = 1$ and constant axial load and uniform bending with lateral brace on the flange in flexural compression, $L_b = 5\text{ft}$	108
Fig. 6.14: Knuckle curves and brace force vs. brace stiffness plots for combined point (nodal) lateral and torsional bracing cases with $n = 1$ and constant axial load and uniform bending with lateral brace on the flange in flexural compression, $L_b = 15\text{ft}$	111
Fig. 6.15: Knuckle curves and brace force vs. brace stiffness plots for combined	

point (nodal) lateral and torsional bracing cases with $n = 1$ and constant axial load and uniform bending with lateral brace on the flange in flexural tension, $L_b = 5\text{ft}$	114
Fig. 6.16: Knuckle curves and brace force vs. brace stiffness plots for combined point (nodal) lateral and torsional bracing cases with $n = 1$ and constant axial load and uniform bending with lateral brace on the flange in flexural tension, $L_b = 15\text{ft}$	117
Fig. 6.17: Knuckle curves and brace force vs. brace stiffness plots for combined shear panel (relative) lateral and torsional bracing cases with $n = 2$ and constant axial load and uniform bending with lateral brace on the flange in flexural compression, $L_b = 5\text{ft}$	120
Fig. 6.18: Knuckle curves and brace force vs. brace stiffness plots for combined shear panel (relative) lateral and torsional bracing cases with $n = 2$ and constant axial load and uniform bending with lateral brace on the flange in flexural compression, $L_b = 15\text{ft}$	125
Fig. 6.19: Knuckle curves and brace force vs. brace stiffness plots for combined shear panel (relative) lateral and torsional bracing cases with $n = 2$ and constant axial load and uniform bending with lateral brace on the flange in flexural tension, $L_b = 5\text{ft}$	130
Fig. 6.20: Knuckle curves and brace force vs. brace stiffness plots for combined shear panel (relative) lateral and torsional bracing cases with $n = 2$ and constant axial load and uniform bending with lateral brace on the flange in flexural tension, $L_b = 15\text{ft}$	135
Fig. 6.21: Plot of lateral brace force versus applied load for BC_UMp_CNTB_n1_Lb5_FFR1 with brace stiffness calculated from Eqs. 6-7 and 6-8	144
Fig. 7.1: Knuckle curves and brace force vs. brace stiffness plots for point (nodal) lateral bracing cases with $n = 1$ and constant axial load and moment gradient 1 loading, $L_b = 5\text{ft}$	150
Fig. 7.2: Knuckle curves and brace force vs. brace stiffness plots for point (nodal) lateral bracing cases with $n = 1$ and constant axial load and moment gradient 1 loading, $L_b = 15\text{ft}$	151
Fig. 7.3: Knuckle curves and brace force vs. brace stiffness plots for shear panel (relative) lateral bracing cases with $n = 2$ and constant axial load and Moment Gradient 1 loading, $L_b = 5\text{ft}$	152
Fig. 7.4: Knuckle curves and brace force vs. brace stiffness plots for shear panel	

(relative) lateral bracing cases with $n = 2$ and constant axial load and Moment Gradient 1 loading, $L_b = 15\text{ft}$	153
Fig. 7.5: Knuckle curves and brace force vs. brace stiffness plots for combined point (nodal) lateral and torsional bracing cases with $n = 1$ and constant axial load and Moment Gradient 1 loading with lateral brace on the flange in flexural compression, $L_b = 5\text{ft}$	156
Fig. 7.6: Knuckle curves and brace force vs. brace stiffness plots for combined point (nodal) lateral and torsional bracing cases with $n = 1$ and constant axial load and Moment Gradient 1 loading with lateral brace on the flange in flexural compression, $L_b = 15\text{ft}$	158
Fig. 7.7: Knuckle curves and brace force vs. brace stiffness plots for combined point (nodal) lateral and torsional bracing cases with $n = 1$ and constant axial load and Moment Gradient 1 loading with lateral brace on the flange in flexural tension, $L_b = 5\text{ft}$	160
Fig. 7.8: Knuckle curves and brace force vs. brace stiffness plots for combined point (nodal) lateral and torsional bracing cases with $n = 1$ and constant axial load and Moment Gradient 1 loading with lateral brace on the flange in flexural tension, $L_b = 15\text{ft}$	162
Fig. 7.9: Knuckle curves and brace force vs. brace stiffness plots for combined shear panel (relative) lateral and torsional bracing cases with $n = 2$ and constant axial load and Moment Gradient 1 loading with lateral brace on the flange in flexural compression, $L_b = 5\text{ft}$	164
Fig. 7.10: Knuckle curves and brace force vs. brace stiffness plots for combined shear panel (relative) lateral and torsional bracing cases with $n = 2$ and constant axial load and Moment Gradient 1 loading with lateral brace on the flange in flexural compression, $L_b = 15\text{ft}$	168
Fig. 7.11: Knuckle curves and brace force vs. brace stiffness plots for combined shear panel (relative) lateral and torsional bracing cases with $n = 2$ and constant axial load and Moment Gradient 1 loading with lateral brace on the flange in flexural tension, $L_b = 5\text{ft}$	172
Fig. 7.12: Knuckle curves and brace force vs. brace stiffness plots for combined shear panel (relative) lateral and torsional bracing cases with $n = 2$ and constant axial load and Moment Gradient 1 loading with lateral brace on the flange in flexural tension, $L_b = 15\text{ft}$	176
Fig. 7.13: Knuckle curves and brace force vs. brace stiffness plots for point (nodal) lateral bracing cases with $n = 1$ and constant axial load and Moment Gradient 2 loading, $L_b = 5\text{ft}$	184

Fig. 7.14: Knuckle curves and brace force vs. brace stiffness plots for point (nodal) lateral bracing cases with $n = 1$ and constant axial load and Moment Gradient 2 loading, $L_b = 15\text{ft}$	185
Fig. 7.15: Knuckle curves and brace force vs. brace stiffness plots for combined point (nodal) lateral and torsional bracing cases with $n = 1$ and constant axial load and Moment Gradient 2 loading with lateral brace on the flange in flexural compression, $L_b = 5\text{ft}$	187
Fig. 7.16: Knuckle curves and brace force vs. brace stiffness plots for combined point (nodal) lateral and torsional bracing cases with $n = 1$ and constant axial load and Moment Gradient 2 loading with lateral brace on the flange in flexural compression, $L_b = 15\text{ft}$	189
Fig. 7.17: Knuckle curves and brace force vs. brace stiffness plots for combined point (nodal) lateral and torsional bracing cases with $n = 1$ and constant axial load and Moment Gradient 2 loading with lateral brace on the flange in flexural tension, $L_b = 5\text{ft}$	191
Fig. 7.18: Knuckle curves and brace force vs. brace stiffness plots for combined point (nodal) lateral and torsional bracing cases with $n = 1$ and constant axial load and Moment Gradient 2 loading with lateral brace on the flange in flexural tension, $L_b = 15\text{ft}$	193
Fig. A.1: Knuckle curves and brace force vs. brace stiffness plots for point (nodal) lateral bracing cases with $n = 1$ and Moment Gradient 1 loading with lateral brace on the flange in compression, $L_b = 5\text{ft}$	203
Fig. A.2: Knuckle curves and brace force vs. brace stiffness plots for point (nodal) lateral bracing cases with $n = 1$ and Moment Gradient 1 loading with lateral brace on the flange in compression, $L_b = 15\text{ft}$	205
Fig. A.3: Knuckle curves and brace force vs. brace stiffness plots for point (nodal) lateral bracing cases with $n = 1$ and Moment Gradient 1 loading with lateral brace on the flange in tension, $L_b = 5\text{ft}$	207
Fig. A.4: Knuckle curves and brace force vs. brace stiffness plots for point (nodal) lateral bracing cases with $n = 1$ and Moment Gradient 1 loading with lateral brace on the flange in tension, $L_b = 15\text{ft}$	209
Fig. A.5: Knuckle curves and brace force vs. brace stiffness plots for shear panel (relative) lateral bracing cases with $n = 2$ and Moment Gradient 1 loading with lateral brace on the flange in compression, $L_b = 5\text{ft}$	211

Fig. A.6: Knuckle curves and brace force vs. brace stiffness plots for shear panel (relative) lateral bracing cases with $n = 2$ and Moment Gradient 1 loading with lateral brace on the flange in compression, $L_b = 15\text{ft}$	215
Fig. A.7: Knuckle curves and brace force vs. brace stiffness plots for shear panel (relative) lateral bracing cases with $n = 2$ and Moment Gradient 1 loading with lateral brace on the flange in tension, $L_b = 5\text{ft}$	218
Fig. A.8: Knuckle curves and brace force vs. brace stiffness plots for shear panel (relative) lateral bracing cases with $n = 2$ and Moment Gradient 1 loading with lateral brace on the flange in tension, $L_b = 15\text{ft}$	221
Fig. A.9: Knuckle curves and brace force vs. brace stiffness plots for point (nodal) lateral bracing cases with $n = 1$, Moment Gradient 2 loading, intermediate transverse load applied at centroid of the mid-span cross-section with lateral brace on the flange in compression, $L_b = 5\text{ft}$	224
Fig. A.10: Knuckle curves and brace force vs. brace stiffness plots for point (nodal) lateral bracing cases with $n = 1$, Moment Gradient 2 loading, intermediate transverse load applied at centroid of the mid-span cross-section with lateral brace on the flange in compression, $L_b = 15\text{ft}$	226
Fig. A.11: Knuckle curves and brace force vs. brace stiffness plots for point (nodal) lateral bracing cases with $n = 1$, Moment Gradient 2 loading, intermediate transverse load applied at centroid of the mid-span cross-section with lateral brace on the flange in tension, $L_b = 5\text{ft}$	228
Fig. A.12: Knuckle curves and brace force vs. brace stiffness plots for point (nodal) lateral bracing cases with $n = 1$, Moment Gradient 2 loading, intermediate transverse load applied at centroid of the mid-span cross-section with lateral brace on the flange in tension, $L_b = 15\text{ft}$	230
Fig. A.13: Knuckle curves and brace force vs. brace stiffness plots for point (nodal) lateral bracing cases with $n = 1$, Moment Gradient 2 loading, intermediate transverse load applied at top flange of the mid-span cross-section with lateral brace on the flange in compression, $L_b = 5\text{ft}$	232
Fig. A.14: Knuckle curves and brace force vs. brace stiffness plots for point (nodal) lateral bracing cases with $n = 1$, Moment Gradient 2 loading, intermediate transverse load applied at top flange of the mid-span cross-section with lateral brace on the flange in compression, $L_b = 15\text{ft}$	234
Fig. A.15: Knuckle curves and brace force vs. brace stiffness plots for point (nodal) lateral bracing cases with $n = 1$, Moment Gradient 2 loading, intermediate transverse load applied at top flange of the mid-span cross-section with lateral brace on the flange in tension, $L_b = 5\text{ft}$	236

Fig. A.16: Knuckle curves and brace force vs. brace stiffness plots for point (nodal) lateral bracing cases with $n = 1$, Moment Gradient 2 loading, intermediate transverse load applied at top flange of the mid-span cross-section with lateral brace on the flange in tension, $L_b = 15\text{ft}$

238

SUMMARY

The ANSI/AISC 360-10 Appendix-6 provisions provide limited guidance on the bracing requirements for beam-columns. In cases involving point (nodal) or shear panel (relative) lateral bracing only, these provisions simply sum the corresponding strength and stiffness requirements for column and beam bracing. Based on prior research evidence, it is expected that this approach is accurate to conservative when the requirements can be logically added. However, in many practical beam-column bracing situations, the requirements cannot be logically added. This is because of the importance of the brace and transverse load position through the cross-section depth, as well as the fact that both torsional and lateral restraint can be important attributes of the general bracing problem. These attributes of the bracing problem can cause the current beam-column bracing requirement predictions to be unconservative.

In addition, limited guidance is available in the broader literature at the current time regarding the appropriate consideration of combined lateral and torsional bracing of I-section beams and beam-columns. Nevertheless, this situation is quite common, particularly for beam-columns, since it is rare that separate and independent lateral bracing systems would be provided for both flanges. More complete guidance is needed for the proper consideration of combined bracing of I-section beams and beam-columns in structural design.

This research focuses on a reasonably comprehensive evaluation of the bracing strength and stiffness requirements for doubly-symmetric I-section beams and beam-columns using refined Finite Element Analysis (FEA) test simulation. The research builds on recent simulation studies of the basic bracing behavior of beams subjected to uniform bending. Various cases of beam members subjected to moment gradient are considered first. This is followed by a wide range of studies of beam-column members subjected to constant axial load and uniform bending as well as axial load combined with moment gradient loading. A range of unbraced lengths are

considered resulting in different levels of plasticity at the member strength limit states. In addition, various bracing configurations are addressed including point (nodal) lateral, shear panel (relative) lateral, point torsional, combined point lateral and point torsional, and combined shear panel lateral and point torsional bracing.

CHAPTER 1: INTRODUCTION

1.1 Problem Statement and Objectives

AISC 360-10 Appendix 6 (AISC 2010) provides equations for design of stability bracing for columns, beams and beam-columns. These equations address both strength and stiffness requirements for stability bracing. This research aims at evaluating the accuracy of the Appendix 6 provisions for beam problems involving moment gradient and transverse load height. It also aims to provide recommendations for design of lateral and combined lateral and torsional bracing systems for beam-column members. This study is part of an overall research program to investigate the stability bracing behavior of beam and beam-column members, and to provide recommendations for potential improvements to AISC 360 Appendix 6.

This research builds on recent test simulation studies of the basic stability bracing behavior of beams subjected to uniform bending (Prado and White 2014). Prado and White (2014) investigated the influence of varying the number of intermediate braces on beam bracing requirements. They also evaluated the impact of inelasticity on bracing requirements, by studying members with unbraced lengths (L_b) close to the AISC L_p and L_r limits as well as within the intermediate range of the AISC inelastic lateral-torsional buckling strength equations. When $(L_b) \leq (L_p)$ the flexural member fails by what can be categorized as plastic lateral-torsional buckling, where the “maximum plateau” flexural resistance of the member is developed. Furthermore, when $(L_p) < (L_b) \leq (L_r)$, the flexural member fails by inelastic lateral-torsional buckling. Finally, when $(L_b) > (L_r)$, the flexural strength limit state under uniform bending moment is elastic lateral-torsional buckling. In addition, Prado and White (2014) studied the benefits of combined lateral and torsional bracing of beams. They considered both lateral bracing at the level of the compression flange as well as at the level of the tension flange in combination with torsional restraint. Lastly, Prado and White (2014) showed that the AISC 360-10 Appendix 6 equations work well in many cases, especially when they are used with the

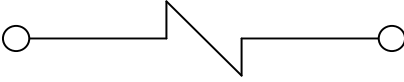
various refinements given in the Specification Commentary. However, improvements were recommended for some situations.

Since Prado and White (2014) only addressed beams subjected to uniform bending, one of the objectives of this research is to build on this work by studying the impact of moment gradient on the beam bracing requirements. Another objective is study the impact of transverse load height and to evaluate the performance of the AISC 360-10 Appendix 6 (AISC 2010) Commentary equations in capturing this effect. Lastly, a central objective of this work is the evaluation of the bracing behavior for beam-columns subjected to uniform bending and to moment gradient loading. The various bracing types considered in this work are as follows:

- Point (nodal) lateral bracing,
- Shear panel (relative) lateral bracing,
- Point torsional bracing,
- Combined point (nodal) lateral and point torsional bracing, and
- Combined shear panel (relative) lateral and point torsional bracing.

Table 1.1 summarizes the graphical symbols used in this work to represent the three basic types of bracing: point lateral, shear panel lateral and point torsional. The member configurations considered in this research for each of these bracing types are summarized in Figs. 1.1 through 1.5. The variable n in Figs. 1.1 through 1.5 indicates the number of intermediate braces. The member end lateral bracing is not shown in these figures.

Table 1.1. Bracing graphics key.

Brace Type	Graphical Symbol
Point (Nodal) lateral brace	
Shear panel (Relative) lateral brace	
Point torsional brace	

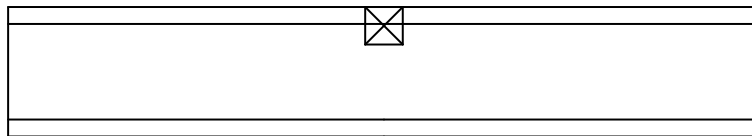


Fig. 1.1. Point (Nodal) lateral bracing with $n = 1$.

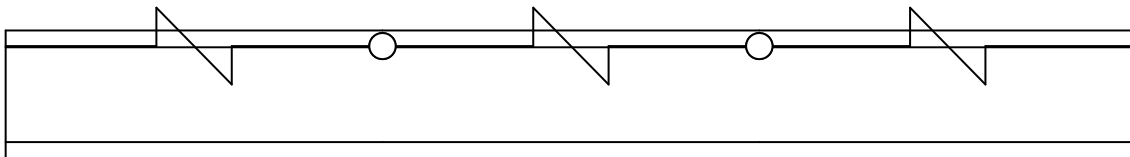


Fig. 1.2. Shear panel (relative) lateral bracing with $n = 2$.

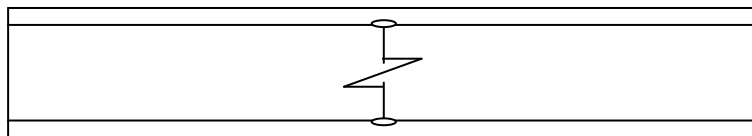


Fig. 1.3. Point torsional bracing with $n = 1$.

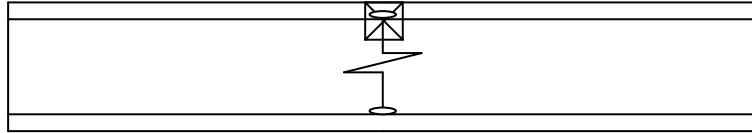


Fig. 1.4. Point torsional and point (nodal) lateral bracing in combination with $n = 1$.

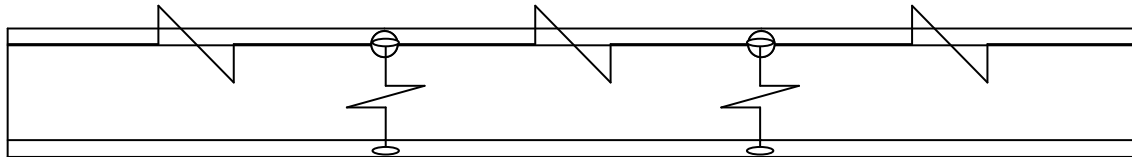


Fig. 1.5 Point torsional and shear panel (relative) lateral bracing in combination with $n = 2$

Prado and White (2014) did not study the bracing requirements for members subjected to combined axial load and bending moment. Furthermore, the AISC 360-10 Appendix 6 provisions provide limited guidance on bracing requirements for beam-columns. In cases involving point (nodal) or shear panel (relative) lateral bracing only, these provisions simply sum the corresponding strength and stiffness requirements for column and beam bracing. Based on prior research evidence (Yura 1993; Yura 1995; Tran 2009; White et al. 2011; Bishop 2013), it is expected that this approach is accurate to conservative where the requirements can be logically added. However, in many practical beam-column bracing situations the requirements cannot be logically added. Therefore, one of the major objectives of this research is to evaluate the bracing requirements and provide recommendations for design of stability bracing for beam-column members.

It is rare that beam-column members would be provided with independent lateral bracing on both flanges. In some cases, lateral bracing would be provided only on the flange in flexural compression; however, it is more common for general beam-columns to have a combination of lateral and torsional bracing. Therefore, another major objective of this research is to study the requirements for combined lateral and torsional bracing, and to provide recommendations for

proper design of combined bracing systems for beams as well as beam-column members. From prior research (Prado and White 2014; Tran 2009), it is known that the behavior of combined bracing systems is different for cases where the lateral bracing is on the flange in flexural compression versus cases where the lateral bracing is on the flange in flexural tension. Hence, both positive and negative bending cases, i.e., cases involving compression on the laterally-braced flange and cases in which the laterally-braced flange is in tension, are studied in this research.

In summary, the main objectives of this research are:

- To evaluate the performance of the AISC 360-10 Appendix 6 equations in accounting for the effect of moment gradient and transverse load height on the bracing requirements for beams.
- To provide recommendations for design of basic lateral bracing systems for beam-column members.
- To provide recommendations for design of combined bracing systems for beam as well as beam-column members.

1.2 Research Methods Employed in this Work

This research involves the use of refined finite element analysis (FEA) test simulation methods to determine the load-deflection and limit load response of beams and beam-columns, and their bracing systems, considering the influence of initial geometric imperfections, residual stress effects, and the overall spread of plasticity throughout the volume of the members. The members are modeled using shell finite elements, and thus the FEA models are capable of capturing general overall member buckling, local buckling and distortional buckling influences

as applicable for the cases studied. The general purpose finite element analysis software ABAQUS version 6.13 (Simulia 2013) is used throughout this research. Details of the FEA models are discussed in Chapter 3.

These refined test simulations are used to generate knuckle curves and brace force versus brace stiffness plots. Knuckle curves are basically plots of the member strength as a function of the brace stiffness. Knuckle curves have been used in prior research, e.g. Stanway et al. (1992a & b), White et al. (2009), Bishop (2013), and Prado and White (2014), for assessing the behavior of stability bracing. Knuckle curves showing the maximum strength or limit load of physical members having initial geometric imperfections and residual stresses are useful in assessing the impact of different characteristics of stability bracing for design. This is because, for strength limit states design, one is interested in the maximum strength behavior of the physical geometrically imperfect elastic/inelastic member or structure.

Figure 1.6 shows an example maximum strength knuckle curve. The specific numerical values for the abscissa and ordinate are immaterial to the discussion of the general knuckle curve characteristics. Generally, maximum strength knuckle curves always asymptote to a horizontal line, corresponding to the maximum resistance of the rigidly-braced structure, as the bracing stiffness is increased. Depending on the specific bracing characteristics, the knuckle curve can have a very gradual or a more abrupt approach to the rigidly-braced strength.

Also of significant importance to stability bracing design is the variation of the brace strength requirements as a function of the provided brace stiffness. Figure 1.7 shows an example plot of this type. Again, the specific values of the ordinate and abscissa are not important to the discussion of the general characteristics here. As long as the member is stable for the case of zero bracing stiffness, the bracing strength requirements increase from zero, for zero stiffness (i.e., no bracing) to a maximum value at an intermediate stiffness value typically close to or

slightly smaller than the stiffness corresponding to the knuckle in the knuckle curve. The brace force then tends to reduce with increasing brace stiffness beyond this value.

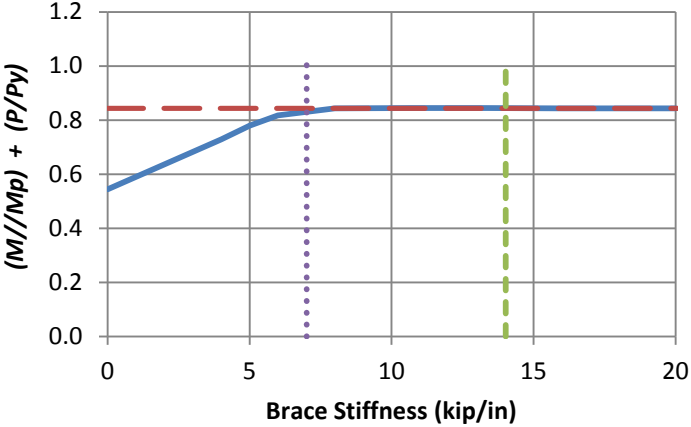


Fig. 1.6. Example maximum strength knuckle curve.

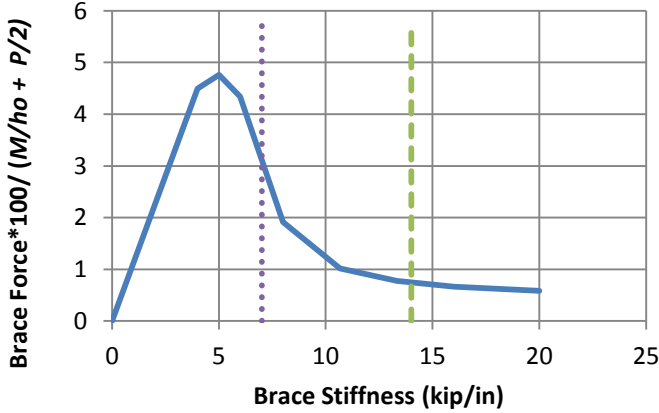


Fig. 1.7. Example brace force versus brace stiffness curve.

As discussed in Section 1.1, one of the major objectives of this research is to provide recommendations for design of combined lateral and torsional bracing, considering the interaction between the separate bracing stiffness's. As such, this research addresses questions

such as: How much torsional bracing is required in combination with a particular amount of lateral bracing to effectively brace a beam or a beam-column?

One way of interpreting the results of combined lateral and torsional bracing cases is by plotting stiffness interaction curves. Figures 1.8 and 1.9 show example bracing stiffness interaction plots for combined bracing cases with lateral bracing on the flange in flexural compression and in flexural tension flange respectively. The bracing stiffness values plotted in the interaction plots are determined as the intersection points of the knuckle curves with the strengths corresponding to 98 and 96 % of the rigidly-braced strengths. The separate 98 and 96 % strength interaction curves in Figs. 1.8 and 1.9 are shown to highlight the nature of the asymptotic strength gain in the knuckle curves with increases in the brace stiffness as the member resistance approaches the rigidly-braced strength.

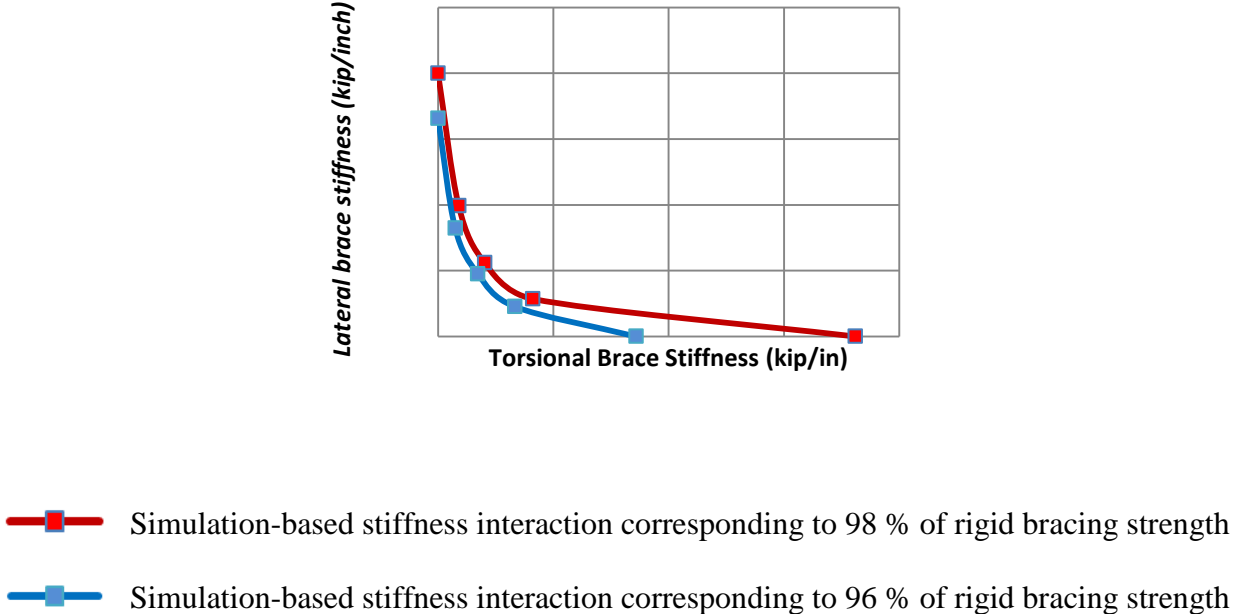


Fig. 1.8. Example bracing stiffness interaction plot for combined bracing cases with lateral bracing on the flange in flexural compression.



- Simulation-based stiffness interaction corresponding to 98 % of rigid bracing strength
- Simulation-based stiffness interaction corresponding to 96 % of rigid bracing strength

Fig. 1.9. Example bracing stiffness interaction plot for combined bracing cases with lateral bracing on the flange in flexural tension.

1.3 Organization

Chapter 2 provides an overview of the design of this research study. Chapter 3 explains the details of the FEA procedures employed for the test simulations conducted in this research. Chapters 4 through 7 explain the results for various loading and bracing configurations considered. Chapter 4 addresses beams subjected to moment gradient loadings, Chapter 5 addresses the influence of transverse load height for beam members, Chapter 6 addresses beam-columns subjected to axial load and uniform bending moment, and Chapter 7 addresses beam-columns subjected to axial load and moment gradient loading. Chapter 8 provides a summary and conclusions.

CHAPTER 2: OVERALL STUDY DESIGN

This chapter explains the overall design of a study to address the research objectives outlined in Section 1.1.

2.1 Study Constants

The constants in the study design of the current research are as follows:

- The steel material is assumed to be A992 Grade 50.
- A W21x44 section is adopted as a representative “beam-type” wide flange section (i.e., W sections with d/b_f greater than about 1.7). In general, it may be useful to consider the behaviour of column-type wide flange sections as well; however, the present studies focus on the bracing of beam-type sections. It is possible that the bracing stiffness and strength requirements will not be sensitive to whether the cross-section is a beam or a column type. The key dimensions and properties of the W21x44 section are $b_f = 6.5$ in, $t_w = 0.35$ in, $d = 20.7$ in, $t_f = 0.45$ in, $A = 13$ in² and h_o (flange centre to centre) = $d - t_f = 20.25$ in, as shown in Fig. 2.1.

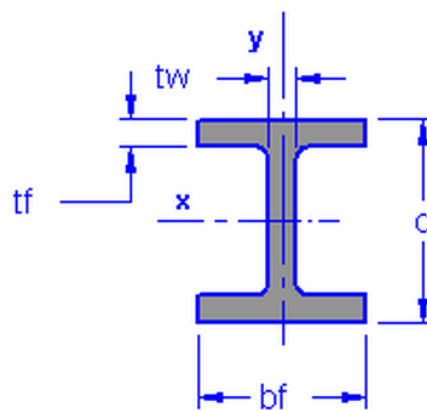


Fig. 2.1. Cross section dimensions of W21X44.

- Equally-spaced and equal-stiffness braces are used throughout this work such that the fundamental bracing behaviour targeted by Appendix 6 of the AISC 360-10 Specification (AISC 2010) can be assessed, and basic extensions of this behaviour pertaining to beams and beam-columns can be studied.
- The member ends are braced laterally at both flanges and the end cross-sections are constrained to enforce Vlasov kinematics (plane sections remain plane with the exception of warping, i.e., cross-bending, of the flanges due to torsion, and no distortion of the cross-section profile). The flanges are free to warp and bend laterally at the member ends.

2.2 Overview of Study Variables and Problem Naming Convention

The study is divided into four major parts:

- a) Beams subjected to moment gradient loading.
- b) Beams with an intermediate transverse load applied at the compression flange, to investigate load height effects.
- c) Beam-columns subjected to constant axial load and uniform bending moment.
- d) Beam-columns subjected to constant axial load and moment gradient loading.

The overall scope and content of these studies can be understood succinctly by considering the naming convention for the various specific cases. This naming convention is summarized in Table 2.1. The names of the test cases are created by assembling the phrases from each of the columns of this table.

The different columns of Table 2.1 are explained in the following subsections. A full factorial study design would make the number of cases to be studied extremely large. Therefore

for each of the four major parts of the study listed above, various cases are identified by a carefully selected combination of the study variables. The subsequent Chapters 4 through 7 explain the details regarding the selection of specific study cases.

Table 2.1. Naming convention for cases studied in this research.

Member Type (a)	Type of loading (b)	Bracing type (c)	Number of intermediate braces (d)	Unbraced length (e)	Torsional to Lateral Bracing stiffness ratio (f)	Flange force ratio (g)
B BC	UMp	NB	n1	Lb5	TLBSR5.7	FFR-0.67
	UMn	RB	n2	Lb10	TLBSR4	FFR-0.5
	MG1p	TB		Lb15	TLBSR1	FFR-0.33
	MG1n	CNTB			TLBSR0.33	FFR0
	MG2pc	CRTB			TLBSR0.25	FFR0.5
	MG2pt				TLBSR0.11	FFR1
	MG2nc					
	MG2nt					
MG3						

2.2.1 Member Type

In column (a) of Table 2.1, ‘B’ represents a beam type member and ‘BC’ represents a beam-column type member.

2.2.2 Type of Loading

Column (b) of Table 2.1 outlines the various loading conditions considered in this research. These are discussed in detail below.

2.2.2.1 Uniform Bending and Moment Gradient Loading

The identifier 'UM' stands for Uniform Bending Moment, and 'MG1', 'MG2' and 'MG3' represent the various moment gradient cases (varied over the full length of the member) as illustrated in Figs. 2.2 through 2.4.

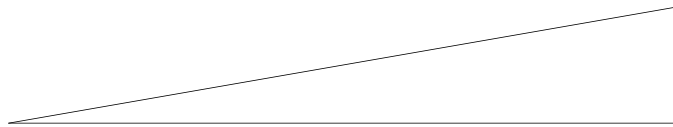


Fig. 2.2. Moment gradient (MG1).



Fig. 2.3. Moment Gradient 2 (MG2).

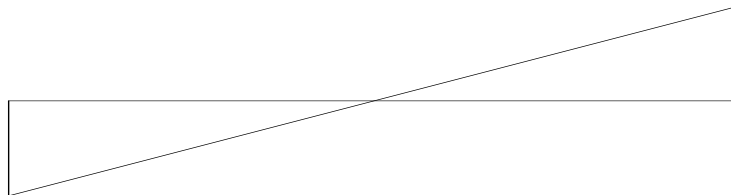


Fig. 2.4. Moment Gradient 3 (MG3).

2.2.2.2 Positive and Negative Bending

One of the objectives of this research is to evaluate the benefit of combined lateral and torsional bracing for beams and beam-columns with:

- a) Lateral bracing on the flange in flexural compression (these cases are referred to as positive bending)
- b) Lateral bracing on the flange in flexural tension (these cases are referred to as negative bending)

Hence, both positive and negative bending cases are considered for the beams and beam-columns having combined lateral and torsional bracing. In column (b) of Table 2.1, the identifier ‘p’ represents positive bending and ‘n’ represents negative bending.

2.2.2.3 Load Position

To evaluate the impact of transverse load height on the stability bracing demands, the following cases are considered:

- a) Load at centroid
- b) Top flange loading

In column (b) of Table 2.1, the identifier ‘c’ represents centroidal loading and ‘t’ represents top flange loading. These cases involve a concentrated load applied at the mid-span of the member, producing the MG2 moment diagram shown in Fig. 2.3. The load positions are illustrated in Figs. 2.5 and 2.6. Two-sided bearing stiffeners having the dimensions 3.075 in x 0.45 in are assumed at the mid-span load location in these tests.

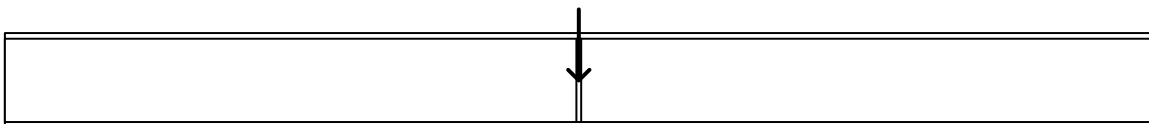


Fig. 2.5. Load at centroid.

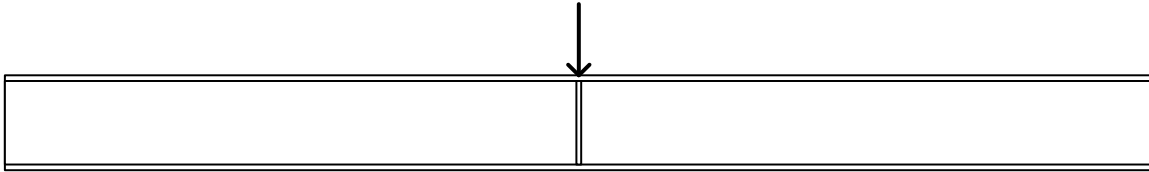


Fig. 2.6. Top flange loading.

2.2.3 Bracing Type and Number of Intermediate Braces

The various bracing types and the number of intermediate brace locations considered in this research are illustrated in Figs. 1.1 through 1.5. In column (c) of Table 2.1, ‘NB’ represents point (nodal) lateral bracing, ‘RB’ represents shear panel (relative) lateral bracing, ‘TB’ represents torsional bracing, ‘CNTB’ represents combined point (nodal) lateral and torsional bracing and ‘CRTB’ represents combined shear panel (relative) lateral and torsional bracing. It should be noted that in all cases in this research, lateral bracing is placed only on the top flange in these elevation views.

As discussed in Section 1.1, Prado and White (2014) addressed the influence of the number of intermediate braces on the bracing requirements. Therefore, consideration of this effect is not the main focus of this research. The point (nodal) lateral bracing as well as the combined point (nodal) lateral and torsional bracing cases are considered here only for $n = 1$ (one intermediate brace location). Shear panel (relative) lateral bracing as well as the combined shear panel (relative) lateral and torsional bracing cases are considered only for $n = 2$ (two intermediate brace locations). Because of the presence of rigid out-of-plane bracing at the member ends, the behavior of shear panel (relative) lateral bracing with $n = 1$ is actually identical to that of point (nodal) lateral bracing with $n = 1$. Therefore, the current work effectively addresses $n = 1$ and 2 for cases involving shear panel lateral bracing, but just $n = 1$ for cases involving point lateral bracing. Again, Prado and White (2014) addressed the impact of a larger number of intermediate brace points on the bracing response, but only in the context of beams subjected to uniform

bending. In column (d) of Table 2.1, ‘n1’ indicates one intermediate brace point and ‘n2’ indicates two intermediate brace points.

2.2.4 Unbraced Length

Prado and White (2014) evaluated the impact of member inelasticity on the bracing requirements by studying W21x44 members with three different unbraced lengths (5 ft, 10 ft and 15 ft). To prevent the number of cases from becoming extremely large, most of the studies in this research are conducted only for unbraced lengths of 5 and 15 ft. The length $L_b = 5$ ft is close to the anchor point $L_p = 4.45$ ft of the AISC beam LTB strength curve for W21x44 members with $F_y = 50$ ksi. In addition, this value corresponds to $L_b/r_y = 47.6$ for Grade 50 W21x44 members, which is a reasonably short unbraced length that leads to extensive spread of yielding throughout the member prior to a weak-axis flexural buckling failure as a column. The length $L_b = 15$ ft is slightly larger than the anchor point $L_r = 13$ ft of the AISC beam LTB strength curve for Grade 50 W21x44 members. This unbraced length corresponds to $L/r_y = 128.7$ for these types of members, which slightly exceeds the length $4.71\sqrt{E/F_y}$ corresponding to the transition between inelastic and elastic column flexural buckling per the AISC column strength curve (AISC 2010). Therefore, the members studied in this research tend to be heavily plastified at their ultimate strength condition for $L_b = 5$ ft, and the members with $L_b = 15$ ft and a small C_b (moment gradient) factor are dominated by elastic stability behavior. In column (e) of Table 2.1, Lb5, Lb10, and Lb15 represent unbraced lengths of 5ft, 10ft and 15ft respectively.

2.2.5 Bracing Stiffness Ratios for Combined Lateral and Torsional Bracing

2.2.5.1 Torsional to Lateral Bracing Stiffness Ratios for Beams

As discussed in Section 1.2, one way of interpreting the results of combined lateral and torsional bracing is by plotting stiffness interaction diagrams. Different torsional to lateral bracing stiffness ratios need to be considered to generate these bracing stiffness interaction plots.

For positive bending cases (i.e., where the lateral bracing is on the flange in flexural compression), the Torsional to Lateral Bracing Stiffness Ratios (TLBSRs) listed in Table 2.2 are considered in this work. The variables referenced in this table are as follows:

β_L = Provided lateral bracing stiffness

β_T = Provided torsional bracing stiffness

β_{Lo} = Base required lateral bracing stiffness for full bracing per the AISC 360-10 Appendix 6 (AISC 2010) rules, including the refinements specified in the Appendix 6 Commentary.

β_{To} = Base required torsional bracing stiffness for full bracing per the AISC 360-10 Appendix 6 (AISC 2010) rules, including the refinements specified in the Appendix 6 Commentary.

Table 2.2. Torsional to Lateral Bracing Stiffness Ratios (TLBSRs) for beams subjected to positive bending.

β_T / β_{To}	β_L / β_{Lo}	$(\beta_T / \beta_{To}) / (\beta_L / \beta_{Lo})$
0.8	0.2	4.0
0.5	0.5	1.0
0.2	0.8	0.25

Full bracing is defined as a case that has sufficient stiffness and strength to develop the maximum member buckling resistance based on a buckling effective length equal to the

unbraced length between the brace points. For prismatic members braced by equally-spaced braces, full bracing produces a buckling mode in which the member buckles in alternate directions in adjacent unbraced lengths and has inflection points at each of the brace locations. Full bracing can refer to an ideal member buckling resistance, or it can refer to the nominal or design buckling resistance of the physical member having generally unavoidable initial imperfections. The bracing stiffness necessary to develop the maximum fully-braced resistance of the physical geometrically imperfect member, and to limit the corresponding brace forces to certain specified limits, is generally larger than the stiffness required to attain the fully-braced eigenvalue buckling resistance of the ideal geometrically perfect member.

In this research, the minimum rigidly-braced strength from test simulations (defined subsequently in Section 4.3) is used as the required moment in determining the above base stiffness requirements. In addition, all the required stiffness's in this research are determined as nominal values, that is, the resistance factor ϕ in the AISC equations is taken equal to 1.0. Prado and White (2014) provide a detailed summary of the AISC Appendix 6 (AISC 2010) equations with all the Commentary refinements included. These equations are not repeated in this report in the interest of keeping the current presentation as succinct as possible.

The TLBSR values for positive bending cases are illustrated in the form of an x-y plot in Fig. 2.7.

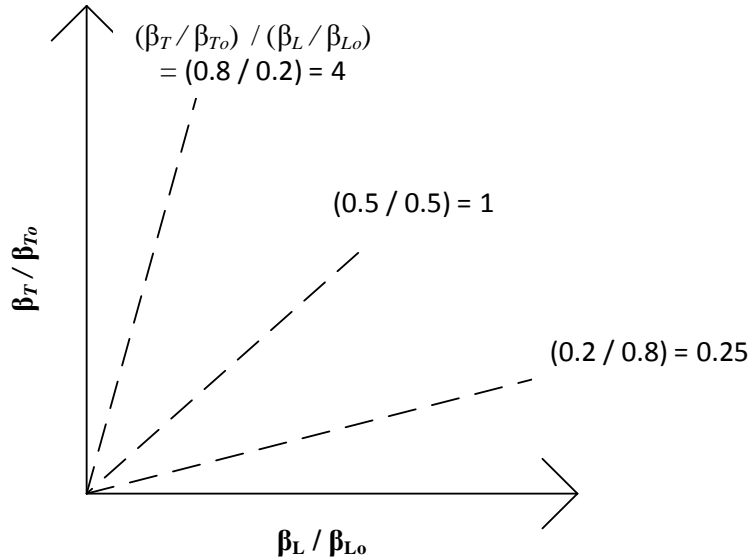


Fig. 2.7. Torsional to lateral bracing stiffness interaction ratios (TLBSRs) for beams subjected to positive bending.

The values 4, 1, and 0.25 shown adjacent to the dashed lines in Fig. 2.7 are the slopes of the corresponding lines. This slope is the TLBSR (i.e., $\text{TLBSR} = (\beta_T / \beta_{T0}) / (\beta_L / \beta_{L0})$). Thus, $\text{TLBSR} = 4$ indicates that:

- The initially targeted and provided lateral bracing stiffness is 0.8 times the base required lateral bracing stiffness as per AISC 360-10 Appendix 6 (AISC 2010) rules including refinements specified in the Appendix 6 Commentary, and
- The initially targeted and provided torsional bracing stiffness is 0.2 times the base required torsional bracing stiffness as per AISC 360-10 Appendix 6 (AISC 2010) rules including refinements specified in the Appendix 6 Commentary.

When generating the knuckle curves corresponding to each TLBSR, the magnitude of torsional and lateral bracing stiffness's in the test simulations is varied such that the TLBSR is kept constant. Therefore, the above stated “initially targeted” values are only used in setting the

TLBSR. Bracing knuckle curves and brace force versus brace stiffness curves are generated in all cases by varying both stiffness's such that the TLBSR is held constant at the selected values.

For negative bending cases (i.e., where the lateral bracing is attached to the flange in flexural tension) the Torsional to Lateral Bracing Stiffness Ratios (TLBSRs) listed in Table 2.3 are considered in this work. These TLBSR values are illustrated in the form of an x-y plot in Fig. 2.8.

Table 2.3. Torsional to Lateral Bracing Stiffness Interaction Ratios (TLBSRs) for beams subjected to negative bending.

β_T / β_{To}	β_L / β_{Lo}	$(\beta_T / \beta_{To}) / (\beta_L / \beta_{Lo})$
0.85	0.15	5.67
0.5	0.5	1.0
0.25	0.75	0.33
0.1	0.9	0.11

In column (f) of Table 2.1, 'TLBSR' stands for Torsional to Lateral Bracing Stiffness Ratio. The number following 'TLBSR' represents the specific value of the ratio, $(\beta_T / \beta_{To}) / (\beta_L / \beta_{Lo})$.

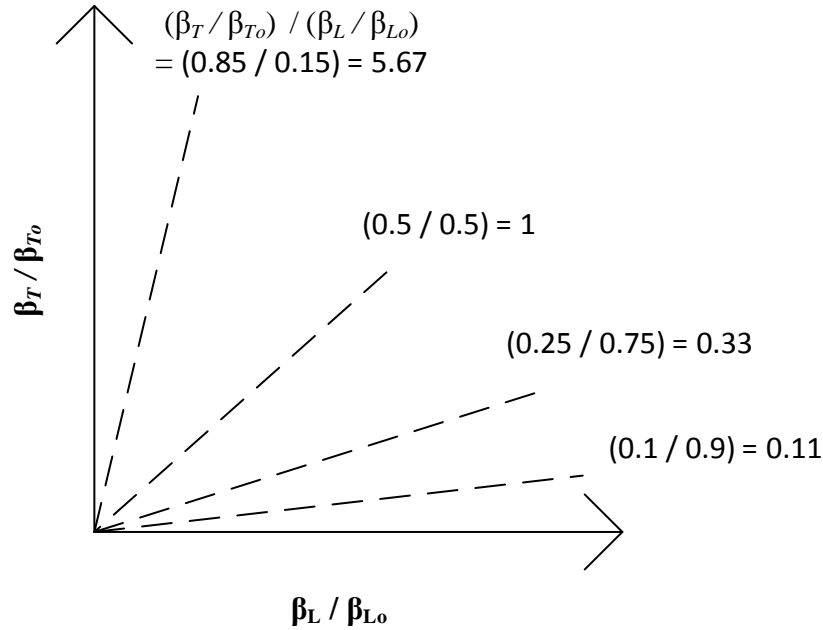


Fig. 2.8. Torsional to lateral bracing stiffness interaction ratios (TLBSRs) for beams subjected to negative bending.

2.2.5.2 Torsional to Lateral Bracing Stiffness Ratios (TLBSRs) and Flange Force Ratios (FFRs) for Beam-Columns

To define a study design for bracing of beam-columns, one needs to select more than just the Torsional to Lateral Bracing Stiffness Ratios (the TLBSRs). One also needs to identify a measure of the member axial force to the member bending moment. In this research, this attribute of the study is quantified by the Effective Flange Force Ratios (FFR). The FFR is the ratio of the effective axial force transmitted by each flange, neglecting any contributions from the member web. That is, in this research, which uses doubly-symmetric W21x44 sections for all of the members, the effective flange force in the member flange loaded in flexural compression is taken as

$$P_{fc} = P / 2 + M_{\max} / h_o$$

where P is the member axial force, taken as positive in compression, M_{max} is the first-order maximum internal moment, and h_o is the distance between the flange centroids. Similarly, the effective flange force for the flange loaded in flexural tension is

$$P_{ft} = P/2 - M_{max} / h_o$$

Therefore, the effective Flange Force Ratio is

$$\text{FFR} = P_{ft} / P_{fc}$$

This ratio is positive when both flanges support a net axial compression, and it is negative when the moment causes an overall net tension in the flange loaded in flexural tension. The following effective flange force ratios are considered for beam-columns subjected to uniform bending in this research: -1, -0.67, -0.33, 0, 0.5, and 1. The following effective flange force ratios are considered for beam-columns subjected to moment gradient loading: -1, -0.5, 0, 0.5, and 1. These ratios are selected such that the following three situations are studied:

- a) One flange in net overall compression and other flange in net overall tension,
- b) One flange in net overall compression and other flange subjected net zero force, and
- c) Both flanges in net overall compression.

Column (g) of Table 2.1 shows the different designations for the flange force ratios used in this research. In column (g) of Table 2.1, 'FFR' stands for the Flange Force Ratio and the number following 'FFR' represents the ratio (P_{ft} / P_{fc}). The FFR values of -1 actually correspond to the beam loading cases, i.e., axial force of zero.

A full factorial study design with different bracing stiffness ratios and effective flange force ratios would make the number of cases to be considered extremely large. Hence a scheme of designing the lateral bracing for a load equal to the axial load and the torsional brace for a load equal to ($M_{max}/h_o + P/2$) is considered in this work. This stems from the fact that the torsional

brace is ineffective for axial load, but the axial load has some effect on the torsional bracing stiffness and strength requirements. The $(P/2)$ term is an ad hoc addition to account for the amplification in the torsional brace demand due to combination of axial and moment loading. In reality an engineer would encounter situations where the lateral bracing may be very stiff or very flexible, e.g., a roof or wall diaphragm composed of stiff precast concrete panels and other cases where the lateral bracing may be relatively flexible, e.g., standing roof panels. In such cases, the lateral bracing would need to be designed generally to accommodate the member axial force. If the bracing stiffness is larger than the minimum requirement to develop the member axial force, then the design is conservative with respect to the lateral bracing. Varying the TLBSRs in a manner other than that indicated by the above minimum requirements, to consider any potential beneficial effects of additional lateral bracing stiffness for relieving the torsional bracing stiffness demands for beam-columns, is not considered in this research. Various general TLBSRs are considered in this research for beams, as discussed in the previous Section 2.2.5.1.

2.3 Example Naming

As indicated above, the various specific beam-column cases studied in this research are named based on the identifiers listed in Table 2.1. For example, a case named B_MG2pt_NB_n1_Lb5 has the loading and geometry shown in Fig. 2.9. This member is a beam, with Moment Gradient 2 loading (resulting in the moment diagram shown in Fig. 2.3), positive bending moment (causing compression on the top flange, where the lateral bracing is provided, transverse load applied at the level of the top flange, nodal (point) lateral bracing with one intermediate brace location, and 5 ft unbraced length between the braced points. In this case, the TLBSR and FFR identifiers are left blank, since these parameters are not relevant to a beam member with point lateral bracing.

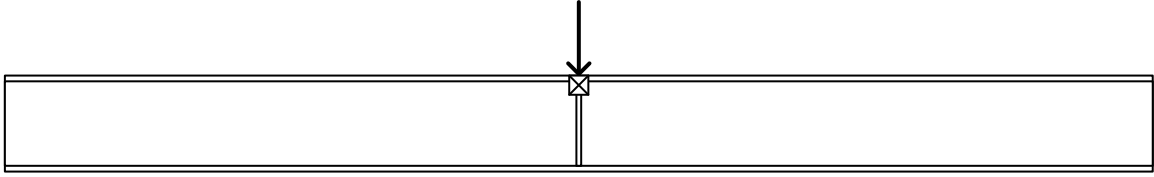


Fig. 2.9 Naming convention example- B_MG2pt_NB_n1_Lb5.

CHAPTER 3: FINITE ELEMENT PROCEDURES

3.1 General Modeling Considerations

The test simulation studies conducted in this research are directed at modelling the overall load-deflection response up to and beyond the peak load capacity of various member and bracing configurations, considering the influence of initial geometric imperfections, residual stress effects, and the overall spread of plasticity throughout the volume of the members. The members are modeled using shell finite elements, and thus the FEA models are capable of capturing general overall member buckling, local buckling and distortional buckling influences as applicable for the cases studied. The different bracing components are modeled using elastic spring elements. Axial load and bending moments are applied at the member ends via concentrated longitudinal axial forces at the web flange juncture points. Figure 3.1 shows a representative case for a beam-column subjected to axial load and uniform bending. Multi-point constraints are applied at the member end cross-sections to enforce Vlasov kinematics at these locations. That is, plane sections are constrained to remain plane in the web as well as in the flanges at the member ends, but the flanges are allowed to rotate freely and independently about a vertical axis through the web. Therefore, warping of the flanges is effectively unrestrained at the member ends. The specific multi-point constraint equations are specified in detail by Kim (2010).

In addition, the vertical displacement of all points on the top and bottom flange are constrained to be equal to the vertical displacement at the corresponding web-flange juncture at each end of the member, such that there is no distortion of the cross-section profile at the member ends.

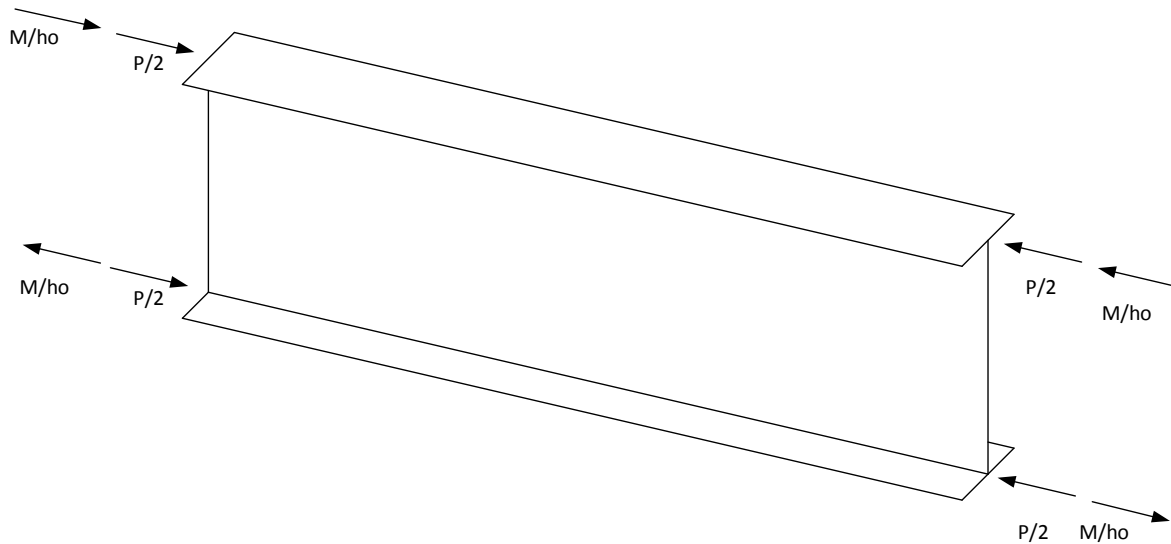


Fig. 3.1. Load application- Axial load and moment.

Because of the application of multi-point constraints at the member ends, the above member end loads do not cause any stress concentrations. The member is supported at one end in the plane of bending by constraining the vertical and longitudinal displacements to zero at the bottom web-flange juncture, and at the other end in the plane of bending by constraining just the vertical displacement to zero. The lateral (out-of-plane) displacements at the member ends are constrained to zero at each web-flange juncture and throughout the height of the web. Self-weight of the member is not included in the analysis.

The general purpose finite element analysis software ABAQUS version 6.13 (Simulia 2013) is used throughout this research. The four-node S4R shell element is used to model both the flanges and the web of the member. The S4R element is a general purpose large strain quadrilateral element which uses a single point numerical integration over its area combined with an algorithm for stabilization of the corresponding spurious zero-energy modes. Twelve elements are used across the width of the flanges and sixteen elements are used through the depth of the

web. An aspect ratio of 1 to 1 is implemented for all the elements in the web. The flange elements are the same length dimensions as the web elements along the longitudinal direction of the member. Figure 3.2 shows a representative finite element model. A five point Simpson's rule is applied for integration of the stresses through the thickness of the shell element. The Riks method is used to perform the incremental-iterative non-linear load-deflection analyses.

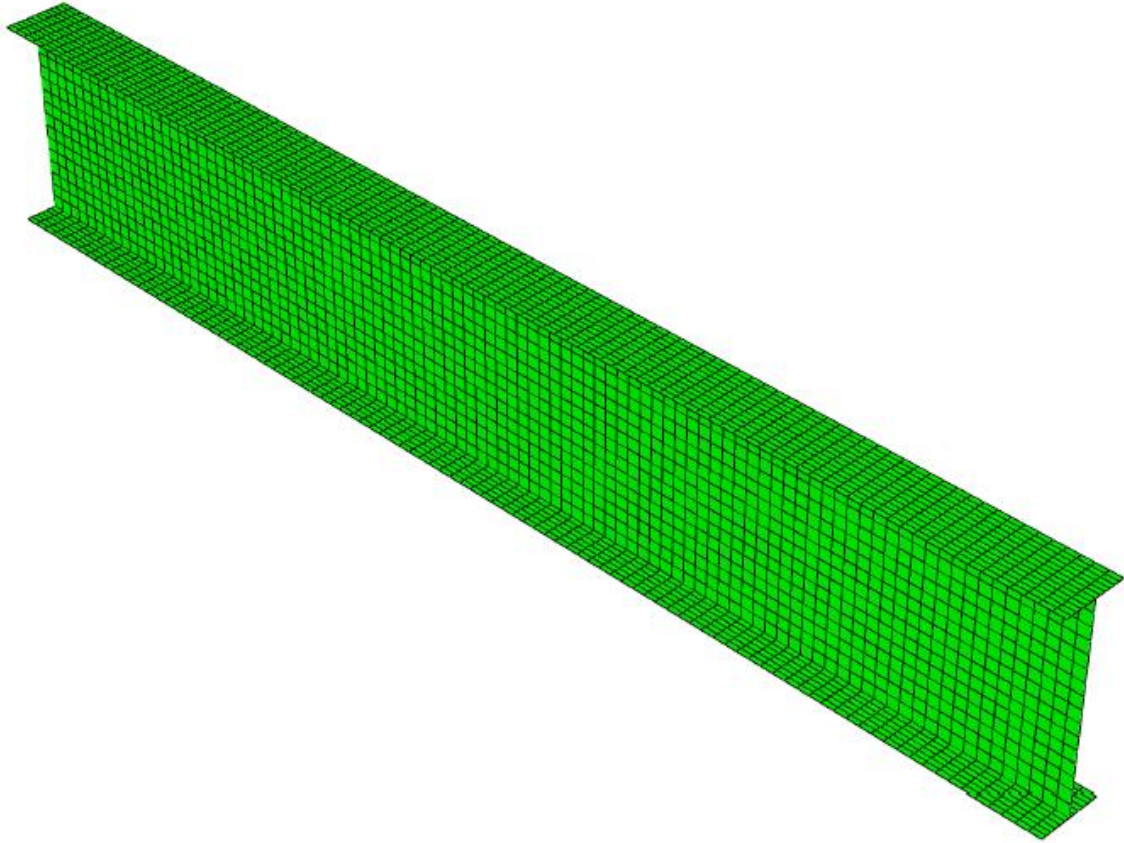


Fig. 3.2. Representative finite element model.

Residual stresses are implemented via a user-defined FORTRAN subroutine. Geometric imperfections are introduced by performing a pre-analysis on the member in which displacements corresponding to the desired geometric imperfection pattern are imposed at

various control points and the member is allowed to elastically deform between these points. The deflections from the pre-analysis are then applied as an initial imperfection on the geometry of the member at the zero load condition in the subsequent test simulation load-deflection analysis. The member is taken as stress and strain-free in this initial imperfect geometry at the beginning of the test simulation, with the exception of the residual stresses.

Force equilibrium is not strictly maintained when the residual stresses are introduced on the imperfect member geometry. The residual stresses are self-equilibrating only on the perfect geometry of the member. As such, a first step of the test simulation analysis is conducted in which the residual stresses are allowed to equilibrate. This results in a relatively small change to the member geometry. This ‘equilibrium step’ is followed by a second step of the test simulation analysis in which load is applied to the member.

3.2 Modelling of Braces

ABAQUS provides two types of spring elements which are used to simulate the bracing components in this research. All the bracing components are modelled as linear elastic springs. Point (nodal) lateral bracing is simulated with the spring type 1 element, which is a grounded spring element. Shear panel (relative) bracing is simulated with the spring type 2, which is a spring element that resists relative displacements in a specified lateral direction between the nodes it connects. In addition, nodal torsional bracing is implemented via the use of the spring type 2 element.

3.3 Material Properties

The material properties of the steel are modelled in all the test simulation studies of this research using the stress-strain curve shown in Fig. 3.3. All the members are assumed to be homogenous and the yield stress of steel, F_y , is taken as 50 ksi. The modulus of elasticity, E is taken as 29000 ksi. The material is modelled with a small tangent stiffness within the yield plateau region of $E/1000$ up to a strain-hardening strain of $\varepsilon_{sh} = 10\varepsilon_y$, where ε_y is the yield strain of the material. Beyond this strain, a constant strain-hardening modulus of $E_{sh} = E/50$ is used up to the ultimate stress level of $F_u = 65$ ksi. The material is modelled as perfectly plastic beyond this point.

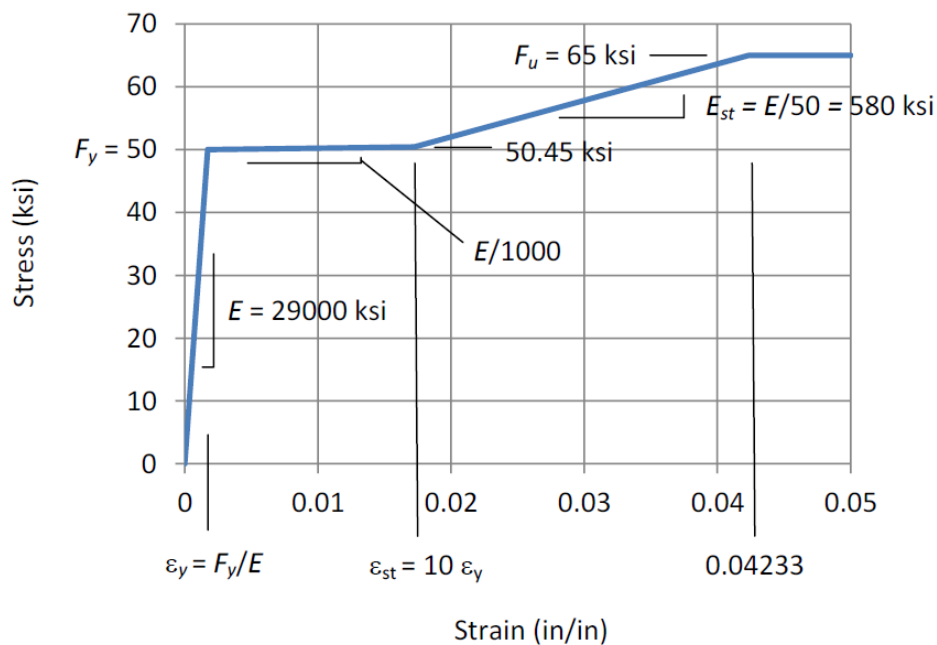


Fig. 3.3. Steel stress-strain curve assumed in the structural analysis.

Since the S4R element in ABAQUS is a large strain formulation, this element actually interprets the input stress versus plastic strain curve associated with Fig. 3.3 as the true stress

versus log strain response. However, for the maximum strains commonly experienced at the limit load of the test simulations, the difference between the uniaxial true-stress versus log strain and engineering stress versus engineering strain is small. The stress-strain curve shown in Fig. 3.3 is a reasonable representation of the true-stress true-strain response of structural steel for stresses up to the level of F_u .

3.4 Residual Stresses

Residual stresses are introduced into rolled structural steel members by uneven cooling after rolling operations, as well as by mill straightening. Flame cutting and welding causes residual stresses in welded I-section members. One of the most commonly accepted models used to represent nominal residual stresses in hot-rolled I-section members is the Lehigh residual stress pattern shown in Fig. 3.4. This pattern has a constant residual tension in the web and a self-equilibrating stress distribution in the flanges with a maximum residual compression of $0.3F_y$ at the tips of the flanges and a linear variation in stress between the flange tips and the above residual tension value at the web-flange juncture. The residual stresses are constant through the thickness of the flange and web plates. The Lehigh residual stress pattern (Galambos and Ketter, 1959) is considered commonly to provide an accurate to relatively conservative assessment of residual stress effects on the inelastic buckling response of rolled wide flange members. The potential conservatism is due to the attribute that the flanges contain a net compressive residual force that is balanced by the web residual tension. The Lehigh residual stress pattern is assumed in all of the studies conducted in this research.

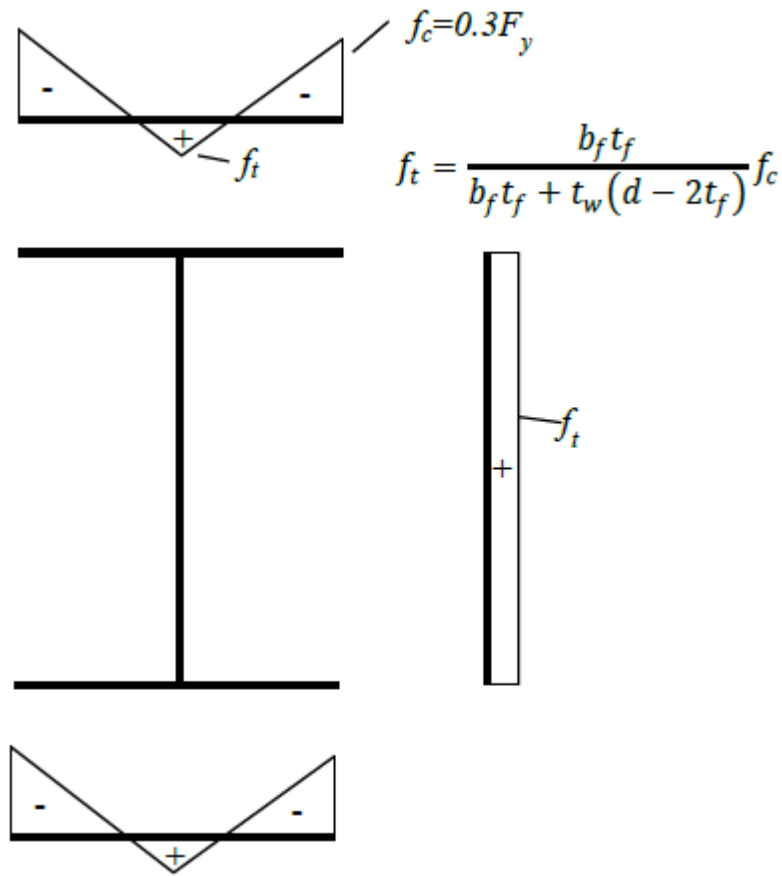


Fig. 3.4. Lehigh residual stress pattern (Galambos and Ketter, 1959).

3.5 Benchmark Studies

Benchmark studies for columns and beams are presented below to illustrate how the capacities obtained from test simulations compare with the strengths predicted by the ANSI/AISC 360 Specification (AISC 2010) as well as the Eurocode 3 Standard (CEN 2005). The results of the column and beam benchmark studies are presented in the following subsections.

3.5.1 Beam Benchmark Study

The results of a beam benchmark study for uniform bending, conducted by Prado and White (2014), is shown in Fig. 3.5. The modelling approach is exactly the same as that used for all of the cases in this research. The beams studied are simply-supported members with no intermediate lateral bracing. A sweep of the compression flange with maximum amplitude of $(L/1000)$ at the mid-span is used, where L is the overall span length.

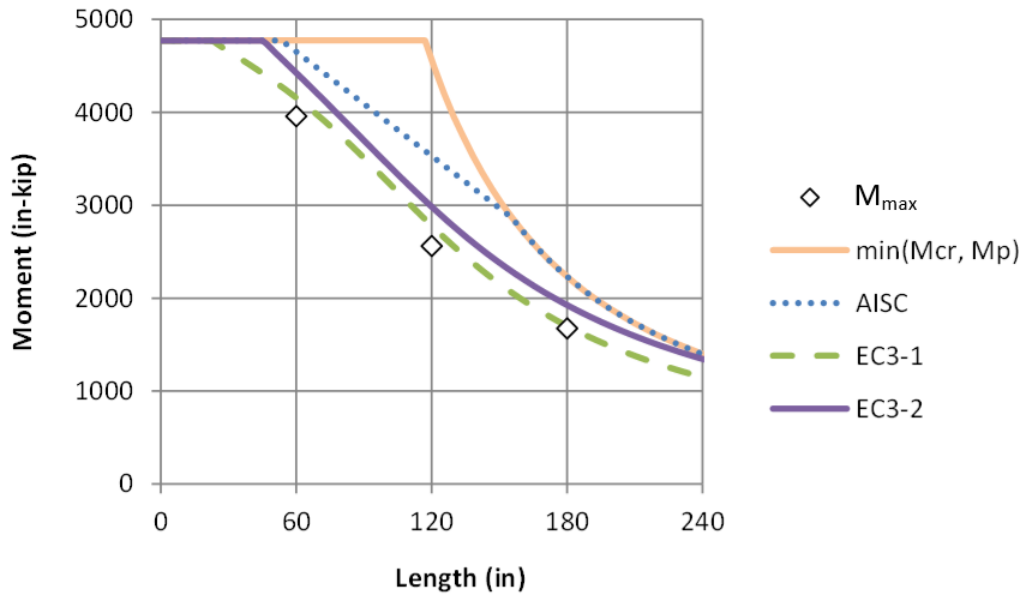


Fig. 3.5. Results of beam benchmark study with uniform bending.

In Fig. 3.5, the maximum strengths determined from the test simulations (M_{max}) are compared to the elastic buckling capacity, capped by the plastic moment of the W21X44 cross-section, as well as to the ANSI-AISC 360-10 and the Eurocode 3 (CEN 2005) predicted strengths. Two curves are shown from the Eurocode 3 provisions, one corresponding to general I-section members and the second providing an enhanced strength estimate intended for application with rolled I-section members and members with a cross-section similar to rolled I-sections. It can be observed that the test simulation strengths are closest to the EC3-1 curve. This is to be expected since the EC3-1 strength curve was developed largely from extensive test simulation studies

similar to the studies conducted here, but with a residual stress pattern that is not quite as damning as the Lehigh residual stress pattern. The use of the Lehigh residual stress pattern reduces the member capacities slightly in comparison to the EC3-1 curve. The EC3-2 and AISC strength curves were developed considering extensive collections of experimental data. Generally, the maximum strengths obtained from test simulations, using typical nominal residual stress patterns along with geometric imperfections set at maximum fabrication and construction tolerances, tend to be smaller on average compared to the strengths from experimental tests. One reason for this behavior is the fact that the imperfections and residual stresses in the experimental tests (and in practice) are not as large as the nominal values typically assumed in simulation studies.

Figure 3.6 shows beam benchmark study results for a basic moment gradient loading case (MG1 in Fig. 2.1) with rigid lateral bracing on the compression flange at the mid-span of the member. The curves in this figure are based on the use of a moment gradient factor C_b of 1.3 for the right-hand critical unbraced length and a $C_b = 1.75$ for the non-critical left-hand unbraced length. Using these C_b values and the approximate procedure recommended by Nethercot and Trahair (1976), the effective length factor for lateral torsional buckling of the right-hand unbraced length is $K = 0.88$ (accounting for the restraint provided by the left-hand non-critical unbraced length to the right-hand critical unbraced length). When $C_b = 1.3$ and $K = 0.88$ are used to evaluate the LTB strength of the right-hand segment, the prediction from the AISC strength curves is basically the theoretical elastic LTB capacity, M_{cr} , capped by the section plastic moment resistance M_p , with the exception of a small deviation close to the length where M_{cr} reaches M_p . Conversely, the two Eurocode strength predictions show a substantial reduction in strength relative to the AISC predictions. The test simulation strengths are again close to the Eurocode 3 predictions, but in this case, the correlation with the rolled I-section EC3-2 curve is somewhat better than with the general I-section EC3-1 curve. The reason for the improved prediction by the EC3-2 curve can be explained as being due to an additional factor, referred to

as f in Eurocode 3, which better accounts for the effect of moment gradient on the inelastic buckling resistance. One can observe that the test simulation predictions are slightly conservative relative to the EC3-2 curve. This is due to the conservative nature of the Lehigh residual stress pattern compared to the base residual stresses utilized in the Eurocode 3 developments. However, at the shortest unbraced length considered in this work (i.e., $L_b = 5$ ft), the beam develops the fully-plastic bending resistance of the cross-section, M_p .

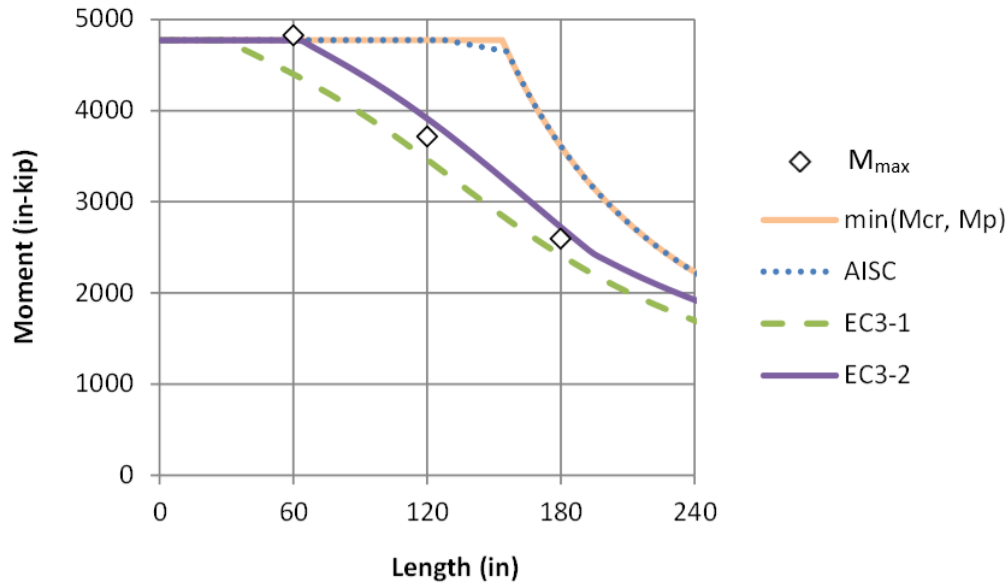


Fig. 3.6. Results of beam benchmark study with Moment Gradient 2 loading.

3.5.2 Column Benchmark Study

The following column benchmark studies are performed using the W21X44 section. The members are flexurally and torsionally simply-supported and have no intermediate brace points. Warping and lateral bending are free at the ends of the members. The modelling approach is exactly the same as that used for all of the studies conducted in this research. An out of straightness of $L/1000$ is used in the weak-axis bending direction as shown in Fig. 3.7, where L is the total length of the column.

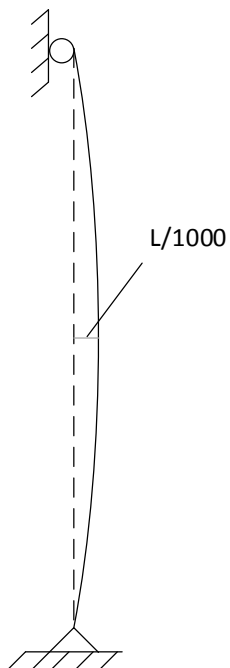


Fig. 3.7. Geometry of the column considered for the benchmark study.

Figure 3.8 shows the results from this benchmark study for 5ft, 10ft and 15ft long columns. The designation EC3 in Figs. 3.8 and 3.9 indicates the applicable Eurocode 3 (CEN 2005) column curve whereas AISC indicates the ANSI/AISC 360-10 column curve.

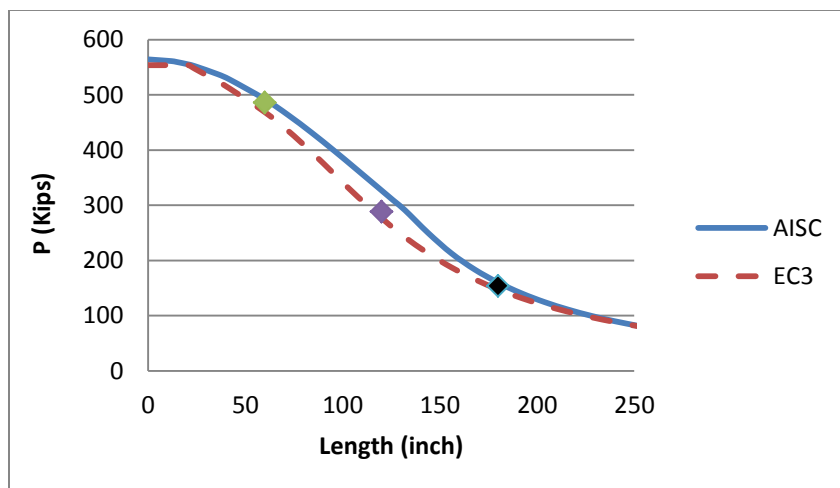


Fig. 3.8. Results of the column benchmark study without local buckling imperfections.

The column benchmark study is repeated with the inclusion of local buckling imperfections to determine their effect on the column capacity. The local buckling imperfection pattern is determined by performing an elastic Eigenvalue buckling analysis. The shape of the lowest local buckling mode is selected and scaled such that the maximum web out-of-flatness is $h/72$. This value is a common fabrication tolerance for welded I-section members (MBMA 2006). The ASTM A6 tolerances for W shapes do not specify any limit on the web out-of-flatness. The resulting flange tilt is well within the ASTM A6 flange tilt tolerance of 5/16 inch, corresponding to $d > 12$ in. Figure 3.9 shows the results for the column strengths after the local buckling imperfections are included. One can observe that the strength of the 5 ft long W21x44 column ($F_y = 50$ ksi) is reduced from 486 kips to 430.5 kips. However, the maximum strengths of the columns having the longer unbraced lengths are practically unchanged due to the inclusion of the local buckling imperfections (reduction by 3.13% and 0.33% for 10ft and 15ft unbraced lengths respectively). This behavior is due to the fact that the W21x44 web is nonslender under pure axial compression; however, for the longer unbraced lengths, the member response is dominated by overall flexural buckling.

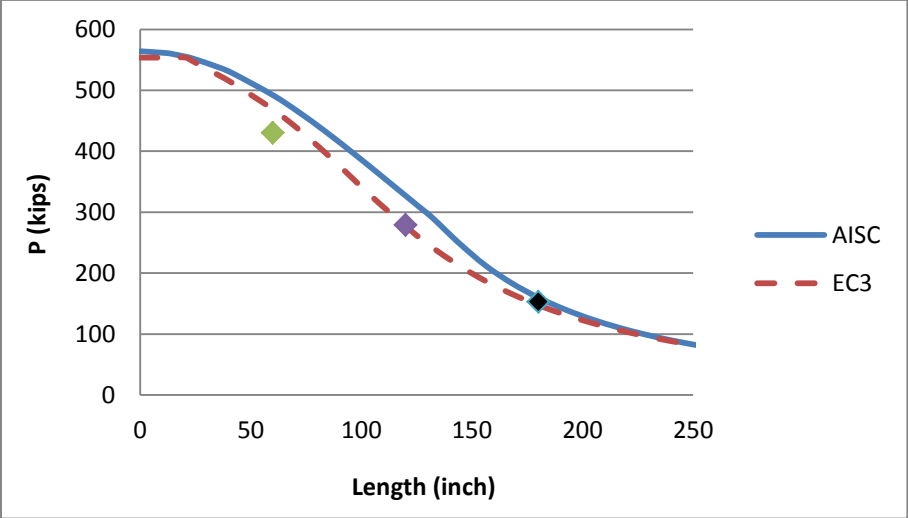


Fig. 3.9 Results of the column benchmark study considering local buckling imperfections.

3.6 Geometric Imperfections in Beams

Wang and Helwig (2005) found that the largest brace forces in fully-braced beams are produced for all practical purposes by giving the compression flange at the brace point having the largest internal moment an out-of-plane initial displacement, leaving the other brace points at their perfect geometry position, and leaving the tension flange straight. Furthermore, to create a maximum out-of-alignment along the compression flange equal to the maximum value of $1/500$ specified in the AISC Code of Standard Practice, this out-of-plane initial displacement is taken as $L_b/500$.

In addition to the above out-of-alignment of the brace points, an out-of-straightness of the compression flange of $L_b/2000$ is imposed in opposite directions on each side of the above critical brace location in this work. This additional “sweep” of the compression flange is applied to avoid cases where the imperfect geometry is completely symmetric about the critical brace location, thus ensuring that the beam fails ultimately in an “S” shape with an inflection point at the brace locations in the test simulations (assuming full bracing). Cases in which the geometry is completely symmetric about the critical brace point, and in which this type of additional out-of-straightness is not modelled, can fail in an unrealistic symmetrical mode about the critical brace location. This can result in larger member strengths and brace force demands than would be expected for the physical member. The value $L_b/2000$ is selected as a reasonable value for the compression flange out-of-straightness that is less than the AISC Code of Standard Practice maximum of $L_b/1000$, and for which the overall imperfection in the unbraced length where the out-of-alignment and out-of-straightness are additive is only slightly larger than that obtained if the compression flange were simply allowed to bend between the brace points based on the offset of $L_b/500$ imposed at the critical brace location.

Figures 3.10 and 3.11 show the imperfection pattern (the out-of-plane lateral displacement of the compression flange) for beams with one and two intermediate brace locations, subjected to

single curvature major-axis bending. The symbol 'X' on the elevation views of the members in these figures indicates the brace point location. Various single curvature bending cases are considered in this research, as discussed in Section 2.2.2. As noted above, the imperfection is applied to the compression flange and the tension flange is constrained to remain straight for these cases. As described in Section 3.1, these imperfections are imposed in a pre-analysis by specifying the desired initial lateral displacements of the compression flange at the critical brace point and at the middle of the unbraced lengths on each side of the brace point. In addition, zero lateral displacement is specified at the corresponding locations on the tension flange in this pre-analysis.

In the cases with two intermediate braces, the compression flange lateral displacement at the middle of the unbraced length further away from the critical brace location is determined from an elastic frame analysis of a prismatic beam with the above displacements imposed at the brace location and the middle of the unbraced lengths on each side of this brace. The value for the elastic deflection obtained at the middle of this additional unbraced length is then imposed on the compression flange of the beam in this unbraced length in the ABAQUS pre-analysis.

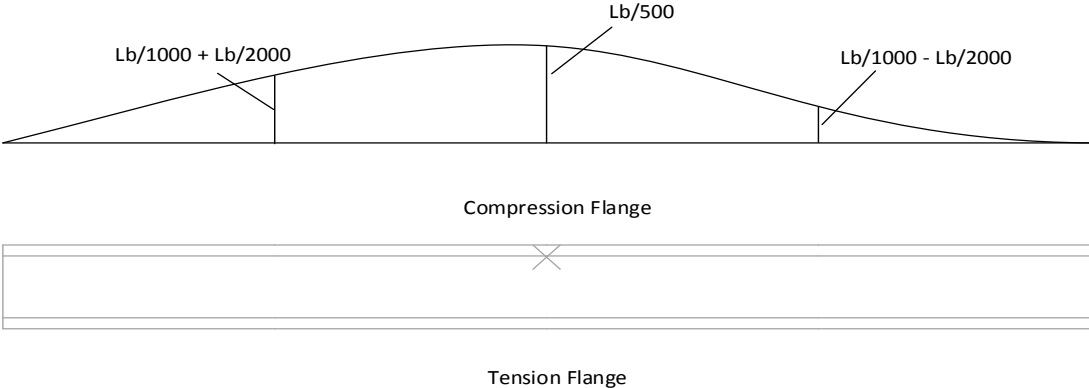


Fig. 3.10. Imperfection pattern for beams subjected to single-curvature bending and containing one intermediate brace point.

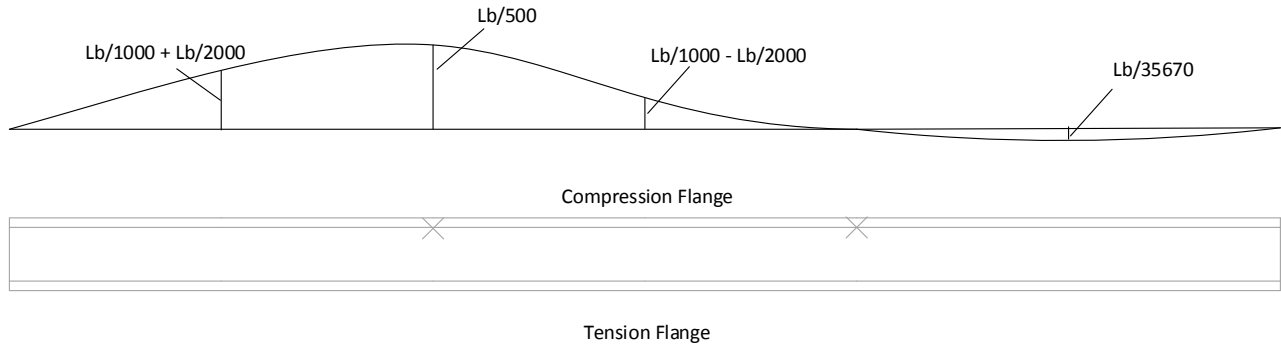


Fig. 3.11. Imperfection pattern for beams subjected to single-curvature bending and containing two intermediate brace points.

It should be noted that the above imperfections are focused on cases in which the members are fully-braced, or in which the members are partially braced but the brace stiffness is approaching the full bracing stiffness. For members with two intermediate braces and relatively flexible partial bracing, the critical geometric imperfections are generally different. For instance, in the limit that the intermediate brace stiffness's are zero, the critical geometric imperfection would involve a single sweep of the compression flange along the entire length of the member. The studies in this research are focused predominantly on cases with full or near full bracing.

3.7 Geometric Imperfections in Beam-Columns

For beam-columns the critical imperfection pattern is taken to depend on the type of bracing as well as the ratio of effective flange force in the flange in flexural tension (P_{ft}) to effective flange force in the flange in flexural compression (P_{fc}). In the limit that the axial force goes to zero, the critical imperfection should correspond to that described above for beams. However, in the limit that the bending moment goes to zero, the critical imperfection should involve an out-of-alignment of both flanges. This attribute of the geometric imperfections is addressed in this work by making the imperfections a function of the effective Flange Force Ratios (the FFRs).

The bracing types considered in this research are discussed in Section 2.2.3 and the ratio of the effective flange forces is discussed in Section 2.2.5.2. The imperfection patterns for beam-columns with lateral bracing only, and combined lateral and torsional bracing are discussed separately in the following subsections.

3.7.1 Beam-column members with point (nodal) lateral or shear panel (relative) lateral bracing only, and bracing provided only on one flange

For beam-columns with bracing only on the flange in flexural compression, when (P_{ft} / P_{fc}) is less than or equal to zero, the member is more like a beam type member because only one flange is in net compression. For these cases the critical imperfection pattern is taken to be the same as that for beams. However, when (P_{ft} / P_{fc}) is greater than zero, the member is more like a column type member because both flanges are in net compression. For these cases the imperfection pattern for the flange in flexural compression is taken to be the same as that for the compression flange in beams. However, since the other flange is subjected to a net compression and is unbraced over the full length of the member, it is specified to have a maximum out of alignment of $L/2000$ at the mid-span (where L is the full member length), with the actual magnitude of out of alignment varying linearly with the ratio (P_{ft} / P_{fc}) .

In summary, the imperfection pattern for beam-columns with lateral bracing only, and with the bracing provided on only one flange, is as shown in Figs. 3.12 and 3.13. The imperfection factor (IF) is a function of the ratio of effective flange force in the flange in flexural tension (P_{ft}) to effective flange force in the flange in flexural compression (P_{fc}). In this research, if $(P_{ft} / P_{fc}) \leq 0$, then IF is taken equal to zero (IF = 0), i.e., the imperfections are the same as if the member were a beam with zero axial loading. If $(P_{ft} / P_{fc}) > 0$, then IF is taken equal to (P_{ft} / P_{fc}) , i.e., as the net axial compression becomes larger in the unbraced flange, the out-of-straightness of this

flange is linearly increased. In the limit that the member is loaded in pure axial compression with zero bending moment, the sweep of the unbraced flange approaches $L/2000$ (i.e., $L_b/1000$).

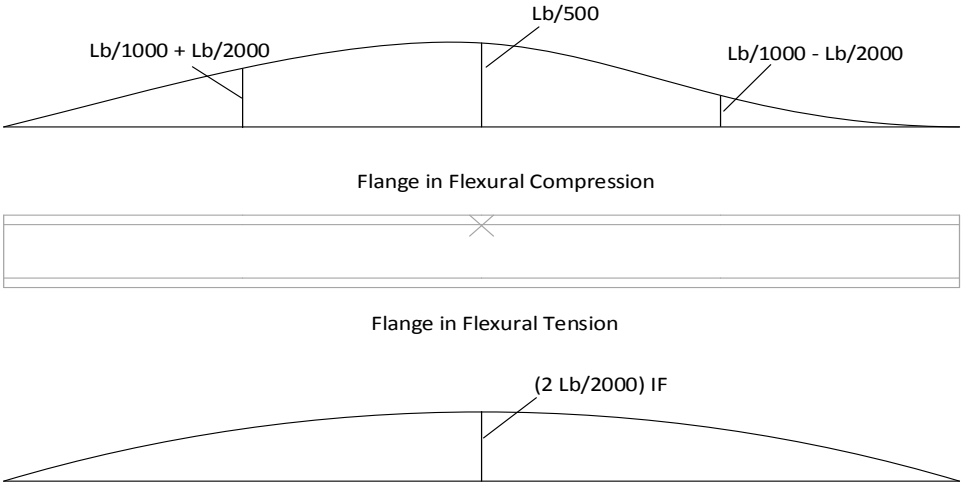


Fig. 3.12. Imperfection pattern for beam-columns with lateral bracing only, bracing only on the flange in flexural compression, and one intermediate brace point.

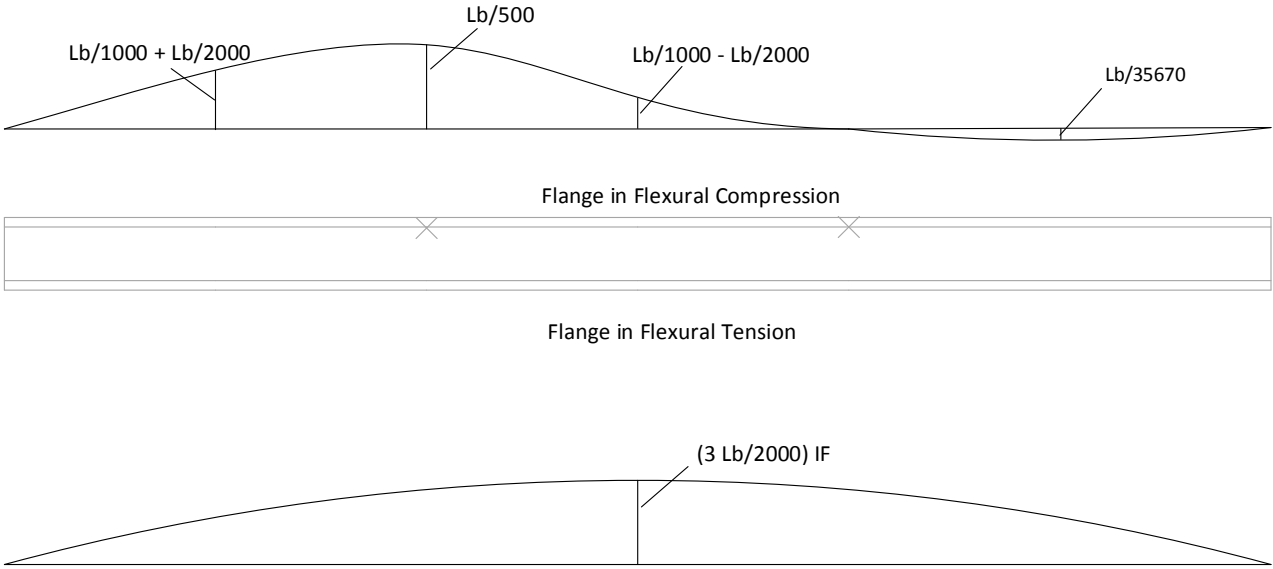


Fig. 3.13. Imperfection pattern for beam-columns with lateral bracing only, bracing only on the flange in flexural compression, and two intermediate brace points.

Figure 3.14 shows end views of the resulting imperfect geometry of the above members with $n = 1$ for three different effective flange force ratios (-0.33, 0.5, and 1).

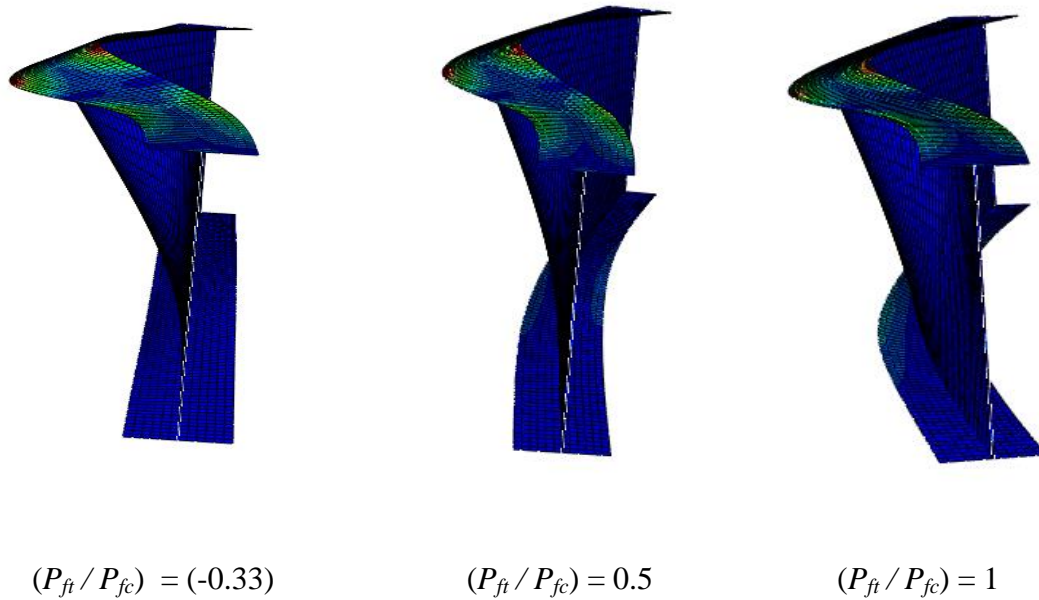


Fig. 3.14. Imperfection pattern in members with a single lateral brace only on the top flange, shown for three different effective flange force ratios.

3.7.2 Beam-column members with combined bracing

For beam-columns with both flanges braced via combined lateral and torsional bracing, if (P_{ft}/P_{fc}) is less than or equal to zero, the member is more like a beam type member because only one flange is in net compression. For these cases the imperfection pattern is taken to be the same as that for beams. However, if (P_{ft}/P_{fc}) is greater than zero, the member is more like a column type member because both flanges are in net compression. For these cases, the imperfection pattern for the flange in flexural compression is taken to be the same as that for the compression flange in beams. Furthermore, since the other flange is also braced and is in compression, it also uses the same imperfection pattern as the compression flange, but the actual magnitude of imperfection is taken as being proportional to the ratio (P_{ft} / P_{fc}) . In the limit that P_{ft} / P_{fc}

approaches zero, the member imperfection is identical to the beam case. However, in the limit that the member is subjected to pure axial compression and P_{ft}/P_{fc} approaches 1.0, both flanges have the same geometric imperfection. The imperfection patterns for beam-columns with combined bracing are summarized in Figs. 3.15 and 3.16.

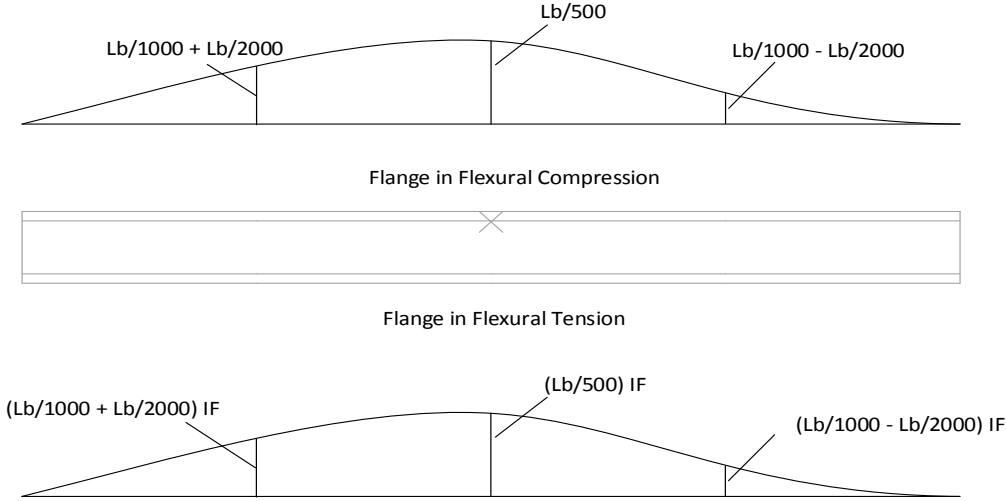


Fig. 3.15. Imperfection pattern for beam-columns with combined lateral and torsional bracing and one intermediate brace point.

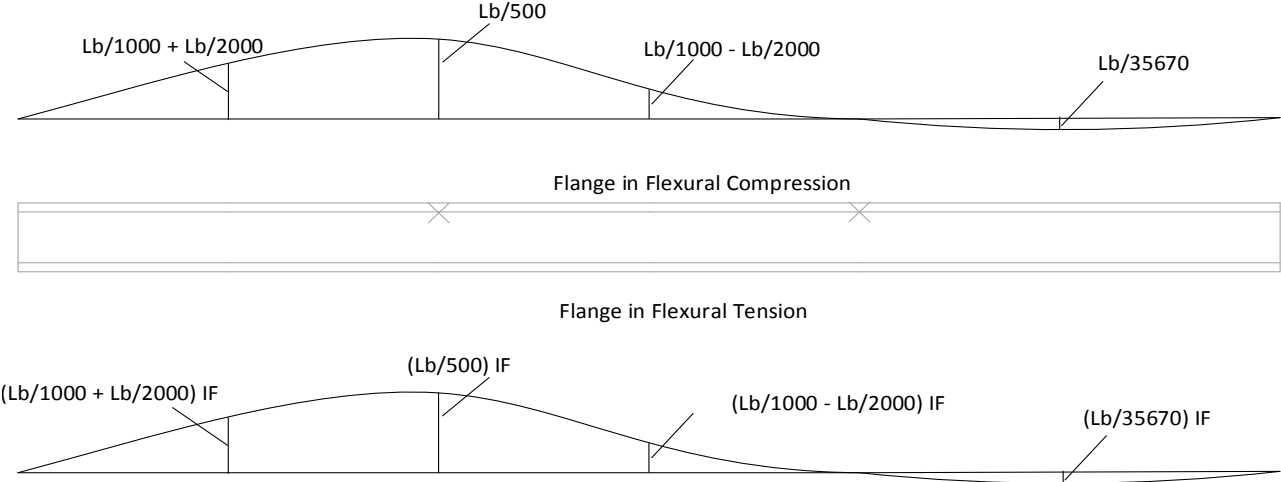


Fig. 3.16. Imperfection pattern for beam-columns with combined lateral and torsional bracing and two intermediate brace points.

If the sign of the bending moment is reversed then the sign on the imperfection patterns on the top and bottom flanges is reversed in the above figures.

The 5 ft unbraced length beam-column moment gradient cases with Moment Gradient 1 loading have difficulty in converging during the load-deflection analysis in some cases, although the solution is successfully continued through the limit load of the member response. To resolve this problem, and to consider the impact of web local buckling displacements on the member resistance, local buckling imperfections also are added to the above imperfections while performing the analyses for these cases. The local buckling imperfections are determined using beam-column loading (i.e., axial load and Moment Gradient 1 loading). The local buckling imperfections are specified in this research only for 5ft unbraced length beam-column moment gradient cases with Moment Gradient 1 loading.

CHAPTER 4: BEAMS SUBJECTED TO MOMENT GRADIENT LOADING

4.1 Overview

This chapter addresses the first major part of this research, beams with moment gradient loading. Section 4.2 gives details of the cases considered. Section 4.3 discusses the member rigidly-braced strengths. Section 4.4 presents the test simulation results.

4.2 Detailed Study Design

The cases considered in this research to study the bracing requirements for beams subjected to moment gradient loadings are listed below. The case naming convention is explained in Sections 2.2 and 2.3.

The cases considered for beams with Moment Gradient 1 loading, single curvature bending with an applied moment on one end and zero moment on the opposite end of the beam, are as follows.

Positive moment loading, basic bracing types:

B_MG1p_NB_n1_Lb5
B_MG1p_NB_n1_Lb15
B_MG1p_RB_n2_Lb5
B_MG1p_RB_n2_Lb15
B_MG1p_TB_n1_Lb5
B_MG1p_TB_n1_Lb15

Positive moment loading, combined point (nodal) lateral and point torsional bracing:

B_MG1p_CNTB_n1_Lb5_TLBSR4
B_MG1p_CNTB_n1_Lb5_TLBSR1
B_MG1p_CNTB_n1_Lb5_TLBSR0.25

B_MG1p_CNTB_n1_Lb15_TLBSR4
B_MG1p_CNTB_n1_Lb15_TLBSR1
B_MG1p_CNTB_n1_Lb15_TLBSR0.25

Positive moment loading, combined shear panel (relative) lateral and point torsional bracing:

B_MG1p_CRTB_n2_Lb5_TLBSR4
B_MG1p_CRTB_n2_Lb5_TLBSR1
B_MG1p_CRTB_n2_Lb5_TLBSR0.25
B_MG1p_CRTB_n2_Lb15_TLBSR4
B_MG1p_CRTB_n2_Lb15_TLBSR1
B_MG1p_CRTB_n2_Lb15_TLBSR0.25

Negative moment loading, combined point (nodal) lateral and point torsional bracing:

B_MG1n_CNTB_n1_Lb5_TLBSR5.67
B_MG1n_CNTB_n1_Lb5_TLBSR1
B_MG1n_CNTB_n1_Lb5_TLBSR0.33
B_MG1n_CNTB_n1_Lb5_TLBSR0.11
B_MG1n_CNTB_n1_Lb15_TLBSR5.67
B_MG1n_CNTB_n1_Lb15_TLBSR1
B_MG1n_CNTB_n1_Lb15_TLBSR0.33
B_MG1n_CNTB_n1_Lb15_TLBSR0.11

Negative moment loading, combined shear panel (relative) lateral and point torsional bracing:

B_MG1n_CRTB_n2_Lb5_TLBSR5.67
B_MG1n_CRTB_n2_Lb5_TLBSR1
B_MG1n_CRTB_n2_Lb5_TLBSR0.33
B_MG1n_CRTB_n2_Lb5_TLBSR0.11
B_MG1n_CRTB_n2_Lb15_TLBSR5.67
B_MG1n_CRTB_n2_Lb15_TLBSR1
B_MG1n_CRTB_n2_Lb15_TLBSR0.33
B_MG1n_CRTB_n2_Lb15_TLBSR0.11

The following cases are considered for beams with Moment Gradient 2 loading, transverse load applied at the centroid of the cross-section at the mid-span of the beam.

Positive moment loading, basic bracing types:

B_MG2pc_NB_n1_Lb5
B_MG2pc_NB_n1_Lb15
B_MG2pc_TB_n1_Lb5
B_MG2pc_TB_n1_Lb15

Positive moment loading, combined point (nodal) lateral and point torsional bracing:

B_MG2pc_CNTB_n1_Lb5_TLBSR4
B_MG2pc_CNTB_n1_Lb5_TLBSR1
B_MG2pc_CNTB_n1_Lb5_TLBSR0.25
B_MG2pc_CNTB_n1_Lb15_TLBSR4
B_MG2pc_CNTB_n1_Lb15_TLBSR1
B_MG2pc_CNTB_n1_Lb15_TLBSR0.25

Negative moment loading, combined point (nodal) lateral and point torsional bracing:

B_MG2nc_CNTB_n1_Lb5_TLBSR5.67
B_MG2nc_CNTB_n1_Lb5_TLBSR1
B_MG2nc_CNTB_n1_Lb5_TLBSR0.33
B_MG2nc_CNTB_n1_Lb5_TLBSR0.11
B_MG2nc_CNTB_n1_Lb15_TLBSR5.67
B_MG2nc_CNTB_n1_Lb15_TLBSR1
B_MG2nc_CNTB_n1_Lb15_TLBSR0.33
B_MG2nc_CNTB_n1_Lb15_TLBSR0.11

4.3 Rigidly Braced Strengths

For a given number of intermediate brace locations, there is a slight difference in the rigidly-braced strength for different bracing types. In this research, the rigidly-braced strength for a given number of intermediate braces is taken as the minimum of the rigidly-braced strengths obtained for the different bracing types. This philosophy simplifies the comparison of the study results. It should be noted that the AISC Specification (AISC 2010) predicts only one strength for the different groups considered, e.g., panel lateral bracing, point lateral bracing, or point torsional bracing. In all of the cases, the minimum rigidly-braced strength is obtained when torsional bracing is used alone, without combining the torsional braces with any lateral bracing. Generally, the rigidly-braced strengths are only slightly different for the different bracing types, but the differences are measureable and notable. As noted previously in Section 2.2.5.1, the minimum rigidly-braced strength is used as the required moment in determining the base bracing stiffness requirements from the AISC Appendix 6 (AISC 2010) equations.

Tables 4.1 and 4.2 give the rigidly-braced strengths for the Moment Gradient 1 loading with $n = 1$ and $n = 2$ respectively. Similarly, Table 4.3 gives the rigidly-braced strengths for the Moment Gradient 2 cases. Tables 4.4 and 4.5 give the rigidly-braced strengths for the Moment Gradient 3 cases with $n = 1$ and $n = 2$.

Table 4.1. Comparison of rigidly-braced strengths for beams with Moment Gradient 1 loading and $n = 1$.

	$L_b = 5\text{ft}$	$L_b = 15\text{ft}$
Combined Point (nodal) lateral and Point torsional bracing	4827 kip-inch	2671 kip-inch
Point (nodal) lateral bracing	4824 kip-inch	2594 kip-inch
Point torsional bracing	4798 kip-inch	2409 kip-inch

Table 4.2 Comparison of rigidly-braced strengths for beams with Moment Gradient 1 loading and $n = 2$

	$L_b = 5\text{ft}$	$L_b = 15\text{ft}$
Shear panel (relative) lateral and Point torsional bracing	4738 kip-inch	2476 kip-inch
Shear panel (relative) lateral bracing	4737 kip-inch	2449 kip-inch
Point torsional bracing	4691 kip-inch	2197 kip-inch

Table 4.3. Comparison of rigidly-braced strengths for beams with Moment Gradient 2 loading and $n = 1$.

	$L_b = 5\text{ft}$	$L_b = 15\text{ft}$
Combined Point (nodal) lateral and Point torsional bracing	4989 kip-inch	3152 kip-inch
Point (nodal) lateral bracing	4989 kip-inch	3149 kip-inch
Point torsional bracing	4913 kip-inch	3069 kip-inch

4.4 Results

The results for the various beam moment gradient loading cases are discussed in the following subsections.

In this research, the torsional bracing stiffness is expressed as an equivalent shear panel (relative) lateral bracing stiffness. This approach of considering the torsional bracing as an equivalent relative lateral bracing, but between the two flanges rather than between two points along the same flange, is discussed in detail in Chapter 2 of Prado and White (2014). A brief explanation of this approach is given below.

Equation (4-1) is the required torsional bracing stiffness per the AISC 360-10 Commentary, which discusses an explicit “top flange loading factor,” designated here by C_{iT} (the second subscript representing “torsional bracing”).

$$\beta_{Tbr} = \pi^2 h_o^2 \left[\frac{\left(\frac{M_{\max}}{C_b h_o} \right)}{P_{ef. eff}} \right] \left[\frac{\left(\frac{M_{\max}}{C_b h_o} \right)}{L_b} \right] \frac{n_T + 1}{n_T} C_{iT} \quad (4-1)$$

where:

h_o = distance between the centroids of the compression and tension flanges;

$\frac{M_{\max}}{C_b}$ = equivalent uniform moment for the critical unbraced length within the member span;

C_b = equivalent uniform moment factor for the critical unbraced length;

$$P_{ef,eff} = \frac{\pi^2 E (I_{eff} / 2)}{L_b^2} = \text{effective elastic lateral buckling resistance of the beam compression flange}$$

based on the unbraced length between the torsional braces, equal to $\frac{\pi^2 EI_{yc}}{L_b^2}$ for a doubly-symmetric

I-section, where I_{yc} is the lateral moment of inertia of the compression flange;

n_T = number of intermediate torsional braces along the beam length; and

C_{iT} = torsional bracing factor accounting for the effects of the height of any transverse loads relative to the depth of the member cross-section.

The format of Eq., (4-1) is different than the corresponding equation in AISC 360-10. However, when C_{iT} is taken conservatively as 1.2, this equation gives identical results to the corresponding Eq. A-6-11 presented in the AISC 360-10 Appendix 6 (AISC 2010). The format used in Eq. (4-1) is useful at emphasizing the contribution from the beam to the resistance of brace point movement via the term $P_{ef,eff}$. Of importance to a number of the subsequent discussions, β_{Tbr} in Eq. (4-1) is 2.0 times what is commonly referred to as the “ideal full bracing stiffness,” defined as the bracing stiffness necessary to develop the moment capacity $M_r = M_n$ before a hypothetical member with zero initial imperfections would fail out-of-plane by buckling between the braced locations.

The torsional brace stiffness requirement may be expressed as an equivalent shear panel (relative) brace stiffness (between the flanges of the I-section) by dividing β_{Tbr} by h_o^2 . This approach to the modeling of torsional bracing is discussed in detail by White and Prado (2014) and by Bishop (2013).

The required torsional brace strength (M_{br}) is estimated in AISC Appendix 6 (AISC 2010) as

$$M_{br} = (\beta_{Tbr}) \theta_o \tag{4-2}$$

where $\theta_o = \frac{L_b}{500h_o}$ is the specified nominal initial twist imperfection.

Chapter 7 of Prado and White (2014) states that the Appendix 6 (AISC 2010) modifier on the

base brace strength requirement, $\frac{1}{2 - \frac{2\beta_{iF.AISC}}{\beta}}$, does not work well in predicting the variation in the torsional brace forces at the member strength limit as a function of the torsional brace stiffness, where $\beta_{iF.AISC}$ is the theoretical ideal full bracing stiffness, estimated as one-half the value from Eq.

4-1. However, Prado and White (2014) suggest that an ad-hoc modifier $\frac{1}{\sqrt{2 - \frac{2\beta_{iF.AISC}}{\beta}}}$ combined

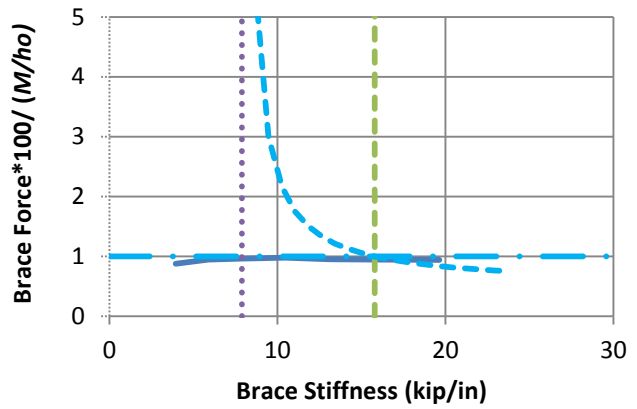
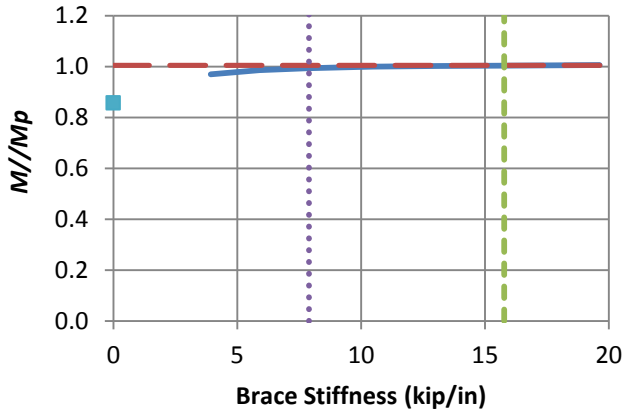
with a base torsional brace strength requirement of 2 %, gives a reasonably good estimate of the torsional brace forces for $\beta \geq 2\beta_{iF.AISC}$. Furthermore, Prado and White (2014) observe that for $\beta < 2\beta_{iF.AISC}$ (i.e., $\beta < \beta_{Tbr}$ from Eq. 4-1), a brace force requirement of 2 % provides an upper bound to the brace forces required to develop 95 % or greater of the load capacity from the test simulations in all cases (i.e., for all brace stiffness values).

In this research, the point and panel lateral bracing stiffness requirements per AISC are obtained from Eq. C-A-6-5, in the Appendix 6 (AISC 2010) Commentary, with $C_b P_f$ taken equal to M_{max}/h_o , where M_{max} is taken as the minimum rigidly-braced strength presented in Section 4.3. The AISC lateral bracing strength requirements are obtained from Eqs. C-A-6-6a and C-A-6-6b, in the Appendix 6 (AISC 2010) Commentary, for shear panel (relative) and point (nodal) lateral bracing respectively. A refined estimate of the required lateral bracing strength can be obtained by using Eq. C-A-6-1, in the Appendix 6 (AISC 2010) Commentary, along with Eqs. C-A-6-6a and C-A-6-6b. A detailed explanation of these AISC Appendix 6 (AISC 2010) equations, with all the Commentary refinements included, can be found in Chapter 2 of Prado and White (2014). It should be noted that, generally, the ideal full bracing stiffness for point lateral and panel lateral bracing is equal to one-half of the nominal AISC required brace stiffness (i.e., the AISC required brace stiffness without the inclusion of the resistance factor ϕ or the safety factor Ω).

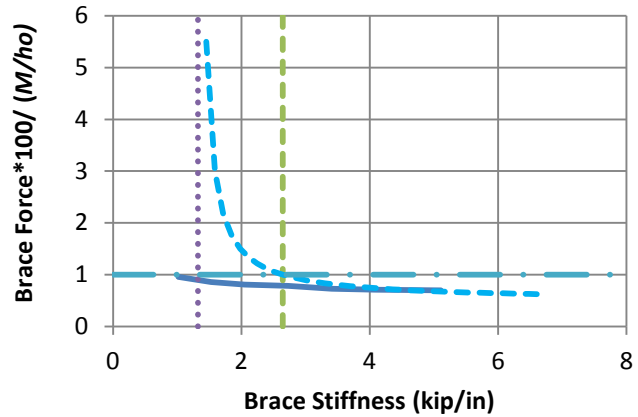
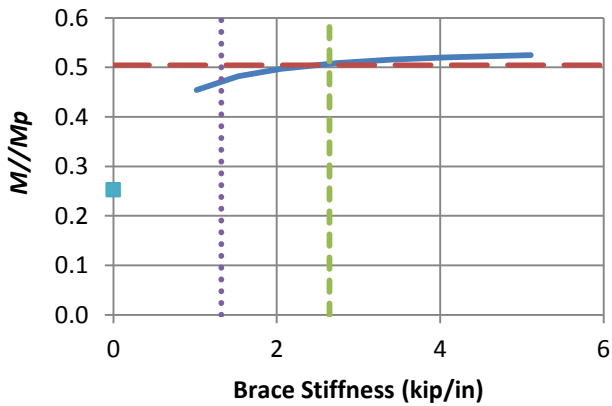
4.4.1 Beams with Moment Gradient 1 loading

The results for the Moment Gradient 1 loading cases are shown in Figs. 4.1 through 4.5. Figures 4.1 through 4.3 show the knuckle curves and brace-force versus brace stiffness curves for the basic point and panel lateral bracing cases and for the point torsional bracing case. In this research, the term M in M/h_o , in all the brace force versus brace stiffness plots, is taken as the maximum moment along the length of the member. Figures 4.4 and 4.5 show the bracing stiffness interaction plots for the combined bracing cases. The method of generating the interaction plots is discussed in Section 1.2. Knuckle curves and brace force versus brace stiffness plots for each of the combined bracing cases are provided in Appendix A.

Table 4.4 compares the results from Figs. 4.1 through 4.3. The torsional bracing stiffness's are reported in this table as the equivalent relative lateral bracing stiffness values. From Column (e) of Table 4.4, it can be observed that the AISC Appendix 6 (AISC 2010) equations (including the Commentary refinements) provide a conservative estimate of the stiffness required to reach 96 % of the rigidly-braced strength for beams with point (nodal) lateral, shear panel (relative) lateral, and point torsional bracing and the 5 ft unbraced lengths. In these cases, the beams experience significant distributed yielding prior to reaching their maximum strength. However, for the 15 ft unbraced lengths, where the beam response is more dominated by elastic stability effects, the bracing stiffness required to reach 96 % of the rigidly-braced strength is slightly larger than the ideal full bracing stiffness values from AISC 360-10. It can be observed that 2.0 times the ideal full bracing stiffness, as calculated by the AISC Appendix 6 (AISC 2010) equations, is sufficient to develop between 96 and 98 % of the minimum rigidly-braced member strength for all of the basic bracing types.



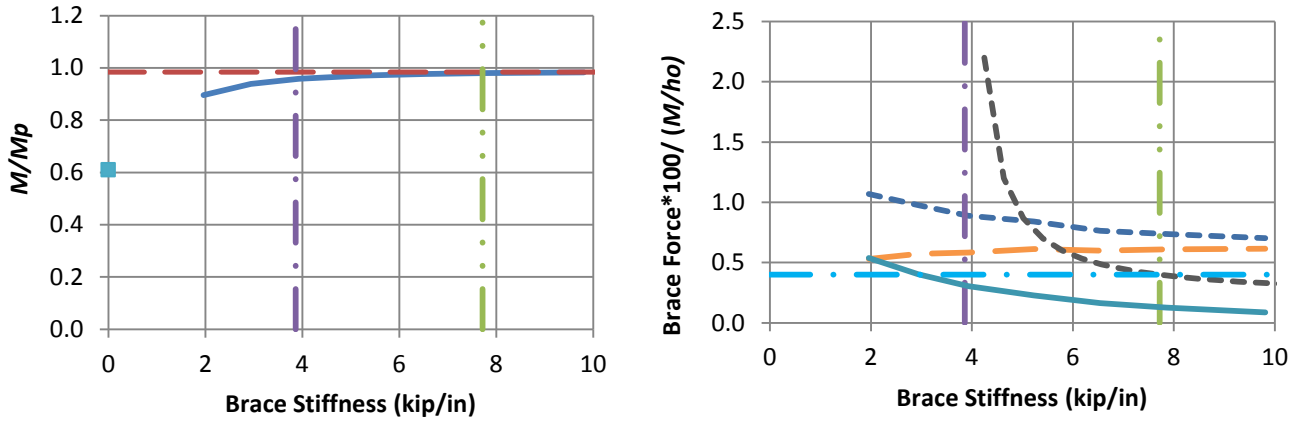
a) B_MG1p_NB_n1_Lb5



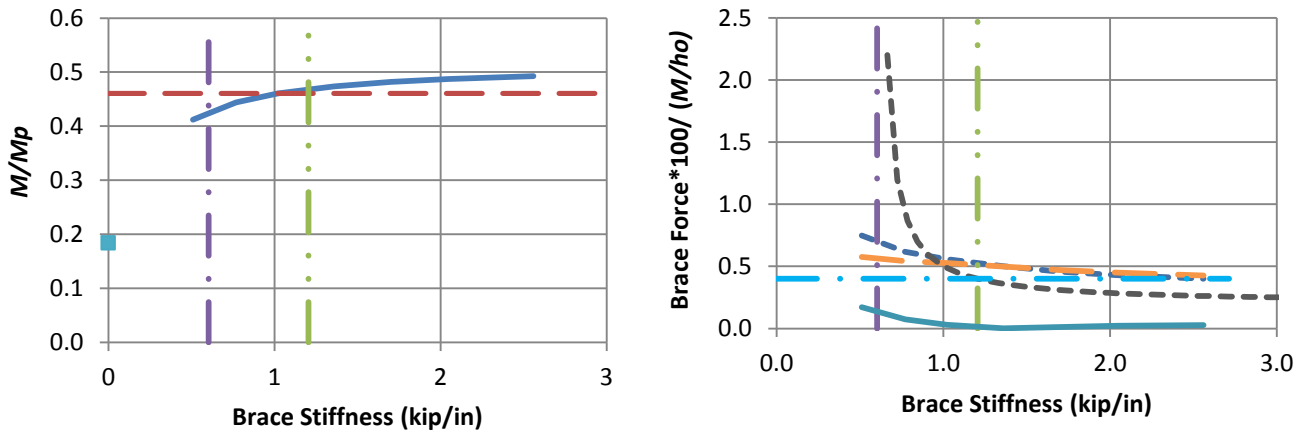
b) B_MG1p_NB_n1_Lb15

- Test simulation results
- - Rigidly-braced strength
- AISC ideal full bracing stiffness
- - - 2x AISC ideal full bracing stiffness (From Eq. C-A-6-5, AISC 360-10, with $C_b P_f$ taken equal to M_{max}/h_o)
- Test simulation strength at zero brace stiffness
- • Base AISC Required Strength Corresponding to $\beta = 2\beta_{iF,AISC}$ (From Eq. C-A-6-6b, AISC 360-10)
- - - Refined Estimate of Required Strength from AISC Commentary (Eq. C-A-6-6b multiplied by Eq. C-A-6-1, AISC 360-10)

Fig. 4.1. Knuckle curves and brace force vs. brace stiffness plots for point (nodal) lateral bracing cases with $n = 1$ and Moment Gradient 1 loading.



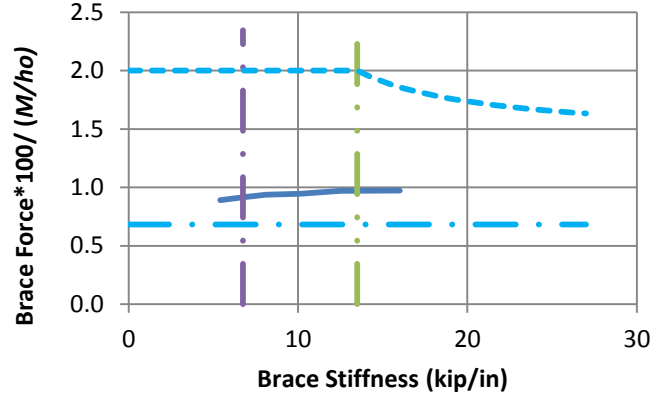
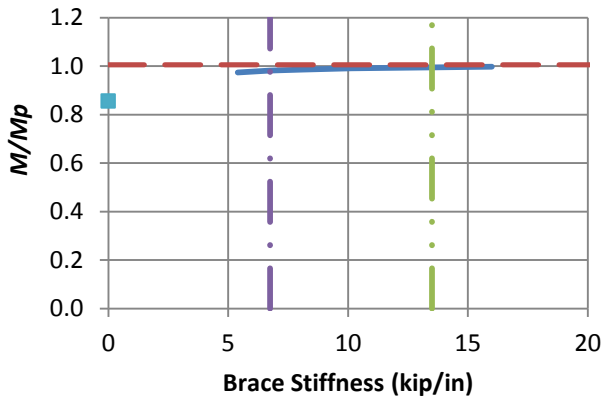
a) B_MG1p_RB_n2_Lb5



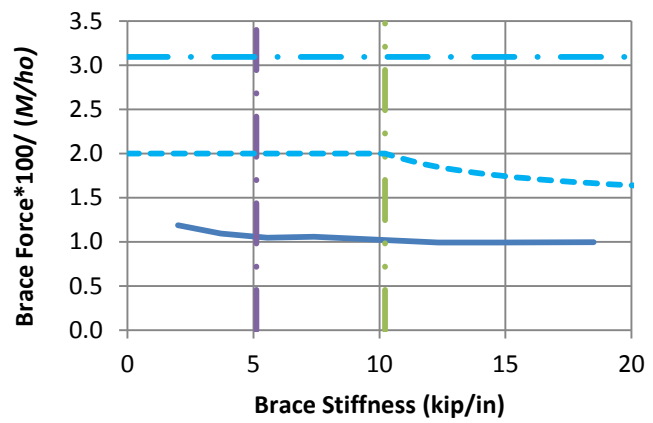
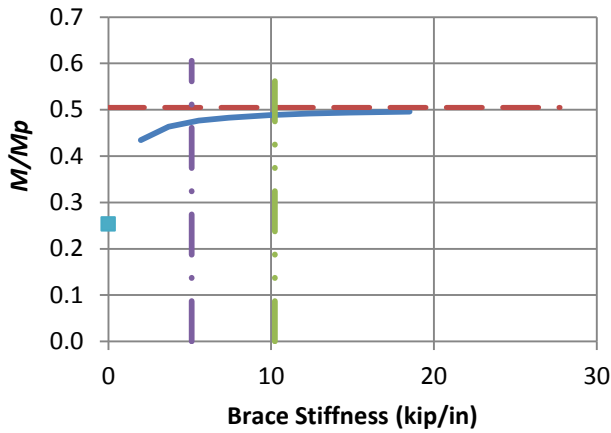
b) B_MG1p_RB_n2_Lb15

- Test simulation results
- · AISC ideal full bracing stiffness
- · 2x AISC ideal full bracing stiffness (From Eq. C-A-6-5, AISC 360-10, with $C_b P_f$ taken equal to M_{max}/h_o)
- - - Left end panel shear force
- Right end panel shear force
- Middle panel shear force
- Test simulation strength at zero brace stiffness
- · Base AISC Required Strength for $\beta = 2\beta_{IF,AISC}$ (Eq. C-A-6-6a, AISC 360-10)
- - - Refined Estimate of Required Strength from AISC Commentary (Eq.C-A-6-6a multiplied by Eq. C-A-6-1, AISC 360-10)
- - - Rigidly-braced strength

Fig. 4.2. Knuckle curves and brace force vs. brace stiffness plots for shear panel (relative) lateral bracing cases with $n = 2$ and Moment Gradient 1 loading.



a) B_MG1p_TB_n1_Lb5



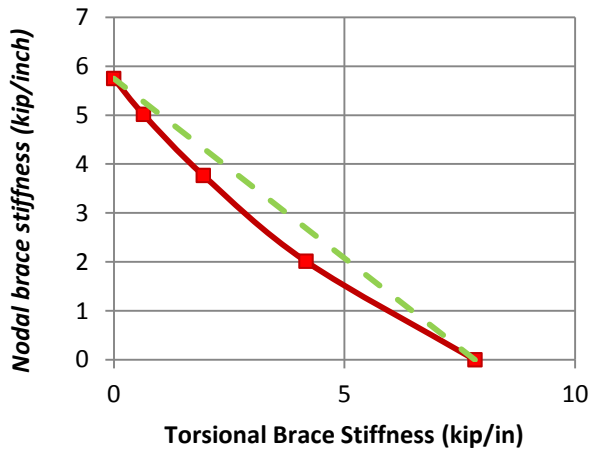
b) B_MG1p_TB_n1_Lb15

- Test simulation results
- · AISC ideal full bracing stiffness
- · 2x AISC ideal full bracing stiffness equal to (β_{Tbr} / h_o^2) , where β_{Tbr} is given in Eq. 4-1
- Test simulation strength at zero brace stiffness
- · Base AISC Required Strength corresponding to $\beta = 2\beta_{iF,AISC}$ (From Eq. 4-2)
- - - Recommended Refined Estimate of Required Strength of 2% with an ad-hoc modifier

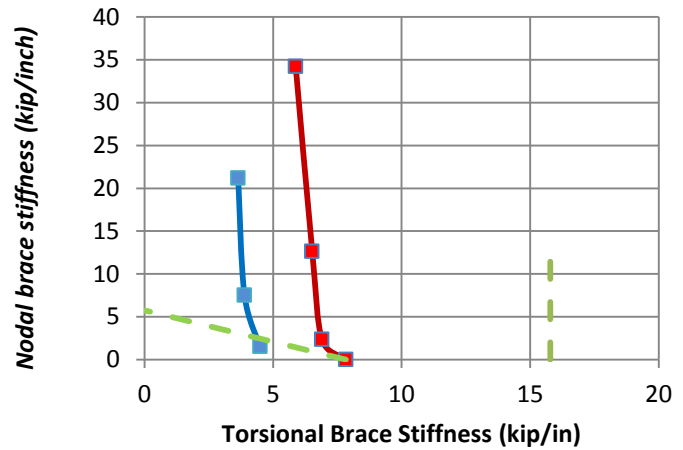
$$\frac{1}{\sqrt{2 - \frac{2\beta_{iF,AISC}}{\beta}}}$$

to account for the variation in torsional brace forces at the member strength limit as a function of the torsional brace stiffness

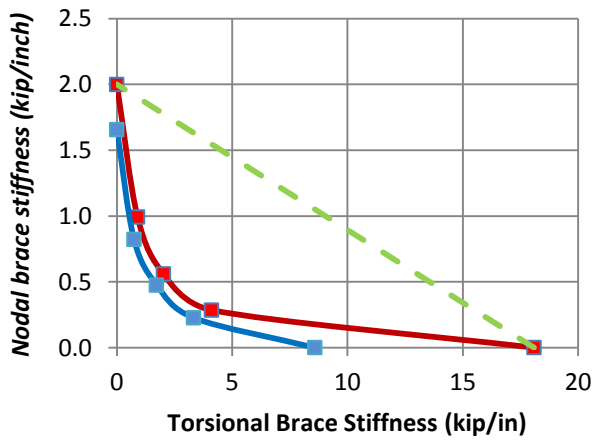
Fig. 4.3. Knuckle curves and brace force vs. brace stiffness plots for point torsional bracing cases with $n = 1$ and Moment Gradient 1 loading.



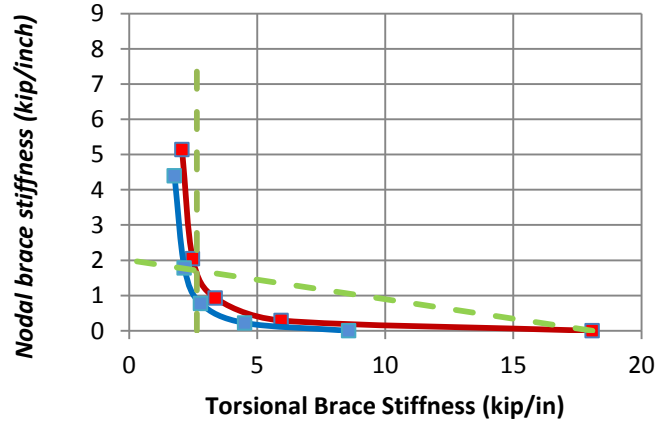
a) 5ft unbraced length (Positive bending)



b) 5ft unbraced length (Negative bending)



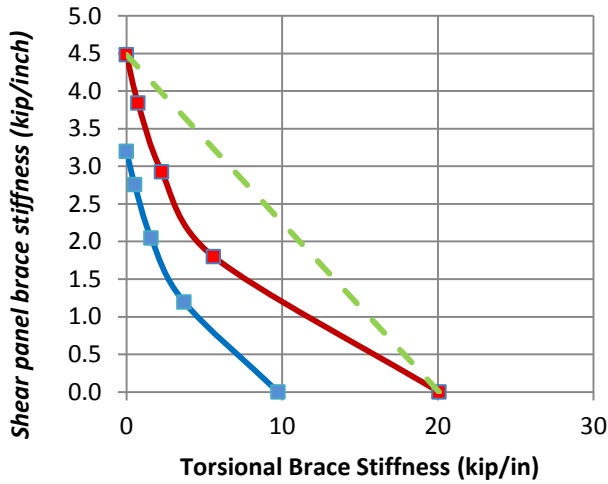
c) 15ft unbraced length (Positive bending)



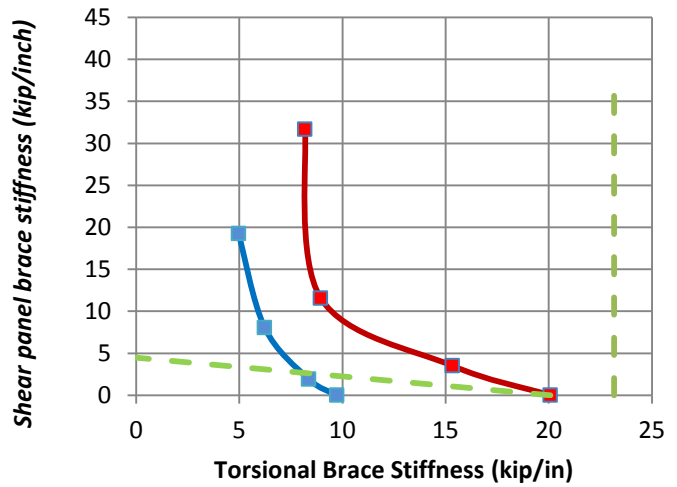
d) 15ft unbraced length (Negative bending)

- Simulation-based stiffness interaction corresponding to 98 % of rigid bracing strength
- Simulation-based stiffness interaction corresponding to 96 % of rigid bracing strength
- - - Recommended design approximation

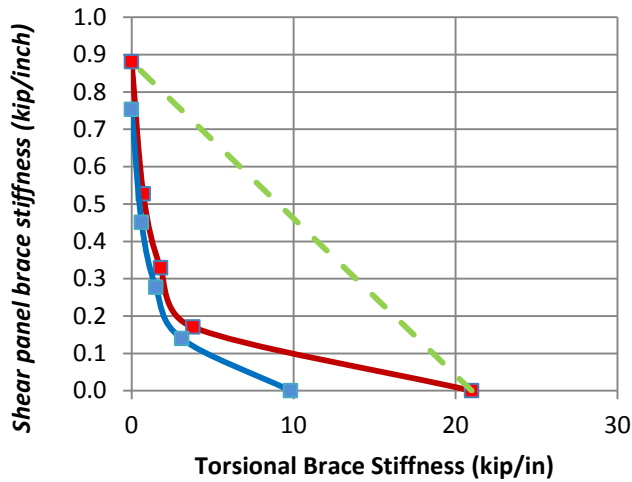
Fig. 4.4. Point (nodal) lateral and point torsional bracing stiffness interactions for Moment Gradient 1 loading and $n = 1$.



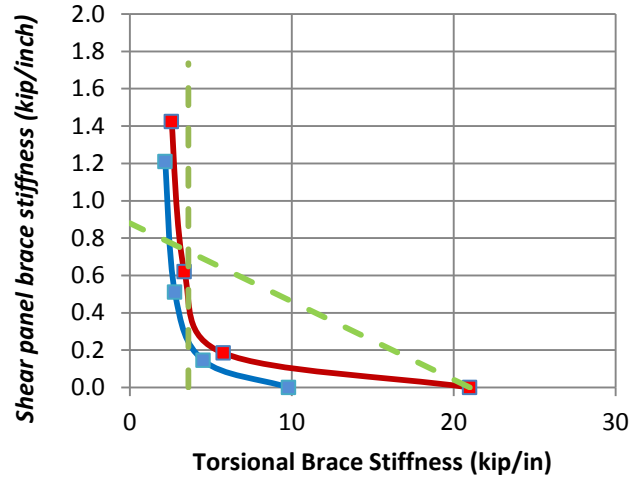
a) 5ft unbraced length (Positive bending)



b) 5ft unbraced length (Negative bending)



c) 15ft unbraced length (Positive bending)



d) 15ft unbraced length (Negative bending)

- Simulation-based stiffness interaction corresponding to 98 % of rigid bracing strength
- Simulation-based stiffness interaction corresponding to 96 % of rigid bracing strength
- - - Recommended design approximation

Fig. 4.5. Shear panel (relative) lateral and point torsional bracing stiffness interactions for Moment Gradient 1 loading and $n = 2$.

Table 4.4. Comparison of simulation results in Figs. 4.1 through 4.3 with AISC predicted ideal full bracing stiffness.

Case (a)	Stiffness corresponding to 98% of simulation rigidly-braced strength (kip/in) (b)	Stiffness corresponding to 96% of simulation rigidly-braced strength (kip/in) (c)	Nominal AISC required full bracing stiffness kip/in (d)	Col. (c) / Col. (d) (e)
B_MG1p_NB_n1_Lb5	5.7	3.8	15.8	0.25
B_MG1p_NB_n1_Lb15	2	1.6	2.6	0.6
B_MG1p_RB_n2_Lb5	4.5	3.2	7.8	0.4
B_MG1p_RB_n2_Lb15	0.9	0.8	1.2	0.65
B_MG1p_TB_n1_Lb5	7.8	5.0	13.4	0.35
B_MG1p_TB_n1_Lb15	16.4	8.1	10.2	0.8

Regarding the AISC bracing required strength estimates, the brace force versus brace stiffness plots in Fig. 4.1 show that the point brace requirements are estimated accurately by the AISC Appendix 6 (AISC 2010) equations at and above $2\beta_{iF.AISC}$. Figure 4.2 shows that the panel brace strength requirements are slightly underestimated for $\beta \geq 2\beta_{iF.AISC}$ for the case with the longer unbraced length. However, the AISC prediction is accurate if the base required brace force is increased from 0.4 % to 0.5 % of the corresponding flange force M_r/h_o . As shown in Fig. 4.2a, the maximum panel brace force requirement at the test limit loads for the 5 ft case are significantly underestimated by the AISC brace strength equations. However, close inspection of the brace force versus applied load curves from the different tests shows that a brace strength requirement of 0.5 % is sufficient to develop very close to the test limit loads for $\beta \geq 2\beta_{iF.AISC}$. Figure 4.6 shows a plot of

brace force versus applied load for B_MG1p_RB_n2_Lb5 case (results for which are shown in Fig. 4.2a) with $\beta = 2\beta_{iF.AISC}$. It can be observed that a brace strength requirement of 0.5 % is sufficient to develop a member strength very close to the test limit load.

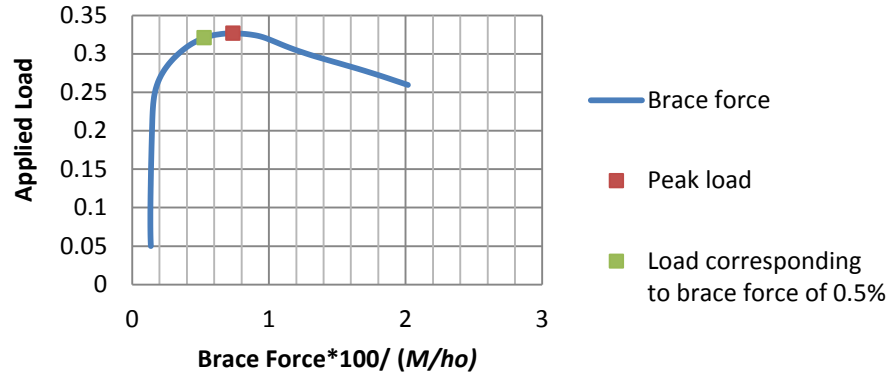


Fig. 4.6. Plot of brace force versus applied load for B_MG1p_RB_n2_Lb5 with $\beta = 2\beta_{iF.AISC}$.

The brace force versus brace stiffness curves in Fig. 4.3 show that the current AISC torsional bracing equations substantially over-estimate the strength requirements for the long unbraced length, where the response is more dominated by elastic stability effects. However, for the short unbraced length, where the beam experiences significant distributed yielding at its strength limit, the AISC estimate significantly underestimates the strength requirements. This is consistent with the findings by Prado and White (2014). However, the brace strength requirement at the test limit load is consistently approximately 1 % for the beams considered in these Moment Gradient 1 tests. This is smaller than the requirements observed for the uniform bending cases considered by Prado and White, where a brace force strength requirement of 2 % of M_r/h_o worked well as a base requirement, and the ad hoc reduction shown for $\beta \geq 2\beta_{iF.AISC}$ provided a good characterization of the required bracing strength.

In the stiffness interaction plots in Figs. 4.4 and 4.5, when the member experiences positive bending, the interaction between the combined lateral (nodal or shear panel) and torsional bracing stiffness requirements is represented conservatively by a simple linear interaction between the lateral

and torsional bracing stiffness's in all the cases studied. The conservative nature is more substantial for larger unbraced lengths.

However, when a member with combined lateral (nodal or shear panel) and torsional bracing is subjected to negative bending, where the laterally-braced top flange is in tension and the bottom flange is in compression, the interaction between the two bracing stiffness requirements is different. In this case, the lateral brace to the tension flange provides negligible benefit to the stability behavior of the beam in the limit that the torsional brace stiffness approaches zero. However, as explained by Prado and White (2014), in the limit that the lateral brace stiffness is rigid, the torsional brace (when modeled as a relative brace between the top and bottom flanges) effectively becomes a point (nodal) lateral brace to the bottom compression flange. This is because the idealization for a point (nodal) lateral brace is simply a grounded spring. In the limit that the lateral brace to the tension flange is rigid, the relative brace between the top and bottom flange is indeed such a grounded spring.

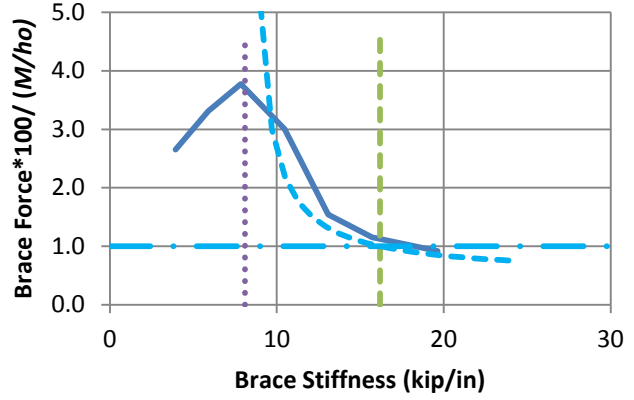
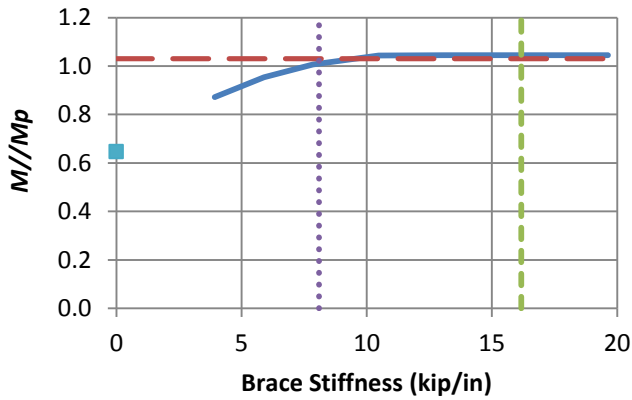
Upon establishing the above concept, then in the limit that the lateral bracing to the tension flange is rigid, one can surmise that the minimum torsional bracing stiffness requirement, expressed as an equivalent relative bracing (i.e., shear spring) stiffness between the top and bottom flange, can be specified simply as the point (nodal) lateral bracing stiffness requirement. However, the lateral bracing stiffness at the tension flange will need to be very large before the required torsional bracing stiffness becomes equal to the ideal bracing stiffness given by half of the value from Eq. C-A-6-5 in AISC 360-10 for point (nodal) lateral brace with $C_b P_f$ taken as M_{max}/h_o . Therefore, a minimum torsional bracing stiffness equal to the nodal bracing value from Eq. C-A-6-5 is recommended.

From Figs. 4.4 and 4.5, it is observed that the behavior for the Moment Gradient 1 cases considered here is essentially the same as that observed by Prado and White (2014) for uniform bending tests. A vertical line at stiffness equal to that from Eq. C-A-6-5 (AISC 360-10) for point (nodal) lateral brace, with $C_b P_f$ taken as M_{max}/h_o , illustrated by the green dashed vertical line in the negative moment based plots, provides an accurate to somewhat conservative minimum limit for the

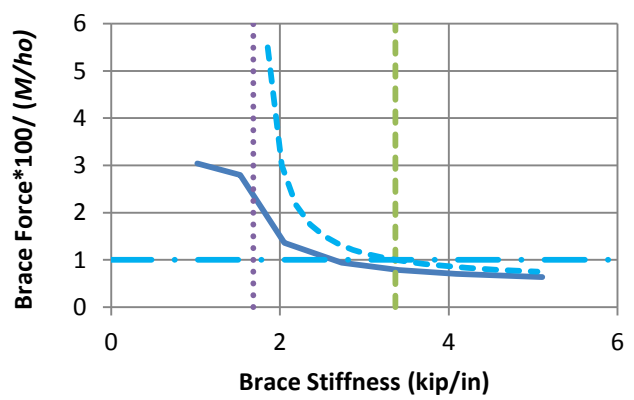
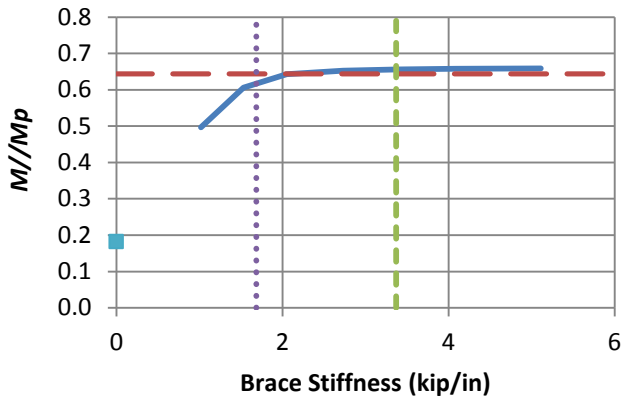
torsional bracing stiffness as the lateral bracing stiffness becomes relatively large. In addition, with the exception of this minimum limit, the torsional bracing stiffness requirement can be reduced by providing a relatively small lateral bracing stiffness, by the same linear interpolation function as shown for the positive moment based plots. One can observe that for some cases, e.g. Figs. 4.4b and 4.5b, the stiffness from Eq. C-A-6-5 in AISC 360-10 for point (nodal) lateral brace with $C_b P_f$ taken as M_{max}/h_o , is greater than the torsional bracing stiffness requirement. In such cases it is recommended that no reduction in the torsional bracing stiffness should be taken accounting for benefits from lateral bracing at the tension flange.

4.4.2 Beams with Moment Gradient 2 loading

The results for Moment Gradient 2 loading are shown in Figs. 4.7 through 4.9. Table 4.5 compares the results from Figs. 4.7 and 4.8. From Column (e), it can be observed that the AISC Appendix 6 (AISC 2010) equations (including the Commentary refinements) provide a conservative estimate of the stiffness required to reach 96 % of the rigidly-braced strength for beams with point (nodal) lateral bracing. Furthermore, $2\beta_{iF.AISC}$ is only slightly smaller than the stiffness needed to develop 96 % of the minimum rigidly-braced strength for the 15 ft torsionally braced case in Fig. 4.8b. However, for the short unbraced length case in Fig. 4.8a (torsional bracing), the knuckle curve approaches the rigidly-braced strength very gradually with increases in the brace stiffness. In this case, a brace stiffness of 35.9 kip/in is required to develop 96 % of the rigidly-braced resistance, whereas the AISC estimated ideal bracing stiffness is only 3.9 kip/in. At $\beta = 2\beta_{iF.AISC}$, the beam strength is still slightly less than 90 % of the rigidly-braced strength for this test. This behavior is considered marginal, but acceptable. A substantial increase in the torsional bracing stiffness would be necessary to achieve 96 % of the rigidly-braced beam strength in this problem.



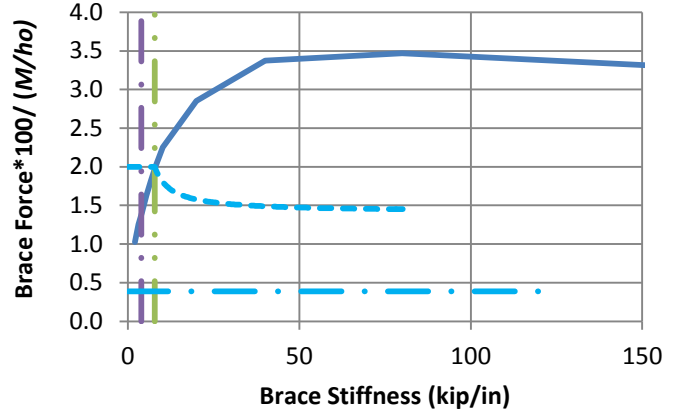
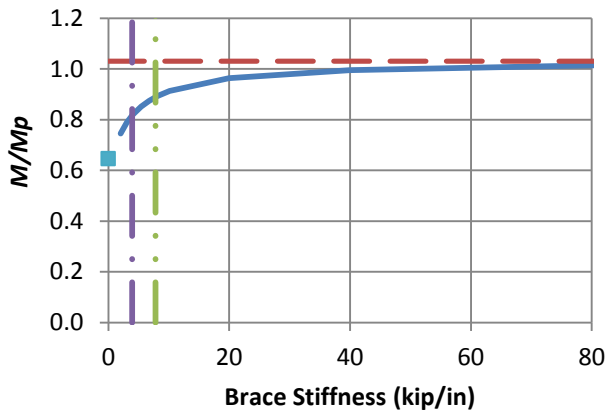
a) B_MG2pc_NB_n1_Lb5



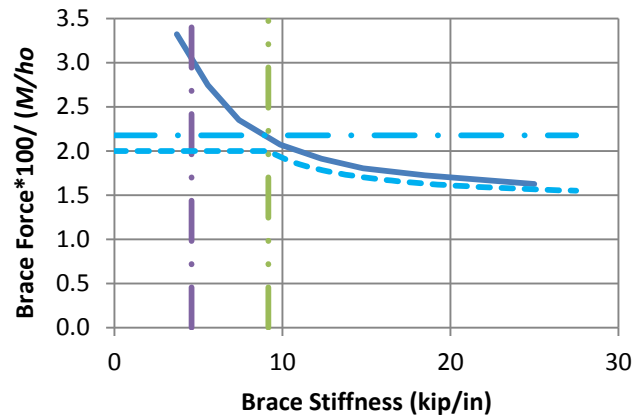
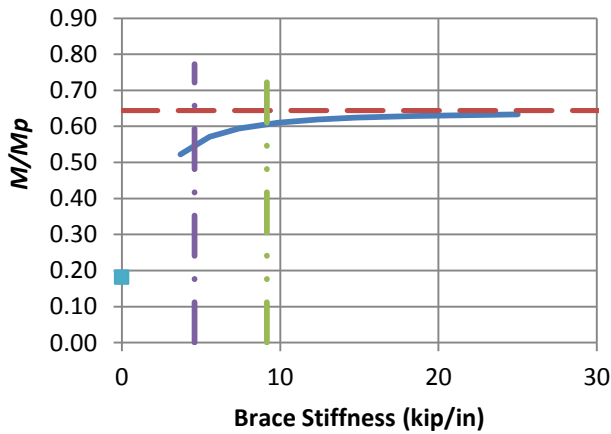
b) B_MG2pc_NB_n1_Lb15

- Test simulation results
- Rigidly-braced strength
- AISC ideal full bracing stiffness
- - - 2x AISC ideal full bracing stiffness (From Eq. C-A-6-5, AISC 360-10, with $C_b P_f$ taken equal to M_{max}/h_o)
- Test simulation strength at zero brace stiffness
- . Base AISC Required Strength Corresponding to $\beta = 2\beta_{iF,AISC}$ (From Eq. C-A-6-6b, AISC 360-10)
- - . Refined Estimate of Required Strength from AISC Commentary (Eq. C-A-6-6b multiplied by Eq. C-A-6-1, AISC 360-10)

Fig. 4.7. Knuckle curves and brace force vs. brace stiffness plots for point (nodal) lateral bracing cases with $n = 1$, Moment Gradient 2, centroidal loading.



a) B_MG2pc_TB_n1_Lb5

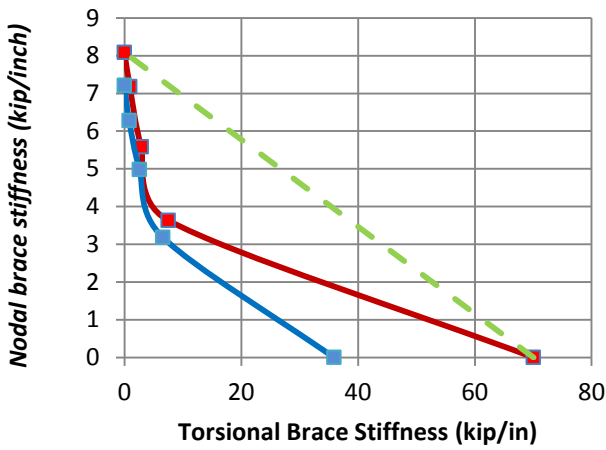


b) B_MG2pc_TB_n1_Lb15

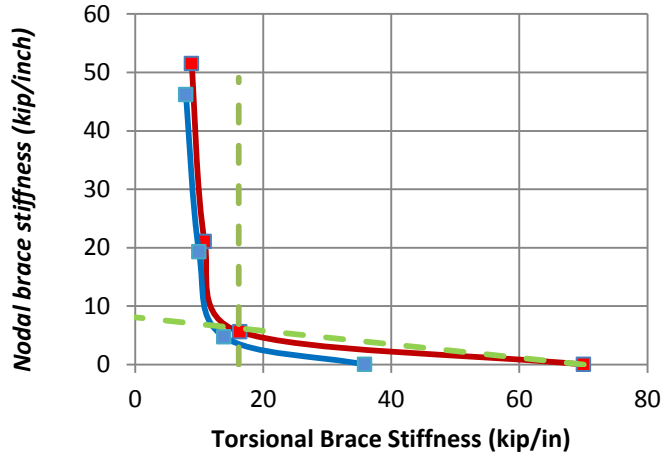
- Test simulation results
- - Rigidly-braced strength
- AISC ideal full bracing stiffness
- 2x AISC ideal full bracing stiffness equal to (β_{Tbr} / h_o^2) , where β_{Tbr} is given in Eq. 4-1
- Test simulation strength at zero brace stiffness
- · Base AISC Required Strength corresponding to $\beta = 2\beta_{IF,AISC}$ (From Eq. 4-2)
- · - · Recommended Refined Estimate of Required Strength of 2% with an ad-hoc modifier

$\frac{1}{\sqrt{2 - \frac{2\beta_{IF,AISC}}{\beta}}}$ to account for the variation in torsional brace forces at the member strength limit as a function of the torsional brace stiffness

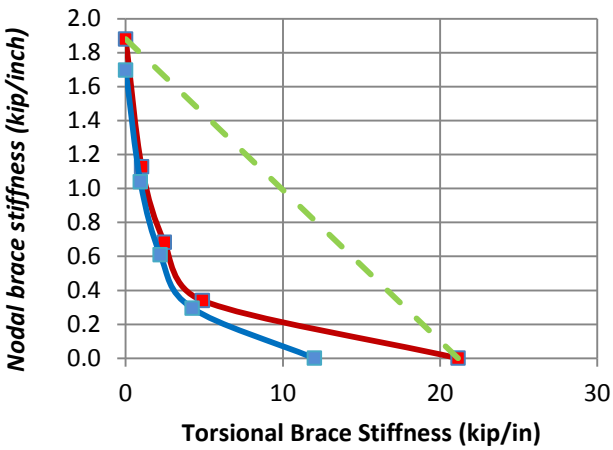
Fig. 4.8. Knuckle curves and brace force vs. brace stiffness plots for torsional bracing cases with $n = 1$, Moment Gradient 2, centroidal loading.



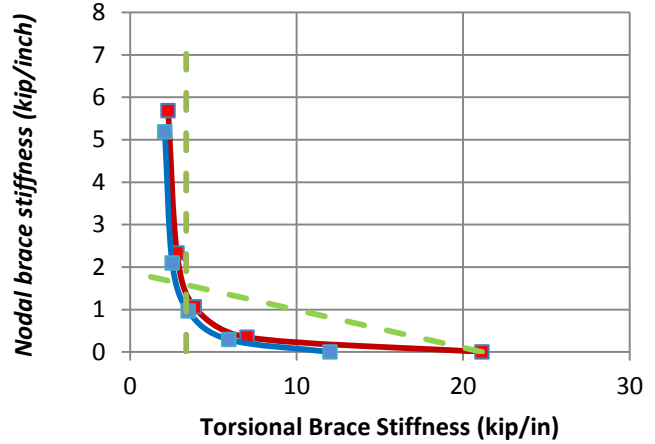
a) 5ft unbraced length (Positive bending)



b) 5ft unbraced length (Negative bending)



c) 15ft unbraced length (Positive bending)



d) 15ft unbraced length (Negative bending)

- Simulation-based stiffness interaction corresponding to 98 % of rigid bracing strength
- Simulation-based stiffness interaction corresponding to 96 % of rigid bracing strength
- - - Recommended design approximation

Fig. 4.9. Point (nodal) lateral and point torsional bracing stiffness interactions for, Moment Gradient 2, centroidal loading and $n = 1$.

Table 4.5. Comparison of simulation results in Figs. 4.7 and 4.8 with AISC predicted ideal full bracing stiffness.

Case (a)	Stiffness corresponding to 98% of simulation rigidly-braced strength (kip/in) (b)	Stiffness corresponding to 96% of simulation rigidly-braced strength (kip/in) (c)	Nominal AISC required full bracing stiffness (kip/in) (d)	Col. (c) / Col. (d) (e)
B_MG2pc_NB_n1_Lb5	8.1	7.2	16.2	0.45
B_MG2pc_NB_n1_Lb15	1.9	1.7	3.4	0.5
B_MG2pc_TB_n1_Lb5	70.1	35.9	7.8	4.6
B_MG2pc_TB_n1_Lb15	21.2	12.0	9.2	1.3

The brace force versus brace stiffness curves in Fig. 4.7 show good correlation between the AISC required point lateral brace strength estimates and the test simulation results even for values somewhat less than $2\beta_{iF.AISC}$. Figure 4.8 shows that the torsional bracing strength requirements are estimated well by the base 2 % bracing requirement recommended by Prado and White (2014) for the 15 ft unbraced length case when $\beta \geq 2\beta_{iF.AISC}$. Also, the AISC Appendix 6 (AISC 2010) base requirement of 2.2 % is an accurate predictor of the brace force requirement at $\beta = 2\beta_{iF.AISC}$ for this case. Furthermore, for the short unbraced length case in this figure, the base strength requirement of $0.02 M_r$ recommended by Prado and White (2014) works well at $\beta = 2\beta_{iF.AISC}$. However, in this case, if the torsional brace stiffness is larger than $2\beta_{iF.AISC}$, a torsional bracing strength of up to 3.5 % of the beam moment is required to develop the limit load of the test. Nevertheless, Fig. 4.10 shows the moment (applied load) versus brace force for the case from Fig. 4.8a where $\beta = 80$ kip/in, which maximizes the torsional brace force as shown in Fig. 4.8b. One can observe that at a brace force of $0.02M_r$, a strength very close to that of the

beam rigidly-braced strength is developed. This is considered to be acceptable behavior for stability bracing design for static loads.

It is important to note that the AISC Commentary prediction based on Eq. (4-2) results in a substantially under-estimated brace strength requirement of less than 0.5 % for all values of the brace stiffness in this problem. This is due to the implicit assumption, in Eq. 4-1, that the elastic stiffness of the beam is available to assist the torsional bracing in resisting the brace point movements. For the short unbraced length case in Fig. 4.8b, the beam is heavily plastified at its strength limit and is not able to provide this elastic resistance to the brace point movement.

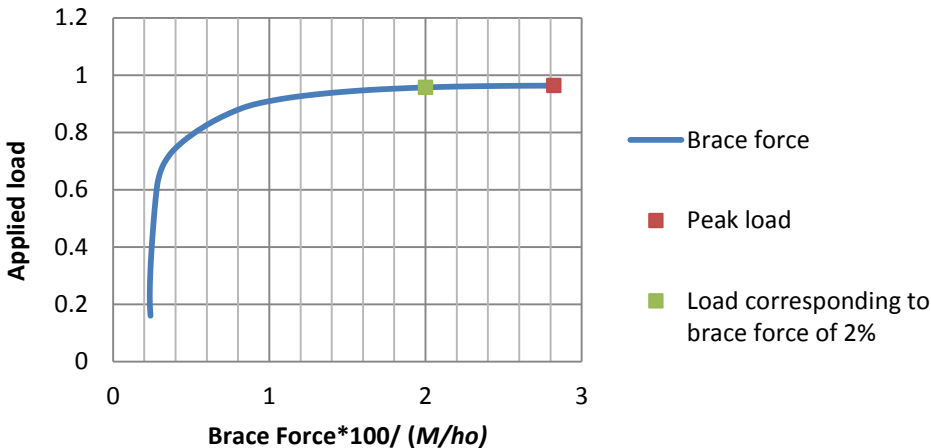


Fig. 4.10. Plot of brace force versus applied load for B_MG2pc_TB_n1_Lb5 with $\beta = 80$ kip/in.

Figure 4.9 shows the bracing stiffness interaction plot for combined point (nodal) lateral and torsional bracing cases. The knuckle curves and brace force versus brace stiffness plots corresponding to every point on the interaction plots are shown in Appendix A. In the plots in Fig. 4.9, when the member experiences positive bending, the linear interaction is conservative compared to the true interaction between the combined lateral and torsional bracing stiffness requirements.

However, when a member with combined lateral (nodal or shear panel) and torsional bracing is subjected to negative bending, where the laterally-braced top flange is in tension and the bottom flange is in compression, the interaction between the two bracing stiffness requirements is different. Based on the results in Fig. 4.9, it is observed that a vertical line at stiffness equal to that from Eq. C-A-6-5 of AISC 360-10 for point (nodal) lateral brace with $C_b P_f$ taken as M_{max}/h_o , illustrated by the green dashed vertical line in the negative moment based plots, provides an accurate to somewhat conservative minimum limit for the torsional bracing stiffness as the lateral bracing stiffness becomes relatively large. In addition, it is observed that, with the exception of this minimum limit, the torsional bracing stiffness requirement can be reduced by providing a relatively small lateral bracing stiffness, by the same linear interpolation function as shown for the positive moment based plots.

Based on the results from Figs. 4.4, 4.5 and 4.9 the following recommendations can be made for bracing stiffness requirements for beams with combined lateral and torsional bracing.

When the lateral bracing is on the flange in compression (i.e., positive bending), the provided lateral and torsional bracing stiffness's should satisfy the requirement in Eq. 4-3,

$$\frac{\beta_T}{\beta_{To}} + \frac{\beta_L}{\beta_{Lo}} \geq 1.0 \quad (4-3)$$

where:

β_L = Provided lateral bracing stiffness

β_T = Provided torsional bracing stiffness

β_{Lo} = Base required lateral bracing stiffness for ideal full bracing per the AISC 360-10 Appendix 6 (AISC 2010) rules, including the refinements specified in the Appendix 6 Commentary.

β_{To} = Base required torsional bracing stiffness for ideal full bracing per the AISC 360-10 Appendix 6 (AISC 2010) rules, including the refinements specified in the Appendix 6 Commentary.

When the lateral bracing is on the flange in tension (i.e., negative bending), the provided lateral and torsional bracing stiffness's should satisfy the above interaction Eq. 4-3. In addition, the required torsional brace stiffness should be greater than or equal to the smaller of β_{To} , or h_o^2 times the point (nodal) lateral bracing stiffness requirement as per AISC, obtained from Eq. C-A-6-5 in the Appendix 6 (AISC 2010) Commentary.

CHAPTER 5: BEAMS WITH TOP FLANGE LOADING

5.1 Overview

This chapter addresses the second major part of this research, beams with the intermediate transverse load applied at the top flange, thus causing an additional destabilizing effect. Section 5.2 gives details of the cases considered. Section 5.3 presents the test simulation results.

5.2 Detailed Study Design

The cases considered in this research, to study the influence of the height of an intermediate transverse load, are listed below. The corresponding cases shown in Section 4.2 for the Moment Gradient 2 loading involve transverse concentrated load applied at the centroidal axis of the members. The following cases are considered for beams with the transverse load applied at the top flange level of the mid-span cross-section, Moment Gradient 2 loading.

Positive moment loading, basic bracing types:

B_MG2pt_NB_n1_Lb5
B_MG2pt_NB_n1_Lb15
B_MG2pt_TB_n1_Lb5
B_MG2pt_TB_n1_Lb15

Positive moment loading, combined point (nodal) lateral and point torsional bracing:

B_MG2pt_CNTB_n1_Lb5_TLBSR4
B_MG2pt_CNTB_n1_Lb5_TLBSR1
B_MG2pt_CNTB_n1_Lb5_TLBSR0.25
B_MG2pt_CNTB_n1_Lb15_TLBSR4
B_MG2pt_CNTB_n1_Lb15_TLBSR1
B_MG2pt_CNTB_n1_Lb15_TLBSR0.25

Negative moment loading, combined point (nodal) lateral and point torsional bracing:

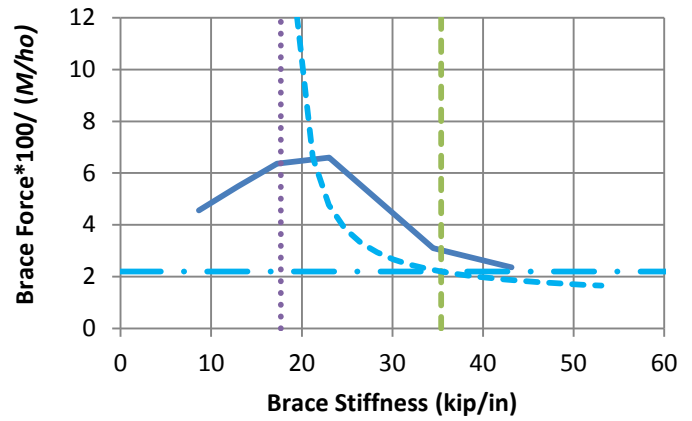
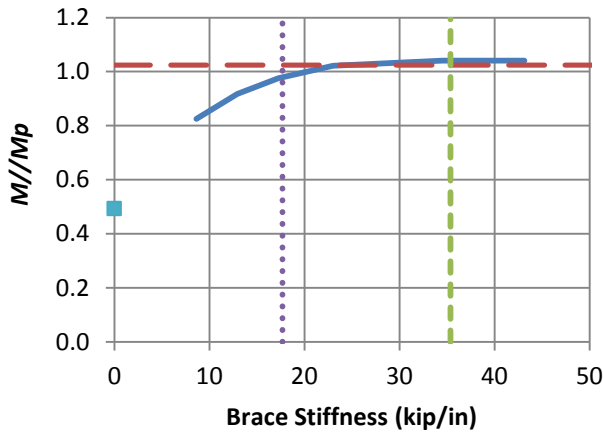
B_MG2nt_CNTB_n1_Lb5_TLBSR5.67
B_MG2nt_CNTB_n1_Lb5_TLBSR1
B_MG2nt_CNTB_n1_Lb5_TLBSR0.33
B_MG2nt_CNTB_n1_Lb5_TLBSR0.11
B_MG2nt_CNTB_n1_Lb15_TLBSR5.67
B_MGnt_CNTB_n1_Lb15_TLBSR1
B_MG2nt_CNTB_n1_Lb15_TLBSR0.33
B_MG2nt_CNTB_n1_Lb15_TLBSR0.11

5.3 Results

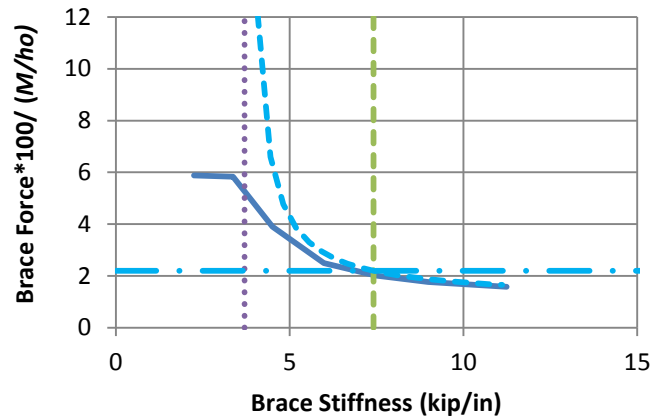
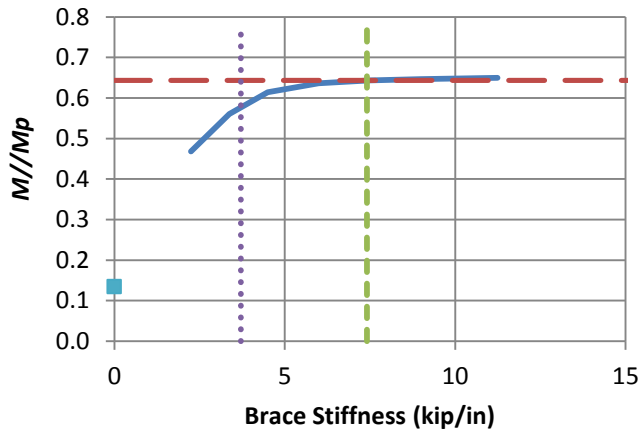
The results for beams with intermediate transverse load applied at centroid of the mid-span cross section are discussed in Section 4.4.2. The results for beams with intermediate transverse load applied at top flange level of the mid-span cross section are shown in Figs. 5.1 through 5.3.

The equations C-A-6-5 and C-A-6-6 in AISC 360-10 have a C_t factor to account for the impact of varying the transverse load height on the bracing stiffness and strength requirements. $C_t = 1$ for centroidal loading and $C_t = 2.2$ for top flange loading with $n = 1$. Similarly, Eq. 4-1 has a C_{iT} factor to account for the effects of the height of any transverse loads relative to the depth of the member cross-section. $C_{iT} = 1.2$ for top flange loading.

Table 5.1 compares the results in Figs. 5.1 and 5.2. Since the values in Col. (e) of Table 5.1 are approximately equal to the values in Col. (e) of Table 4.5, it can be concluded that the C_t and C_{iT} factors do a good job of estimating the impact of transverse load height on the bracing stiffness requirements.



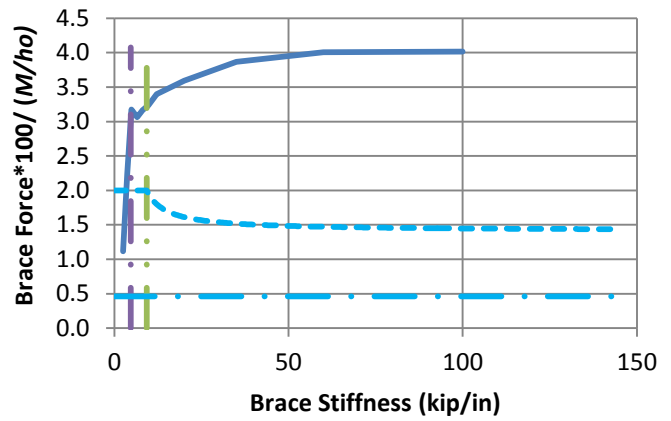
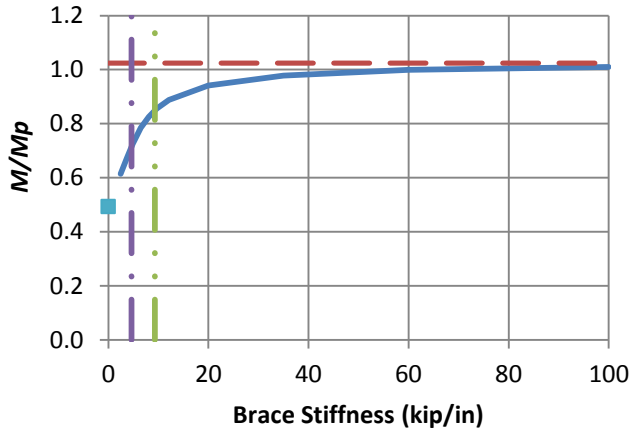
a) B_MG2pt_NB_n1_Lb5



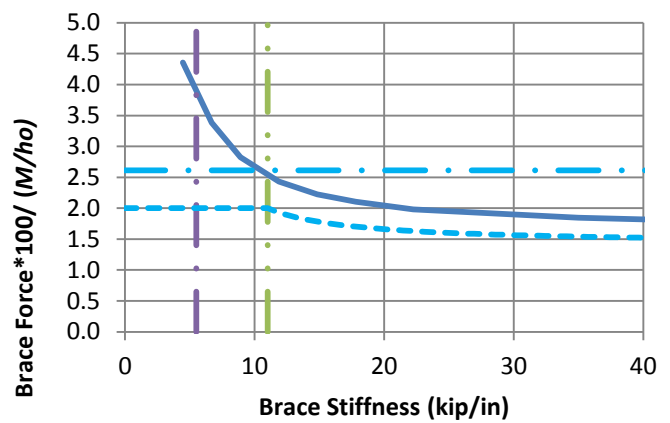
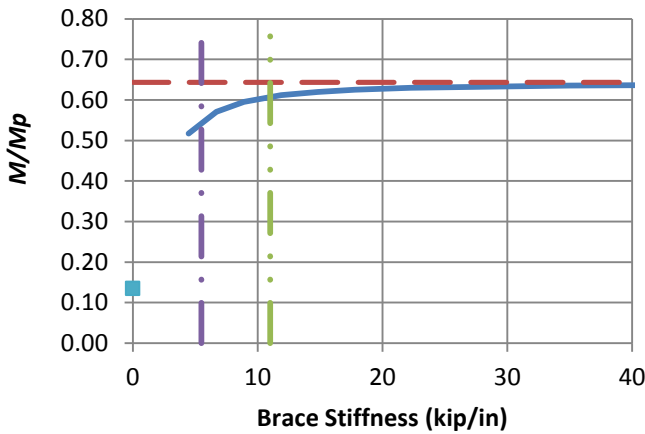
b) B_MG2pt_NB_n1_Lb15

- Test simulation results
- - Rigidly-braced strength
- ⋯ AISC ideal full bracing stiffness
- - - 2x AISC ideal full bracing stiffness (From Eq. C-A-6-5, AISC 360-10, with $C_b P_f$ taken equal to M_{max}/h_o)
- Test simulation strength at zero brace stiffness
- . Base AISC Required Strength Corresponding to $\beta = 2\beta_{iF,AISC}$ (From Eq. C-A-6-6b, AISC 360-10)
- - - . Refined Estimate of Required Strength from AISC Commentary (Eq. C-A-6-6b multiplied by Eq. C-A-6-1, AISC 360-10)

Fig. 5.1. Knuckle curves and brace force vs. brace stiffness plots for point (nodal) lateral bracing cases with $n = 1$, Moment Gradient 2, top flange loading.



a) B_MG2pt_TB_n1_Lb5



b) B_MG2pt_TB_n1_Lb15

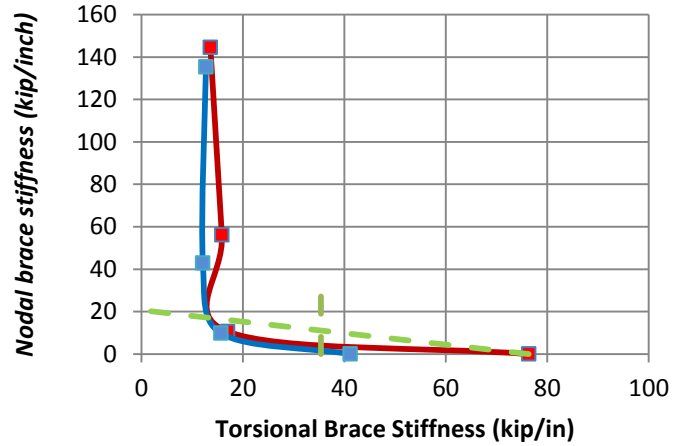
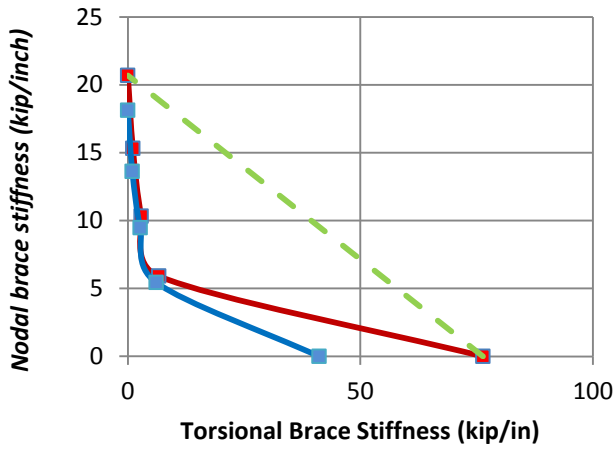
- Test simulation results
- Rigidly-braced strength
- AISC ideal full bracing stiffness
- 2x AISC ideal full bracing stiffness equal to (β_{Tbr} / h_o^2) , where β_{Tbr} is given in Eq.4-1
- Test simulation strength at zero brace stiffness
- Base AISC Required Strength corresponding to $\beta = 2\beta_{IF,AISC}$ (From Eq. 4-2)
- Recommended Refined Estimate of Required Strength of 2% with an ad-hoc modifier

$$\frac{1}{\sqrt{2 - \frac{2\beta_{IF,AISC}}{\beta}}}$$

to account for the variation in torsional brace forces at the member strength limit

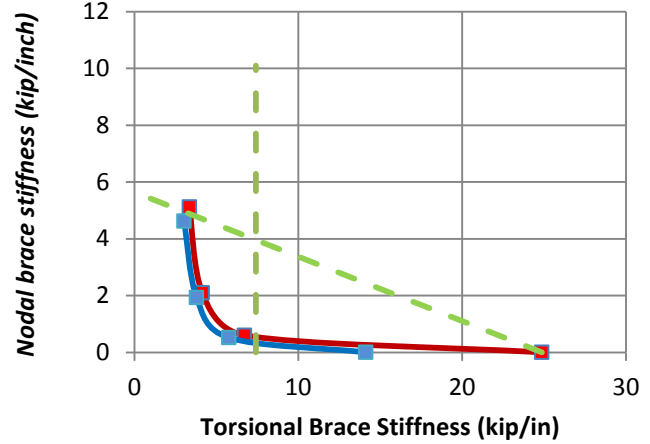
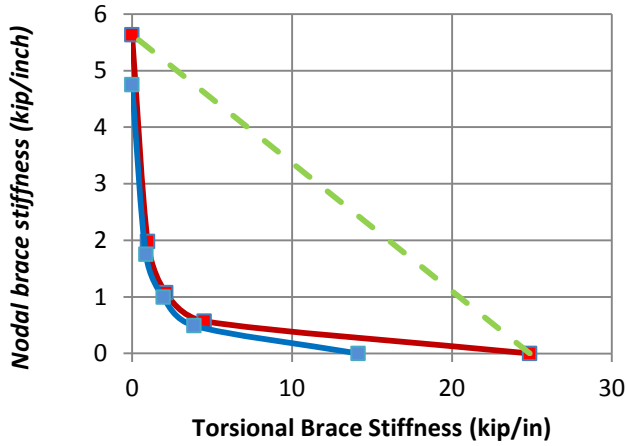
as a function of the torsional brace stiffness

Fig. 5.2. Knuckle curves and brace force vs. brace stiffness plots for torsional bracing cases with $n = 1$, Moment Gradient 2, top flange loading.



a) 5ft unbraced length (Positive bending)

b) 5ft unbraced length (Negative bending)



c) 15ft unbraced length (Positive bending)

d) 15ft unbraced length (Negative bending)

- Simulation-based stiffness interaction corresponding to 98 % of Rigidly-braced strength
- Simulation-based stiffness interaction corresponding to 96 % of Rigidly-braced strength
- - - Recommended design approximation

Fig. 5.3. Point (nodal) lateral and point torsional bracing stiffness interactions for, Moment Gradient 2, top flange loading and $n = 1$.

Table 5.1. Comparison of simulation results in Figs. 5.1 and 5.2 with AISC predicted ideal full bracing stiffness.

Case (a)	Stiffness corresponding to 98% of simulation rigidly-braced strength (kip/in) (b)	Stiffness corresponding to 96% of simulation rigidly-braced strength (kip/in) (c)	Nominal AISC required full bracing stiffness (kip/in) (d)	Col. (c) / Col. (d) (e)
B_MG2pt_NB_n1_Lb5	20.7	18.1	35.4	0.5
B_MG2pt_NB_n1_Lb15	5.6	4.8	7.4	0.65
B_MG2pt_TB_n1_Lb5	76.4	41.2	9.2	4.45
B_MG2pt_TB_n1_Lb15	24.9	14.1	11	1.3

From Figs. 4.7 and 5.1, one can observe that the C_t factor does not fully account for the impact of the load height on the bracing strength requirements. The increase in the required brace strength at a brace stiffness of $2\beta_{iF.AISC}$ in Fig. 5.1 versus Fig 4.7 is 2.73 (3.0/1.1) for the case with 5 ft unbraced length, and it is 2.5 (2/0.8) for the case with 15 ft unbraced length, instead of the C_t factor value of 2.2. However, it is important to note that both the AISC Specification (AISC 2010) equations as well as the test simulation models do not account for the benefits of tipping restraint from the applied loading. The AISC Specification (AISC 2010) as well as the test simulation models consider that the load is applied as a point load at the middle of the flange. However, in actual structures the load is applied to the beams through secondary members or the slab. This loading condition commonly provides a beneficial tipping restraint effect. Additional discussion of tipping restraint effects is provided by Yura (2001).

It can be observed from Fig. 5.2a that the base strength requirement of $0.02 M_r$, recommended by Prado and White (2014) is unconservative at $\beta = 2\beta_{iF,AISC}$. However, Fig. 5.4 shows the moment (applied load) versus brace force plot for B_MG2pt_TB_n1_Lb5 with $\beta = 2\beta_{iF,AISC}$. It can be observed that at a brace force of $0.02M_r$, strength very close to that of the beam rigidly-braced strength is developed. This is considered to be acceptable behavior for stability bracing design for static loads.

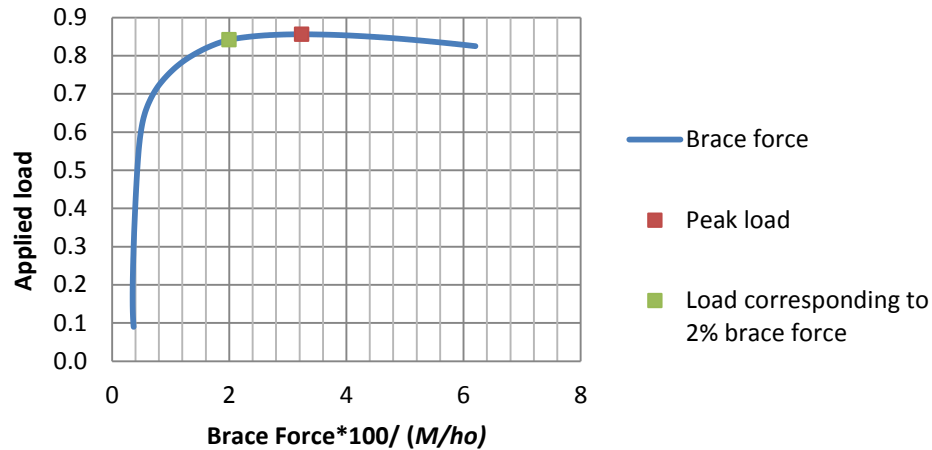


Fig. 5.4. Plot of brace force versus applied load for B_MG2pt_TB_n1_Lb5 with $\beta = 2\beta_{iF,AISC}$.

Figures 4.8 and 5.3 show the bracing stiffness interaction plots for combined bracing cases. The knuckle curves and brace force versus brace stiffness plots corresponding to every point on the interaction plots are shown in Appendix A. In the above plots, when the member experiences positive bending, the linear interaction is conservative compared to the true interaction between the combined lateral and torsional bracing stiffness requirements.

Based on the results shown in Figs. 4.9 and 5.3, it is observed that for the negative bending based plots, a vertical line at stiffness equal to that from Eq. C-A-6-5 of AISC 360-10 for point (nodal) lateral brace, with $C_b P_f$ taken as M_{max}/h_o , provides an accurate to somewhat conservative minimum limit for the required torsional bracing stiffness as the lateral bracing stiffness becomes relatively large in all cases. This is illustrated by the green dashed vertical line in the negative

moment based plots. In addition, it is observed that, with the exception of this minimum limit, the torsional bracing stiffness requirement can be reduced by providing a relatively small lateral bracing stiffness, by the same linear interpolation function as shown for the positive moment based plots. Therefore, the recommendations for consideration of the interaction between the lateral and torsional brace stiffness's explained at the end of Section 4.4.2 can also be applied to cases where the transverse loads are applied at the "top" flange, causing additional destabilizing effects.

CHAPTER 6: BEAM-COLUMNS SUBJECTED TO AXIAL LOAD AND UNIFORM BENDING MOMENT

6.1 Overview

This chapter addresses the third major part of this research, beam-columns subjected to axial load and uniform bending moment. Section 6.2 gives details of the cases considered. Section 6.3 presents the test simulation results.

6.2 Detailed Study Design

The cases considered in this research to study the bracing requirements for beam-columns subjected to axial load and uniform bending moment are listed below:

Base bracing types, with axial load and positive moment loading such that only one flange is in net compression:

BC_UMp_NB_n1_Lb5_FFR-0.67
BC_UMp_NB_n1_Lb5_FFR-0.33
BC_UMp_NB_n1_Lb5_FFR0
BC_UMp_NB_n1_Lb10_FFR-0.67
BC_UMp_NB_n1_Lb10_FFR-0.33
BC_UMp_NB_n1_Lb10_FFR0
BC_UMp_NB_n1_Lb15_FFR-0.67
BC_UMp_NB_n1_Lb15_FFR-0.33
BC_UMp_NB_n1_Lb15_FFR0
BC_UMp_RB_n2_Lb5_FFR-0.67
BC_UMp_RB_n2_Lb5_FFR-0.33

BC_UMp_RB_n2_Lb5_FFR0
BC_UMp_RB_n2_Lb10_FFR-0.67
BC_UMp_RB_n2_Lb10_FFR-0.33
BC_UMp_RB_n2_Lb10_FFR0
BC_UMp_RB_n2_Lb15_FFR-0.67
BC_UMp_RB_n2_Lb15_FFR-0.33
BC_UMp_RB_n2_Lb15_FFR0

Base bracing types, with axial load and positive moment loading such that both flanges are in net compression:

BC_UMp_NB_n1_Lb5_FFR0.5
BC_UMp_NB_n1_Lb5_FFR1
BC_UMp_NB_n1_Lb10_FFR0.5
BC_UMp_NB_n1_Lb10_FFR1
BC_UMp_NB_n1_Lb15_FFR0.5
BC_UMp_NB_n1_Lb15_FFR1
BC_UMp_RB_n2_Lb5_FFR0.5
BC_UMp_RB_n2_Lb5_FFR1
BC_UMp_RB_n2_Lb10_FFR0.5
BC_UMp_RB_n2_Lb10_FFR1
BC_UMp_RB_n2_Lb15_FFR0.5
BC_UMp_RB_n2_Lb15_FFR1

Combined lateral and torsional bracing, with axial load and positive moment loading such that only one flange is in net compression:

BC_UMp_CNTB_n1_Lb5_FFR-0.67
BC_UMp_CNTB_n1_Lb5_FFR-0.33
BC_UMp_CNTB_n1_Lb5_FFR0
BC_UMp_CNTB_n1_Lb15_FFR-0.67
BC_UMp_CNTB_n1_Lb15_FFR-0.33
BC_UMp_CNTB_n1_Lb15_FFR0
BC_UMp_CRTB_n2_Lb5_FFR-0.67
BC_UMp_CRTB_n2_Lb5_FFR-0.33
BC_UMp_CRTB_n2_Lb5_FFR0
BC_UMp_CRTB_n2_Lb15_FFR-0.67
BC_UMp_CRTB_n2_Lb15_FFR-0.33
BC_UMp_CRTB_n2_Lb15_FFR0

Combined lateral and torsional bracing, with axial load and positive moment loading such that both flanges are in net compression:

BC_UMp_CNTB_n1_Lb5_FFR0.5
BC_UMp_CNTB_n1_Lb5_FFR1
BC_UMp_CNTB_n1_Lb15_FFR0.5
BC_UMp_CNTB_n1_Lb15_FFR1
BC_UMp_CRTB_n2_Lb5_FFR0.5
BC_UMp_CRTB_n2_Lb5_FFR1
BC_UMp_CRTB_n2_Lb15_FFR0.5
BC_UMp_CRTB_n2_Lb15_FFR1

Combined lateral and torsional bracing, with axial load and negative moment loading such that only one flange is in net compression:

BC_UMn_CNTB_n1_Lb5_FFR-0.67
BC_UMn_CNTB_n1_Lb5_FFR-0.33
BC_UMn_CNTB_n1_Lb5_FFR0
BC_UMn_CNTB_n1_Lb15_FFR-0.67
BC_UMn_CNTB_n1_Lb15_FFR-0.33
BC_UMn_CNTB_n1_Lb15_FFR0
BC_UMn_CRTB_n2_Lb5_FFR-0.67
BC_UMn_CRTB_n2_Lb5_FFR-0.33
BC_UMn_CRTB_n2_Lb5_FFR0
BC_UMn_CRTB_n2_Lb15_FFR-0.67
BC_UMn_CRTB_n2_Lb15_FFR-0.33
BC_UMn_CRTB_n2_Lb15_FFR0

Combined lateral and torsional bracing, with axial load and negative moment loading such that both flanges are in net compression:

BC_UMn_CNTB_n1_Lb5_FFR0.5
BC_UMn_CNTB_n1_Lb5_FFR1
BC_UMn_CNTB_n1_Lb15_FFR0.5
BC_UMn_CNTB_n1_Lb15_FFR1
BC_UMn_CRTB_n2_Lb5_FFR0.5
BC_UMn_CRTB_n2_Lb5_FFR1
BC_UMn_CRTB_n2_Lb15_FFR0.5
BC_UMn_CRTB_n2_Lb15_FFR1

6.3 Results

Results for the various cases of beam-columns with axial load and uniform bending are discussed in the following subsections.

6.3.1 Beam-Columns with Lateral Bracing Only, Located on the Flange Subjected to Flexural Compression

Per Appendix 6 Section 6.4 of AISC 360-10, the bracing requirements for beam-columns should be obtained by superposition of the bracing requirements for compression and those for flexure. The corresponding refined equations can be found in Sections 6.2 and 6.3 of the Commentary to AISC 360-10. Section 6.4 requires the column bracing to be designed for axial load P and the beam bracing to be designed for M/h_o . Therefore, the bracing requirements for beam-columns per AISC 360-10 are:

$$\text{Stiffness} = 2 \left[\frac{N_i P}{L_b} + \frac{N_i C_i C_d \left(\frac{M}{h_o} \right)}{L_b} \right] \quad (6-1)$$

$$\text{Strength} = 1\% \text{ of } \left[P + C_i C_d \left(\frac{M}{h_o} \right) \right] \text{ for Point (nodal) lateral brace} \quad (6-2a)$$

$$= 0.4\% \text{ of } \left[P + C_i C_d \left(\frac{M}{h_o} \right) \right] \text{ for Shear panel (relative) lateral brace} \quad (6-2b)$$

where:

$N_i = 1$ for shear panel (relative) lateral bracing

= $(4-2/n)$ for Point (nodal) lateral bracing

$C_i = 1$ for centroidal loading

= $1+(1.2/n)$ for top-flange loading

n = number of intermediate braces

L_b = unbraced length

C_d = double curvature factor, which accounts for the potential larger demands on the lateral bracing in unbraced lengths containing inflection points

= $1+(M_S/M_L)^2$ when an inflection point occurs within one of the unbraced lengths adjacent to the brace being considered

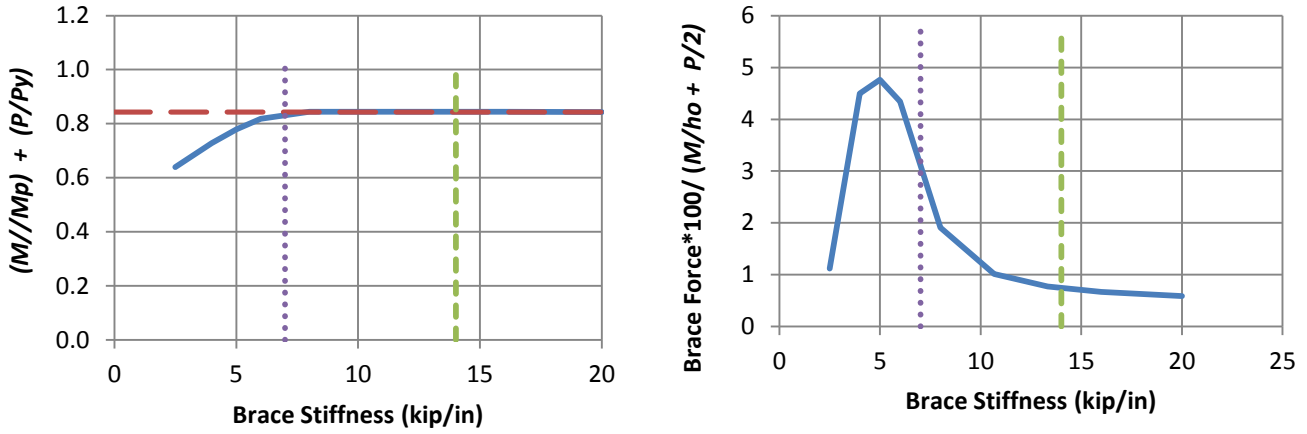
= 1.0 when neither of the unbraced lengths adjacent to the brace contains an inflection point, or when an inflection point exists within one of these lengths, but is closer to the adjacent brace location

M_S = smallest moment within the two unbraced lengths adjacent to the brace under consideration

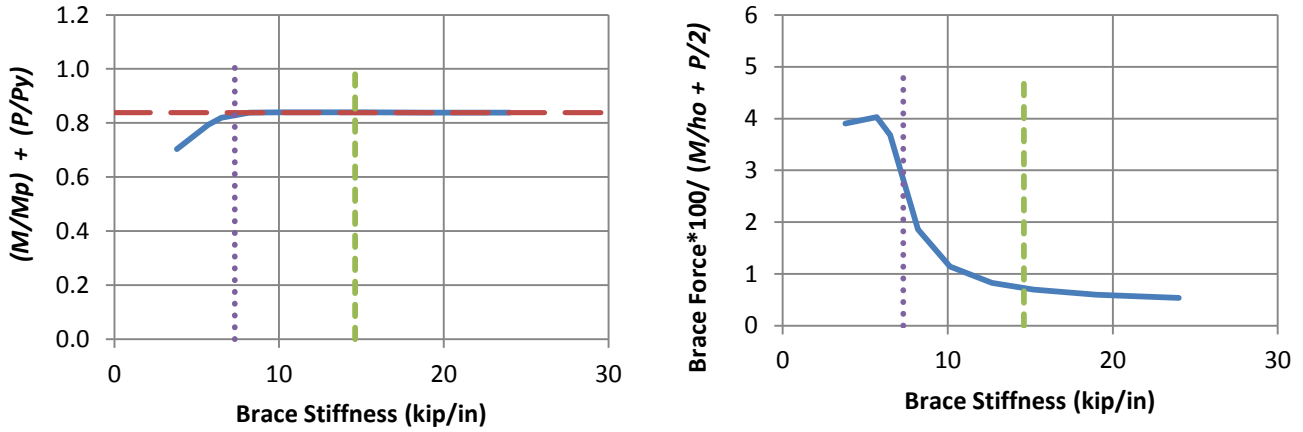
M_L = largest moment within the two unbraced lengths adjacent to the brace under consideration

The definitions provided for C_d in the AISC 360-10 Commentary are ambiguous. The above definitions of C_d are from White et al. (2011), and are based on a detailed evaluation of the original developments of the C_d equation by Yura (2001). However, it is important to recognize that it is intended that both flanges must be braced at a brace point associated with $C_d > 1$. Most often, this is accomplished by some combination of lateral and torsional bracing. Rarely would an independent lateral bracing system be placed on both flanges. In the current work, reversed curvature bending is not considered for the case of lateral bracing only, with the bracing located on just one flange.

Per Section 6.4 of the AISC Commentary, the above approach for obtaining the bracing requirements for beam-columns will tend to be conservative. Figures 6.1 through 6.12 show the results from test simulation for the selected beam-column cases of this type. The ordinate of the knuckle curve graphs is taken as $M/M_p + P/P_y$ in these figures. This is a reasonable normalized ordinate allowing the engineer to ascertain the effect of increasing the bracing stiffness values on the beam-column strength. The ordinate of the required brace force versus brace stiffness curves is normalized either by $M/h_o + P/2$ or by $M/h_o + 2.5P$. The rationale for these ordinate values is explained in detail below.



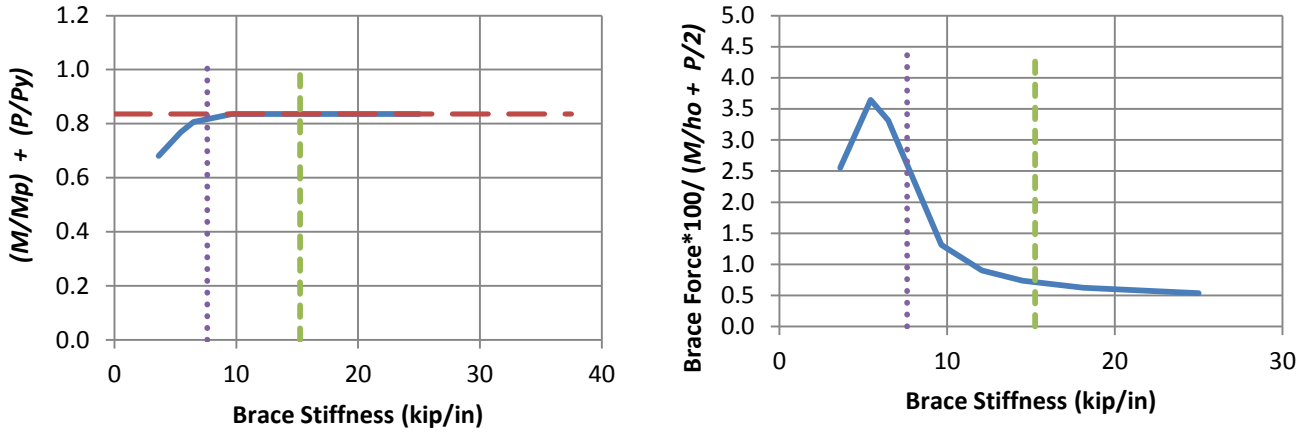
a) BC_UMp_NB_n1_Lb5_FFR-0.67



b) BC_UMp_NB_n1_Lb5_FFR-0.33

- Test simulation results
- - Rigidly-braced strength
- ⋯ 0.5 times bracing stiffness from Eq. 6-3
- - Bracing stiffness from Eq. 6-3

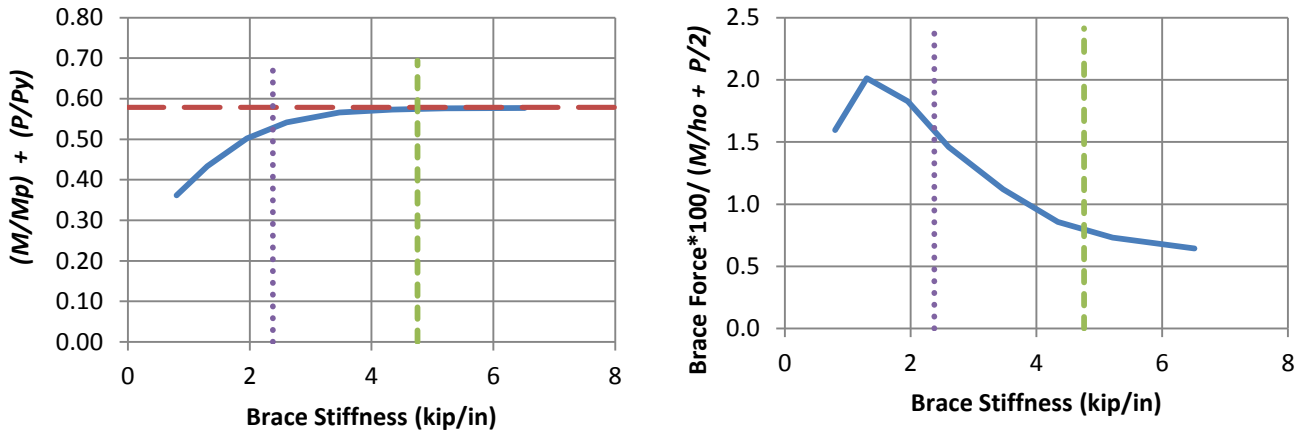
Fig. 6.1. Knuckle curves and brace force vs. brace stiffness plots for point (nodal) lateral bracing cases with $n = 1$ and constant axial load and uniform bending with effective flange force ratio $(P_{ft}/P_{fc}) \leq 0$, $L_b = 5\text{ft}$.



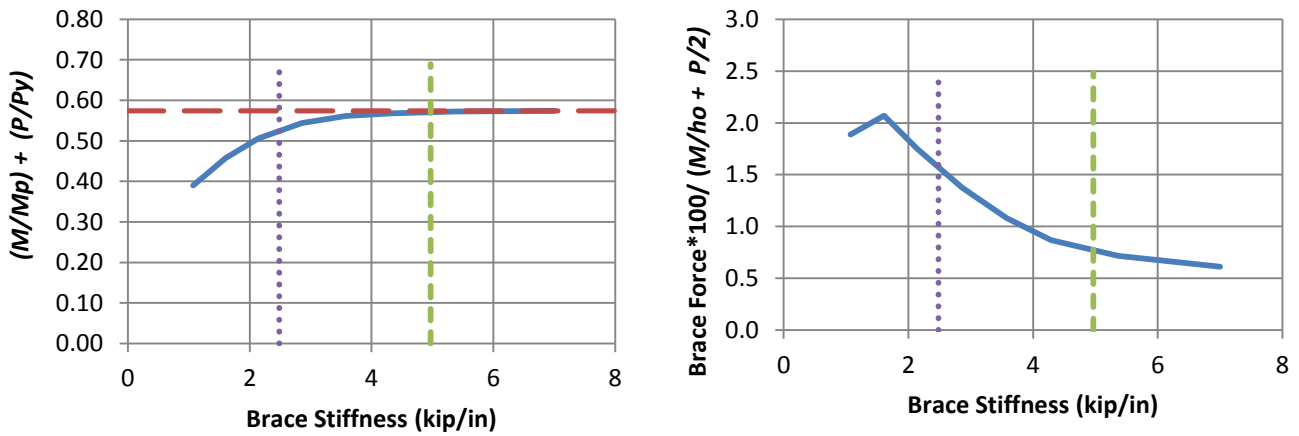
c) BC_UMp_NB_n1_Lb5_FFR0

- Test simulation results
- - Rigidly-braced strength
- ⋯ 0.5 times bracing stiffness from Eq. 6-3
- - Bracing stiffness from Eq. 6-3

Fig. 6.1. (continued) Knuckle curves and brace force vs. brace stiffness plots for point (nodal) lateral bracing cases with $n = 1$ and constant axial load and uniform bending with effective flange force ratio $(P_{f\ell} / P_{fc}) \leq 0$, $L_b = 5\text{ft}$.



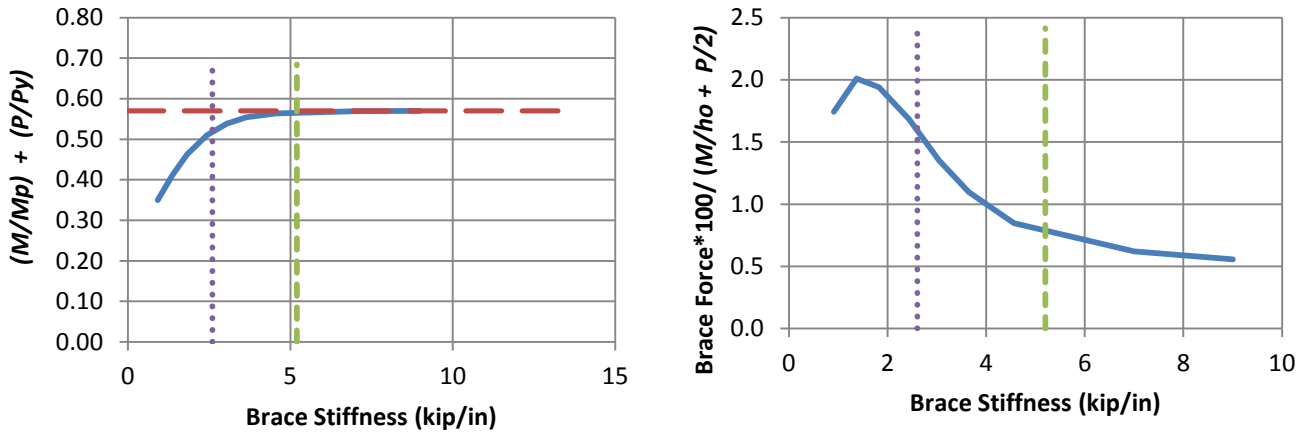
a) BC_UMp_NB_n1_Lb10_FFR-0.67



b) BC_UMp_NB_n1_Lb10_FFR-0.33

- Test simulation results
- - Rigidly-braced strength
- ⋯ 0.5 times bracing stiffness from Eq. 6-3
- - Bracing stiffness from Eq. 6-3

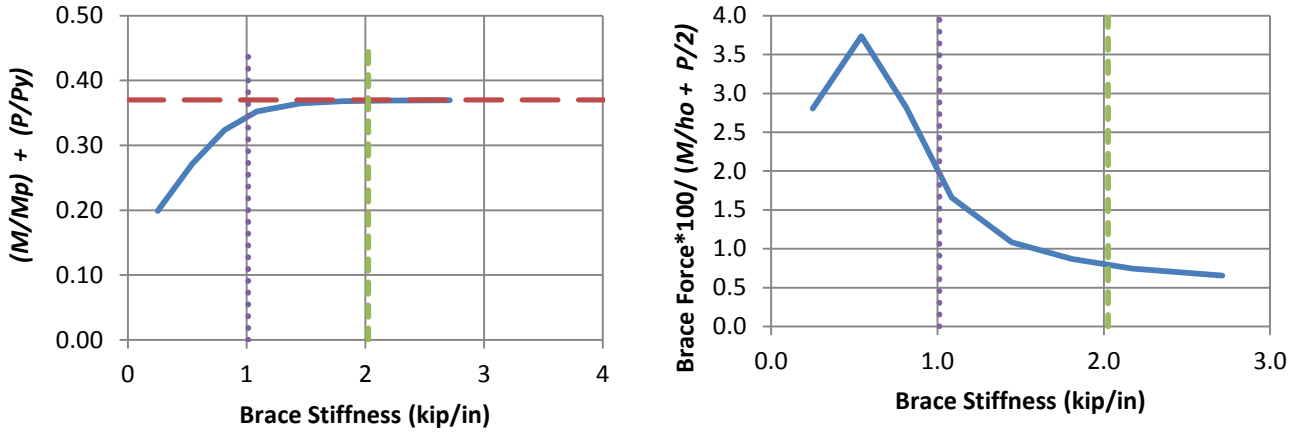
Fig. 6.2. Knuckle curves and brace force vs. brace stiffness plots for point (nodal) lateral bracing cases with $n = 1$ and constant axial load and uniform bending with effective flange force ratio $(P_{ft}/P_{fc}) \leq 0$, $L_b = 10\text{ft}$.



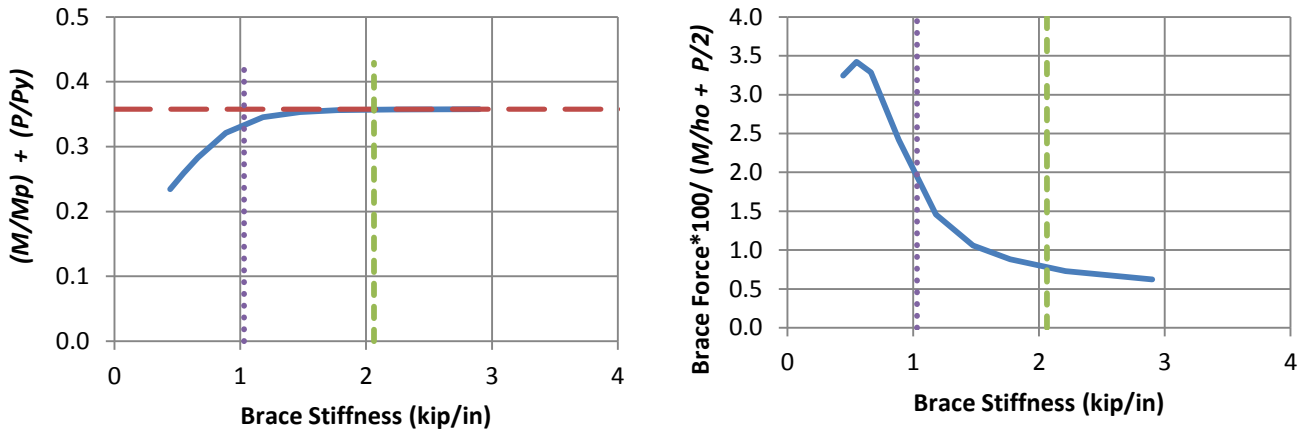
c) BC_UMp_NB_n1_Lb10_FFR0

- Test simulation results
- - Rigidly-braced strength
- ⋯ 0.5 times bracing stiffness from Eq. 6-3
- - Bracing stiffness from Eq. 6-3

Fig. 6.2. (continued) Knuckle curves and brace force vs. brace stiffness plots for point (nodal) lateral bracing cases with $n = 1$ and constant axial load and uniform bending with effective flange force ratio $(P_{ft}/P_{fc}) \leq 0$, $L_b = 10\text{ft}$.



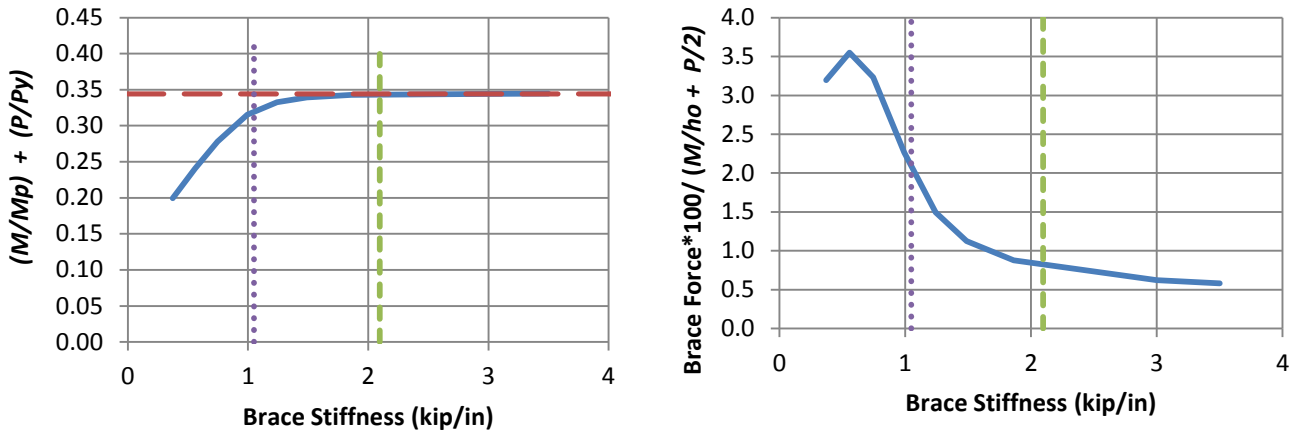
a) BC_UMp_NB_n1_Lb15_FFR-0.67



b) BC_UMp_NB_n1_Lb15_FFR-0.33

- Test simulation results
- - Rigidly-braced strength
- ⋯ 0.5 times bracing stiffness from Eq. 6-3
- - Bracing stiffness from Eq. 6-3

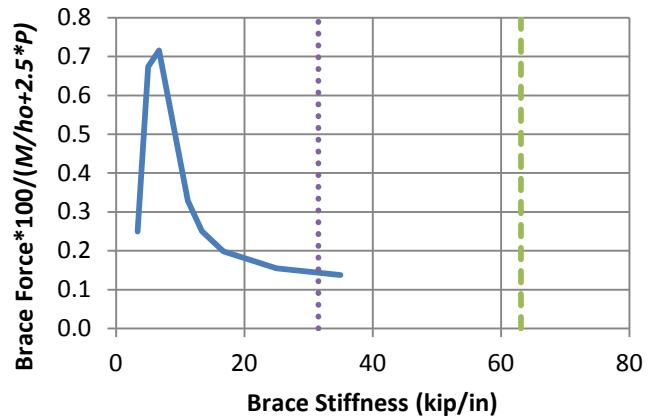
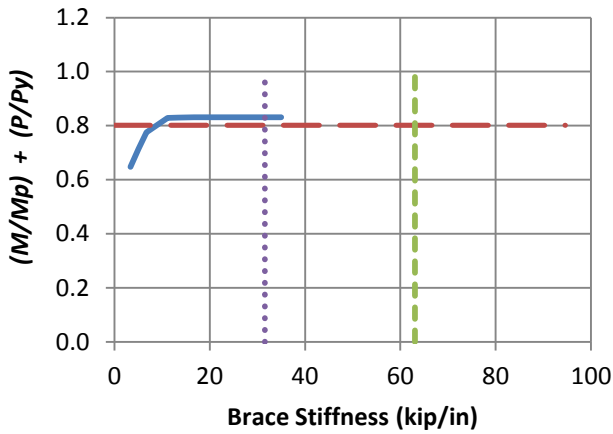
Fig. 6.3. Knuckle curves and brace force vs. brace stiffness plots for point (nodal) lateral bracing cases with $n = 1$ and constant axial load and uniform bending with effective flange force ratio $(P_{fc}/P_y) \leq 0$, $L_b = 15$ ft.



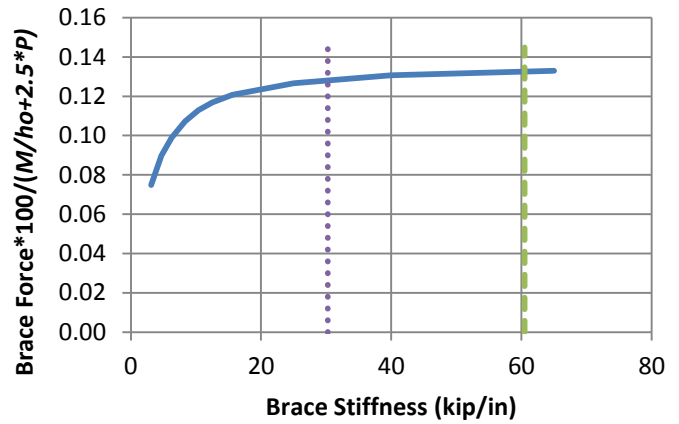
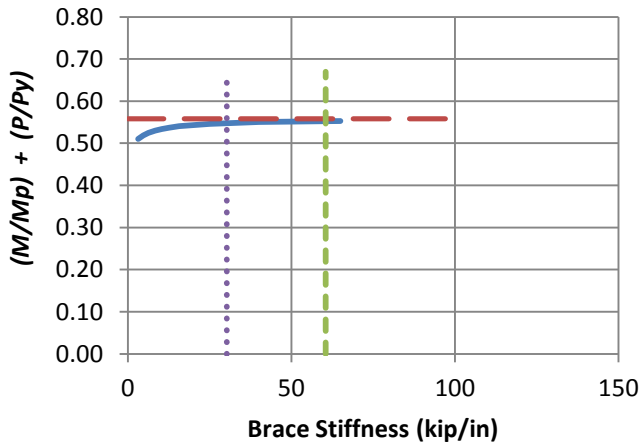
c) BC_UMp_NB_n1_Lb15_FFR0

- Test simulation results
- - Rigidly-braced strength
- ⋯ 0.5 times bracing stiffness from Eq. 6-3
- - Bracing stiffness from Eq. 6-3

Fig. 6.3. (continued) Knuckle curves and brace force vs. brace stiffness plots for point (nodal) lateral bracing cases with $n = 1$ and constant axial load and uniform bending with effective flange force ratio $(P_{ft}/P_{fc}) \leq 0$, $L_b = 15$ ft.



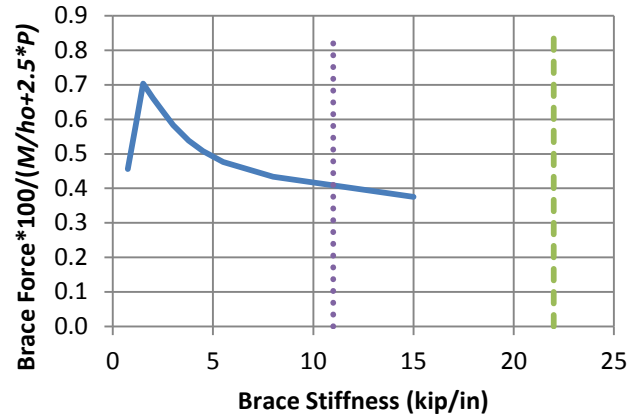
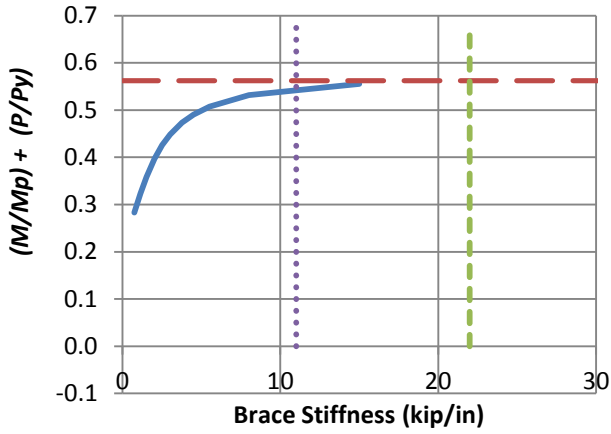
a) BC_UMp_NB_n1_Lb5_FFR0.5



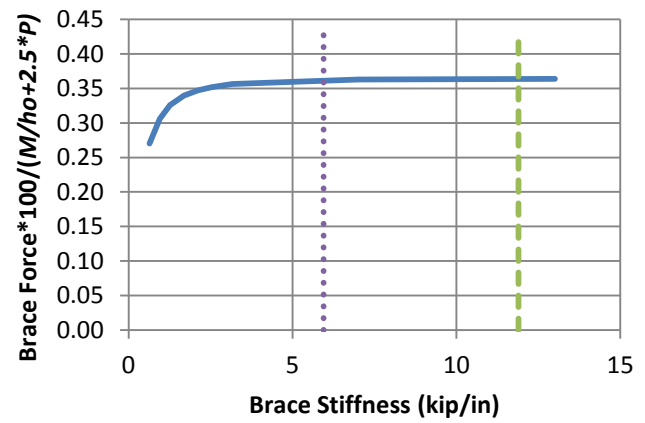
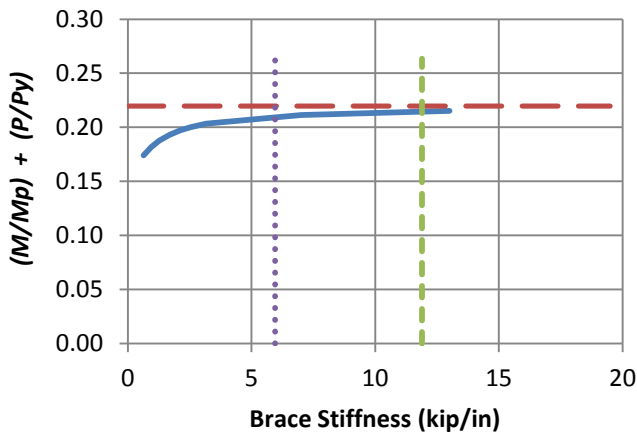
b) BC_UMp_NB_n1_Lb5_FFR1

- Test simulation results
- - Rigidly-braced strength
- ⋯ 0.5 times bracing stiffness from Eq. 6-5
- - Bracing stiffness from Eq. 6-5

Fig. 6.4. Knuckle curves and brace force vs. brace stiffness plots for point (nodal) lateral bracing cases with $n = 1$ and constant axial load and uniform bending with effective flange force ratio (P_{ft}/P_{fc}) > 0 , $L_b = 5\text{ft}$.



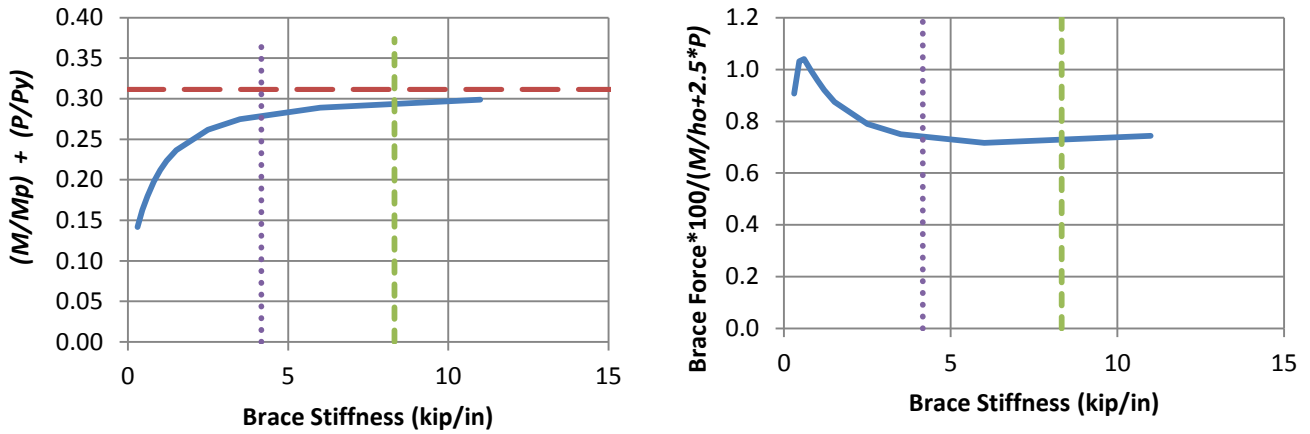
a) BC_UMp_NB_n1_Lb10_FFR0.5



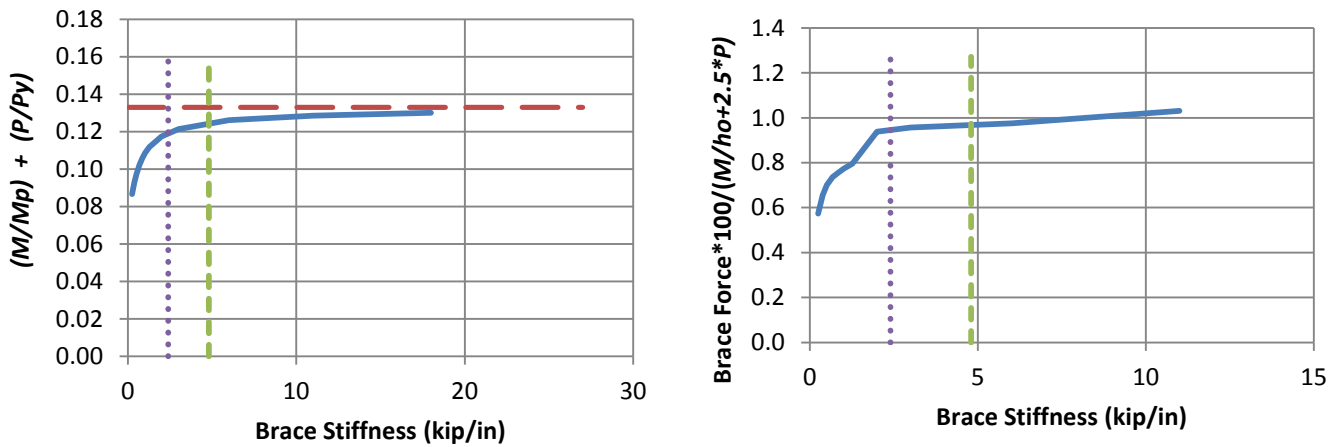
b) BC_UMp_NB_n1_Lb10_FFR1

- Test simulation results
- - Rigidly-braced strength
- ⋯ 0.5 times bracing stiffness from Eq. 6-5
- - Bracing stiffness from Eq. 6-5

Fig. 6.5. Knuckle curves and brace force vs. brace stiffness plots for point (nodal) lateral bracing cases with $n = 1$ and constant axial load and uniform bending with effective flange force ratio (P_{ft}/P_{fc}) > 0 , $L_b = 10$ ft.



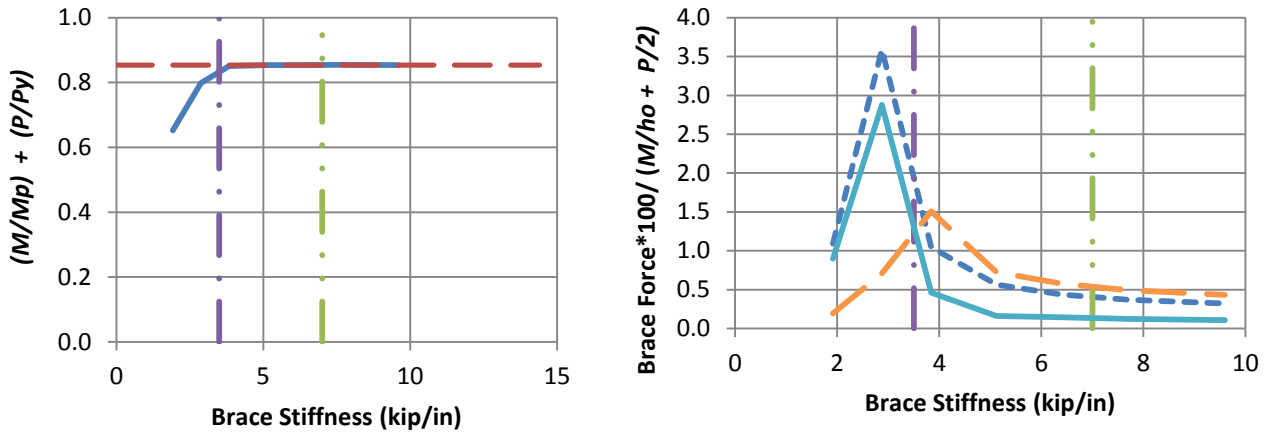
a) BC_UMp_NB_n1_Lb15_FFR0.5



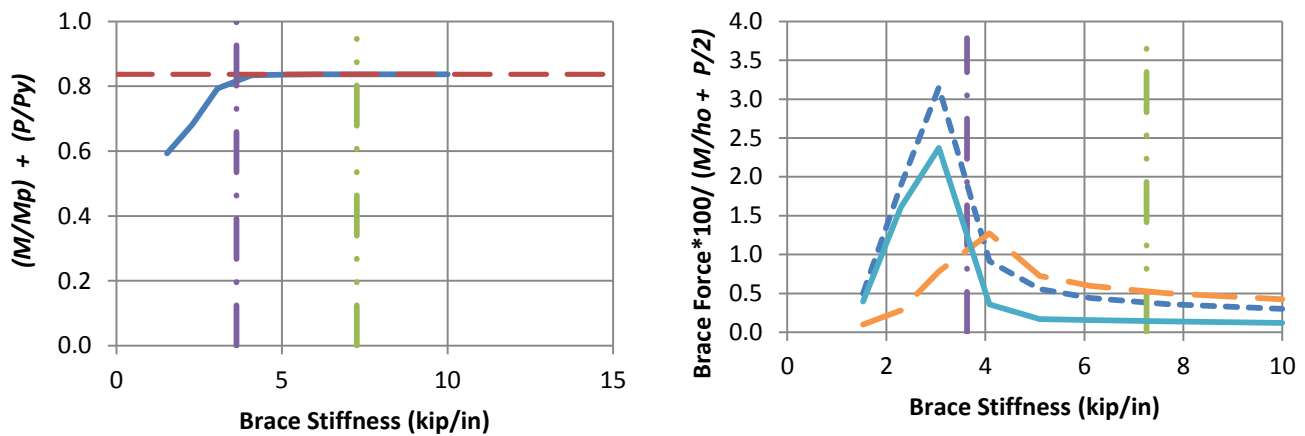
b) BC_UMp_NB_n1_Lb15_FFR1

- Test simulation results
- - Rigidly-braced strength
- ⋯ 0.5 times bracing stiffness from Eq. 6-5
- - Bracing stiffness from Eq. 6-5

Fig. 6.6. Knuckle curves and brace force vs. brace stiffness plots for point (nodal) lateral bracing cases with $n = 1$ and constant axial load and uniform bending with effective flange force ratio (P_{ft}/P_{fc}) > 0 , $L_b = 15$ ft.



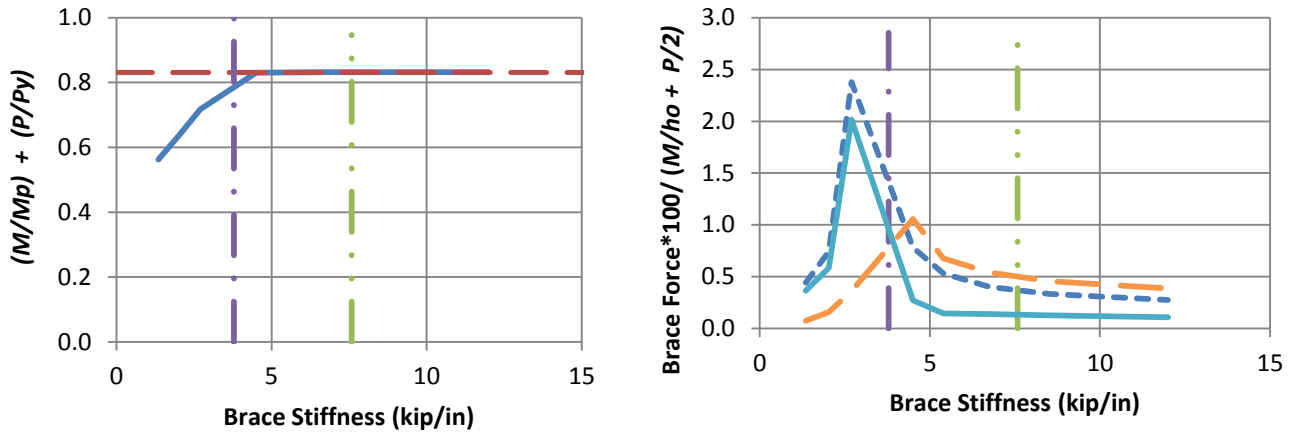
a) BC_UMp_RB_n2_Lb5_FFR-0.67



b) BC_UMp_RB_n2_Lb5_FFR-0.33

- Test simulation results
- - Rigidly-braced strength
- 0.5 times bracing stiffness from Eq. 6-3
- · - Left end panel shear force
- Right end panel shear force
- Bracing stiffness from Eq. 6-3
- · - Middle panel shear force

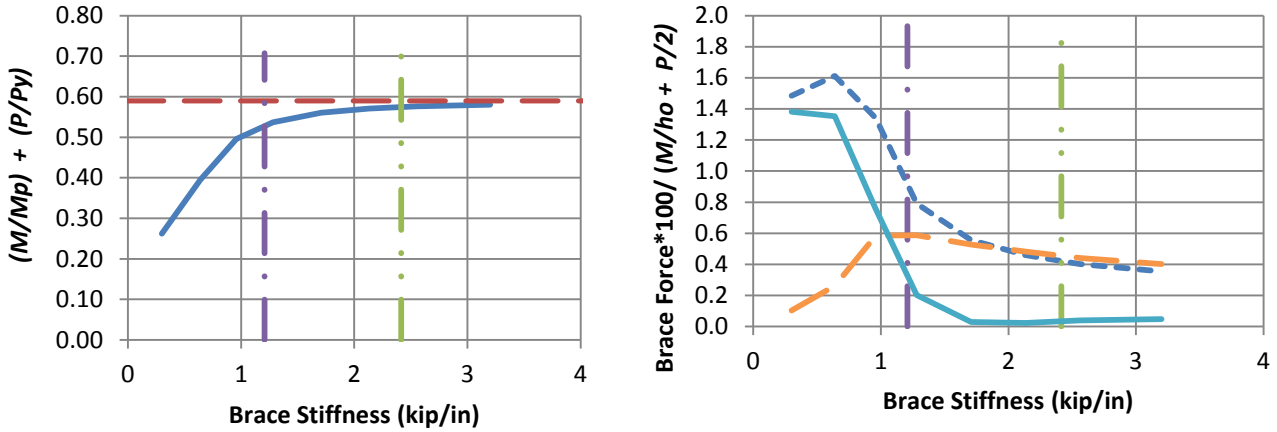
Fig. 6.7. Knuckle curves and brace force vs. brace stiffness plots for shear panel (relative) lateral bracing cases with $n = 2$ and constant axial load and uniform bending with effective flange force ratio $(P_{ft}/P_{fc}) \leq 0$, $L_b = 5$ ft.



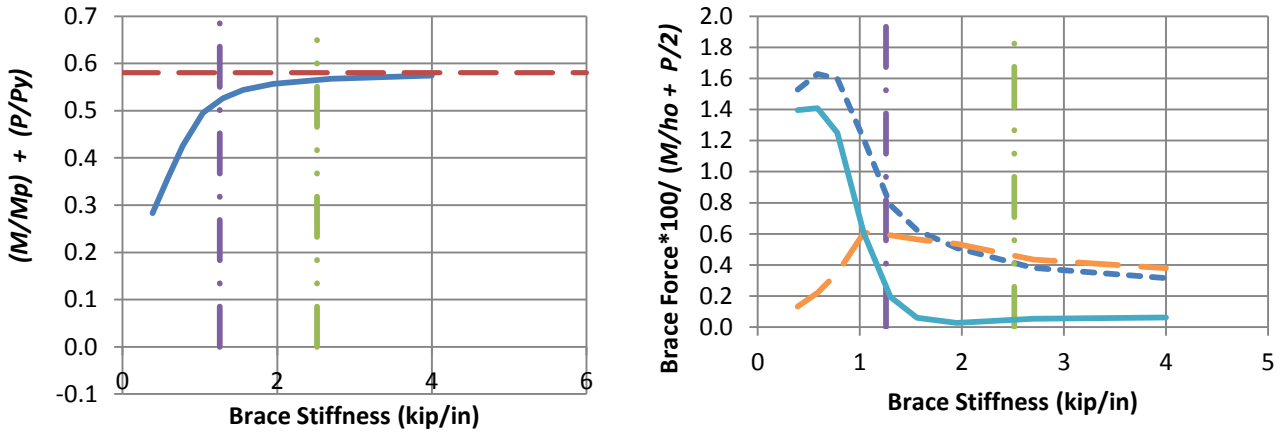
c) BC_UMp_RB_n2_Lb5_FFR0

- Test simulation results
- - Rigidly-braced strength
- 0.5 times bracing stiffness from Eq. 6-3
- Bracing stiffness from Eq. 6-3
- - Left end panel shear force
- Right end panel shear force
- - Middle panel shear force

Fig. 6.7. (continued) Knuckle curves and brace force vs. brace stiffness plots for shear panel (relative) lateral bracing cases with $n = 2$ and constant axial load and uniform bending with effective flange force ratio $(P_{ft}/P_{fc}) \leq 0$, $L_b = 5$ ft.



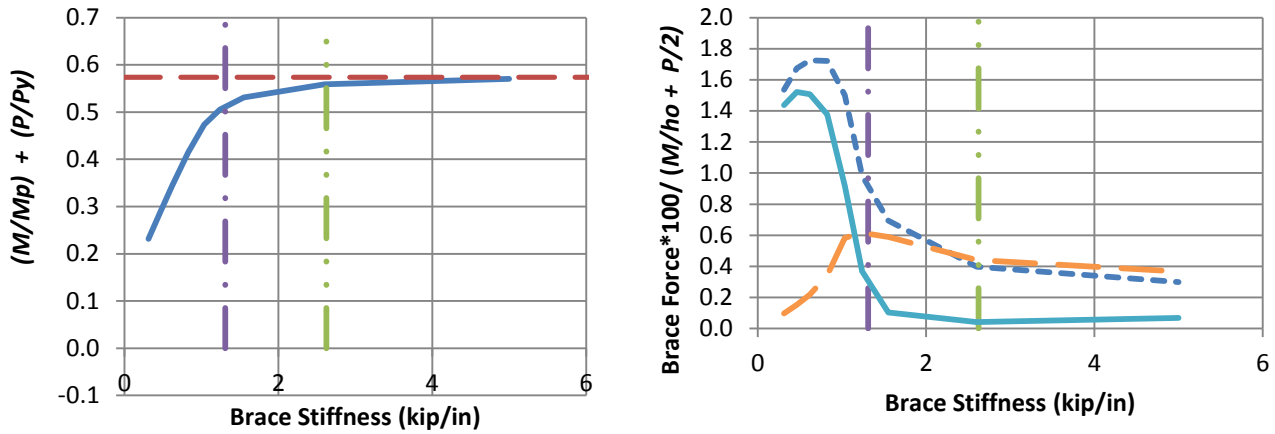
a) BC_UMp_RB_n2_Lb10_FFR-0.67



b) BC_UMp_RB_n2_Lb10_FFR-0.33

- Test simulation results
- - Rigidly-braced strength
- 0.5 times bracing stiffness from Eq. 6-3
- Bracing stiffness from Eq. 6-3
- · - Left end panel shear force
- Right end panel shear force
- · - Middle panel shear force

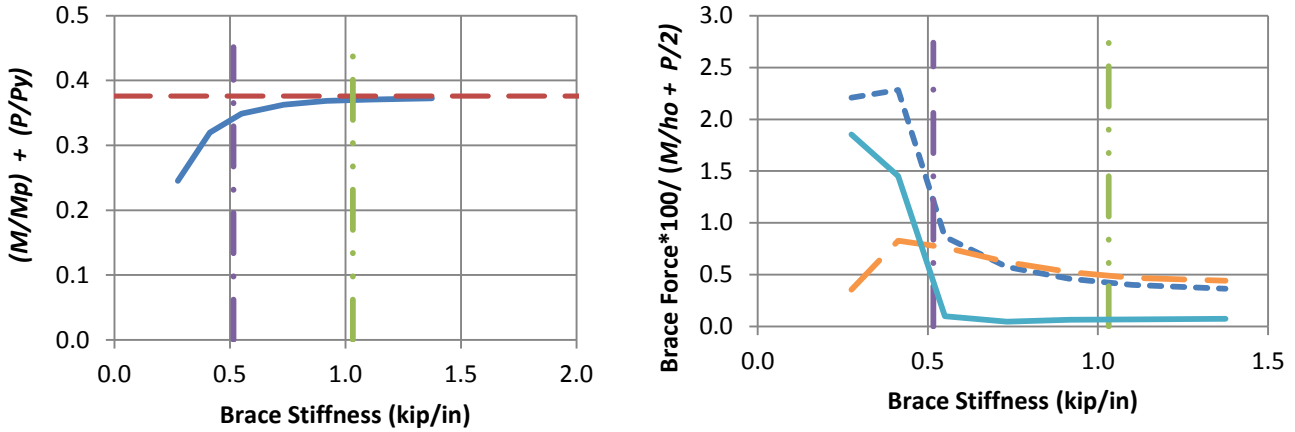
Fig. 6.8. Knuckle curves and brace force vs. brace stiffness plots for shear panel (relative) lateral bracing cases with $n = 2$ and constant axial load and uniform bending with effective flange force ratio $(P_{fv}/P_{fc}) \leq 0$, $L_b = 10\text{ft}$.



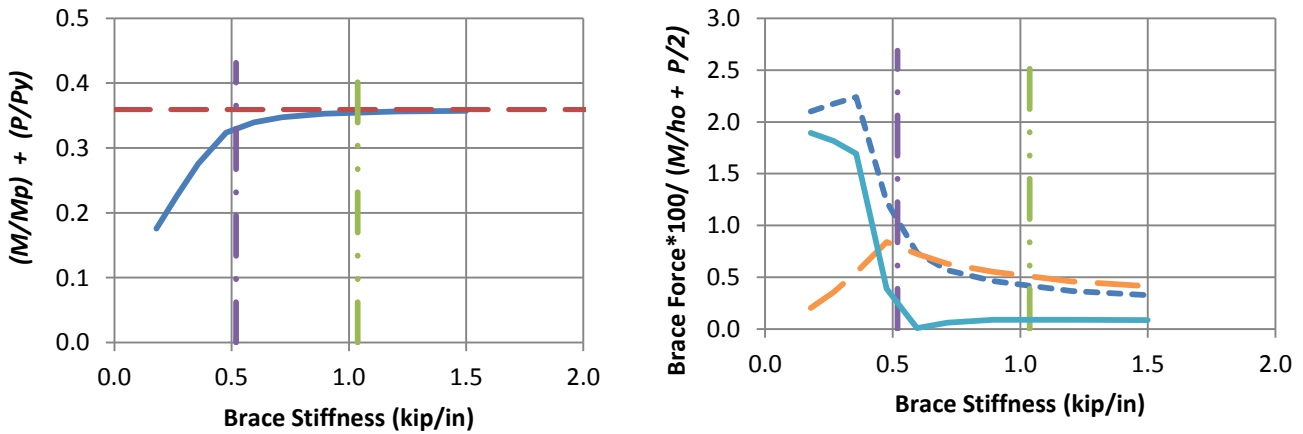
c) BC_UMp_RB_n2_Lb10_FFR0

- Test simulation results
- - Rigidly-braced strength
- 0.5 times bracing stiffness from Eq. 6-3
- Bracing stiffness from Eq. 6-3
- - Left end panel shear force
- Right end panel shear force
- - Middle panel shear force

Fig. 6.8. (continued) Knuckle curves and brace force vs. brace stiffness plots for shear panel (relative) lateral bracing cases with $n = 2$ and constant axial load and uniform bending with effective flange force ratio $(P_{ft}/P_{fc}) \leq 0$, $L_b = 10$ ft.



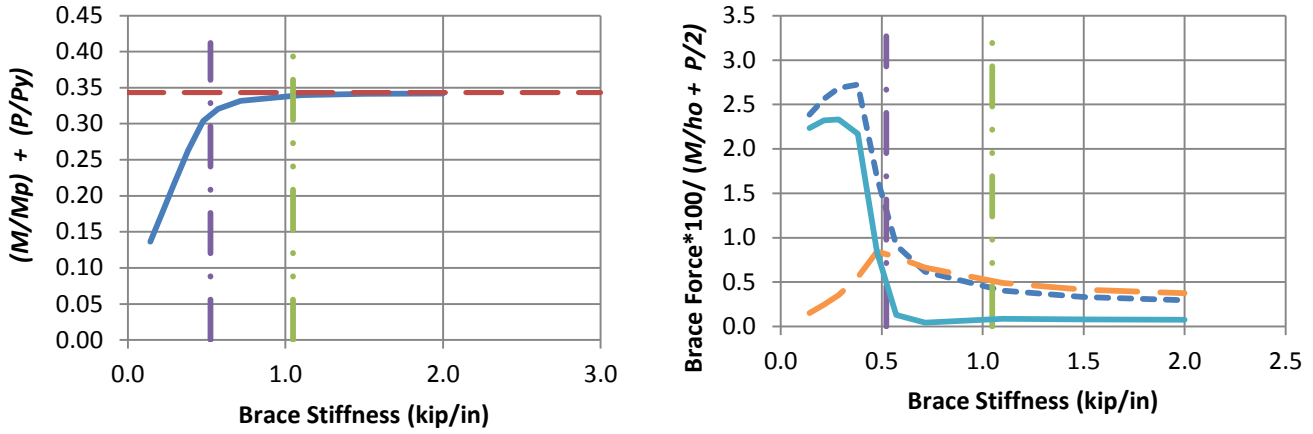
a) BC_UMp_RB_n2_Lb15_FFR-0.67



b) BC_UMp_RB_n2_Lb15_FFR-0.33

- Test simulation results
- 0.5 times bracing stiffness from Eq. 6-3
- Bracing stiffness from Eq. 6-3
- - - Left end panel shear force
- - - Middle panel shear force
- - - Rigidly-braced strength
- Right end panel shear force

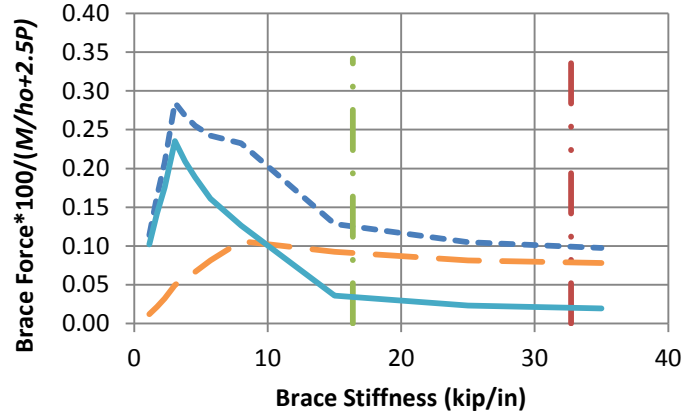
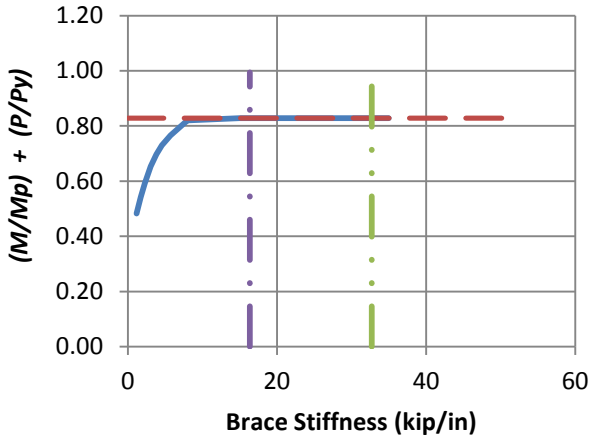
Fig. 6.9. Knuckle curves and brace force vs. brace stiffness plots for shear panel (relative) lateral bracing cases with $n = 2$ and constant axial load and uniform bending with effective flange force ratio $(P_{ft}/P_{fc}) \leq 0$, $L_b = 15$ ft.



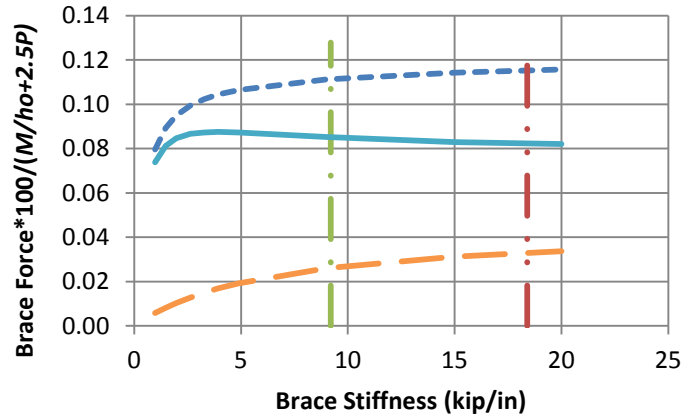
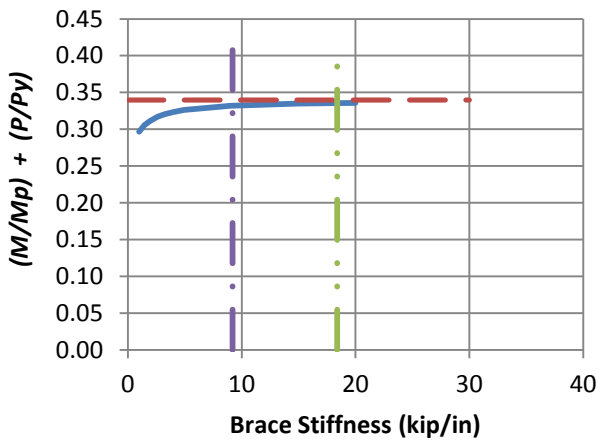
c) BC_UMp_RB_n2_Lb15_FFR0

- Test simulation results
- - Rigidly-braced strength
- 0.5 times bracing stiffness from Eq. 6-3
- Bracing stiffness from Eq. 6-3
- - Left end panel shear force
- Right end panel shear force
- - Middle panel shear force

Fig. 6.9. (continued) Knuckle curves and brace force vs. brace stiffness plots for shear panel (relative) lateral bracing cases with $n = 2$ and constant axial load and uniform bending with effective flange force ratio $(P_{fv}/P_{fc}) \leq 0$, $L_b = 15$ ft.



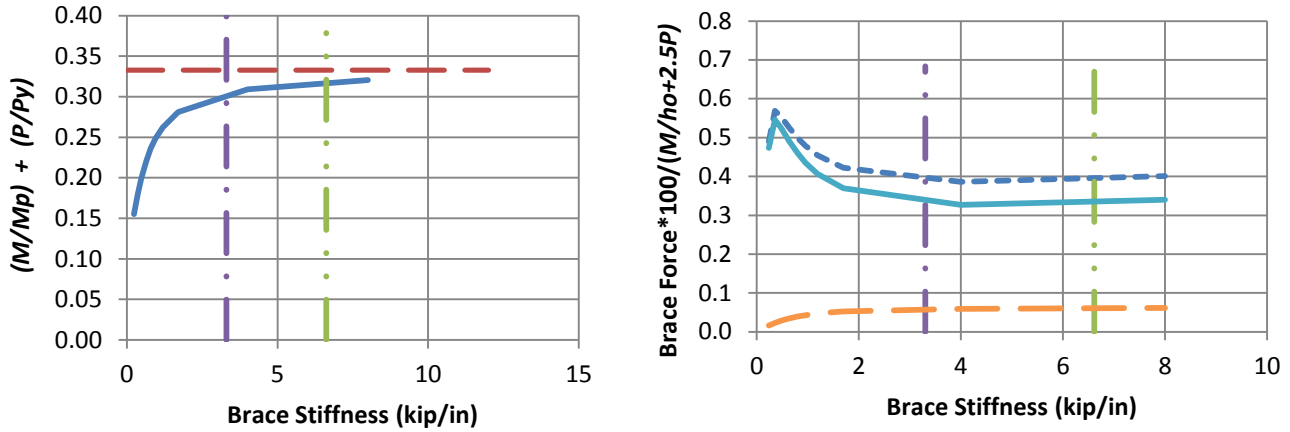
a) BC_UMp_RB_n2_Lb5_FFR0.5



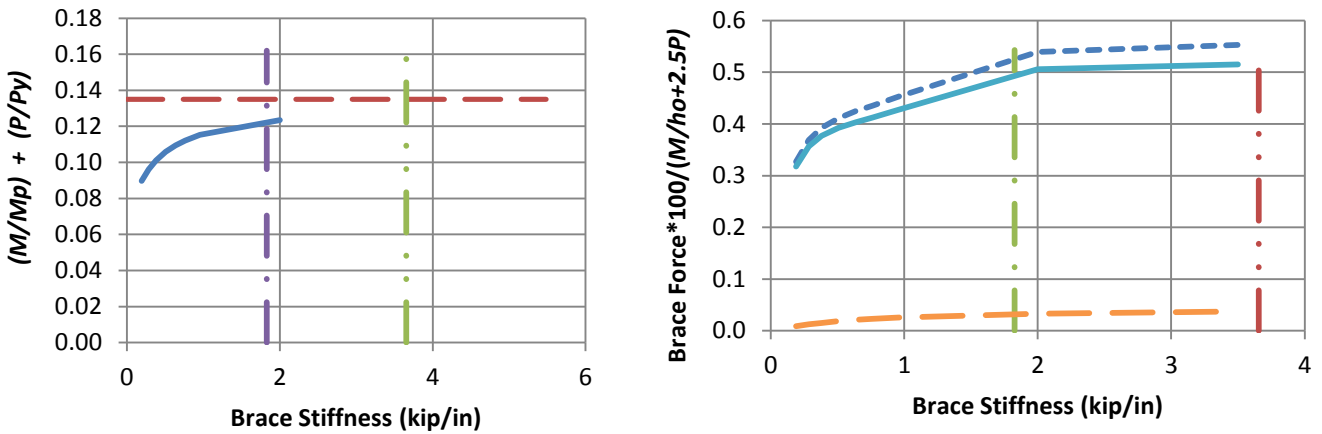
b) BC_UMp_RB_n2_Lb5_FFR1

- Test simulation results
 - 0.5 times bracing stiffness from Eq. 6-5
 - Bracing stiffness from Eq. 6-5
 - - - Left end panel shear force
 - - - Middle panel shear force
- - - Rigidly-braced strength
 - Right end panel shear force

Fig. 6.10. Knuckle curves and brace force vs. brace stiffness plots for shear panel (relative) lateral bracing cases with $n = 2$ and constant axial load and uniform bending with effective flange force ratio $(P_{ft}/P_{fc}) > 0$, $L_b = 5$ ft.



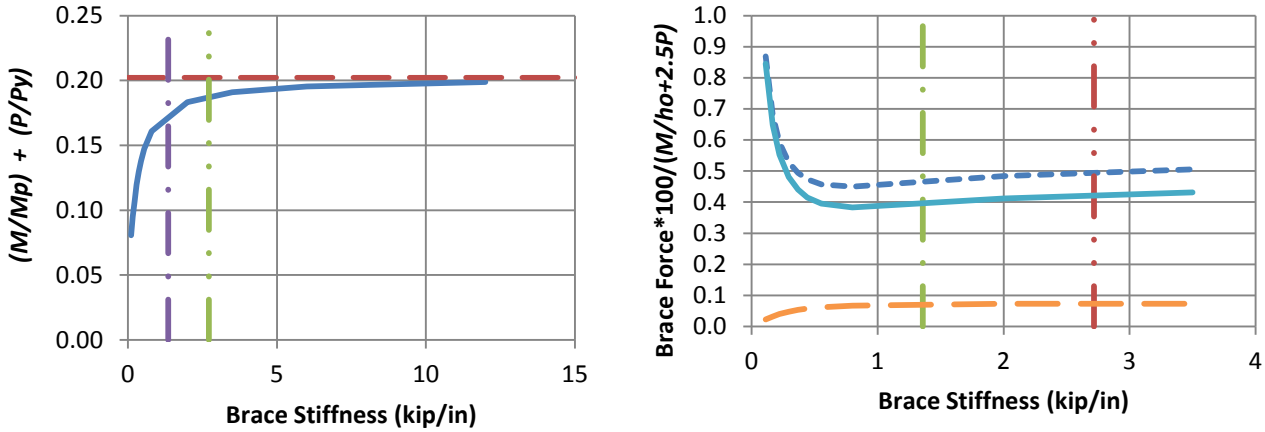
a) BC_UMp_RB_n2_Lb10_FFR0.5



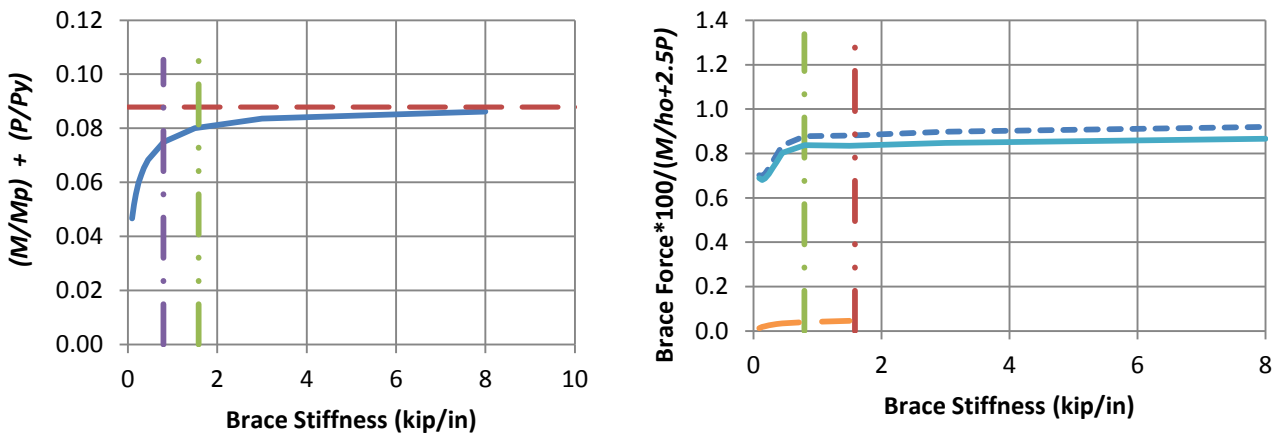
b) BC_UMp_RB_n2_Lb10_FFR1

- Test simulation results
- - Rigidly-braced strength
- 0.5 times bracing stiffness from Eq. 6-5
- Bracing stiffness from Eq. 6-5
- · - Left end panel shear force
- Right end panel shear force
- · - Middle panel shear force

Fig. 6.11. Knuckle curves and brace force vs. brace stiffness plots for shear panel (relative) lateral bracing cases with $n = 2$ and constant axial load and uniform bending with effective flange force ratio $(P_{f\bar{f}}/P_{fc}) > 0$, $L_b = 10\text{ft}$.



a) BC_UMp_RB_n2_Lb15_FFR0.5



b) BC_UMp_RB_n2_Lb15_FFR1

- Test simulation results
- 0.5 times bracing stiffness from Eq. 6-5
- Bracing stiffness from Eq. 6-5
- - - Left end panel shear force
- - - Middle panel shear force
- - - Rigidly-braced strength
- Right end panel shear force

Fig. 6.12. Knuckle curves and brace force vs. brace stiffness plots for shear panel (relative) lateral bracing cases with $n = 2$ and constant axial load and uniform bending with effective flange force ratio $(P_{f\ell} / P_{fc}) > 0$, $L_b = 15$ ft.

The approach given by Eqs. 6-1 and 6-2 is found to be conservative for situations where $(P_{ft}/P_{fc}) \leq 0$. However, it is found to be unconservative for situations in which $(P_{ft}/P_{fc}) > 0$. Hence the following estimates of the bracing requirements for beam-columns are recommended:

Cases with an Effective Flange Force Ratio $(P_{ft}/P_{fc}) \leq 0$

Based on the results from Figs. 6.1 through 6.3 and Figs. 6.7 through 6.9 it can be observed that for all beam-column cases where the effective flange force ratio $(P_{ft}/P_{fc}) \leq 0$ (i.e., only one flange is in compression), the bracing requirements from Eqs. 6-1 and 6-2 are conservative. The results in Figs. 6.1 through 6.3 and Figs. 6.7 through 6.9 clearly show that it is sufficient for the bracing to be designed for the column effect $P/2$ and the beam effect M/h_o . In addition to this finding, based on the results for shear panel (relative) lateral bracing in Figs. 6.7 through 6.9, it can be observed that a value of 0.5% is more appropriate than a value of 0.4% for the bracing strength predictions.

Hence the following equations could be used for obtaining the bracing requirements for all cases where the effective flange force ratio $(P_{ft}/P_{fc}) \leq 0$.

$$\text{Stiffness} = 2 \left[\frac{N_i \left(\frac{P}{2} \right)}{L_b} + \frac{N_i C_t \left(\frac{M}{h_o} \right)}{L_b} \right] \quad (6-3)$$

$$\text{Strength} = 1\% \text{ of } \left[\frac{P}{2} + C_t \left(\frac{M}{h_o} \right) \right] \text{ for Point (nodal) lateral brace} \quad (6-4a)$$

$$= 0.5\% \text{ of } \left[\frac{P}{2} + C_t \left(\frac{M}{h_o} \right) \right] \text{ for Shear panel (relative) lateral brace} \quad (6-4b)$$

Table 6.1 compares the results from Figs. 6.1 through 6.3 and Figs. 6.7 through 6.9.

Table 6.1. Comparison of simulation results in Figs. 6.1 through 6.3 and Figs. 6.7 through 6.9 with Eq. 6-3.

Case (a)	Stiffness corresponding to 96% of simulation rigidly-braced strength (kip/in) (b)	Required bracing stiffness from Eq. 6-3 kip/in (c)	Col. (b) / Col. (c) (d)
BC_UMp_NB_n1_Lb5_FFR-0.67	5.78	14.00	0.42
BC_UMp_NB_n1_Lb5_FFR-0.33	6.05	14.60	0.42
BC_UMp_NB_n1_Lb5_FFR0	6.41	15.24	0.42
BC_UMp_NB_n1_Lb10_FFR-0.67	3.09	4.76	0.65
BC_UMp_NB_n1_Lb10_FFR-0.33	3.17	4.96	0.64
BC_UMp_NB_n1_Lb10_FFR0	3.38	5.20	0.65
BC_UMp_NB_n1_Lb15_FFR-0.67	1.17	2.02	0.58
BC_UMp_NB_n1_Lb15_FFR-0.33	1.16	2.06	0.56
BC_UMp_NB_n1_Lb15_FFR0	1.21	2.10	0.58
BC_UMp_RB_n2_Lb5_FFR-0.67	3.27	7.00	0.47
BC_UMp_RB_n2_Lb5_FFR-0.33	3.29	7.26	0.46
BC_UMp_RB_n2_Lb5_FFR0	3.99	7.58	0.53
BC_UMp_RB_n2_Lb10_FFR-0.67	1.94	2.42	0.81
BC_UMp_RB_n2_Lb10_FFR-0.33	1.98	2.52	0.79
BC_UMp_RB_n2_Lb10_FFR0	2.3	2.62	0.88
BC_UMp_RB_n2_Lb15_FFR-0.67	0.71	1.04	0.69
BC_UMp_RB_n2_Lb15_FFR-0.33	0.68	1.04	0.66
BC_UMp_RB_n2_Lb15_FFR0	0.69	1.04	0.66

From Column (d) of Table 6.1, it can be observed that the bracing stiffness calculated by Eq. 6-3 is sufficient to develop 96 % of the minimum rigidly-braced member strength for all of the basic bracing types when $(P_{ft}/P_{fc}) \leq 0$. Based on the brace force versus brace stiffness plots in Figs. 6.1 through 6.3 and Figs. 6.7 through 6.9, it can be observed that Eqs. 6-4a and 6-4b do an accurate to somewhat conservative job of estimating the brace strength requirements.

Cases with Effective Flange Force Ratio $(P_{ft}/P_{fc}) > 0$

The following equations can be used for obtaining the bracing requirements for all cases where the effective flange force ratio $(P_{ft}/P_{fc}) > 0$.

$$\text{Stiffness} = 2 \left[\frac{N_i (2.5P)}{L_b} + \frac{N_i C_t \left(\frac{M}{h_o} \right)}{L_b} \right] \quad (6-5)$$

$$\text{Strength} = 1\% \text{ of } \left[2.5P + C_t \left(\frac{M}{h_o} \right) \right] \text{ for Point (nodal) lateral brace} \quad (6-6a)$$

$$= 0.5\% \text{ of } \left[2.5P + C_t \left(\frac{M}{h_o} \right) \right] \text{ for Shear panel (relative) lateral brace} \quad (6-6b)$$

Table 6.2 compares the results from Figs. 6.4 through 6.6 and Figs. 6.10 through 6.12, which correspond to this range of the P_{ft}/P_{fc} ratio.

Table 6.2. Comparison of simulation results in Figs. 6.4 through 6.6 and Figs. 6.10 through 6.12 with Eq. 6-5.

Case (a)	Stiffness corresponding to 96% of simulation rigidly-braced strength (kip/in) (b)	Required bracing stiffness from Eq. 6-5 kip/in (c)	Col. (b) / Col. (c) (d)
BC_UMp_NB_n1_Lb5_FFR0.5	0.7	63.08	0.01
BC_UMp_NB_n1_Lb5_FFR1	11.89	60.48	0.20
BC_UMp_NB_n1_Lb10_FFR0.5	10.36	22.00	0.47
BC_UMp_NB_n1_Lb10_FFR1	6.67	11.90	0.56
BC_UMp_NB_n1_Lb15_FFR0.5	11.2	8.32	1.35
BC_UMp_NB_n1_Lb15_FFR1	9.16	4.80	1.91
BC_UMp_RB_n2_Lb5_FFR0.5	6.96	32.72	0.22
BC_UMp_RB_n2_Lb5_FFR1	4.8	18.40	0.26
BC_UMp_RB_n2_Lb10_FFR0.5	7.61	6.62	1.15
BC_UMp_RB_n2_Lb10_FFR1	5.43	3.66	1.49
BC_UMp_RB_n2_Lb15_FFR0.5	5.29	2.72	1.95
BC_UMp_RB_n2_Lb15_FFR1	4.31	1.58	2.72

From Column (d) of Table 6.2, it can be observed that the bracing stiffness calculated by Eq. 6-5 is unconservative for cases in which the (L/r) value of the unbraced flange (flange loaded in flexural tension) is large. For the other cases (i.e., cases with one intermediate brace and unbraced lengths of 5 ft and 10 ft, and cases with two intermediate braces and unbraced length of 5 ft) the bracing stiffness calculated by Eq. 6-5 is conservative. Similarly, from Figs. 6.4 through 6.6 and Figs. 6.10

through 6.12, it can be observed that the bracing strength calculated by Eq. 6-6 is conservative for all cases except Fig. 6.12b for which (L/r) value of the unbraced flange is large. If the (L/r) value of the unbraced flange is restricted to 200, then Eqs. 6-5 and 6-6 with $2P$ instead of $2.5P$, gives acceptable results.

6.3.2 Beam-Columns with Combined Lateral and Torsional Bracing

When both flanges have to be braced in beam-column members, it is rare that independent lateral bracing would be provided at both flanges. The more common situation is for beam-columns to have a combination of lateral and torsional bracing. As discussed in Section 2.2.5.2, for beam-columns with combined lateral and torsional bracing, it is recommended to design the lateral bracing for a load equal to the axial load (P) and the torsional brace for a load equal to $(M/h_o + P/2)$.

The corresponding bracing stiffness requirements for beam-columns are:

$$\text{Lateral bracing} = \frac{2N_i P}{L_b} \quad (6-7)$$

$$\text{Torsional bracing} = 10 \left[\frac{\left(\frac{M}{C_b h_o} + \frac{P}{2} \right)}{P_{e,eff}} \right] \left[\frac{\left(\frac{M}{C_b h_o} + \frac{P}{2} \right)}{L_b} \right] \left[\frac{n_T + 1}{n_T} \right] C_{tT} \quad (6-8)$$

where:

n_T = number of intermediate torsional brace points

L_b = unbraced length

C_b = Lateral-torsional buckling modification factor

$C_{tT} = 1.2$ when the transverse loading is applied at the flange level in a way that

is detrimental to the member stability (this occurs when the transverse

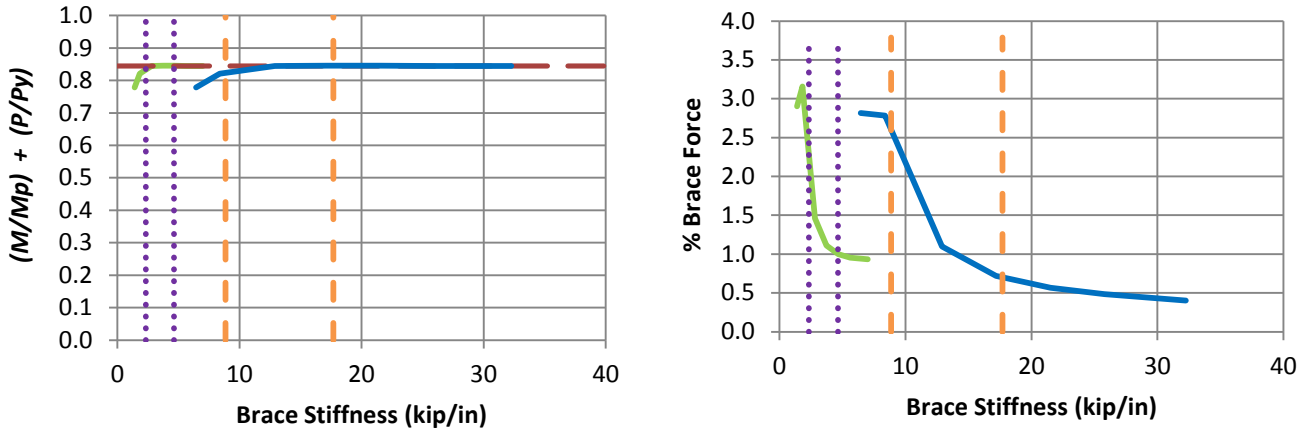
loading is applied at the flange level and is directed towards the member shear center from its point of application), assuming that substantial tipping restraint does not exist at the transverse loading points.

= 1 otherwise

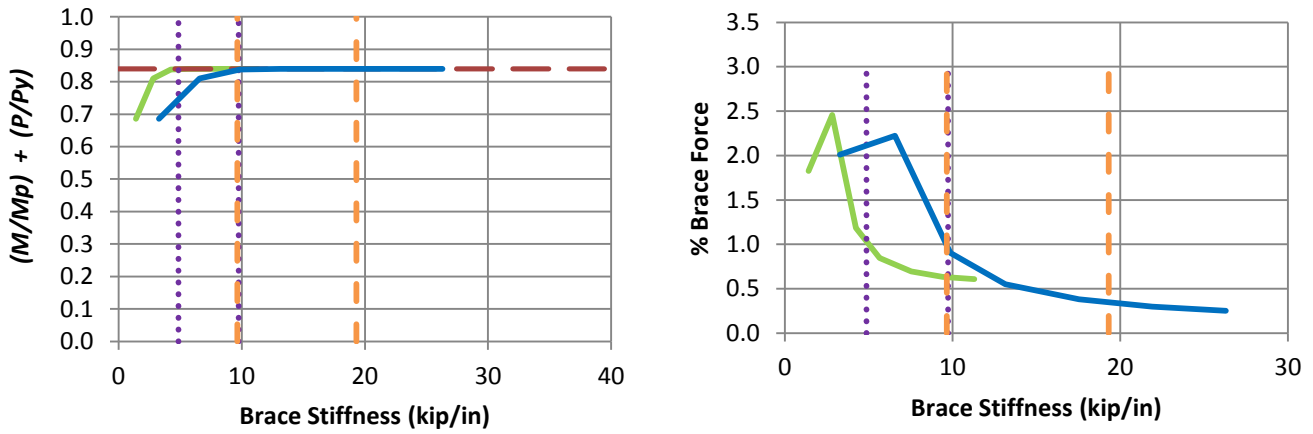
$$P_{e,eff} = \frac{\pi^2 E \left(\frac{I_y}{2} \right)}{L_b^2} = \text{effective flange buckling load for doubly-symmetric I-section members.}$$

Figures 6.13 through 6.20 show the results for beam-columns with combined lateral and torsional bracing. The lateral brace force in Figs. 6.13 through 6.20 is expressed as percentage of P . The torsional brace force in these figures is expressed as percentage of $M/h_o + P/2$.

Tables 6.3 and 6.4 compare the results from Figs. 6.13 through 6.20. From Column (d) of these tables, it can be observed that the bracing stiffness calculated by Eqs. 6-7 and 6-8 is sufficient to develop 96 % of the minimum rigidly-braced member strength for all of the combined bracing cases.



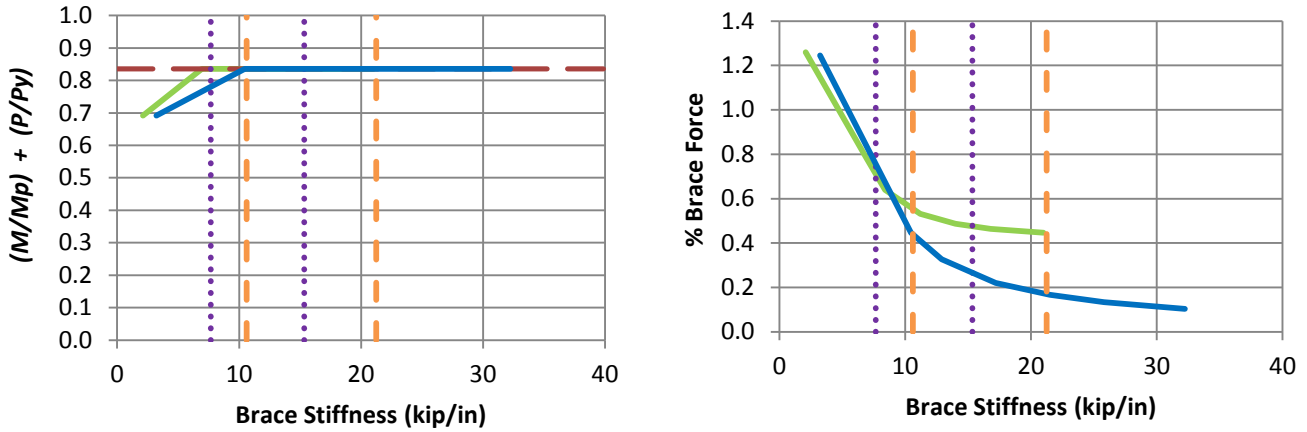
a) BC_UMp_CNTB_n1_Lb5_FFR-0.67



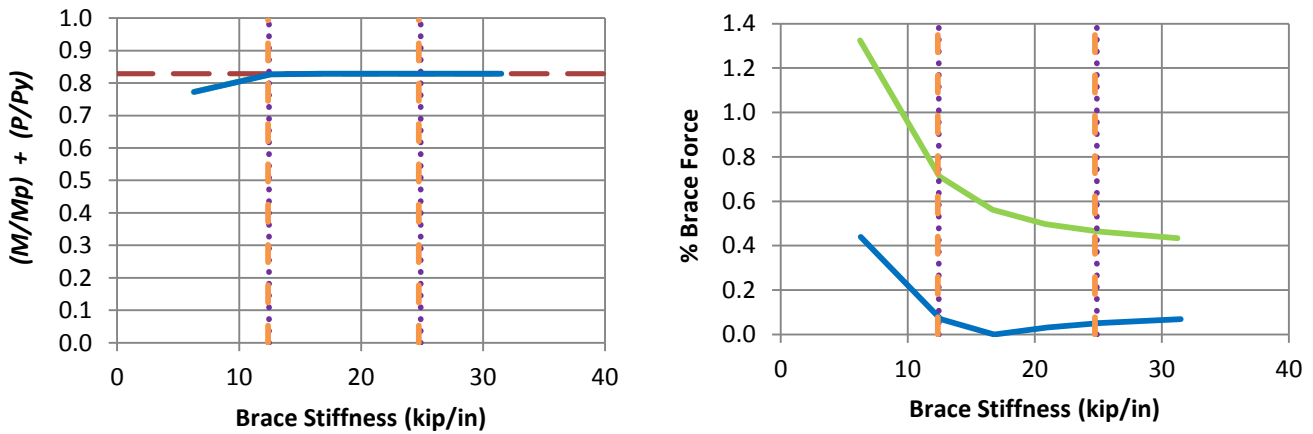
b) BC_UMp_CNTB_n1_Lb5_FFR-0.33

- Rigidly-braced strength
- Test simulation results corresponding to torsional brace
- Test simulation results corresponding to lateral brace
- ⋯ 1x and 0.5x lateral bracing stiffness from Eq. 6-7
- 1x and 0.5x torsional bracing stiffness from Eq. 6-8

Fig. 6.13. Knuckle curves and brace force vs. brace stiffness plots for combined point (nodal) lateral and torsional bracing cases with $n = 1$ and constant axial load and uniform bending with lateral brace on the flange in flexural compression, $L_b = 5\text{ft}$.



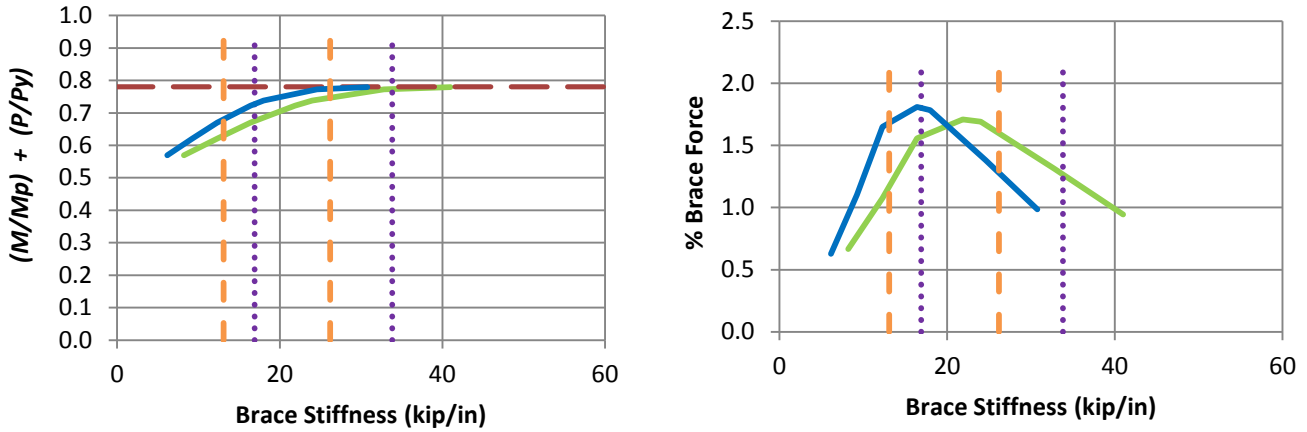
c) BC_UMp_CNTB_n1_Lb5_FFR0



d) BC_UMp_CNTB_n1_Lb5_FFR0.5

- Rigidly-braced strength
- Test simulation results corresponding to torsional brace
- Test simulation results corresponding to lateral brace
- 1x and 0.5x lateral bracing stiffness from Eq. 6-7
- - - 1x and 0.5x torsional bracing stiffness from Eq. 6-8

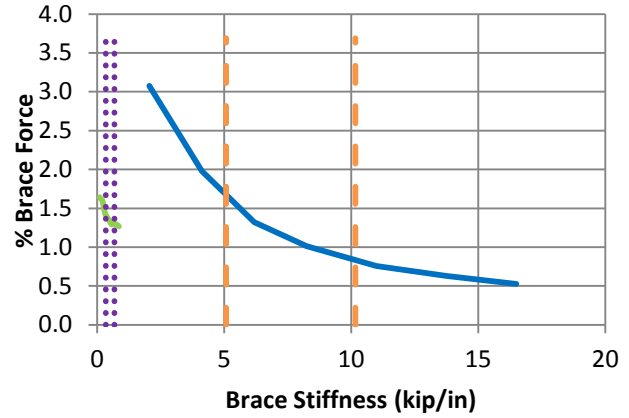
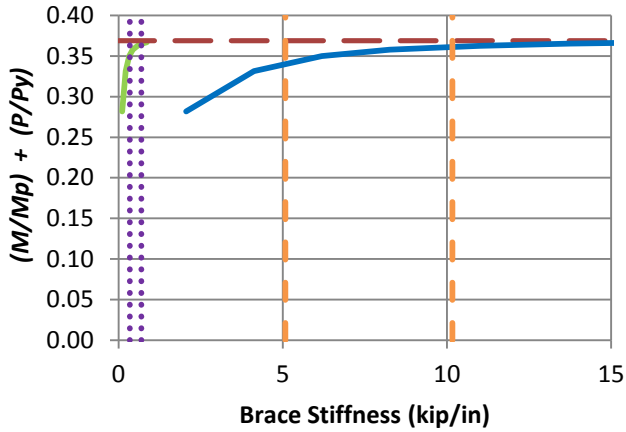
Fig. 6.13. (continued) Knuckle curves and brace force vs. brace stiffness plots for combined point (nodal) lateral and torsional bracing cases with $n = 1$ and constant axial load and uniform bending with lateral brace on the flange in flexural compression, $L_b = 5$ ft.



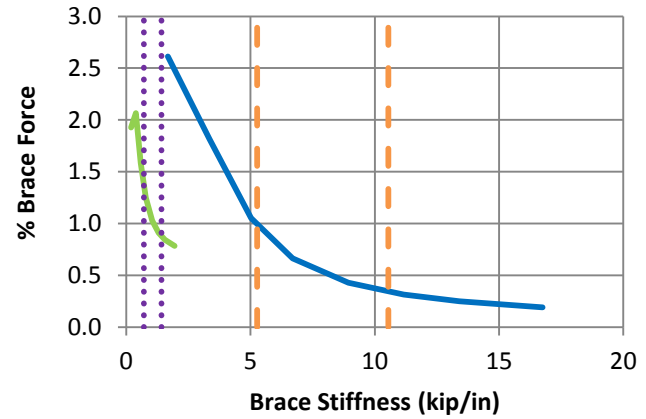
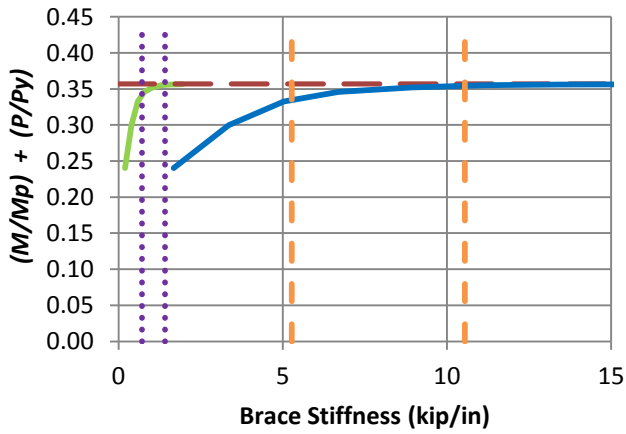
e) BC_UMp_CNTB_n1_Lb5_FFR1

- Rigidly-braced strength
- Test simulation results corresponding to torsional brace
- Test simulation results corresponding to lateral brace
- 1x and 0.5x lateral bracing stiffness from Eq. 6-7
- 1x and 0.5x torsional bracing stiffness from Eq. 6-8

Fig. 6.13. (continued) Knuckle curves and brace force vs. brace stiffness plots for combined point (nodal) lateral and torsional bracing cases with $n = 1$ and constant axial load and uniform bending with lateral brace on the flange in flexural compression, $L_b = 5\text{ft}$.



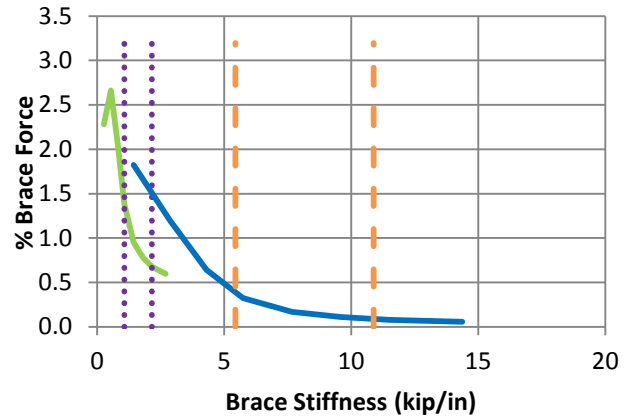
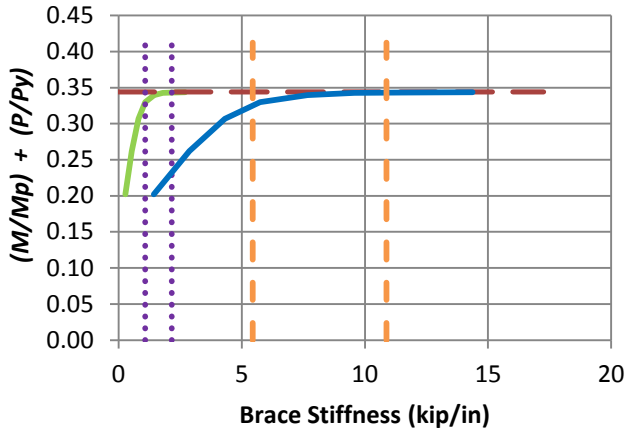
a) BC_UMp_CNTB_n1_Lb15_FFR-0.67



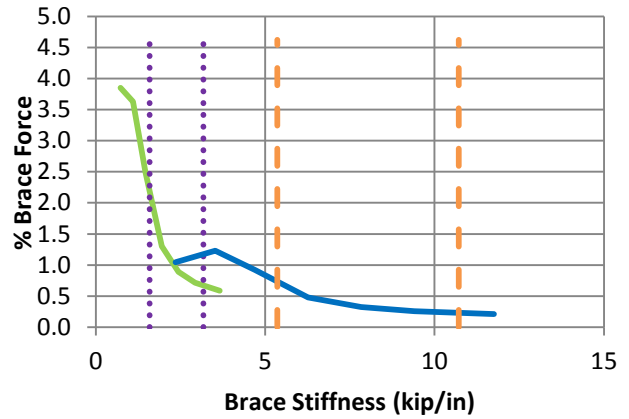
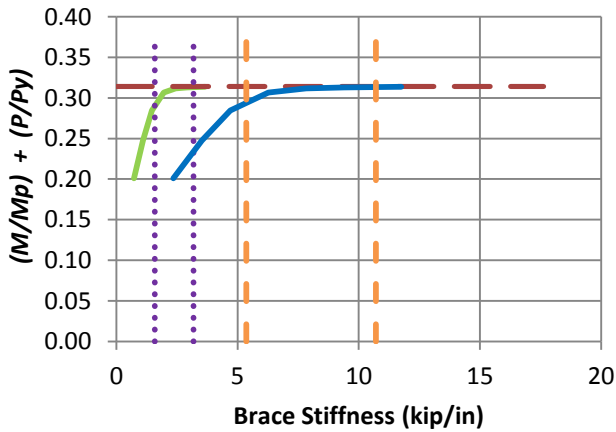
b) BC_UMp_CNTB_n1_Lb15_FFR-0.33

- Rigidly-braced strength
- Test simulation results corresponding to torsional brace
- Test simulation results corresponding to lateral brace
- 1x and 0.5x lateral bracing stiffness from Eq. 6-7
- 1x and 0.5x torsional bracing stiffness from Eq. 6-8

Fig. 6.14. Knuckle curves and brace force vs. brace stiffness plots for combined point (nodal) lateral and torsional bracing cases with $n = 1$ and constant axial load and uniform bending with lateral brace on the flange in flexural compression, $L_b = 15$ ft.



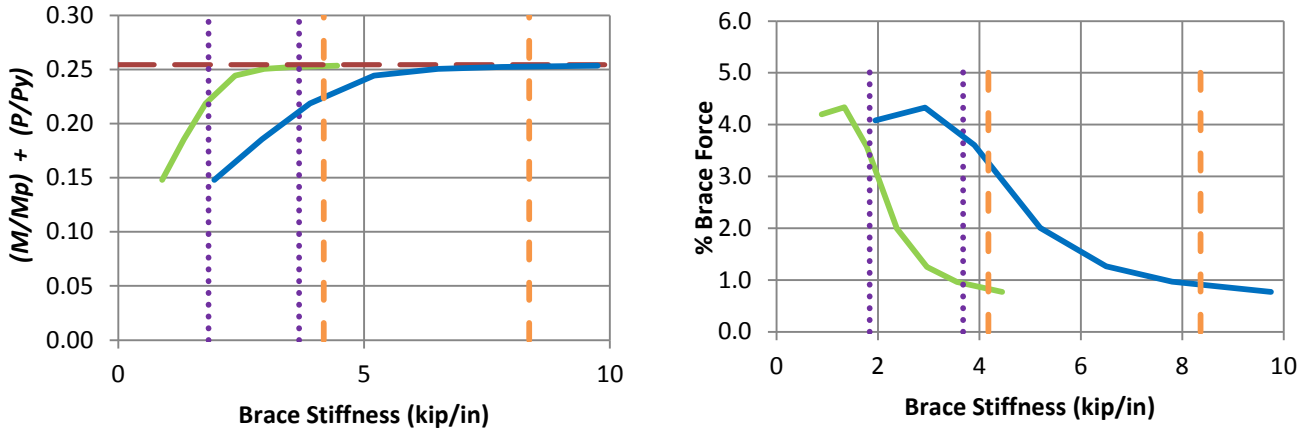
c) BC_UMp_CNTB_n1_Lb15_FFR0



d) BC_UMp_CNTB_n1_Lb15_FFR0.5

- Rigidly-braced strength
- Test simulation results corresponding to torsional brace
- Test simulation results corresponding to lateral brace
- 1x and 0.5x lateral bracing stiffness from Eq. 6-7
- - - 1x and 0.5x torsional bracing stiffness from Eq. 6-8

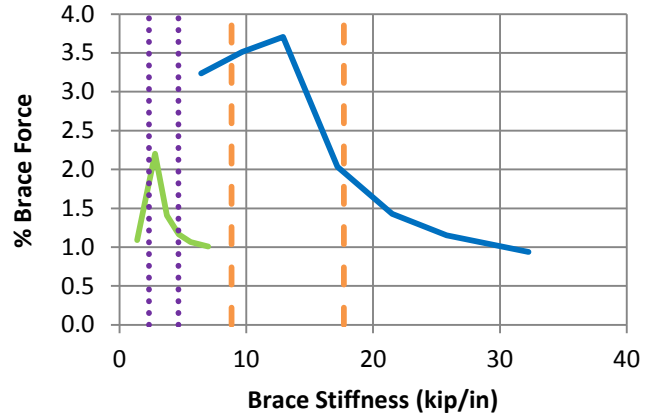
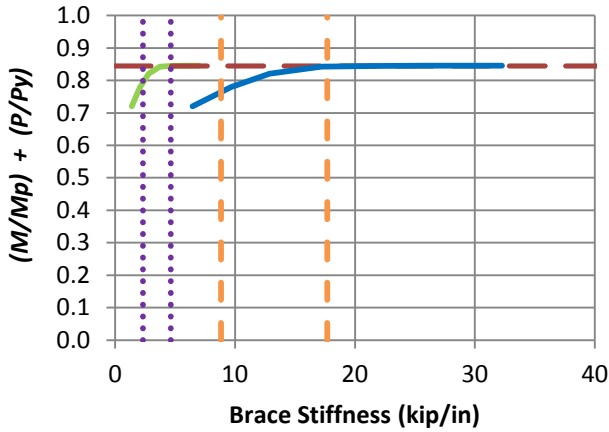
Fig. 6.14. (continued) Knuckle curves and brace force vs. brace stiffness plots for combined point (nodal) lateral and torsional bracing cases with $n = 1$ and constant axial load and uniform bending with lateral brace on the flange in flexural compression, $L_b = 15$ ft.



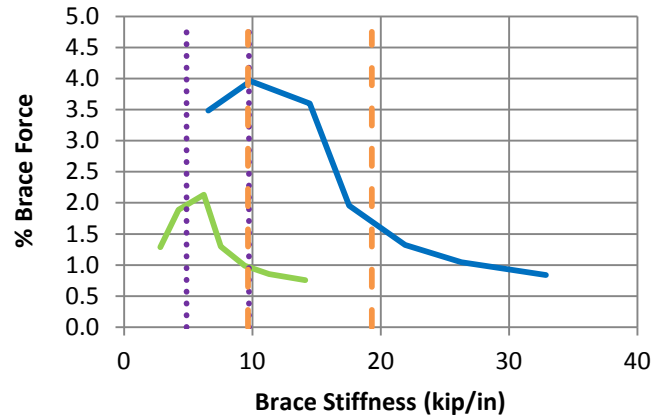
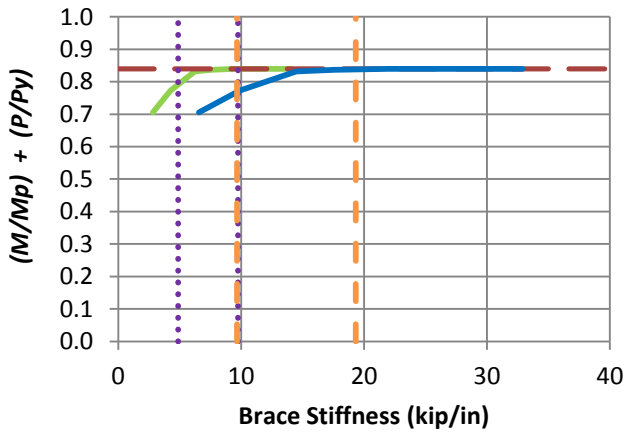
e) BC_UMp_CNTB_n1_Lb15_FFR1

- Rigidly-braced strength
- Test simulation results corresponding to torsional brace
- Test simulation results corresponding to lateral brace
- 1x and 0.5x lateral bracing stiffness from Eq. 6-7
- - - 1x and 0.5x torsional bracing stiffness from Eq. 6-8

Fig. 6.14. (continued) Knuckle curves and brace force vs. brace stiffness plots for combined point (nodal) lateral and torsional bracing cases with $n = 1$ and constant axial load and uniform bending with lateral brace on the flange in flexural compression, $L_b = 15\text{ft}$.



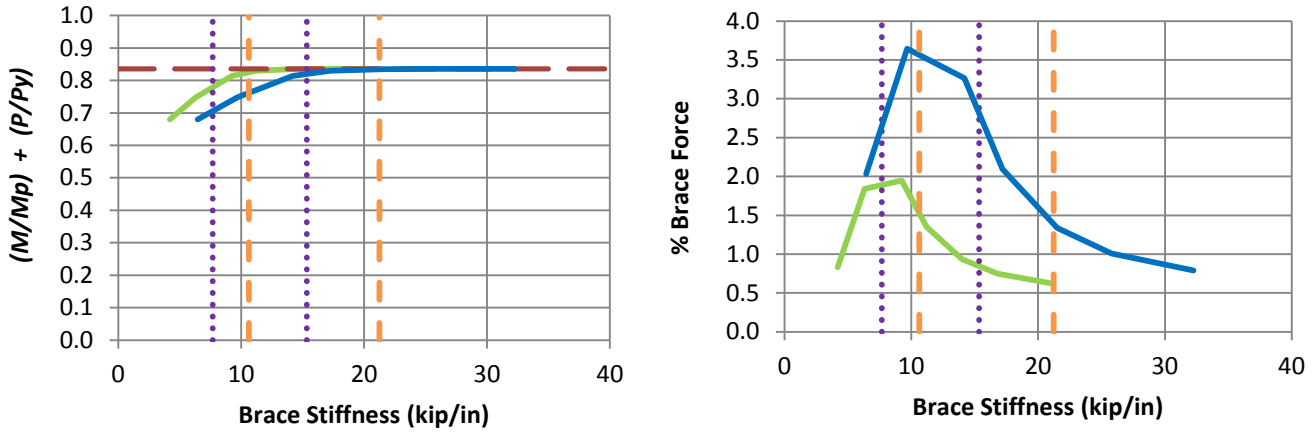
a) BC_N_CNTB_n1_Lb5_FFR-0.67



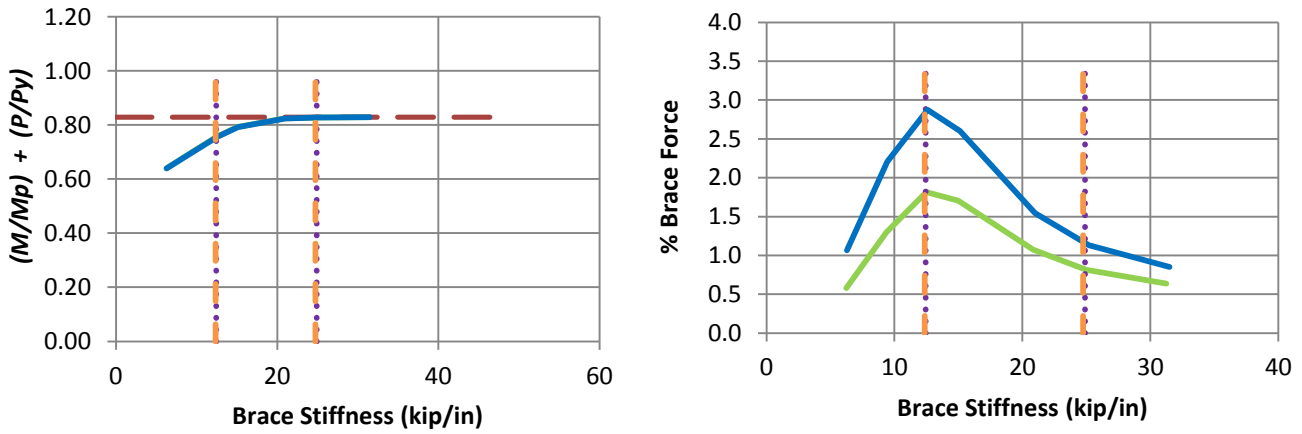
b) BC_UMn_CNTB_n1_Lb5_FFR-0.33

- Rigidly-braced strength
- Test simulation results corresponding to torsional brace
- Test simulation results corresponding to lateral brace
- ⋯ 1x and 0.5x lateral bracing stiffness from Eq. 6-7
- - - 1x and 0.5x torsional bracing stiffness from Eq. 6-8

Fig. 6.15. Knuckle curves and brace force vs. brace stiffness plots for combined point (nodal) lateral and torsional bracing cases with $n = 1$ and constant axial load and uniform bending with lateral brace on the flange in flexural tension, $L_b = 5\text{ft}$.



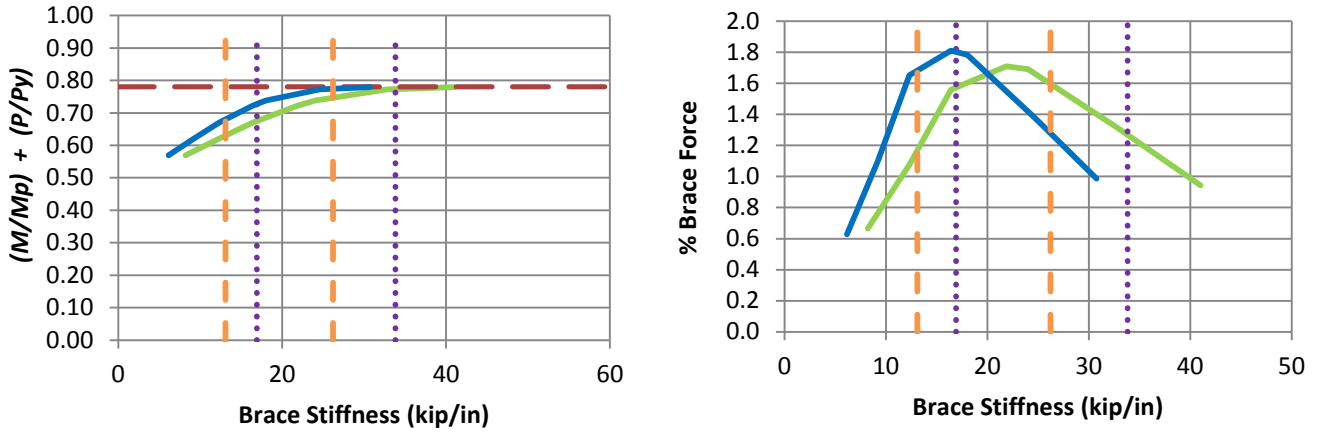
c) BC_UMn_CNTB_n1_Lb5_FFR0



d) BC_UMn_CNTB_n1_Lb5_FFR0.5

- Rigidly-braced strength
- Test simulation results corresponding to torsional brace
- Test simulation results corresponding to lateral brace
- 1x and 0.5x lateral bracing stiffness from Eq. 6-7
- 1x and 0.5x torsional bracing stiffness from Eq. 6-8

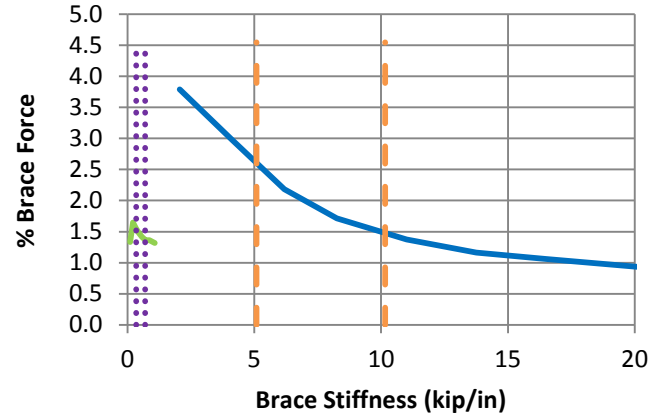
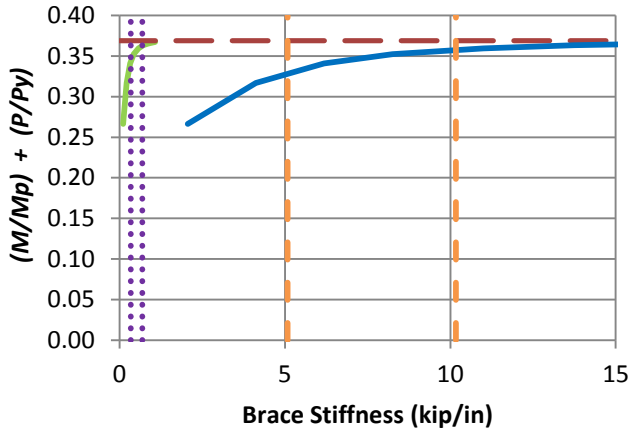
Fig. 6.15. (continued) Knuckle curves and brace force vs. brace stiffness plots for combined point (nodal) lateral and torsional bracing cases with $n = 1$ and constant axial load and uniform bending with lateral brace on the flange in flexural tension, $L_b = 5\text{ft}$.



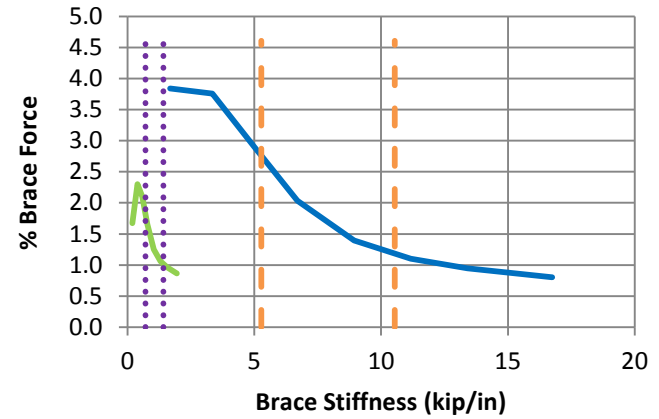
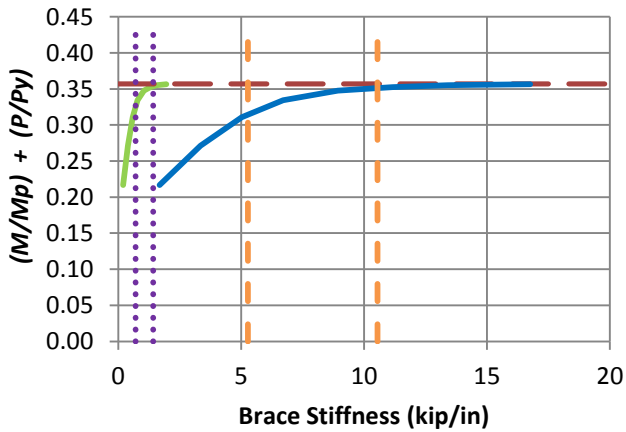
e) BC_UMn_CNTB_n1_Lb5_FFR1

- Rigidly-braced strength
- Test simulation results corresponding to torsional brace
- Test simulation results corresponding to lateral brace
- 1x and 0.5x lateral bracing stiffness from Eq. 6-7
- 1x and 0.5x torsional bracing stiffness from Eq. 6-8

Fig. 6.15. (continued) Knuckle curves and brace force vs. brace stiffness plots for combined point (nodal) lateral and torsional bracing cases with $n = 1$ and constant axial load and uniform bending with lateral brace on the flange in flexural tension, $L_b = 5\text{ft}$.



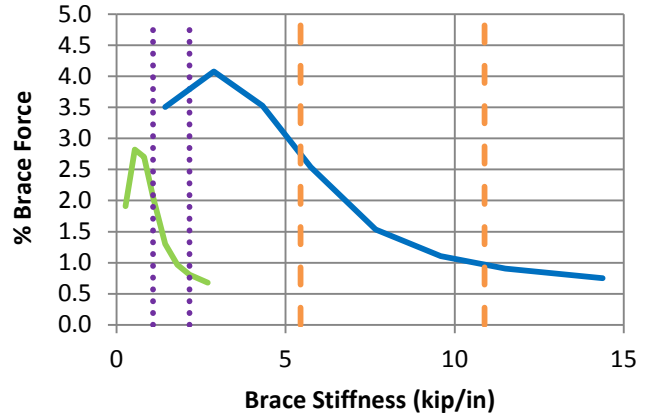
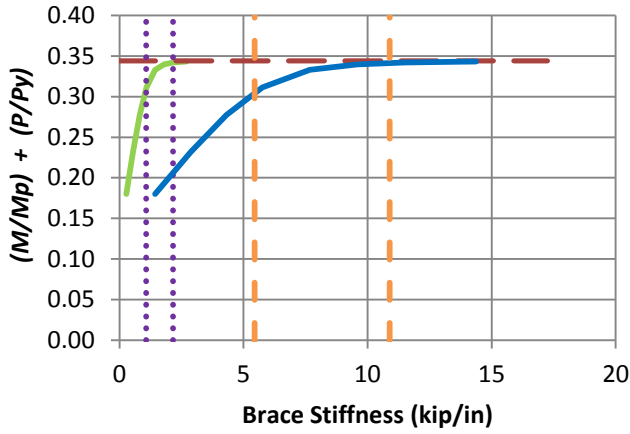
a) BC_UMn_CNTB_n1_Lb15_FFR-0.67



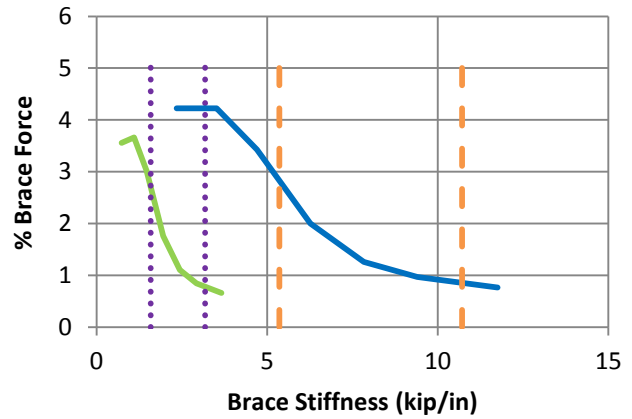
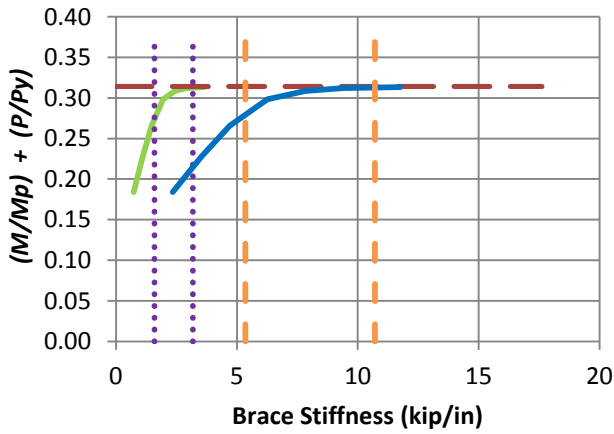
b) BC_UMn_CNTB_n1_Lb15_FFR-0.33

- — Rigidly-braced strength
- Test simulation results corresponding to torsional brace
- Test simulation results corresponding to lateral brace
- ⋯⋯⋯ 1x and 0.5x lateral bracing stiffness from Eq. 6-7
- - - 1x and 0.5x torsional bracing stiffness from Eq. 6-8

Fig. 6.16. Knuckle curves and brace force vs. brace stiffness plots for combined point (nodal) lateral and torsional bracing cases with $n = 1$ and constant axial load and uniform bending with lateral brace on the flange in flexural tension, $L_b = 15\text{ft}$.



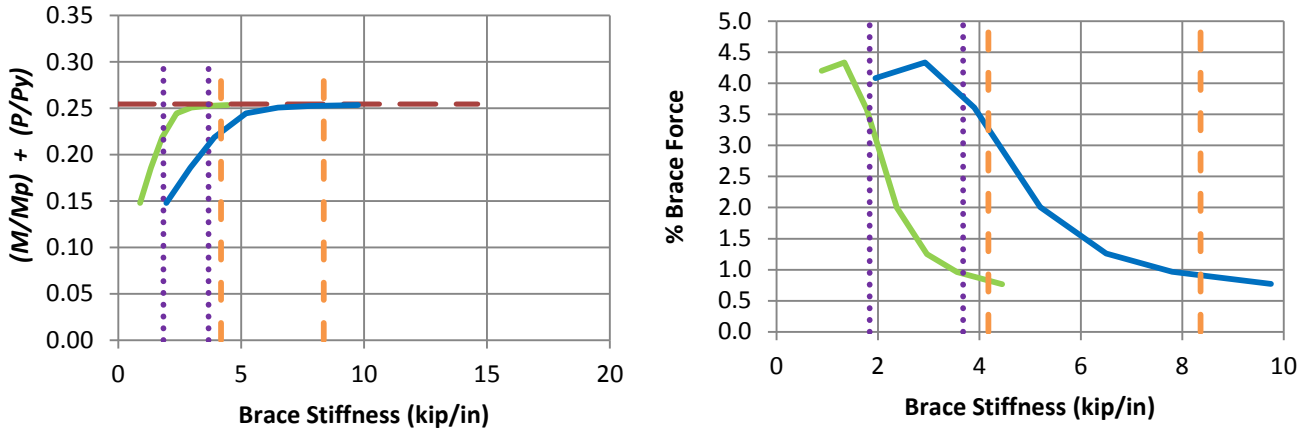
c) BC_UMn_CNTB_n1_Lb15_FFR0



d) BC_UMn_CNTB_n1_Lb15_FFR0.5

- Rigidly-braced strength
- Test simulation results corresponding to torsional brace
- Test simulation results corresponding to lateral brace
- 1x and 0.5x lateral bracing stiffness from Eq. 6-7
- - - 1x and 0.5x torsional bracing stiffness from Eq. 6-8

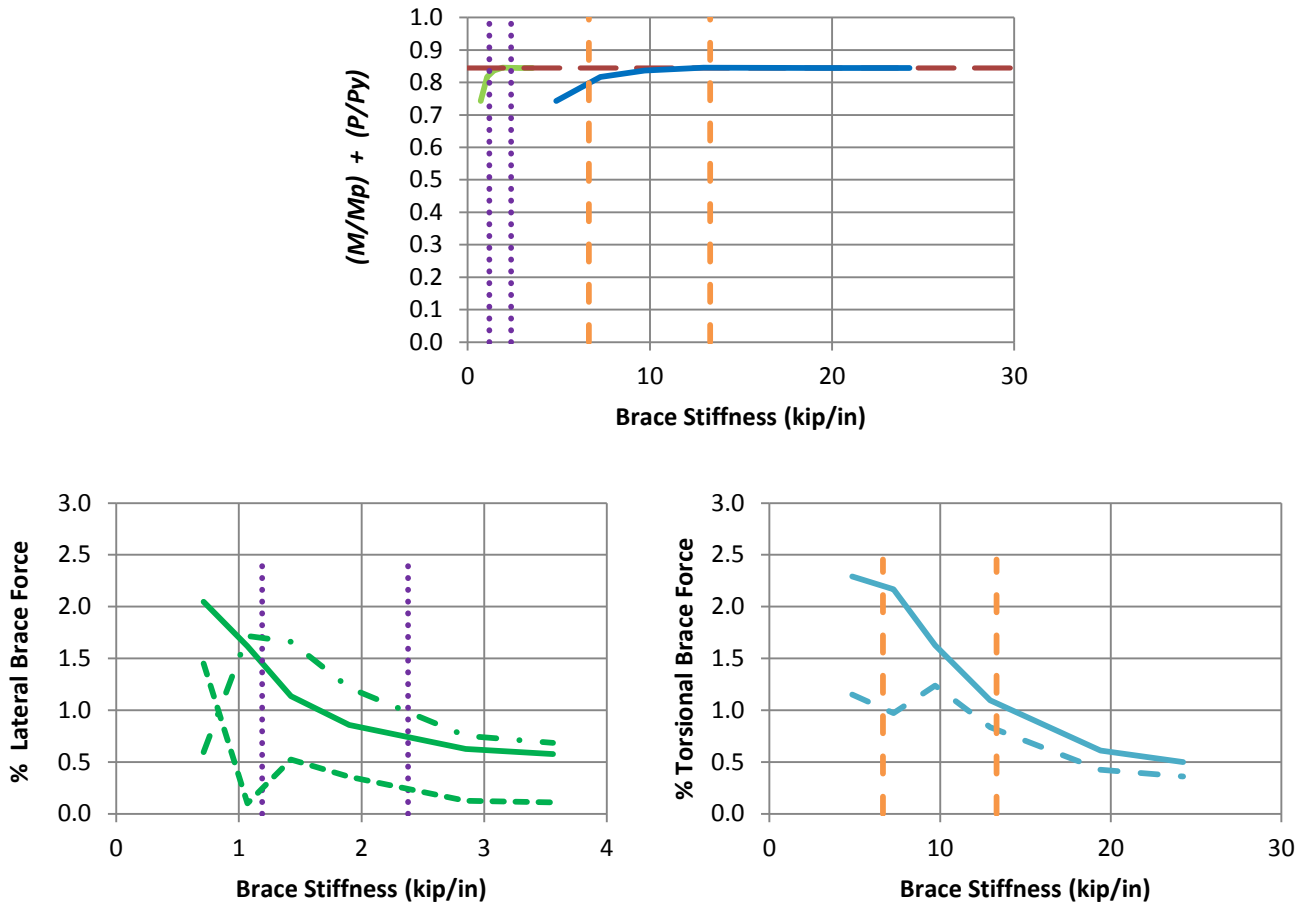
Fig. 6.16. (continued) Knuckle curves and brace force vs. brace stiffness plots for combined point (nodal) lateral and torsional bracing cases with $n = 1$ and constant axial load and uniform bending with lateral brace on the flange in flexural tension, $L_b = 15\text{ft}$.



e) BC_UMn_CNTB_n1_Lb15_FFR1

- Rigidly-braced strength
- Test simulation results corresponding to torsional brace
- Test simulation results corresponding to lateral brace
- 1x and 0.5x lateral bracing stiffness from Eq. 6-7
- - - 1x and 0.5x torsional bracing stiffness from Eq. 6-8

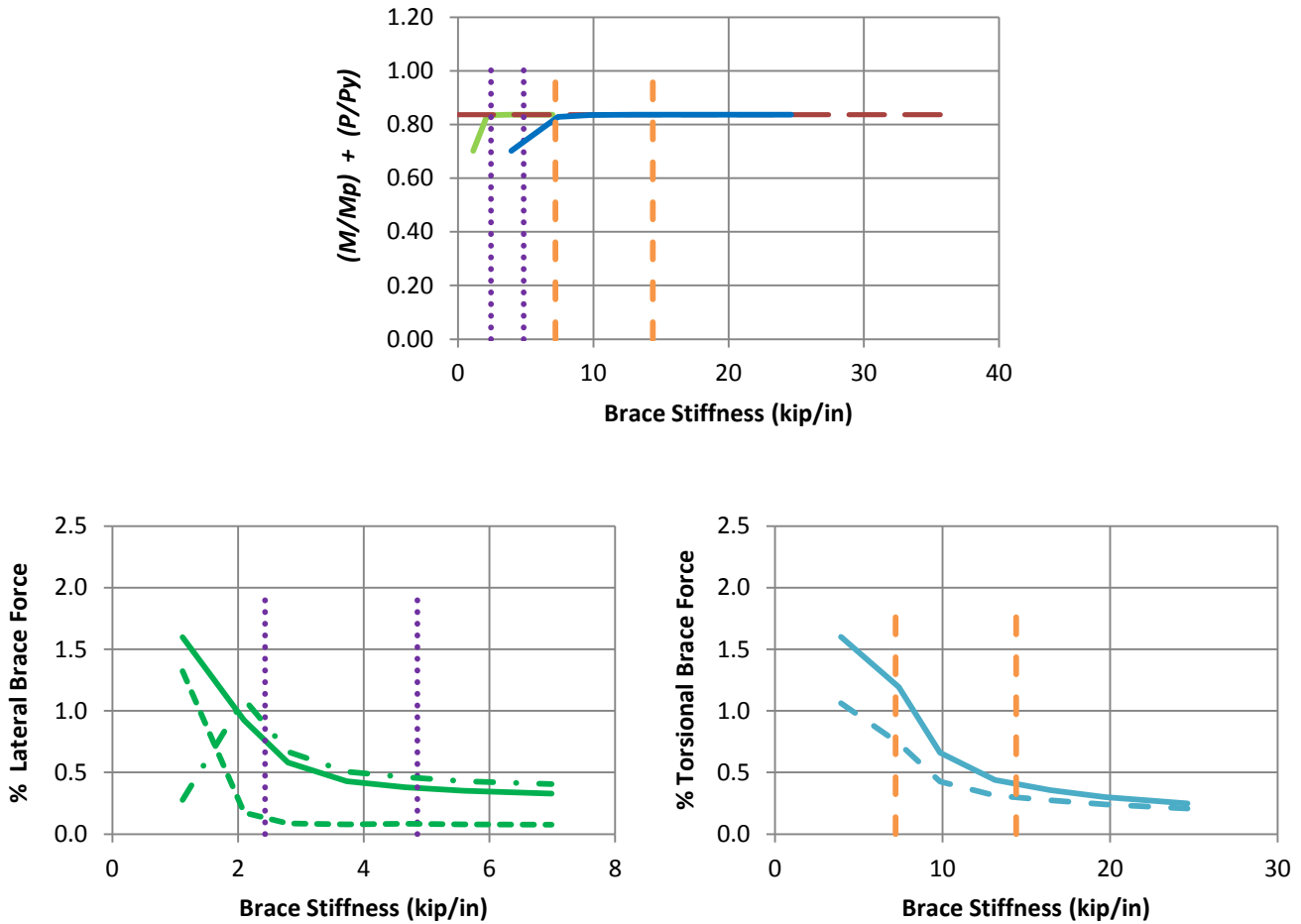
Fig. 6.16. (continued) Knuckle curves and brace force vs. brace stiffness plots for combined point (nodal) lateral and torsional bracing cases with $n = 1$ and constant axial load and uniform bending with lateral brace on the flange in flexural tension, $L_b = 15$ ft.



a) BC_UMp_CRTB_n2_Lb5_FFR-0.67

- Rigidly-braced strength
- Test simulation results corresponding to torsional brace
- Test simulation results corresponding to lateral brace
- 1x and 0.5x lateral bracing stiffness from Eq. 6-7
- - - 1x and 0.5x torsional bracing stiffness from Eq. 6-8
- Left end panel shear force
- - - Right end panel shear force
- Torsional brace force 1
- - - Middle panel shear force
- Torsional brace force 2

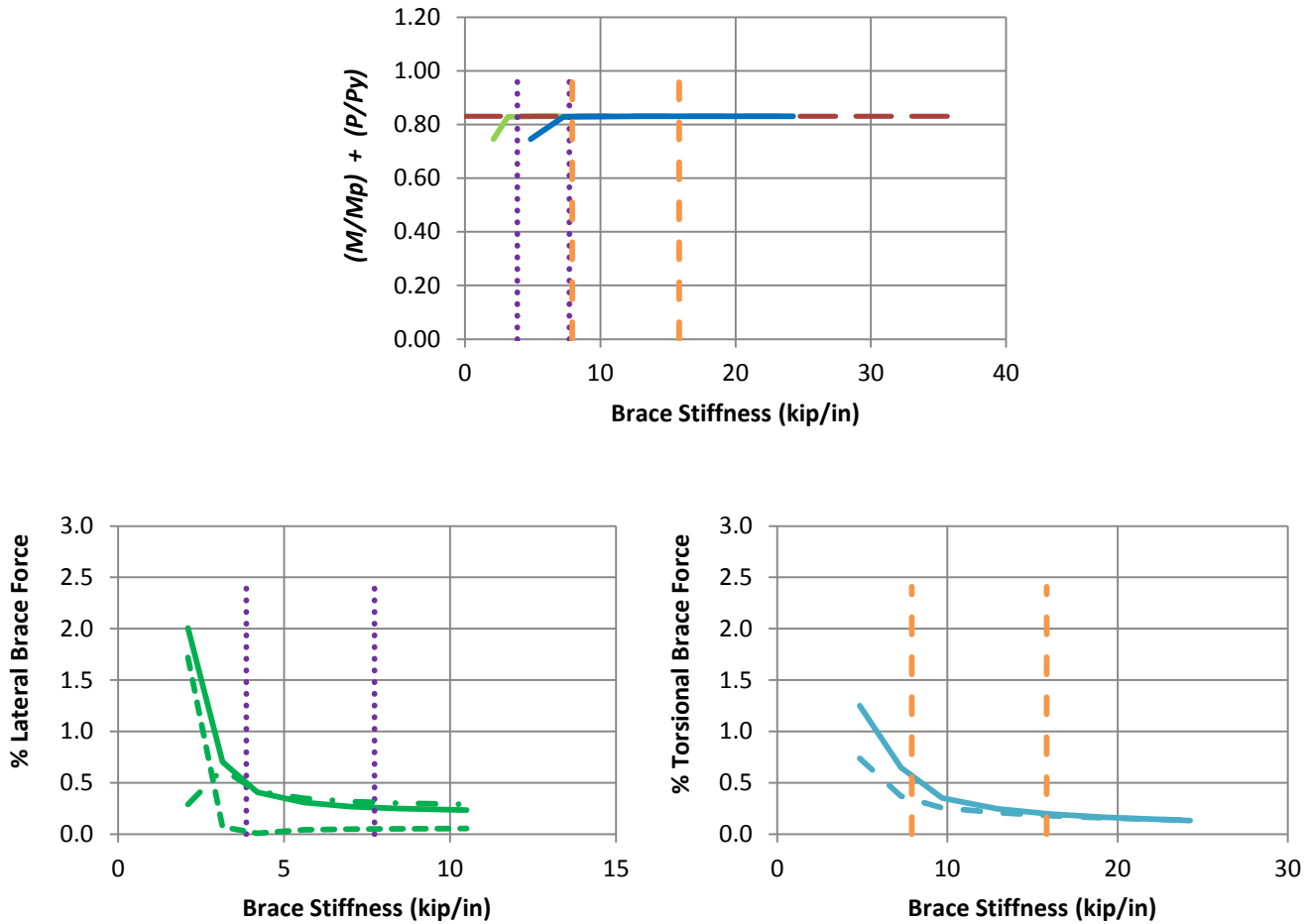
Fig. 6.17. Knuckle curves and brace force vs. brace stiffness plots for combined shear panel (relative) lateral and torsional bracing cases with $n = 2$ and constant axial load and uniform bending with lateral brace on the flange in flexural compression, $L_b = 5$ ft.



b) BC_UMp_CRTB_n2_Lb5_FFR-0.33

- Rigidly-braced strength
- Test simulation results corresponding to torsional brace
- Test simulation results corresponding to lateral brace
- 1x and 0.5x lateral bracing stiffness from Eq. 6-7
- - - 1x and 0.5x torsional bracing stiffness from Eq. 6-8
- Left end panel shear force
- - - Right end panel shear force
- . - Middle panel shear force
- Torsional brace force 1
- - - Torsional brace force 2

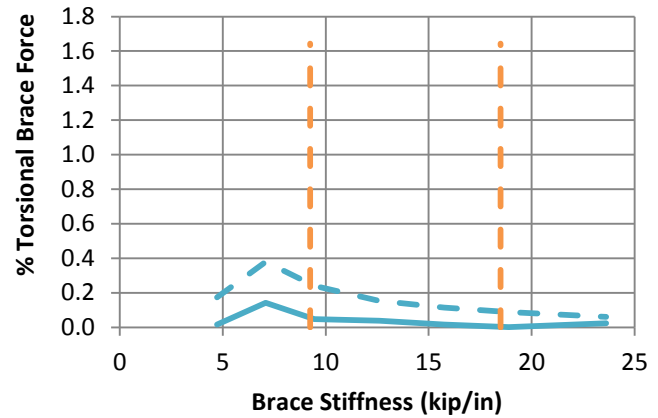
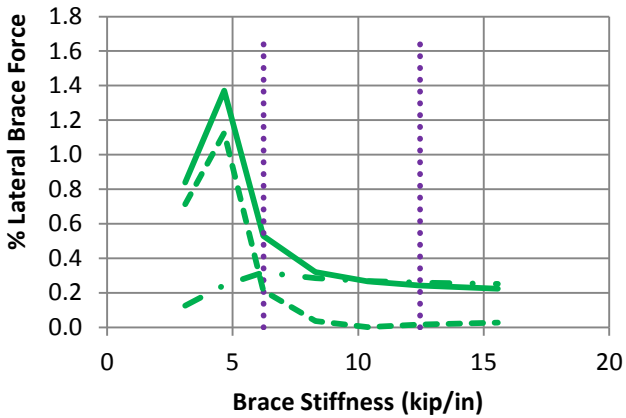
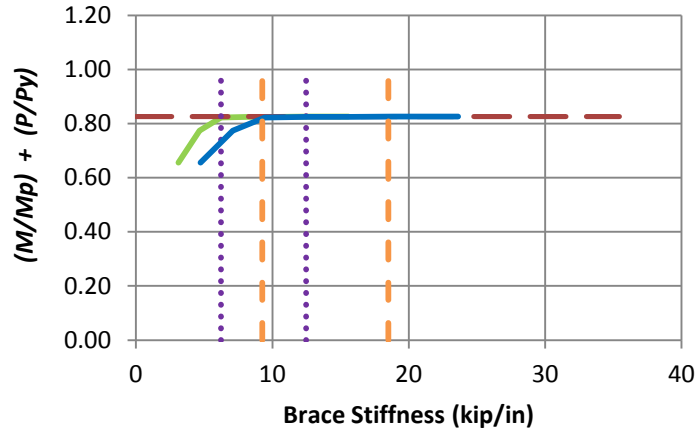
Fig. 6.17. (continued) Knuckle curves and brace force vs. brace stiffness plots for combined shear panel (relative) lateral and torsional bracing cases with $n = 2$ and constant axial load and uniform bending with lateral brace on the flange in flexural compression, $L_b = 5$ ft.



c) BC_UMp_CRTB_n2_Lb5_FFR0

- — Rigidly-braced strength
- Test simulation results corresponding to torsional brace
- Test simulation results corresponding to lateral brace
- 1x and 0.5x lateral bracing stiffness from Eq. 6-7
- — 1x and 0.5x torsional bracing stiffness from Eq. 6-8
- Left end panel shear force
- Right end panel shear force
- • — Middle panel shear force
- Torsional brace force 1
- Torsional brace force 2

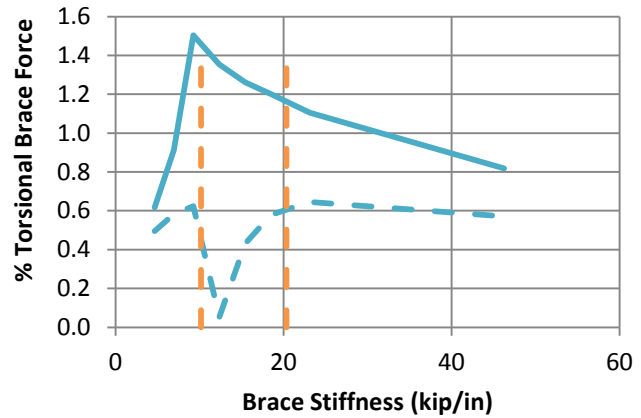
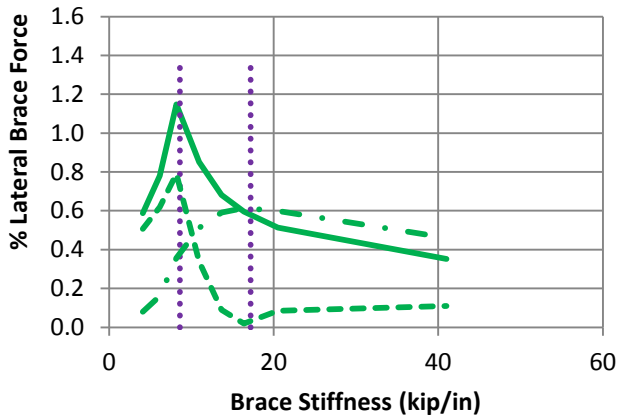
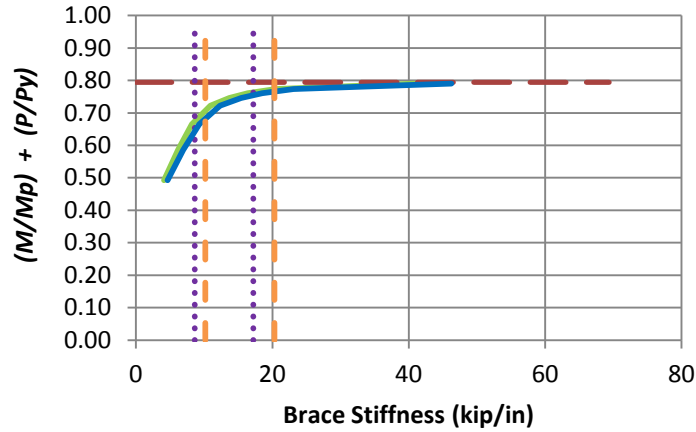
Fig. 6.17. (continued) Knuckle curves and brace force vs. brace stiffness plots for combined shear panel (relative) lateral and torsional bracing cases with $n = 2$ and constant axial load and uniform bending with lateral brace on the flange in flexural compression, $L_b = 5$ ft.



d) BC_UMp_CRTB_n2_Lb5_FFR0.5

- Rigidly-braced strength
- Test simulation results corresponding to torsional brace
- Test simulation results corresponding to lateral brace
- 1x and 0.5x lateral bracing stiffness from Eq. 6-7
- - - 1x and 0.5x torsional bracing stiffness from Eq. 6-8
- Left end panel shear force
- - - Right end panel shear force
- . - Middle panel shear force
- Torsional brace force 1
- Torsional brace force 2

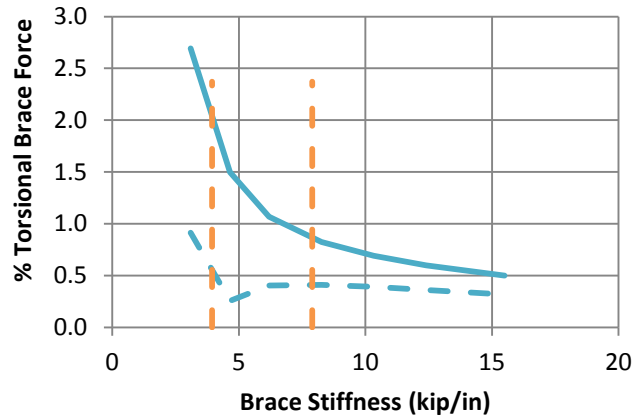
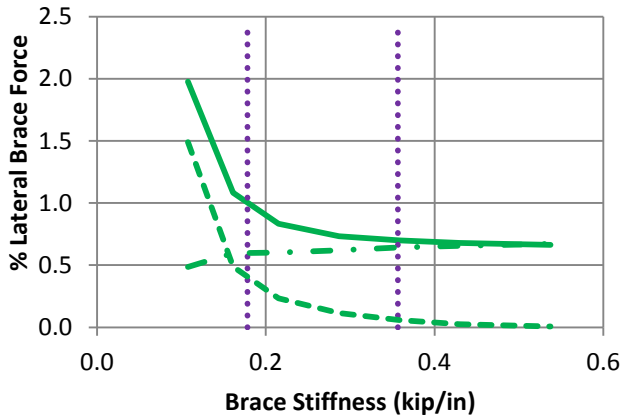
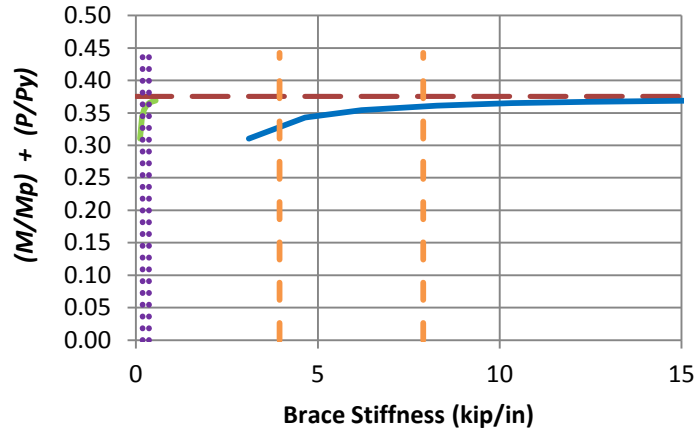
Fig. 6.17. (continued) Knuckle curves and brace force vs. brace stiffness plots for combined shear panel (relative) lateral and torsional bracing cases with $n = 2$ and constant axial load and uniform bending with lateral brace on the flange in flexural compression, $L_b = 5\text{ft}$.



e) BC_UMp_CRTB_n2_Lb5_FFR1

- Rigidly-braced strength
- Test simulation results corresponding to torsional brace
- Test simulation results corresponding to lateral brace
- 1x and 0.5x lateral bracing stiffness from Eq. 6-7
- - - 1x and 0.5x torsional bracing stiffness from Eq. 6-8
- Left end panel shear force
- - - Right end panel shear force
- . - Middle panel shear force
- Torsional brace force 1
- - - Torsional brace force 2

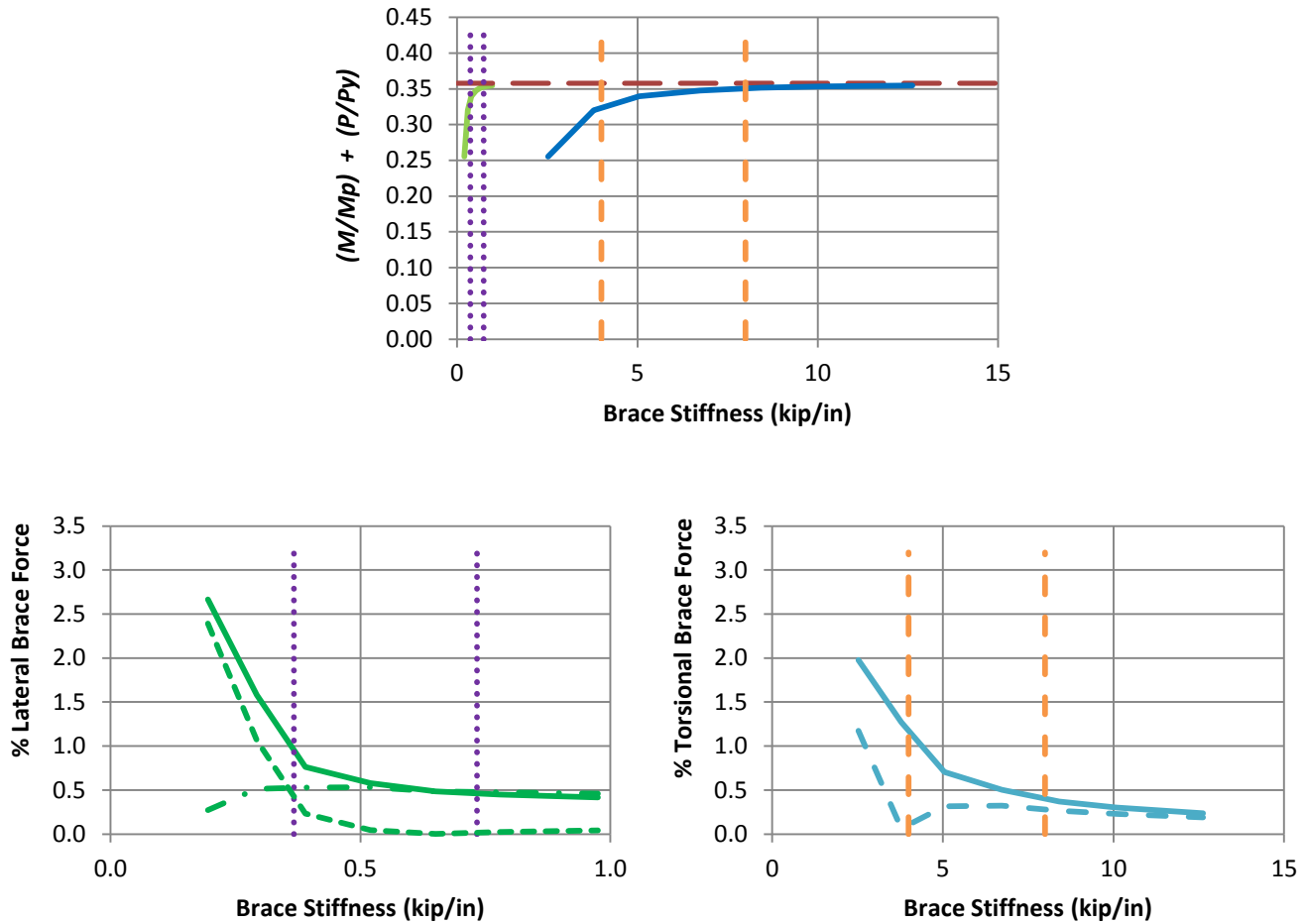
Fig. 6.17. (continued) Knuckle curves and brace force vs. brace stiffness plots for combined shear panel (relative) lateral and torsional bracing cases with $n = 2$ and constant axial load and uniform bending with lateral brace on the flange in flexural compression, $L_b = 5\text{ft}$.



a) BC_UMp_CRTB_n2_Lb15_FFR-0.67

- Rigidly-braced strength
- Test simulation results corresponding to torsional brace
- Test simulation results corresponding to lateral brace
- 1x and 0.5x lateral bracing stiffness from Eq. 6-7
- 1x and 0.5x torsional bracing stiffness from Eq. 6-8
- Left end panel shear force
- Right end panel shear force
- Middle panel shear force
- Torsional brace force 1
- Torsional brace force 2

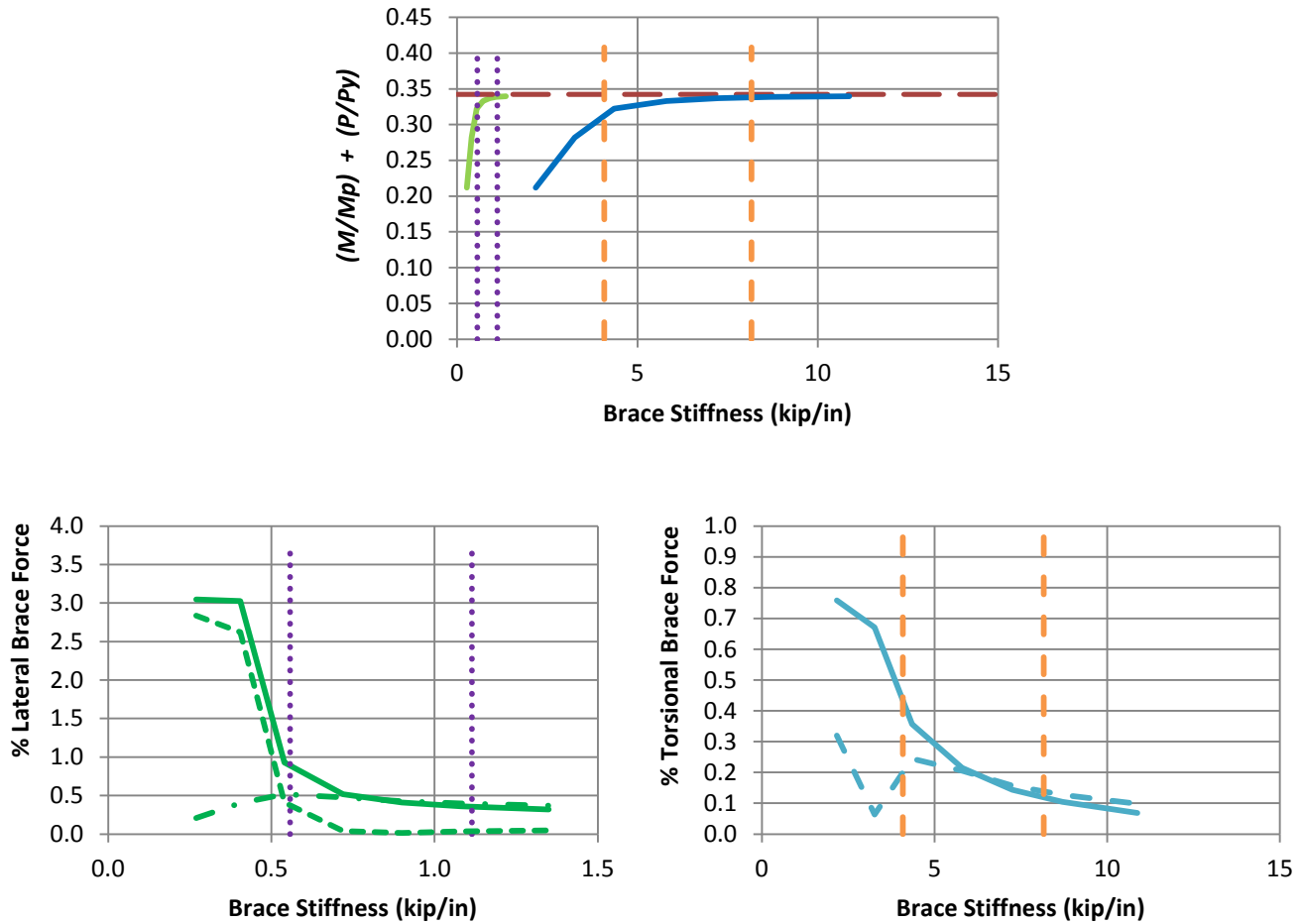
Fig. 6.18. Knuckle curves and brace force vs. brace stiffness plots for combined shear panel (relative) lateral and torsional bracing cases with $n = 2$ and constant axial load and uniform bending with lateral brace on the flange in flexural compression, $L_b = 15$ ft.



b) BC_UMp_CRTB_n2_Lb15_FFR-0.33

- Rigidly-braced strength
- Test simulation results corresponding to torsional brace
- Test simulation results corresponding to lateral brace
- 1x and 0.5x lateral bracing stiffness from Eq. 6-7
- - - 1x and 0.5x torsional bracing stiffness from Eq. 6-8
- Left end panel shear force
- - - Right end panel shear force
- . - Middle panel shear force
- Torsional brace force 1
- - - Torsional brace force 2

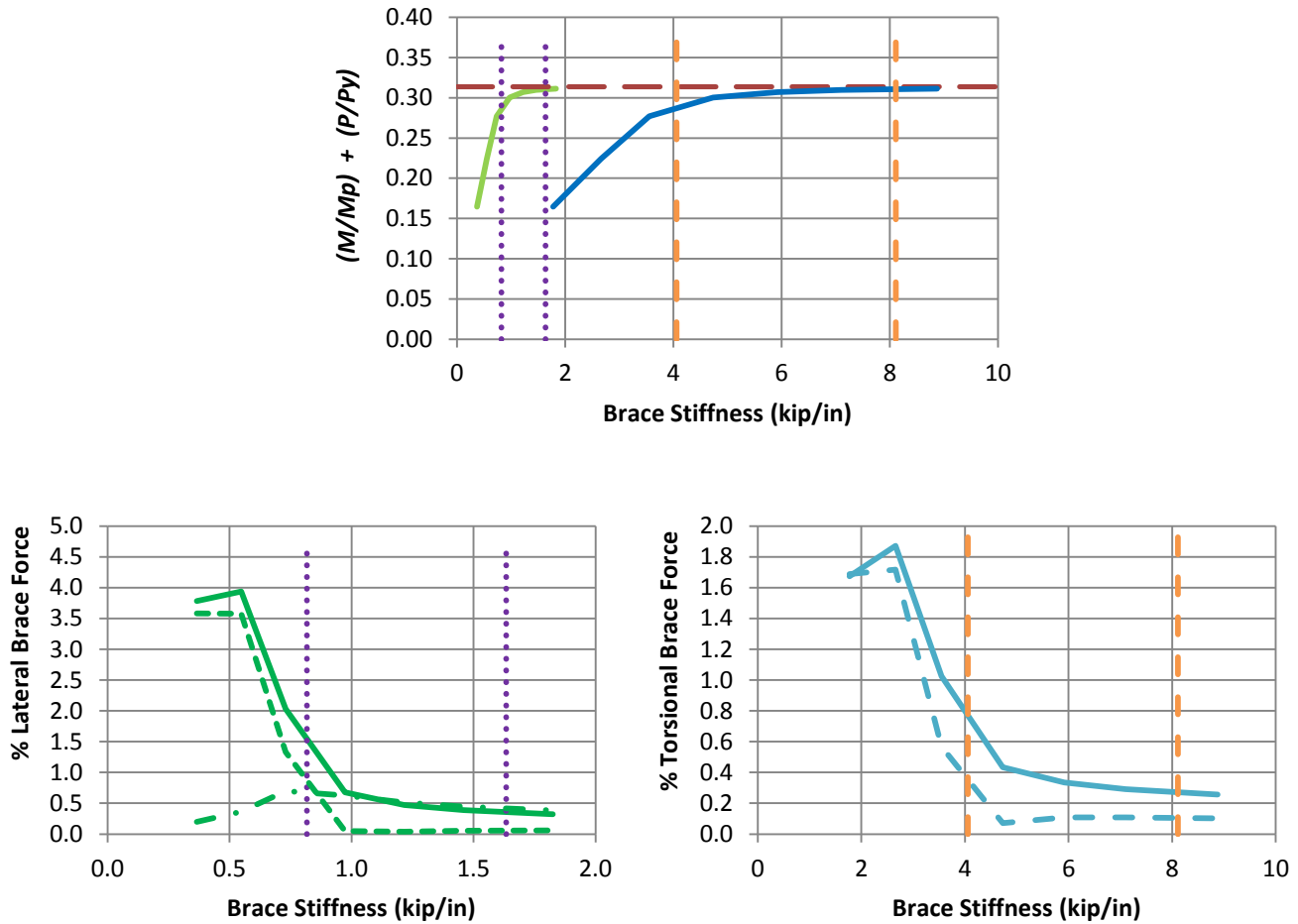
Fig. 6.18. (continued) Knuckle curves and brace force vs. brace stiffness plots for combined shear panel (relative) lateral and torsional bracing cases with $n = 2$ and constant axial load and uniform bending with lateral brace on the flange in flexural compression, $L_b = 15$ ft.



c) BC_UMp_CRTB_n2_Lb15_FFR0

- Rigidly-braced strength
- Test simulation results corresponding to torsional brace
- Test simulation results corresponding to lateral brace
- 1x and 0.5x lateral bracing stiffness from Eq. 6-7
- - - 1x and 0.5x torsional bracing stiffness from Eq. 6-8
- Left end panel shear force
- - - Right end panel shear force
- . - Middle panel shear force
- Torsional brace force 1
- - - Torsional brace force 2

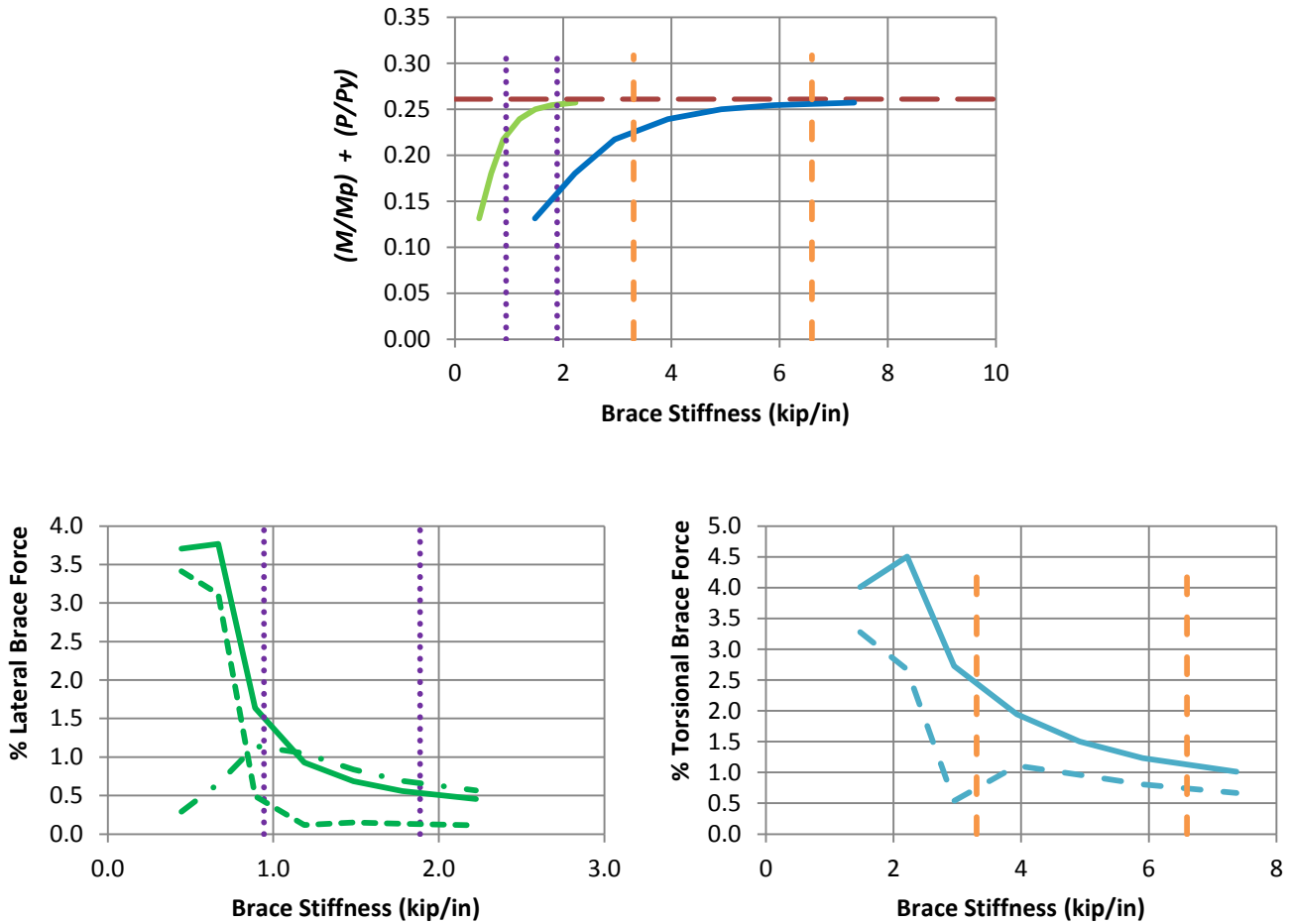
Fig. 6.18. (continued) Knuckle curves and brace force vs. brace stiffness plots for combined shear panel (relative) lateral and torsional bracing cases with $n = 2$ and constant axial load and uniform bending with lateral brace on the flange in flexural compression, $L_b = 15$ ft.



d) BC_UMp_CRTB_n2_Lb15_FFR0.5

- Rigidly-braced strength
- Test simulation results corresponding to torsional brace
- Test simulation results corresponding to lateral brace
- 1x and 0.5x lateral bracing stiffness from Eq. 6-7
- - - 1x and 0.5x torsional bracing stiffness from Eq. 6-8
- Left end panel shear force
- - - Right end panel shear force
- . - Middle panel shear force
- Torsional brace force 1
- - - Torsional brace force 2

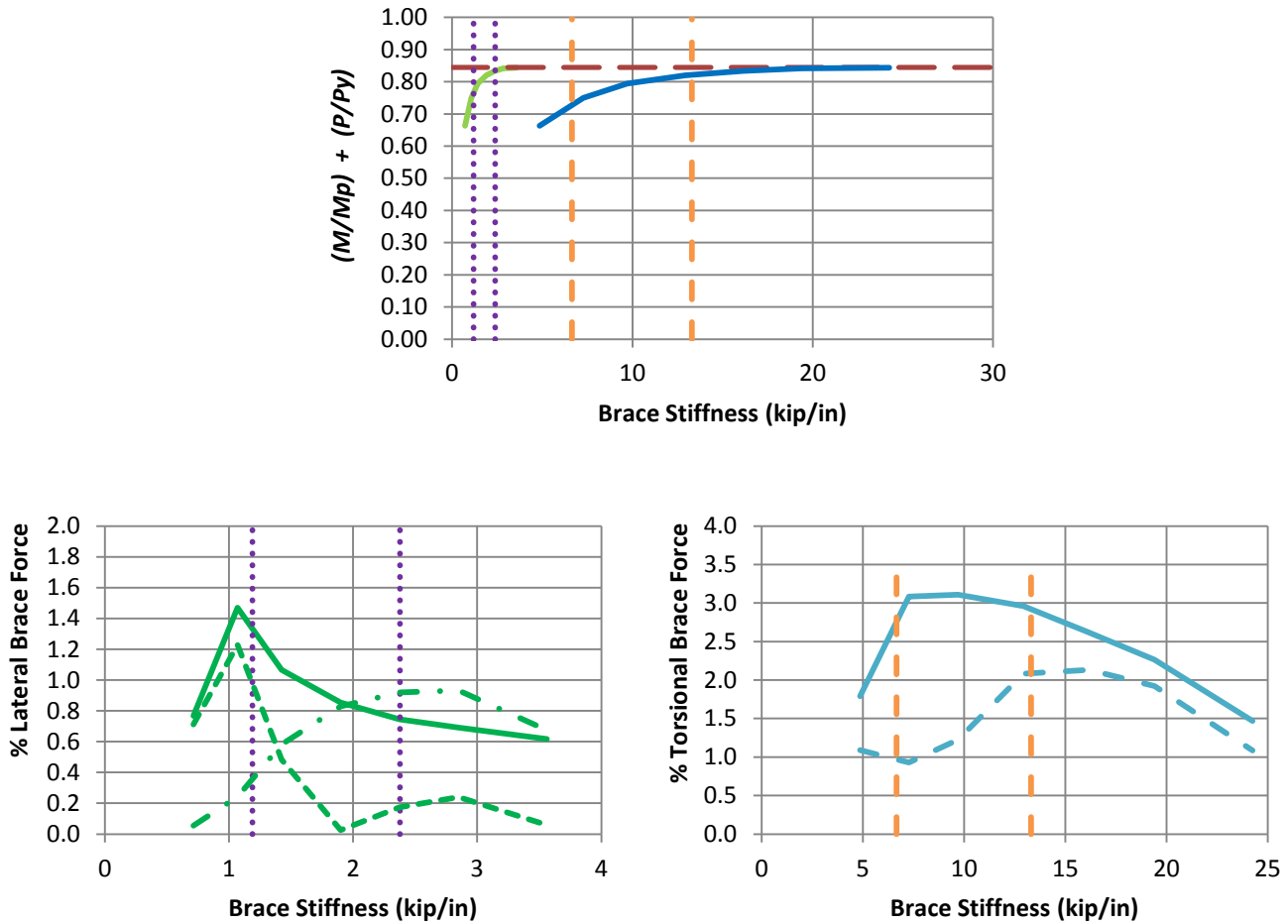
Fig. 6.18. (continued) Knuckle curves and brace force vs. brace stiffness plots for combined shear panel (relative) lateral and torsional bracing cases with $n = 2$ and constant axial load and uniform bending with lateral brace on the flange in flexural compression, $L_b = 15$ ft.



e) BC_UMp_CRTB_n2_Lb15_FFR1

- Rigidly-braced strength
- Test simulation results corresponding to torsional brace
- Test simulation results corresponding to lateral brace
- 1x and 0.5x lateral bracing stiffness from Eq. 6-7
- - - 1x and 0.5x torsional bracing stiffness from Eq. 6-8
- Left end panel shear force
- - - Right end panel shear force
- . - Middle panel shear force
- Torsional brace force 1
- - - Torsional brace force 2

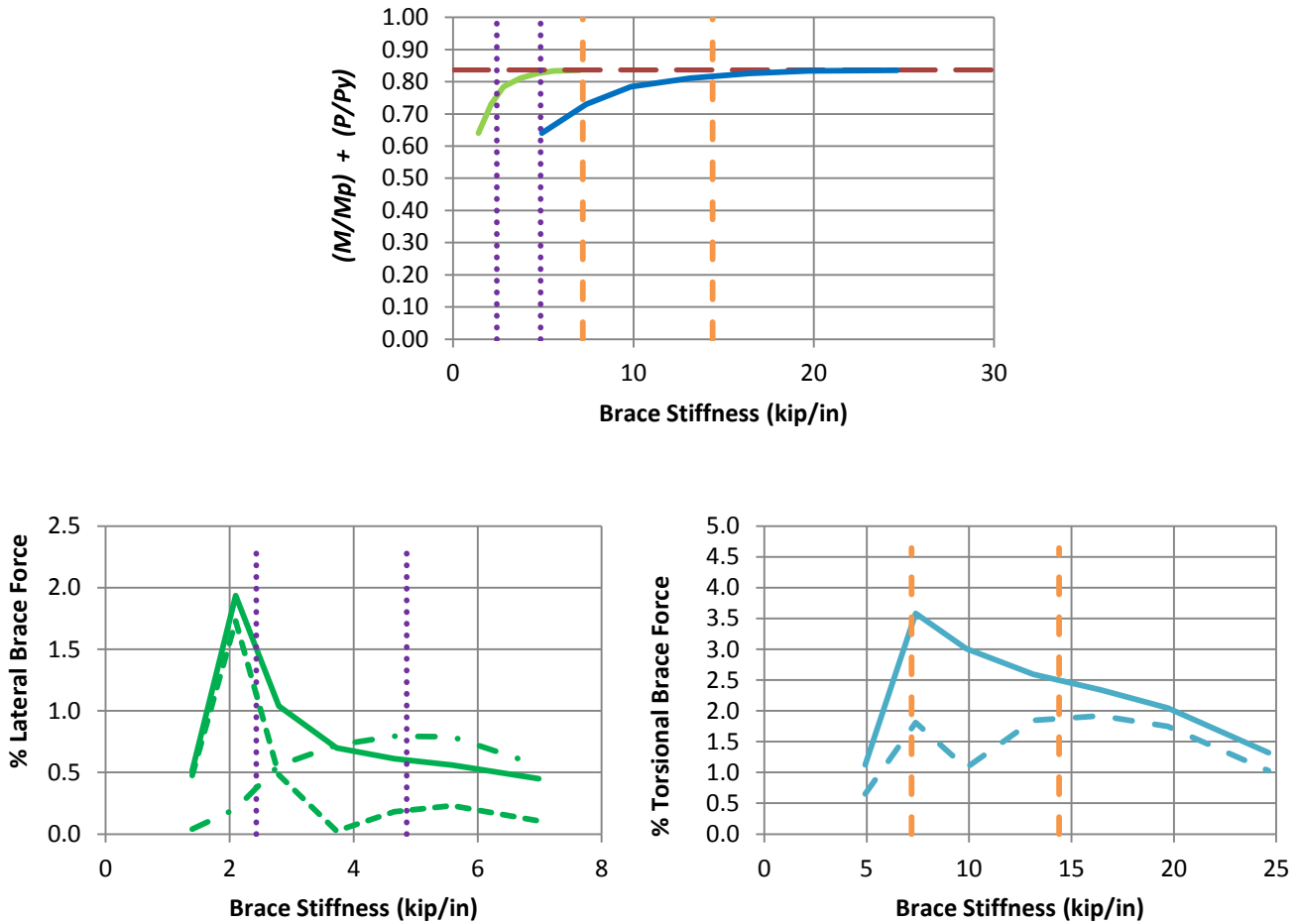
Fig. 6.18. (continued) Knuckle curves and brace force vs. brace stiffness plots for combined shear panel (relative) lateral and torsional bracing cases with $n = 2$ and constant axial load and uniform bending with lateral brace on the flange in flexural compression, $L_b = 15$ ft.



a) BC_UMn_CRTB_n2_Lb5_FFR-0.67

- Rigidly-braced strength
- Test simulation results corresponding to torsional brace
- Test simulation results corresponding to lateral brace
- 1x and 0.5x lateral bracing stiffness from Eq. 6-7
- - - 1x and 0.5x torsional bracing stiffness from Eq. 6-8
- Left end panel shear force
- - - Right end panel shear force
- . - Middle panel shear force
- Torsional brace force 1
- - - Torsional brace force 2

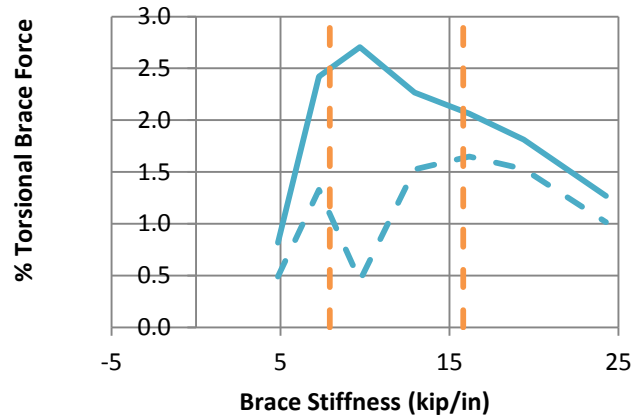
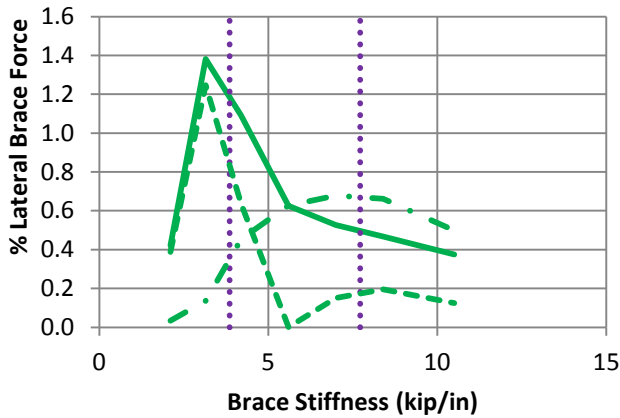
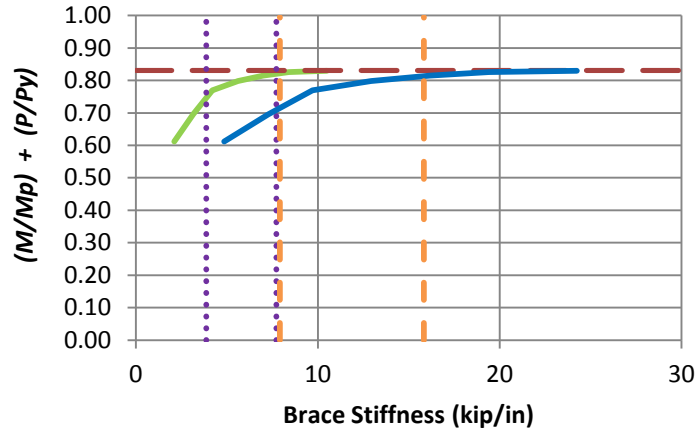
Fig. 6.19. Knuckle curves and brace force vs. brace stiffness plots for combined shear panel (relative) lateral and torsional bracing cases with $n = 2$ and constant axial load and uniform bending with lateral brace on the flange in flexural tension, $L_b = 5$ ft.



b) BC_UMn_CRTB_n2_Lb5_FFR-0.33

- Rigidly-braced strength
- Test simulation results corresponding to torsional brace
- Test simulation results corresponding to lateral brace
- 1x and 0.5x lateral bracing stiffness from Eq. 6-7
- 1x and 0.5x torsional bracing stiffness from Eq. 6-8
- Left end panel shear force
- Right end panel shear force
- Middle panel shear force
- Torsional brace force 1
- Torsional brace force 2

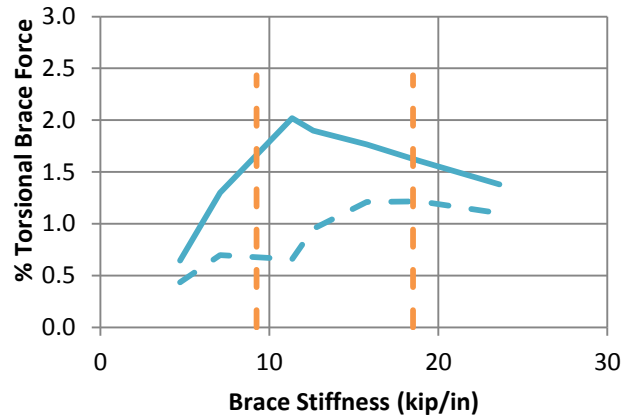
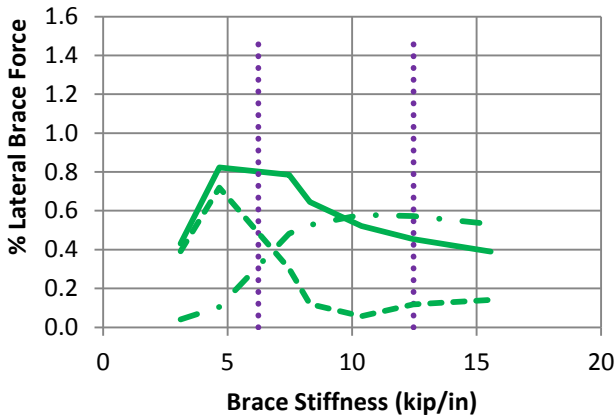
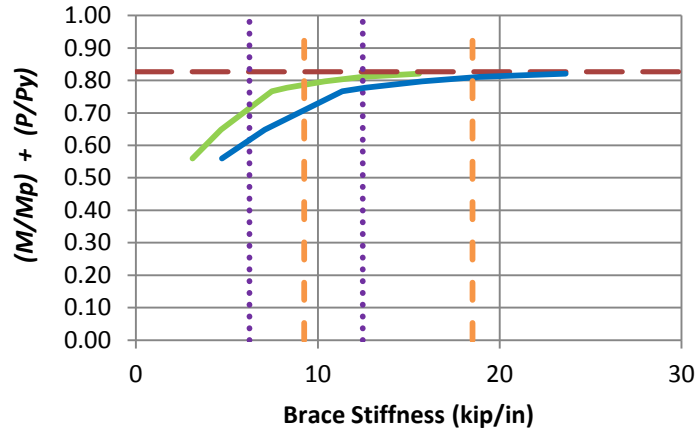
Fig. 6.19. (continued) Knuckle curves and brace force vs. brace stiffness plots for combined shear panel (relative) lateral and torsional bracing cases with $n = 2$ and constant axial load and uniform bending with lateral brace on the flange in flexural tension, $L_b = 5$ ft.



c) BC_UMn_CRTB_n2_Lb5_FFR0

- — Rigidly-braced strength
- Test simulation results corresponding to torsional brace
- Test simulation results corresponding to lateral brace
- ⋯ 1x and 0.5x lateral bracing stiffness from Eq. 6-7
- — 1x and 0.5x torsional bracing stiffness from Eq. 6-8
- Left end panel shear force
- - - Right end panel shear force
- · - Middle panel shear force
- Torsional brace force 1
- - - Torsional brace force 2

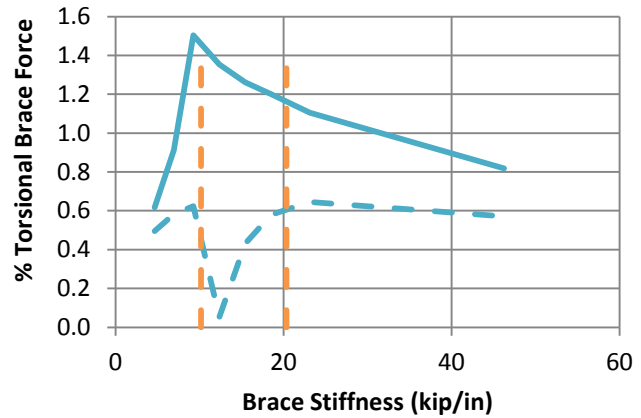
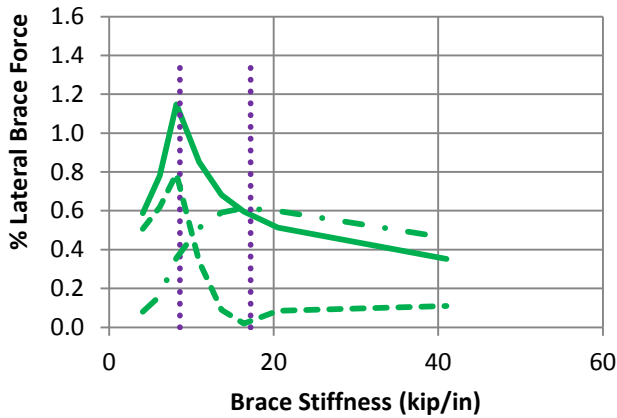
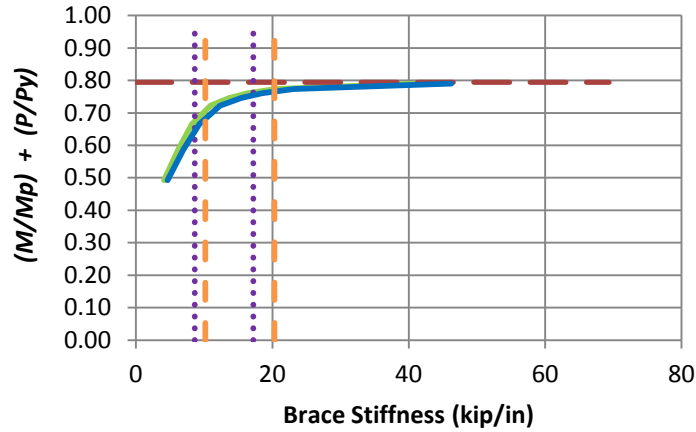
Fig. 6.19. (continued) Knuckle curves and brace force vs. brace stiffness plots for combined shear panel (relative) lateral and torsional bracing cases with $n = 2$ and constant axial load and uniform bending with lateral brace on the flange in flexural tension, $L_b = 5$ ft.



d) BC_UMn_CRTB_n2_Lb5_FFR0.5

- Rigidly-braced strength
- Test simulation results corresponding to torsional brace
- Test simulation results corresponding to lateral brace
- 1x and 0.5x lateral bracing stiffness from Eq. 6-7
- - - 1x and 0.5x torsional bracing stiffness from Eq. 6-8
- Left end panel shear force
- - - Right end panel shear force
- . - Middle panel shear force
- Torsional brace force 1
- - - Torsional brace force 2

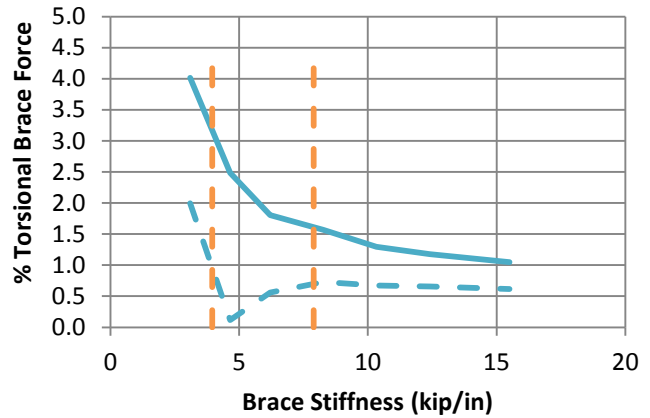
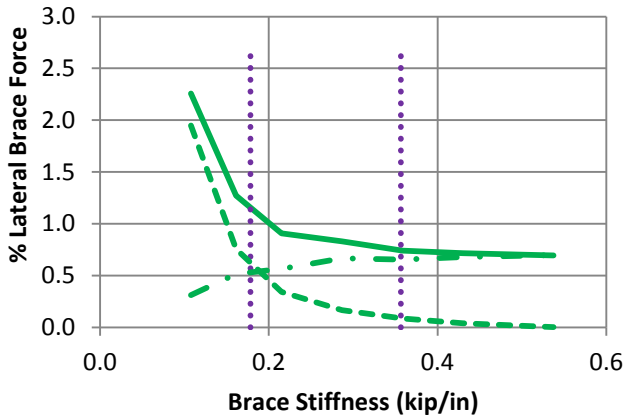
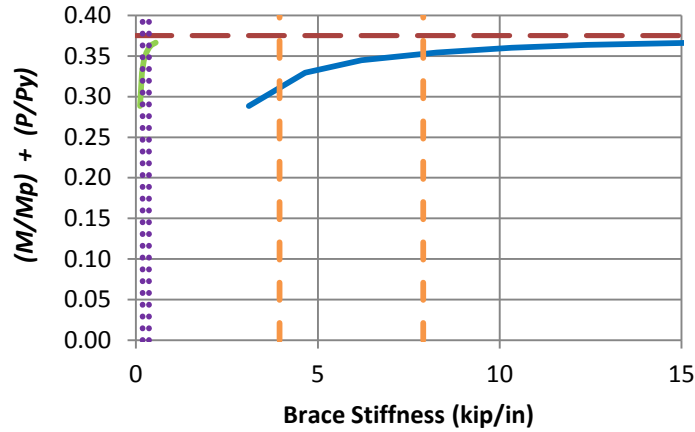
Fig. 6.19. (continued) Knuckle curves and brace force vs. brace stiffness plots for combined shear panel (relative) lateral and torsional bracing cases with $n = 2$ and constant axial load and uniform bending with lateral brace on the flange in flexural tension, $L_b = 5$ ft.



e) BC_UMn_CRTB_n2_Lb5_FFR1

- Rigidly-braced strength
- Test simulation results corresponding to torsional brace
- Test simulation results corresponding to lateral brace
- 1x and 0.5x lateral bracing stiffness from Eq. 6-7
- - - 1x and 0.5x torsional bracing stiffness from Eq. 6-8
- Left end panel shear force
- - - Right end panel shear force
- . - Middle panel shear force
- Torsional brace force 1
- - - Torsional brace force 2

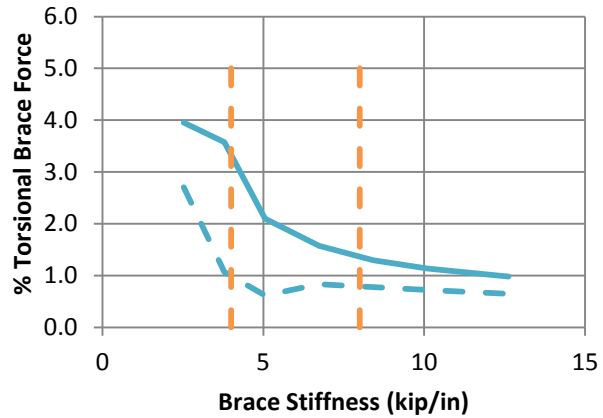
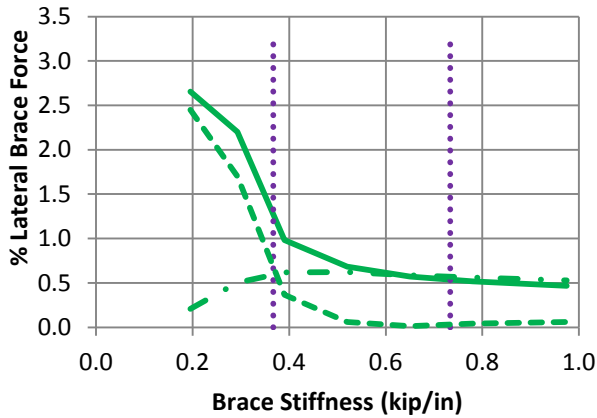
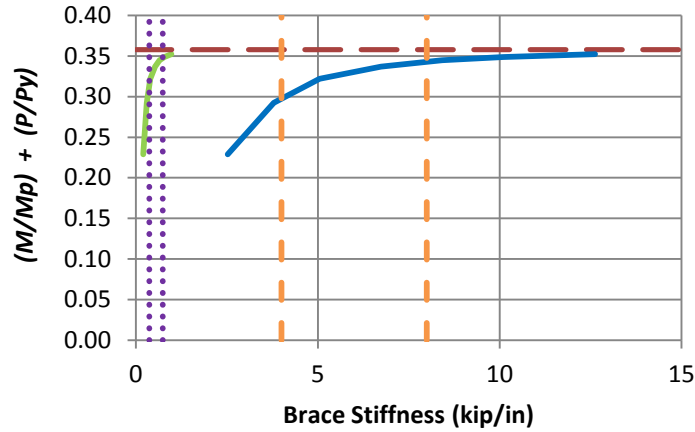
Fig. 6.19. (continued) Knuckle curves and brace force vs. brace stiffness plots for combined shear panel (relative) lateral and torsional bracing cases with $n = 2$ and constant axial load and uniform bending with lateral brace on the flange in flexural tension, $L_b = 5\text{ft}$.



a) BC_UMn_CRTB_n2_Lb15_FFR-0.67

- Rigidly-braced strength
- Test simulation results corresponding to torsional brace
- Test simulation results corresponding to lateral brace
- 1x and 0.5x lateral bracing stiffness from Eq. 6-7
- 1x and 0.5x torsional bracing stiffness from Eq. 6-8
- Left end panel shear force
- Right end panel shear force
- Middle panel shear force
- Torsional brace force 1
- Torsional brace force 2

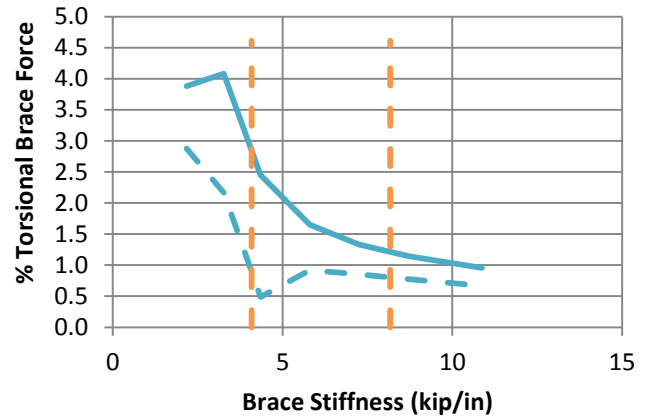
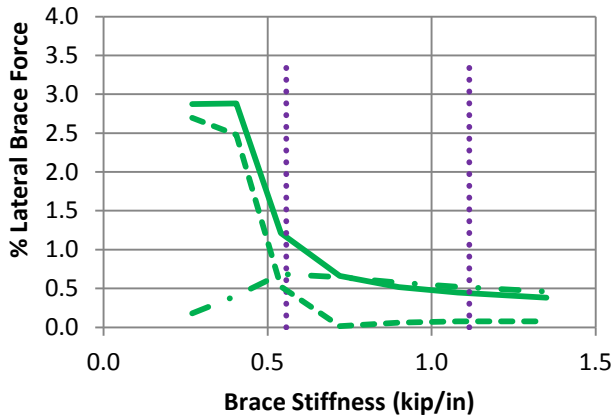
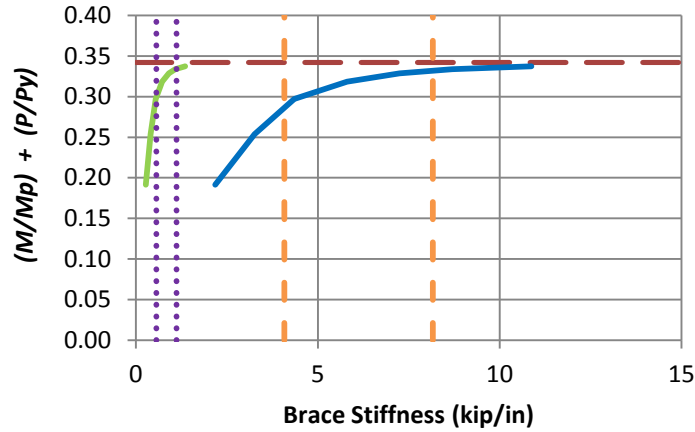
Fig. 6.20. Knuckle curves and brace force vs. brace stiffness plots for combined shear panel (relative) lateral and torsional bracing cases with $n = 2$ and constant axial load and uniform bending with lateral brace on the flange in flexural tension, $L_b = 15\text{ft}$.



b) BC_UMn_CRTB_n2_Lb15_FFR-0.33

- — Rigidly-braced strength
- Test simulation results corresponding to torsional brace
- Test simulation results corresponding to lateral brace
- 1x and 0.5x lateral bracing stiffness from Eq. 6-7
- — 1x and 0.5x torsional bracing stiffness from Eq. 6-8
- Left end panel shear force
- — Right end panel shear force
- • — Middle panel shear force
- Torsional brace force 1
- — Torsional brace force 2

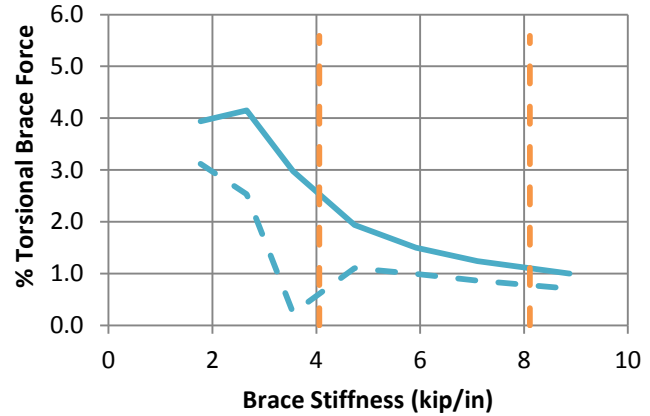
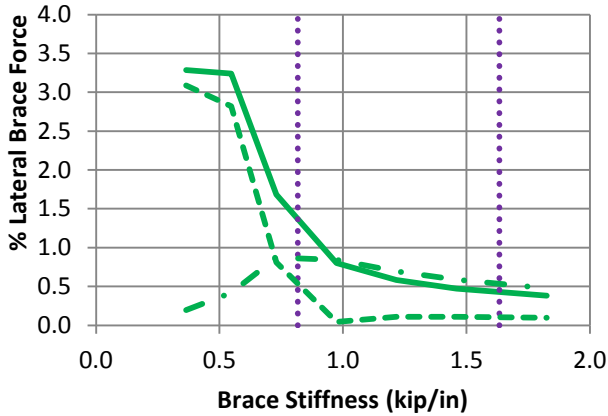
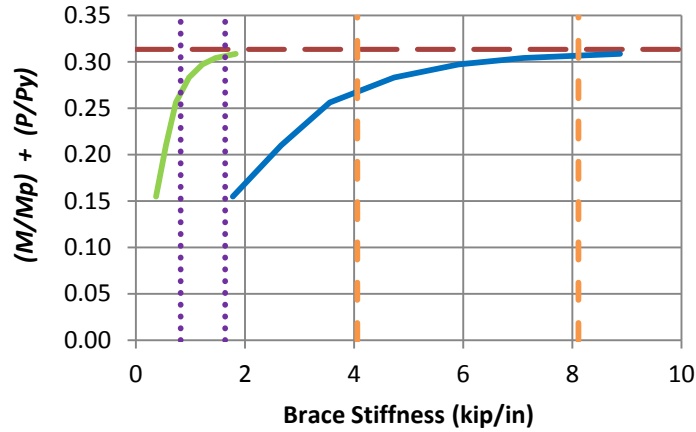
Fig. 6.20. (continued) Knuckle curves and brace force vs. brace stiffness plots for combined shear panel (relative) lateral and torsional bracing cases with $n = 2$ and constant axial load and uniform bending with lateral brace on the flange in flexural tension, $L_b = 15$ ft.



c) BC_UMn_CRTB_n2_Lb15_FFR0

- Rigidly-braced strength
- Test simulation results corresponding to torsional brace
- Test simulation results corresponding to lateral brace
- 1x and 0.5x lateral bracing stiffness from Eq. 6-7
- - - 1x and 0.5x torsional bracing stiffness from Eq. 6-8
- Left end panel shear force
- - - Right end panel shear force
- . - Middle panel shear force
- Torsional brace force 1
- - - Torsional brace force 2

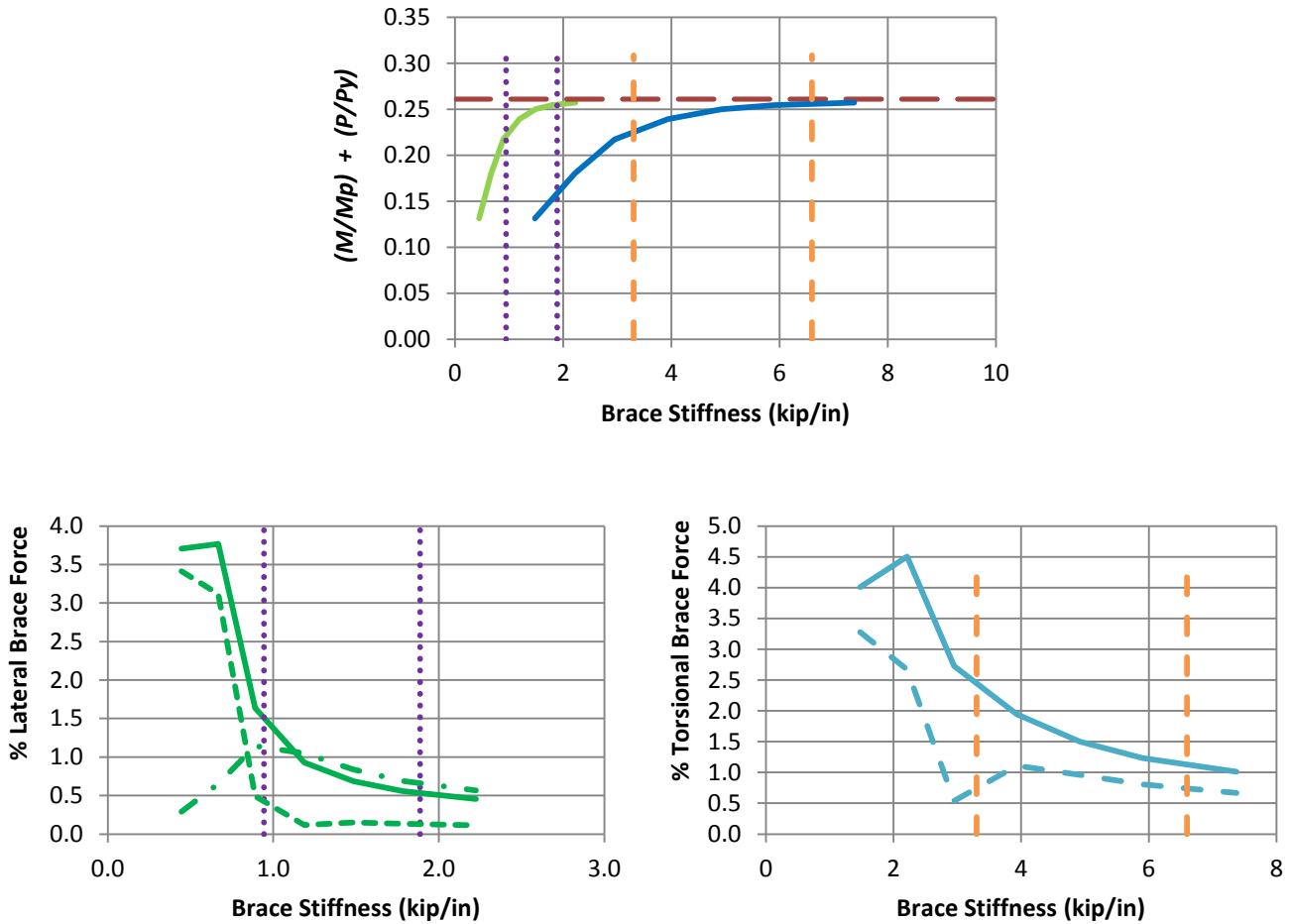
Fig. 6.20. (continued) Knuckle curves and brace force vs. brace stiffness plots for combined shear panel (relative) lateral and torsional bracing cases with $n = 2$ and constant axial load and uniform bending with lateral brace on the flange in flexural tension, $L_b = 15$ ft.



d) BC_UMn_CRTB_n2_Lb15_FFR0.5

- — Rigidly-braced strength
- Test simulation results corresponding to torsional brace
- Test simulation results corresponding to lateral brace
- 1x and 0.5x lateral bracing stiffness from Eq. 6-7
- - - 1x and 0.5x torsional bracing stiffness from Eq. 6-8
- Left end panel shear force
- - - Right end panel shear force
- . - Middle panel shear force
- Torsional brace force 1
- - - Torsional brace force 2

Fig. 6.20. (continued) Knuckle curves and brace force vs. brace stiffness plots for combined shear panel (relative) lateral and torsional bracing cases with $n = 2$ and constant axial load and uniform bending with lateral brace on the flange in flexural tension, $L_b = 15$ ft.



e) BC_UMn_CRTB_n2_Lb15_FFR1

- Rigidly-braced strength
- Test simulation results corresponding to torsional brace
- Test simulation results corresponding to lateral brace
- 1x and 0.5x lateral bracing stiffness from Eq. 6-7
- - - 1x and 0.5x torsional bracing stiffness from Eq. 6-8
- Left end panel shear force
- - - Right end panel shear force
- . - Middle panel shear force
- Torsional brace force 1
- - - Torsional brace force 2

Fig. 6.20. (continued) Knuckle curves and brace force vs. brace stiffness plots for combined shear panel (relative) lateral and torsional bracing cases with $n = 2$ and constant axial load and uniform bending with lateral brace on the flange in flexural tension, $L_b = 15\text{ft}$.

Table 6.3. Comparison of simulation results in Figs. 6.13 through 6.20 with Eq. 6-7.

Case (a)	Lateral bracing stiffness corresponding to 96% of simulation rigidly-braced strength (kip/in) (b)	Required lateral bracing stiffness from Eq. 6-7 (kip/in) (c)	Col. (b) / Col. (c) (d)
BC_UMp_CNTB_n1_Lb5_FFR-0.67	1.72	4.64	0.37
BC_UMp_CNTB_n1_Lb5_FFR-0.33	2.77	9.74	0.29
BC_UMp_CNTB_n1_Lb5_FFR0	5.81	15.34	0.38
BC_UMp_CNTB_n1_Lb5_FFR0.5	8.84	24.90	0.36
BC_UMp_CNTB_n1_Lb5_FFR1	26.91	33.82	0.80
BC_UMp_CNTB_n1_Lb15_FFR-0.67	0.38	0.68	0.56
BC_UMp_CNTB_n1_Lb15_FFR-0.33	0.74	1.42	0.52
BC_UMp_CNTB_n1_Lb15_FFR0	1.08	2.16	0.50
BC_UMp_CNTB_n1_Lb15_FFR0.5	1.84	3.18	0.58
BC_UMp_CNTB_n1_Lb15_FFR1	2.37	3.18	0.75
BC_UMp_CRTB_n2_Lb5_FFR-0.67	1.04	2.38	0.44
BC_UMp_CRTB_n2_Lb5_FFR-0.33	1.9	4.86	0.39
BC_UMp_CRTB_n2_Lb5_FFR0	2.76	7.72	0.36
BC_UMp_CRTB_n2_Lb5_FFR0.5	5.26	12.46	0.42
BC_UMp_CRTB_n2_Lb5_FFR1	16.75	17.20	0.98
BC_UMp_CRTB_n2_Lb15_FFR-0.67	0.28	0.36	0.79
BC_UMp_CRTB_n2_Lb15_FFR-0.33	0.45	0.74	0.62
BC_UMp_CRTB_n2_Lb15_FFR0	0.64	1.12	0.58

Table 6.3.(continued) Comparison of simulation results in Figs. 6.13 through 6.20 with Eq. 6-7.

Case (a)	Lateral bracing stiffness corresponding to 96% of simulation rigidly- braced strength (kip/in) (b)	Required lateral bracing stiffness from Eq. 6-7 (kip/in) (c)	Col. (b) / Col. (c) (d)
BC_UMp_CRTB_n2_Lb15_FFR0.5	1	1.64	0.62
BC_UMp_CRTB_n2_Lb15_FFR1	1.53	1.88	0.81
BC_UMn_CNTB_n1_Lb5_FFR-0.67	2.62	4.64	0.57
BC_UMn_CNTB_n1_Lb5_FFR-0.33	5.33	9.74	0.55
BC_UMn_CNTB_n1_Lb5_FFR0	8.7	15.34	0.57
BC_UMn_CNTB_n1_Lb5_FFR0.5	15.63	24.90	0.63
BC_UMn_CNTB_n1_Lb5_FFR1	26.91	33.82	0.80
BC_UMn_CNTB_n1_Lb15_FFR-0.67	0.47	0.68	0.68
BC_UMn_CNTB_n1_Lb15_FFR-0.33	0.95	1.42	0.67
BC_UMn_CNTB_n1_Lb15_FFR0	1.4	2.16	0.65
BC_UMn_CNTB_n1_Lb15_FFR0.5	2.1	3.18	0.66
BC_UMn_CNTB_n1_Lb15_FFR1	2.37	3.18	0.75
BC_UMn_CRTB_n2_Lb5_FFR-0.67	1.73	2.38	0.73
BC_UMn_CRTB_n2_Lb5_FFR-0.33	3.46	4.86	0.71
BC_UMn_CRTB_n2_Lb5_FFR0	5.56	7.72	0.72
BC_UMn_CRTB_n2_Lb5_FFR0.5	9.91	12.46	0.80
BC_UMn_CRTB_n2_Lb5_FFR1	16.75	17.20	0.98
BC_UMn_CRTB_n2_Lb15_FFR-0.67	0.36	0.36	1.02
BC_UMn_CRTB_n2_Lb15_FFR-0.33	0.63	0.74	0.86
BC_UMn_CRTB_n2_Lb15_FFR0	0.89	1.12	0.81
BC_UMn_CRTB_n2_Lb15_FFR0.5	1.35	1.64	0.83
BC_UMn_CRTB_n2_Lb15_FFR1	1.53	1.88	0.81

Table 6.4. Comparison of simulation results in Figs. 6.13 through 6.20 with Eq. 6-8.

Case (a)	Torsional bracing stiffness corresponding to 96% of simulation rigidly-braced strength (kip/in) (b)	Required torsional bracing stiffness from Eq. 6-8 (kip/in) (c)	Col. (c) / Col. (d) (d)
BC_UMp_CNTB_n1_Lb5_FFR-0.67	7.91	17.70	0.45
BC_UMp_CNTB_n1_Lb5_FFR-0.33	6.45	19.32	0.34
BC_UMp_CNTB_n1_Lb5_FFR0	8.78	21.24	0.42
BC_UMp_CNTB_n1_Lb5_FFR0.5	8.91	24.74	0.36
BC_UMp_CNTB_n1_Lb5_FFR1	20.19	26.20	0.77
BC_UMp_CNTB_n1_Lb15_FFR-0.67	7.33	10.16	0.72
BC_UMp_CNTB_n1_Lb15_FFR-0.33	6.34	10.54	0.60
BC_UMp_CNTB_n1_Lb15_FFR0	5.78	10.88	0.53
BC_UMp_CNTB_n1_Lb15_FFR0.5	5.9	10.72	0.55
BC_UMp_CNTB_n1_Lb15_FFR1	5.2	10.72	0.49
BC_UMp_CRTB_n2_Lb5_FFR-0.67	7.09	13.30	0.54
BC_UMp_CRTB_n2_Lb5_FFR-0.33	6.69	14.40	0.47
BC_UMp_CRTB_n2_Lb5_FFR0	6.37	15.82	0.41
BC_UMp_CRTB_n2_Lb5_FFR0.5	7.99	18.50	0.43
BC_UMp_CRTB_n2_Lb5_FFR1	18.9	20.32	0.93
BC_UMp_CRTB_n2_Lb15_FFR-0.67	8.06	7.90	1.02
BC_UMp_CRTB_n2_Lb15_FFR-0.33	5.88	8.00	0.74
BC_UMp_CRTB_n2_Lb15_FFR0	5.17	8.16	0.64

Table 6.4.(continued) Comparison of simulation results in Figs. 6.13 through 6.20 with Eq. 6-8.

Case (a)	Lateral bracing stiffness corresponding to 96% of simulation rigidly- braced strength (kip/in) (b)	Required lateral bracing stiffness from Eq. 6-8 (kip/in) (c)	Col. (b) / Col. (c) (d)
BC_UMp_CRTB_n2_Lb15_FFR0.5	4.87	8.12	0.60
BC_UMp_CRTB_n2_Lb15_FFR1	5.08	6.60	0.77
BC_UMn_CNTB_n1_Lb5_FFR-0.67	12.09	17.70	0.69
BC_UMn_CNTB_n1_Lb5_FFR-0.33	12.41	19.32	0.65
BC_UMn_CNTB_n1_Lb5_FFR0	13.37	21.24	0.63
BC_UMn_CNTB_n1_Lb5_FFR0.5	15.75	24.74	0.64
BC_UMn_CNTB_n1_Lb5_FFR1	20.19	26.20	0.77
BC_UMn_CNTB_n1_Lb15_FFR-0.67	8.95	10.16	0.88
BC_UMn_CNTB_n1_Lb15_FFR-0.33	8.15	10.54	0.78
BC_UMn_CNTB_n1_Lb15_FFR0	7.44	10.88	0.69
BC_UMn_CNTB_n1_Lb15_FFR0.5	6.72	10.72	0.63
BC_UMn_CNTB_n1_Lb15_FFR1	5.2	10.72	0.49
BC_UMn_CRTB_n2_Lb5_FFR-0.67	11.78	13.30	0.89
BC_UMn_CRTB_n2_Lb5_FFR-0.33	12.18	14.40	0.85
BC_UMn_CRTB_n2_Lb5_FFR0	12.84	15.82	0.81
BC_UMn_CRTB_n2_Lb5_FFR0.5	15.05	18.50	0.82
BC_UMn_CRTB_n2_Lb5_FFR1	18.9	20.32	0.93
BC_UMn_CRTB_n2_Lb15_FFR-0.67	10.41	7.90	1.32
BC_UMn_CRTB_n2_Lb15_FFR-0.33	8.17	8.00	1.02
BC_UMn_CRTB_n2_Lb15_FFR0	7.21	8.16	0.89
BC_UMn_CRTB_n2_Lb15_FFR0.5	6.55	8.12	0.81
BC_UMn_CRTB_n2_Lb15_FFR1	5.08	6.60	0.77

The following bracing strength requirements are recommended based on the results from Figs. 6.13 through 6.20.

$$\text{Lateral bracing strength} = 1\% \text{ of } P \quad (6-9)$$

$$\text{Torsional bracing strength} = 2\% \text{ of } (M + Ph_o/2) \quad (6-10)$$

These recommendations do an accurate to conservative job of predicting the bracing strength requirements. They give slightly unconservative results in some cases. However, a close inspection of the brace force versus applied load curves for these cases with stiffness's calculated from Eqs. 6-7 and 6-8 show that the above bracing strength recommendations are sufficient to develop member strength very close to the test limit load. An example case is BC_UMp_CNTB_n1_Lb5_FFR1, the results for which are shown in Fig. 6.13e. The lateral brace force versus applied load curve for this case, with brace stiffness calculated from Eqs. 6-7 and 6-8, is shown in Fig. 6.21. It can be observed that a lateral brace strength requirement of 1 % of P is sufficient to develop member strength very close to the test limit load.

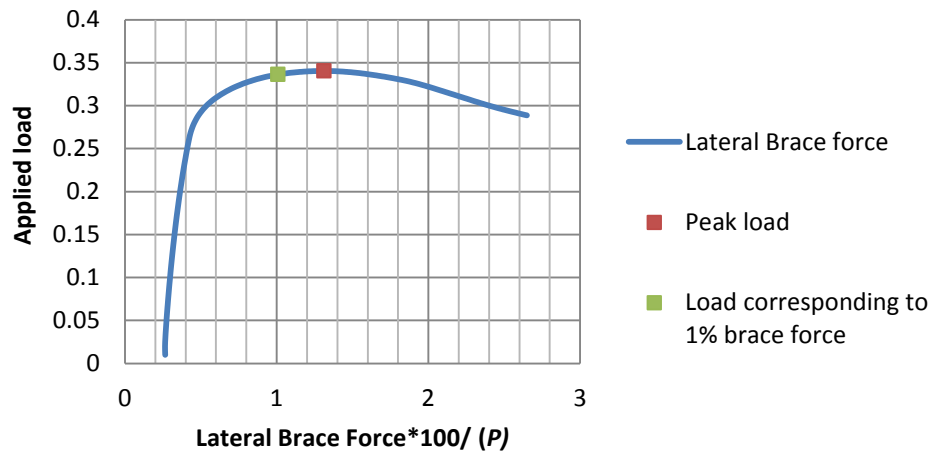


Fig. 6.21. Plot of lateral brace force versus applied load for BC_UMp_CNTB_n1_Lb5_FFR1 with brace stiffness calculated from Eqs. 6-7 and 6-8.

CHAPTER 7: BEAM-COLUMNS SUBJECTED TO AXIAL LOAD AND MOMENT GRADIENT LOADING

7.1 Overview

This chapter addresses the fourth major part of this research, beam-columns subjected to axial load and moment gradient loading. Section 7.2 gives details of the cases considered. Section 7.3 presents the test simulation results.

7.2 Detailed Study Design

The cases considered in this research to study the bracing requirements for beam-columns subjected to axial load and moment gradient loading are listed below.

Cases considered for beam-columns with Moment Gradient 1 loading are as follows:

Basic bracing types, axial load and positive Moment Gradient 1 loading such that only one flange is in net compression:

BC_MG1p_NB_n1_Lb5_FFR-0.5
BC_MG1p_NB_n1_Lb5_FFR0
BC_MG1p_NB_n1_Lb15_FFR-0.5
BC_MG1p_NB_n1_Lb15_FFR0
BC_MG1p_RB_n2_Lb5_FFR-0.5
BC_MG1p_RB_n2_Lb5_FFR0
BC_MG1p_RB_n2_Lb15_FFR-0.5
BC_MG1p_RB_n2_Lb15_FFR0

Combined lateral and torsional brace, axial load and positive Moment Gradient 1 loading such that only one flange is in net compression:

BC_MG1p_CNTB_n1_Lb5_FFR-0.5
BC_MG1p_CNTB_n1_Lb5_FFR0
BC_MG1p_CNTB_n1_Lb15_FFR-0.5
BC_MG1p_CNTB_n1_Lb15_FFR0
BC_MG1p_CRTB_n2_Lb5_FFR-0.5
BC_MG1p_CRTB_n2_Lb5_FFR0
BC_MG1p_CRTB_n2_Lb15_FFR-0.5
BC_MG1p_CRTB_n2_Lb15_FFR0

Combined lateral and torsional brace, axial load and positive Moment Gradient 1 loading such that both flanges are in net compression:

BC_MG1p_CNTB_n1_Lb5_FFR0.5
BC_MG1p_CNTB_n1_Lb5_FFR1
BC_MG1p_CNTB_n1_Lb15_FFR0.5
BC_MG1p_CNTB_n1_Lb15_FFR1
BC_MG1p_CRTB_n2_Lb5_FFR0.5
BC_MG1p_CRTB_n2_Lb5_FFR1
BC_MG1p_CRTB_n2_Lb15_FFR0.5
BC_MG1p_CRTB_n2_Lb15_FFR1

Combined lateral and torsional brace, axial load and negative Moment Gradient 1 loading such that only one flange is in net compression:

BC_MG1n_CNTB_n1_Lb5_FFR-0.5
BC_MG1n_CNTB_n1_Lb5_FFR0
BC_MG1n_CNTB_n1_Lb15_FFR-0.5
BC_MG1n_CNTB_n1_Lb15_FFR0
BC_MG1n_CRTB_n2_Lb5_FFR-0.5
BC_MG1n_CRTB_n2_Lb5_FFR0
BC_MG1n_CRTB_n2_Lb15_FFR-0.5
BC_MG1n_CRTB_n2_Lb15_FFR0

Combined lateral and torsional brace, axial load and negative Moment Gradient 1 loading such that both flanges are in net compression:

BC_MG1n_CNTB_n1_Lb5_FFR0.5
BC_MG1n_CNTB_n1_Lb5_FFR1
BC_MG1n_CNTB_n1_Lb15_FFR0.5
BC_MG1n_CNTB_n1_Lb15_FFR1
BC_MG1n_CRTB_n2_Lb5_FFR0.5
BC_MG1n_CRTB_n2_Lb5_FFR1
BC_MG1n_CRTB_n2_Lb15_FFR0.5
BC_MG1n_CRTB_n2_Lb15_FFR1

Cases considered for beam-columns with Moment Gradient 2 loading are as follows:

Basic bracing types, axial load and positive Moment Gradient 2 loading such that only one flange is in net compression:

BC_MG2p_NB_n1_Lb5_FFR-0.5
BC_MG2p_NB_n1_Lb5_FFR0
BC_MG2p_NB_n1_Lb15_FFR-0.5
BC_MG2p_NB_n1_Lb15_FFR0

Combined lateral and torsional brace, axial load and positive Moment Gradient 2 loading such that only one flange is in net compression:

BC_MG2p_CNTB_n1_Lb5_FFR-0.5
BC_MG2p_CNTB_n1_Lb5_FFR0
BC_MG2p_CNTB_n1_Lb15_FFR-0.5
BC_MG2p_CNTB_n1_Lb15_FFR0

Combined lateral and torsional brace, axial load and positive Moment Gradient 2 loading such that both flanges are in net compression:

BC_MG2p_CNTB_n1_Lb5_FFR0.5
BC_MG2p_CNTB_n1_Lb5_FFR1
BC_MG2p_CNTB_n1_Lb15_FFR0.5
BC_MG2p_CNTB_n1_Lb15_FFR1

Combined lateral and torsional brace, axial load and negative Moment Gradient 2 loading such that only one flange is in net compression:

BC_MG2n_CNTB_n1_Lb5_FFR-0.5
BC_MG2n_CNTB_n1_Lb5_FFR0

BC_MG2n_CNTB_n1_Lb15_FFR-0.5
BC_MG2n_CNTB_n1_Lb15_FFR0

Combined lateral and torsional brace, axial load and negative Moment Gradient 2 loading such that both flanges are in net compression:

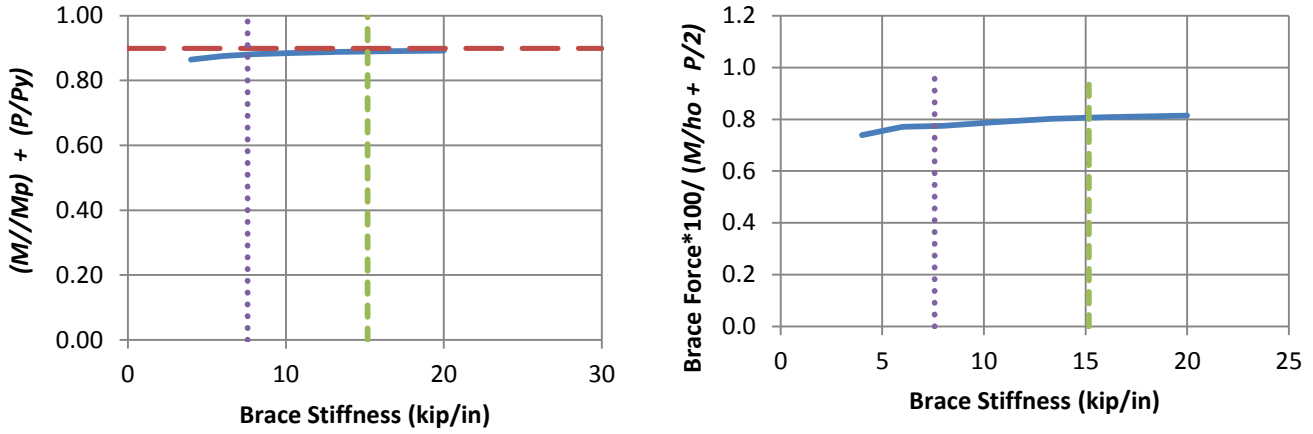
BC_MG2n_CNTB_n1_Lb5_FFR0.5
BC_MG2n_CNTB_n1_Lb5_FFR1
BC_MG2n_CNTB_n1_Lb15_FFR0.5
BC_MG2n_CNTB_n1_Lb15_FFR1

7.3 Results

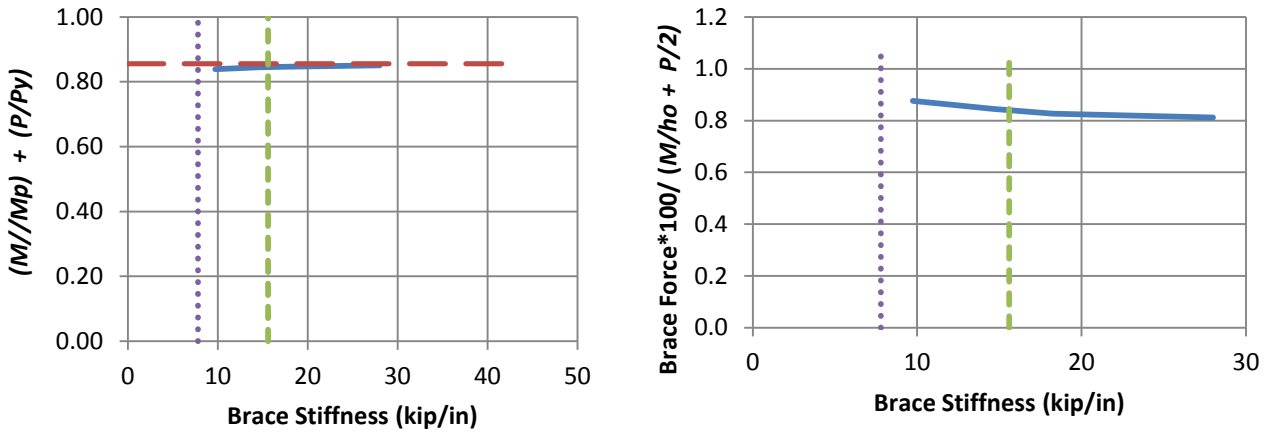
Results for the various beam-column moment gradient loading cases are shown in the following subsections.

7.3.1 Beam-Columns with Moment Gradient 1 Loading

Results for beam-columns with Moment Gradient 1 loading and lateral bracing only are shown in Figs. 7.1 through 7.4. Table 7.1 compares the results from these figures.



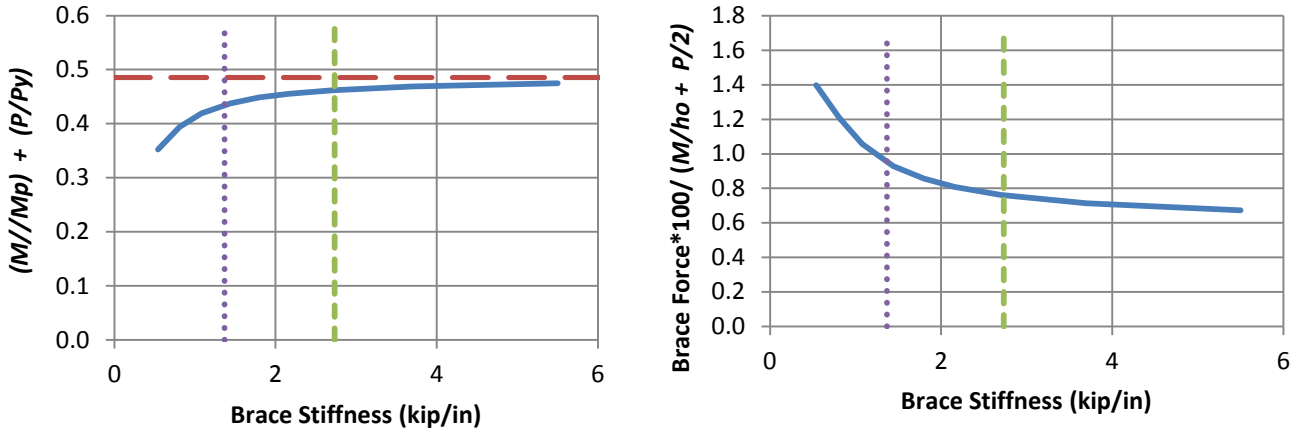
a) BC_MG1p_NB_n1_Lb5_FFR-0.5



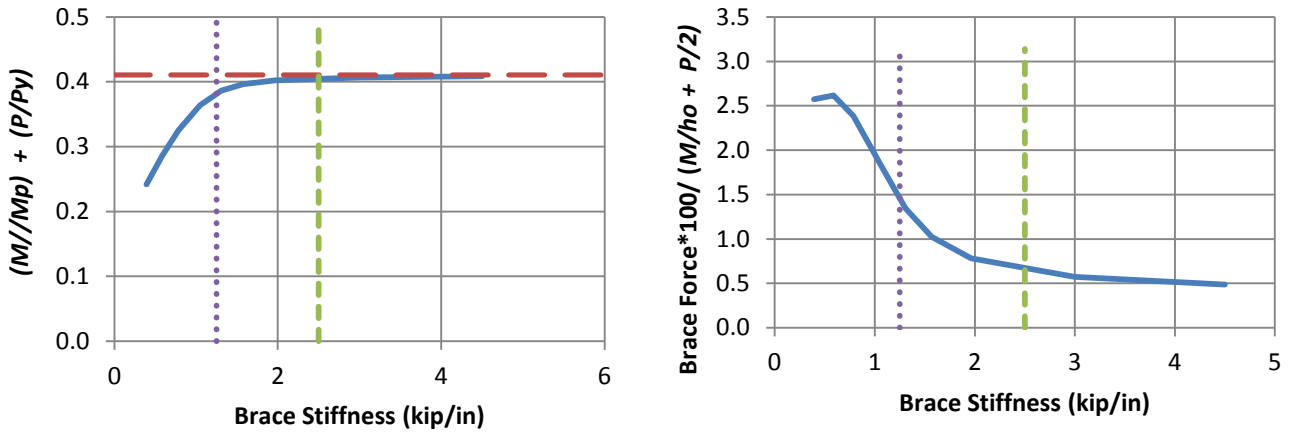
b) BC_MG1p_NB_n1_Lb5_FFR0

- Test simulation results
- - Rigidly-braced strength
- ⋯ 0.5 times bracing stiffness from Eq. 6-3
- - Bracing stiffness from Eq. 6-3

Fig. 7.1. Knuckle curves and brace force vs. brace stiffness plots for point (nodal) lateral bracing cases with $n = 1$ and constant axial load and Moment Gradient 1 loading, $L_b = 5$ ft.



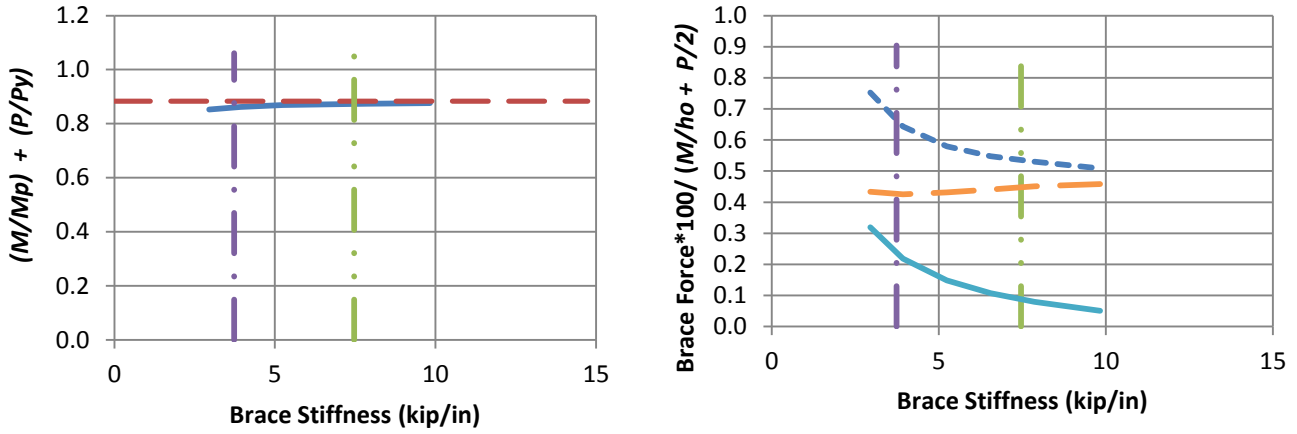
a) BC_MG1p_NB_n1_Lb15_FFR-0.5



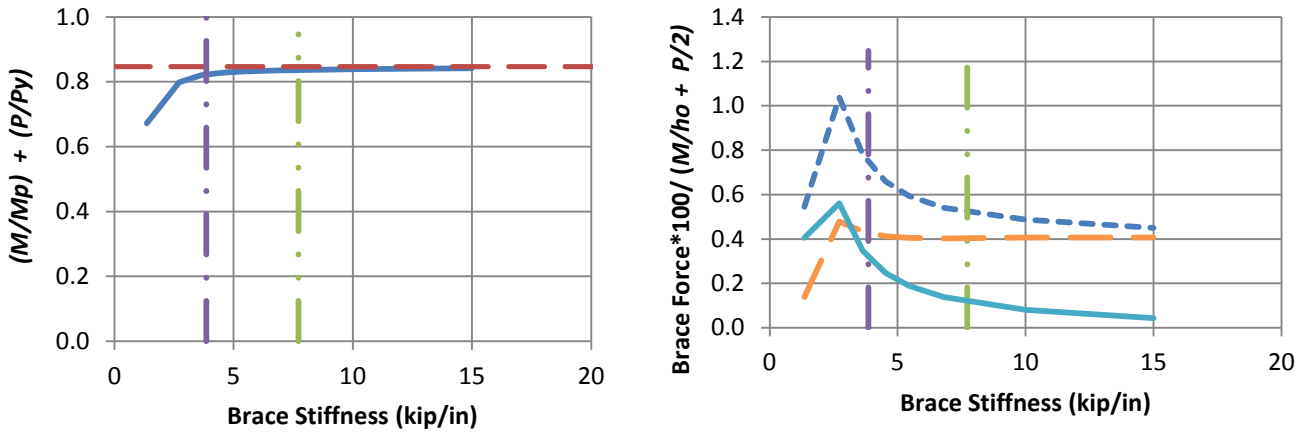
b) BC_MG1p_NB_n1_Lb15_FFR0

- Test simulation results
- - Rigidly-braced strength
- ⋯ 0.5 times bracing stiffness from Eq. 6-3
- - Bracing stiffness from Eq. 6-3

Fig. 7.2. Knuckle curves and brace force vs. brace stiffness plots for point (nodal) lateral bracing cases with $n = 1$ and constant axial load and Moment Gradient 1 loading, $L_b = 15$ ft.



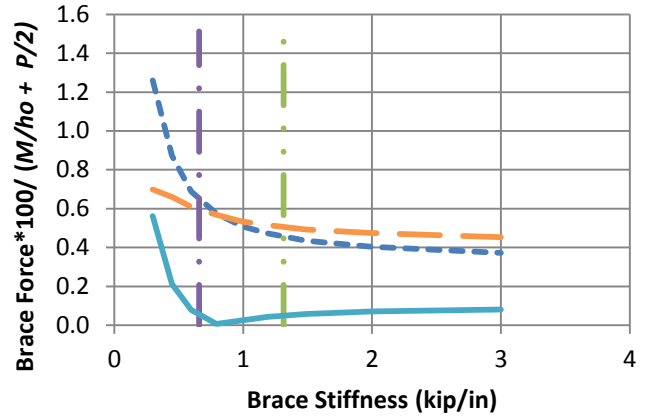
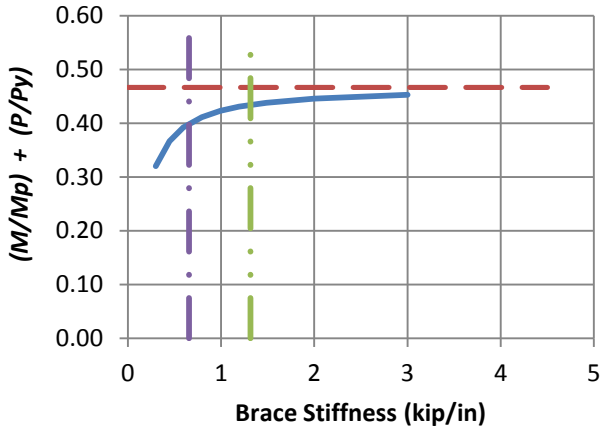
a) BC_MG1p_RB_n2_Lb5_FFR-0.5



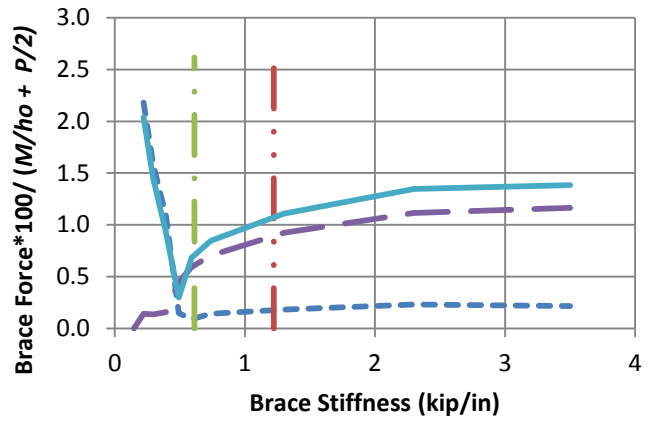
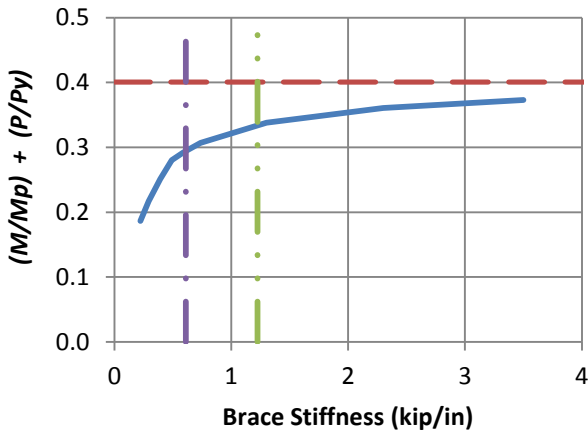
b) BC_MG1p_RB_n2_Lb5_FFR0

- Test simulation results
- - Rigidly-braced strength
- . Bracing stiffness from Eq. 6-3
- . Left end panel shear force
- Right end panel shear force
- - Middle panel shear force
- . 0.5 times bracing stiffness from Eq. 6-3

Fig. 7.3. Knuckle curves and brace force vs. brace stiffness plots for shear panel (relative) lateral bracing cases with $n = 2$ and constant axial load and Moment Gradient 1 loading, $L_b = 5$ ft.



a) BC_MG1p_RB_n2_Lb15_FFR-0.5



b) BC_MG1p_RB_n2_Lb15_FFR0

- Test simulation results
- - Rigidly-braced strength
- 0.5 times bracing stiffness from Eq. 6-3
- Bracing stiffness from Eq. 6-3
- - · Left end panel shear force
- Right end panel shear force
- - Middle panel shear force

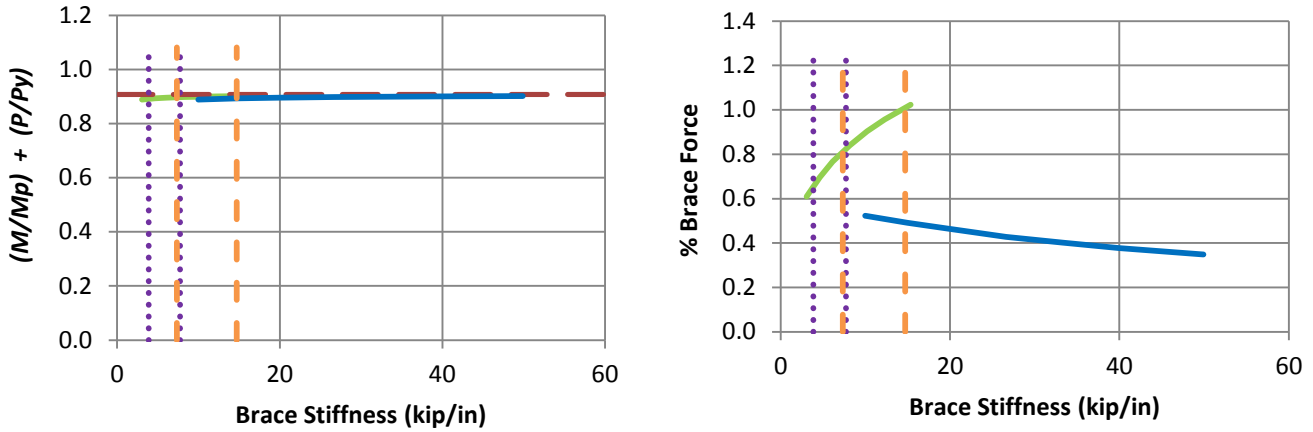
Fig. 7.4. Knuckle curves and brace force vs. brace stiffness plots for shear panel (relative) lateral bracing cases with $n = 2$ and constant axial load and Moment Gradient 1 loading, $L_b = 15$ ft.

Table 7.1. Comparison of simulation results in Figs. 7.1 through 7.4 with Eq. 6-3.

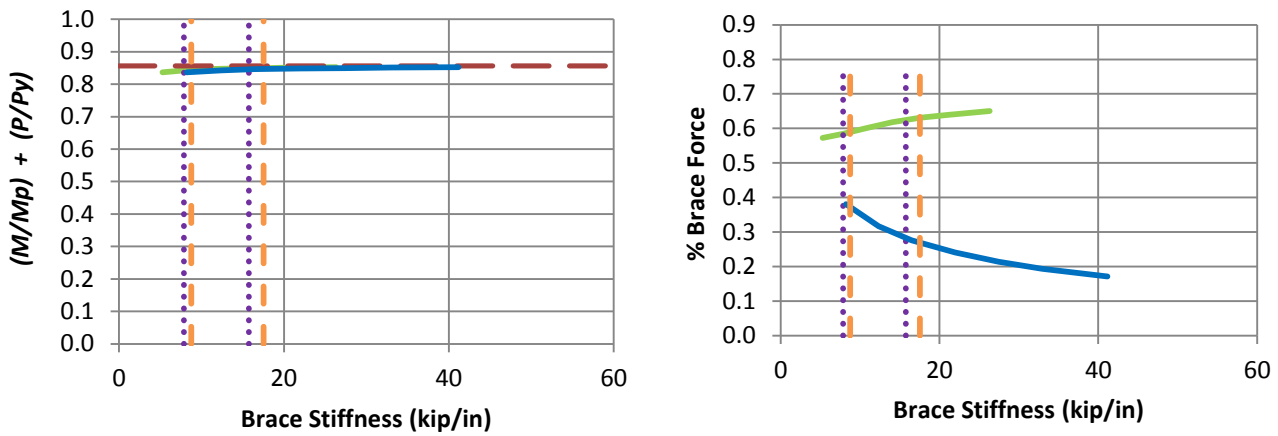
Case (a)	Stiffness corresponding to 96% of simulation rigidly-braced strength (kip/in) (b)	Required bracing stiffness from Eq. 6-3 kip/in (c)	Col. (b) / Col. (c) (d)
BC_MG1p_NB_n1_Lb5_FFR-0.5	3.5	15.16	0.23
BC_MG1p_NB_n1_Lb5_FFR0	5.39	15.60	0.35
BC_MG1p_NB_n1_Lb15_FFR-0.5	3.29	2.74	0.69
BC_MG1p_NB_n1_Lb15_FFR0	1.52	2.50	0.61
BC_MG1p_RB_n2_Lb5_FFR-0.5	2.89	7.46	0.39
BC_MG1p_RB_n2_Lb5_FFR0	3.33	7.72	0.43
BC_MG1p_RB_n2_Lb15_FFR-0.5	2.29	1.32	1.74
BC_MG1p_RB_n2_Lb15_FFR0	1.74	1.22	1.43

From Column (d) of Table 7.1, it can be observed that the bracing stiffness calculated by Eq. 6-3 is conservative for all cases except those for which the (L/r) value of the unbraced flange (flange loaded in flexural tension) is large. This behavior is similar to the one observed in Chapter 6, for beam-column members with only lateral bracing on one flange, and subjected to axial load and uniform bending. Similarly from Figs. 7.1 through 7.4, it can be observed that the bracing strength calculated by Eq. 6-4 is accurate to slightly conservative for all cases except BC_MG1p_RB_n2_Lb15_FFR0, for which (L/r) value of the unbraced flange is large.

Results for beam-columns with Moment Gradient 1 loading, and combined lateral and torsional bracing are shown in Figs. 7.5 through 7.12. The lateral brace force in these figures is expressed as percentage with respect to P . The torsional brace force is expressed as percentage with respect to $M/h_o+P/2$. From Figs. 7.5 through 7.12. it can be observed that the bracing strength requirement predicted by Eq. 6-9 and 6-10 is conservative. Tables 7.2 and 7.3 compare the results from these figures.



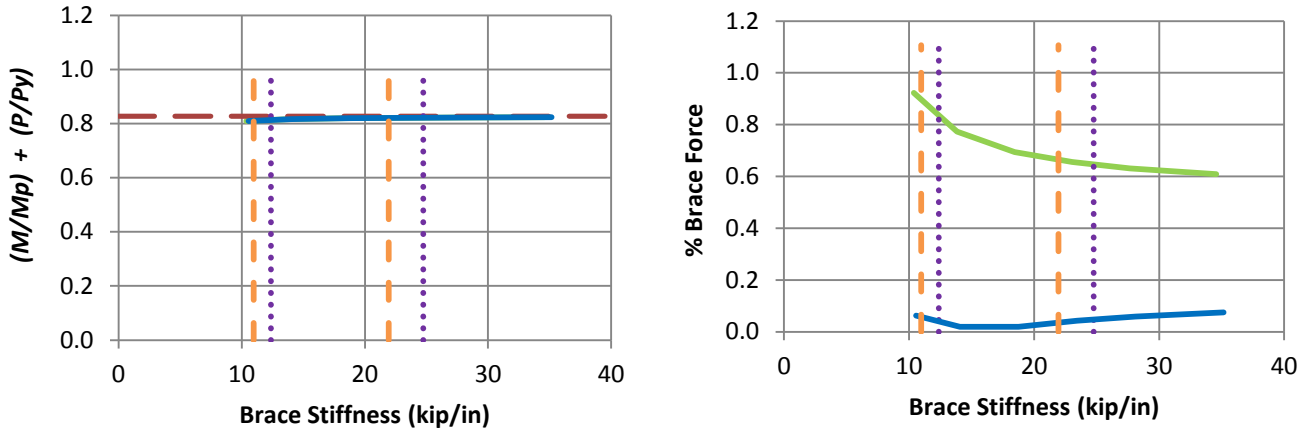
a) BC_MG1p_CNTB_n1_Lb5_FFR-0.5



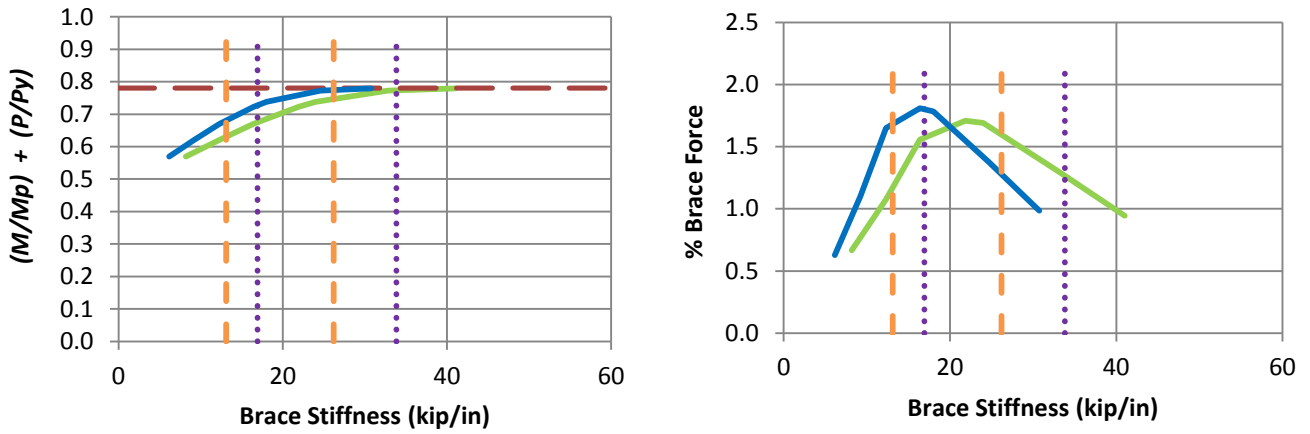
b) BC_MG1p_CNTB_n1_Lb5_FFR0

- Rigidly-braced strength
- Test simulation results corresponding to torsional brace
- Test simulation results corresponding to lateral brace
- 1x and 0.5x lateral bracing stiffness from Eq. 6-7
- 1x and 0.5x torsional bracing stiffness from Eq. 6-8

Fig. 7.5. Knuckle curves and brace force vs. brace stiffness plots for combined point (nodal) lateral and torsional bracing cases with $n = 1$ and constant axial load and Moment Gradient 1 loading with lateral brace on the flange in flexural compression, $L_b = 5$ ft.



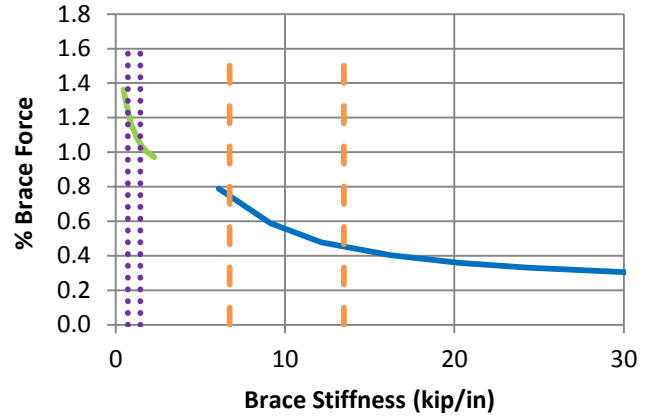
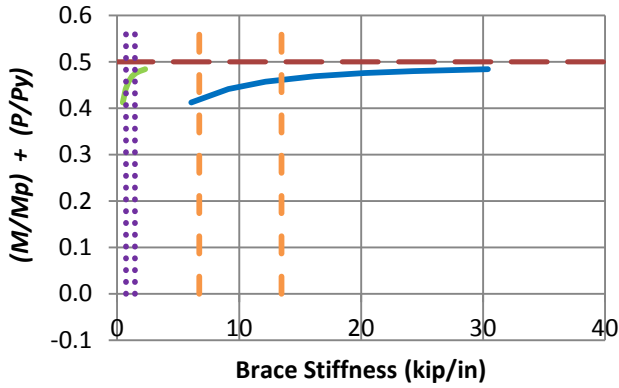
c) BC_MG1p_CNTB_n1_Lb5_FFR0.5



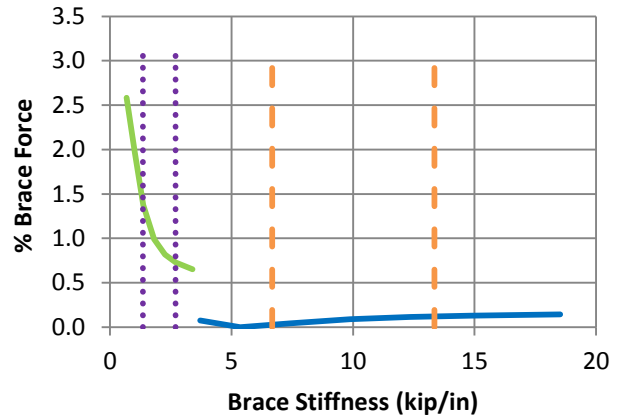
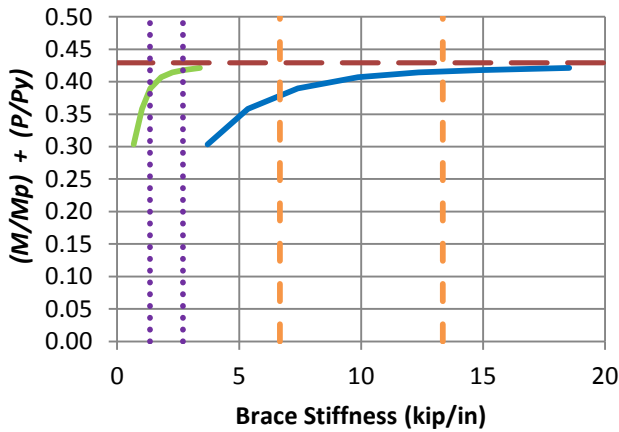
d) BC_MG1p_CNTB_n1_Lb5_FFR1

- Rigidly-braced strength
- Test simulation results corresponding to torsional brace
- Test simulation results corresponding to lateral brace
- 1x and 0.5x lateral bracing stiffness from Eq. 6-7
- 1x and 0.5x torsional bracing stiffness from Eq. 6-8

Fig. 7.5. (continued) Knuckle curves and brace force vs. brace stiffness plots for combined point (nodal) lateral and torsional bracing cases with $n = 1$ and constant axial load and Moment Gradient 1 loading with lateral brace on the flange in flexural compression, $L_b = 5$ ft.



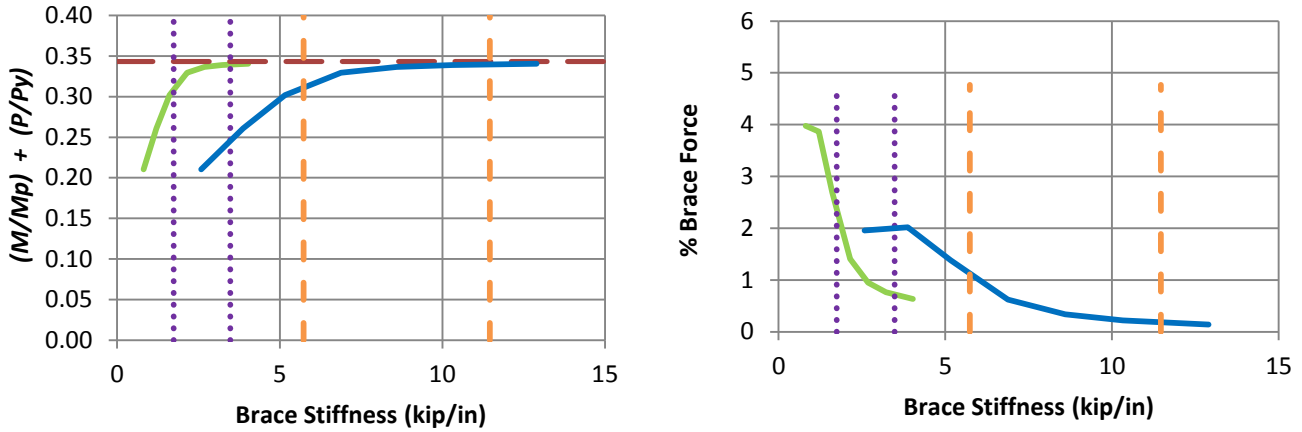
a) BC_MG1p_CNTB_n1_Lb15_FFR-0.5



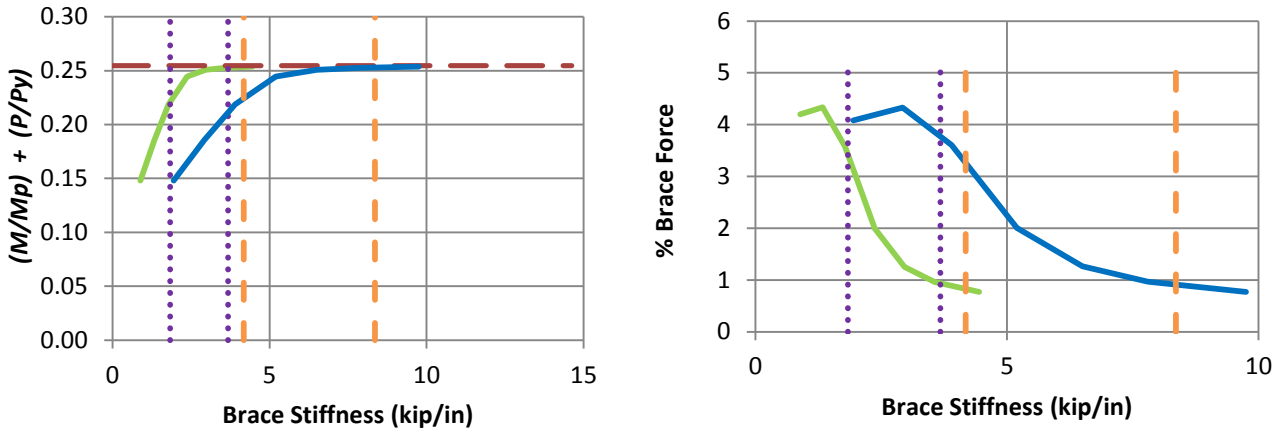
b) BC_MG1p_CNTB_n1_Lb15_FFR0

- Rigidly-braced strength — Test simulation results corresponding to torsional brace
- Test simulation results corresponding to lateral brace
- 1x and 0.5x lateral bracing stiffness from Eq. 6-7
- - - 1x and 0.5x torsional bracing stiffness from Eq. 6-8

Fig. 7.6. Knuckle curves and brace force vs. brace stiffness plots for combined point (nodal) lateral and torsional bracing cases with $n = 1$ and constant axial load and Moment Gradient 1 loading with lateral brace on the flange in flexural compression, $L_b = 15$ ft.



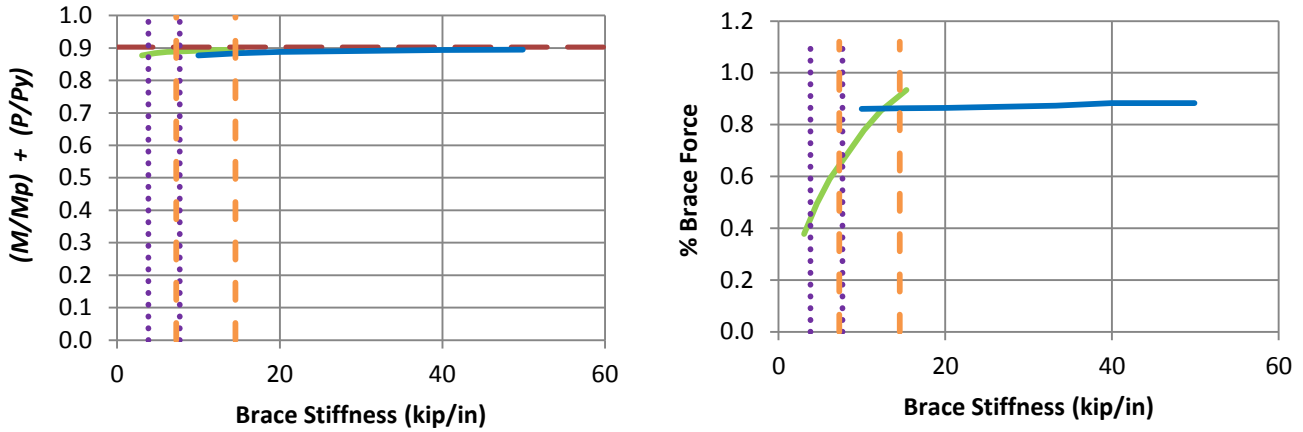
c) BC_MG1p_CNTB_n1_Lb15_FFR0.5



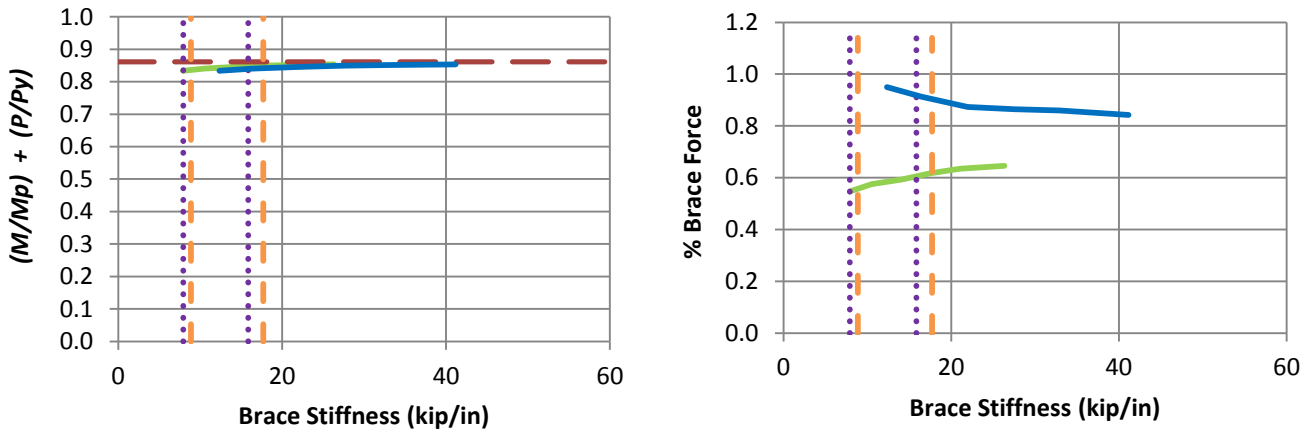
d) BC_MG1p_CNTB_n1_Lb15_FFR1

- Rigidly-braced strength
- Test simulation results corresponding to torsional brace
- Test simulation results corresponding to lateral brace
- ⋯ 1x and 0.5x lateral bracing stiffness from Eq. 6-7
- 1x and 0.5x torsional bracing stiffness from Eq. 6-8

Fig. 7.6. (continued) Knuckle curves and brace force vs. brace stiffness plots for combined point (nodal) lateral and torsional bracing cases with $n = 1$ and constant axial load and Moment Gradient 1 loading with lateral brace on the flange in flexural compression, $L_b = 15$ ft.



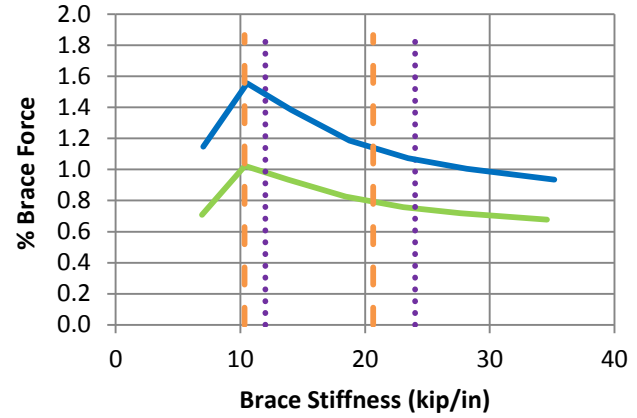
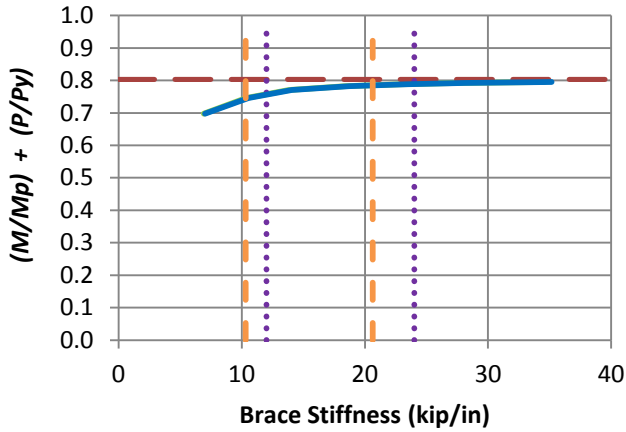
a) BC_MG1n_CNTB_n1_Lb5_FFR-0.5



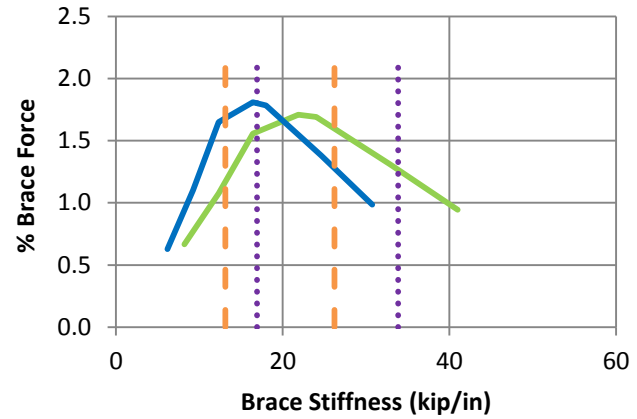
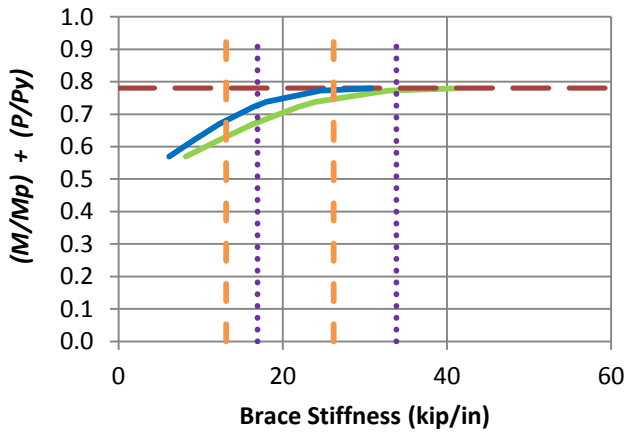
b) BC_MG1n_CNTB_n1_Lb5_FFR0

- Rigidly-braced strength
- Test simulation results corresponding to torsional brace
- Test simulation results corresponding to lateral brace
- 1x and 0.5x lateral bracing stiffness from Eq. 6-7
- 1x and 0.5x torsional bracing stiffness from Eq. 6-8

Fig. 7.7. Knuckle curves and brace force vs. brace stiffness plots for combined point (nodal) lateral and torsional bracing cases with $n = 1$ and constant axial load and Moment Gradient 1 loading with lateral brace on the flange in flexural tension, $L_b = 5$ ft.



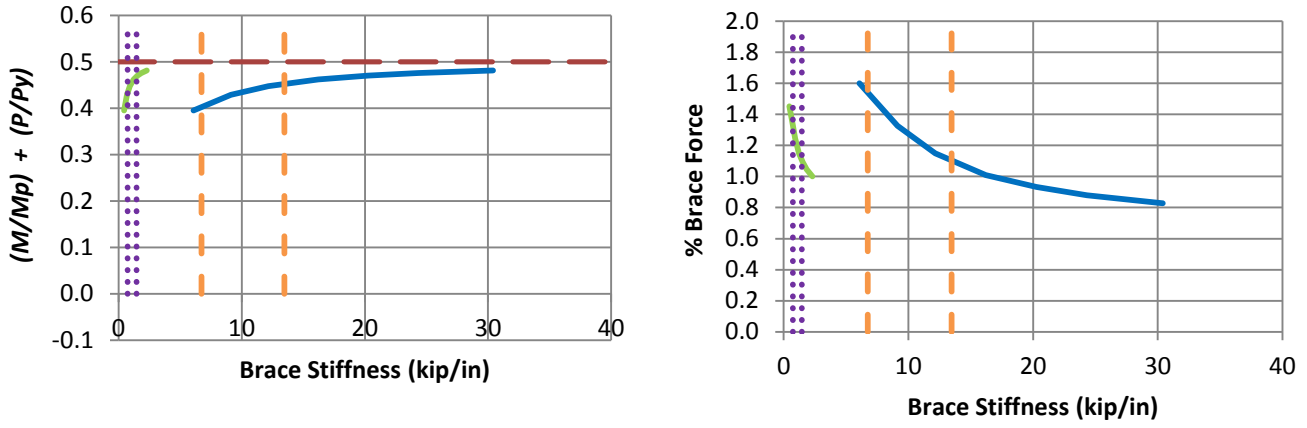
c) BC_MG1n_CNTB_n1_Lb5_FFR0.5



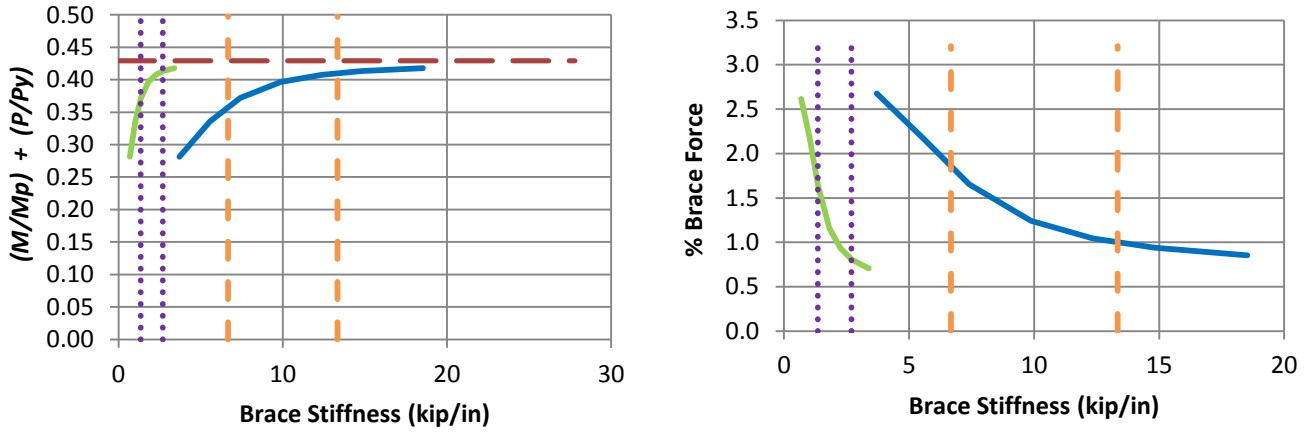
d) BC_MG1n_CNTB_n1_Lb5_FFR1

- Rigidly-braced strength
- Test simulation results corresponding to torsional brace
- Test simulation results corresponding to lateral brace
- 1x and 0.5x lateral bracing stiffness from Eq. 6-7
- 1x and 0.5x torsional bracing stiffness from Eq. 6-8

Fig. 7.7. (continued) Knuckle curves and brace force vs. brace stiffness plots for combined point (nodal) lateral and torsional bracing cases with $n = 1$ and constant axial load and Moment Gradient 1 loading with lateral brace on the flange in flexural tension, $L_b = 5$ ft.



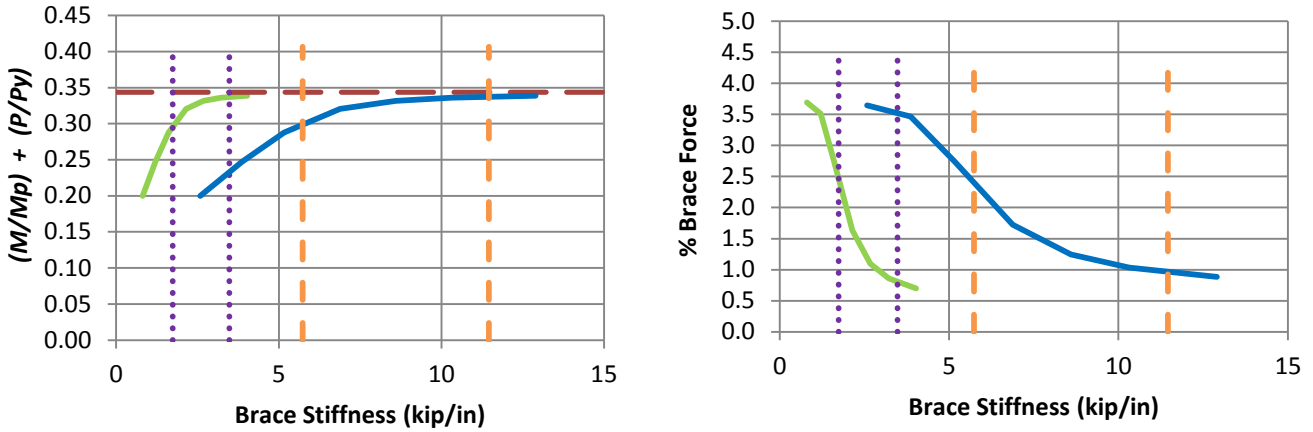
a) BC_MG1n_CNTB_n1_Lb15_FFR-0.5



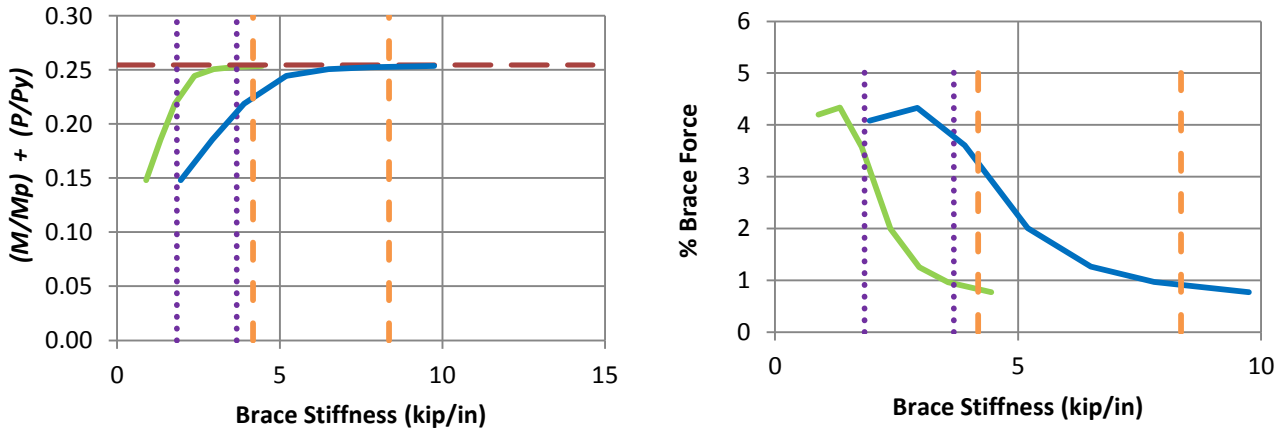
b) BC_MG1n_CNTB_n1_Lb15_FFR0

- Rigidly-braced strength
- Test simulation results corresponding to torsional brace
- Test simulation results corresponding to lateral brace
- 1x and 0.5x lateral bracing stiffness from Eq. 6-7
- 1x and 0.5x torsional bracing stiffness from Eq. 6-8

Fig. 7.8. Knuckle curves and brace force vs. brace stiffness plots for combined point (nodal) lateral and torsional bracing cases with $n = 1$ and constant axial load and Moment Gradient 1 loading with lateral brace on the flange in flexural tension, $L_b = 15$ ft.



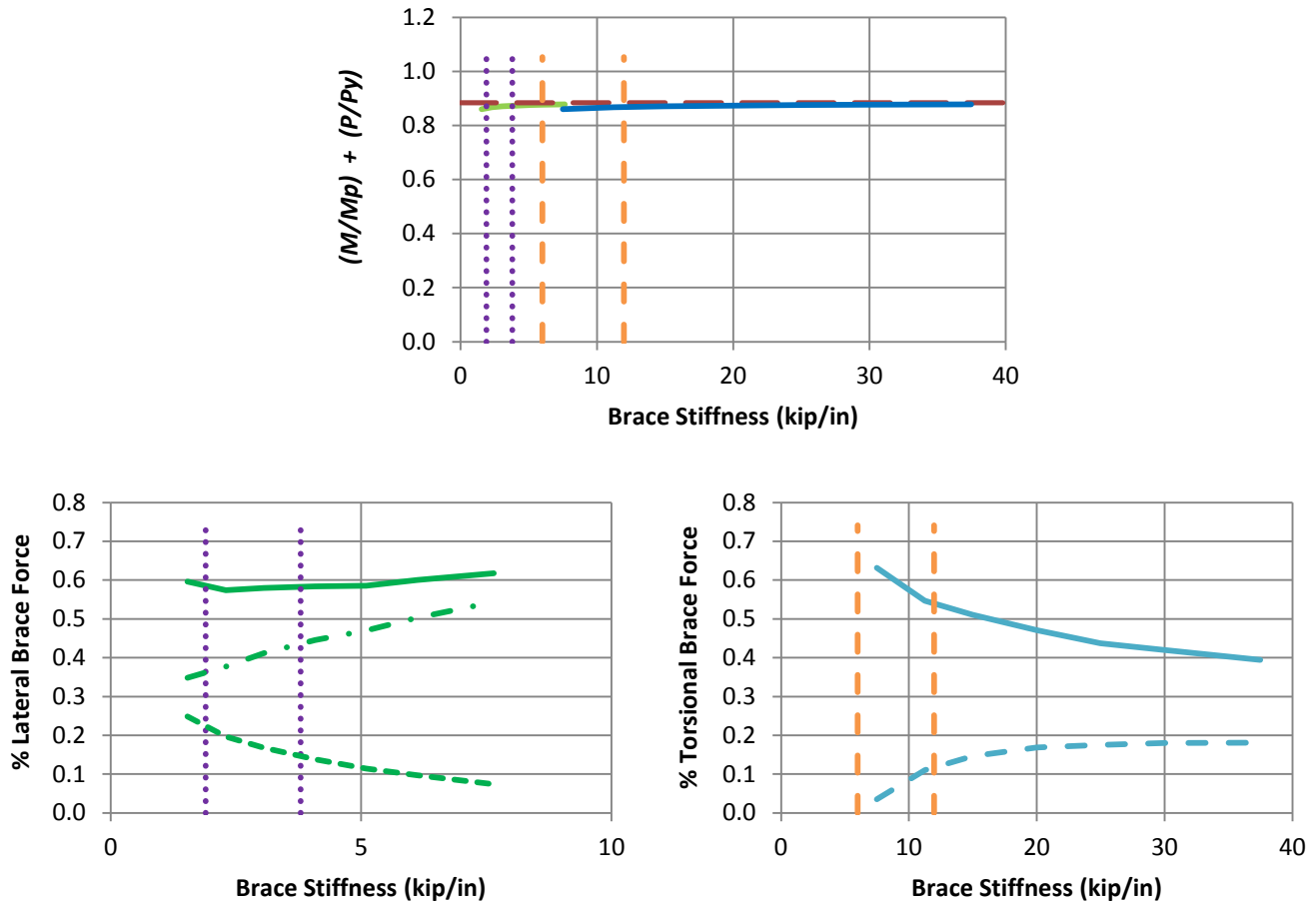
c) BC_MG1n_CNTB_n1_Lb15_FFR0.5



d) BC_MG1n_CNTB_n1_Lb15_FFR1

- Rigidly-braced strength
- Test simulation results corresponding to torsional brace
- Test simulation results corresponding to lateral brace
- ⋯ 1x and 0.5x lateral bracing stiffness from Eq. 6-7
- - - 1x and 0.5x torsional bracing stiffness from Eq. 6-8

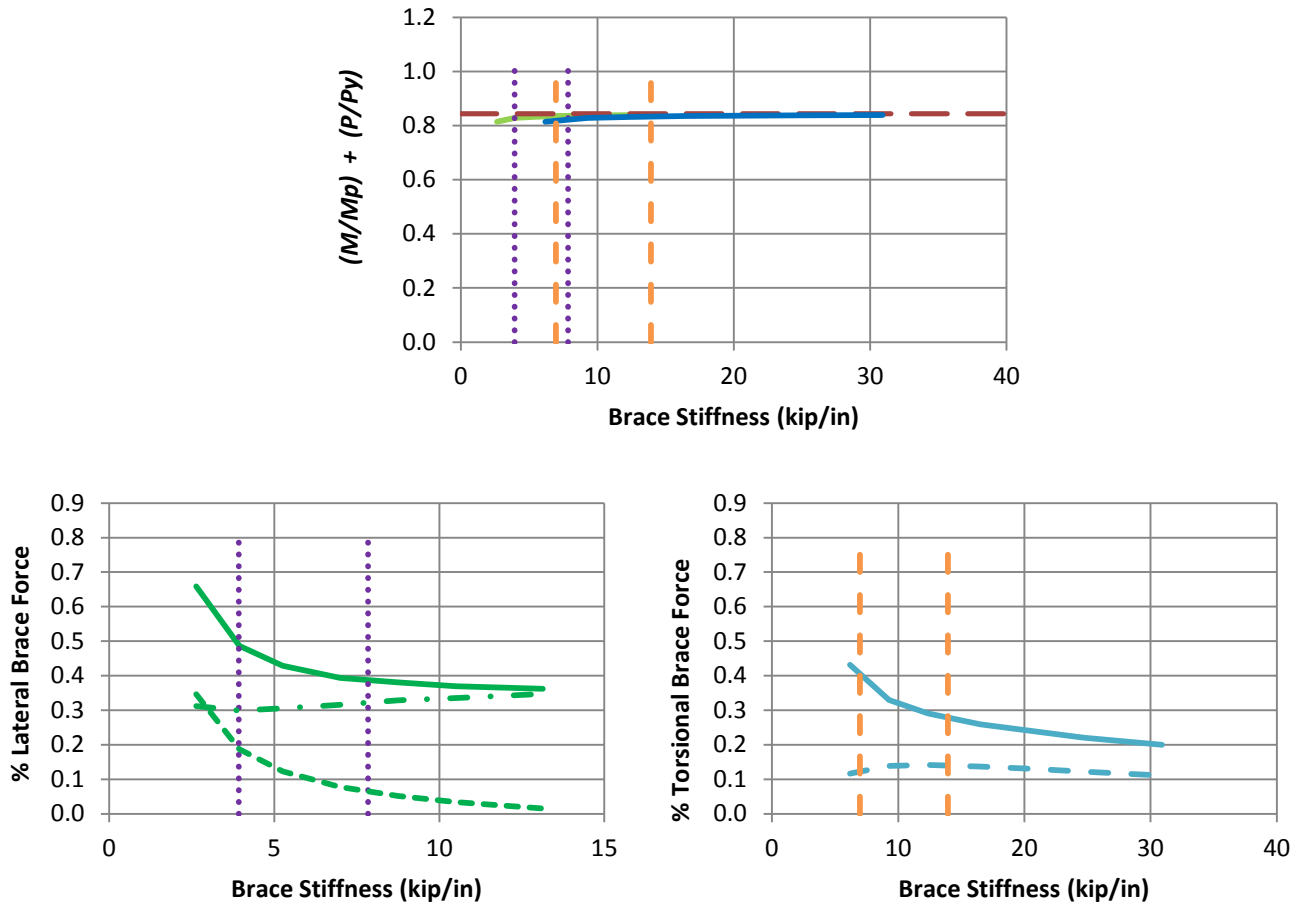
Fig. 7.8. (continued) Knuckle curves and brace force vs. brace stiffness plots for combined point (nodal) lateral and torsional bracing cases with $n = 1$ and constant axial load and Moment Gradient 1 loading with lateral brace on the flange in flexural tension, $L_b = 15$ ft.



f) BC_MG1p_CRTB_n2_Lb5_FFR-0.5

- Rigidly-braced strength
- Test simulation results corresponding to torsional brace
- Test simulation results corresponding to lateral brace
- 1x and 0.5x lateral bracing stiffness from Eq. 6-7
- - - 1x and 0.5x torsional bracing stiffness from Eq. 6-8
- Left end panel shear force
- - - Right end panel shear force
- . - Middle panel shear force
- Torsional brace force 1
- Torsional brace force 2

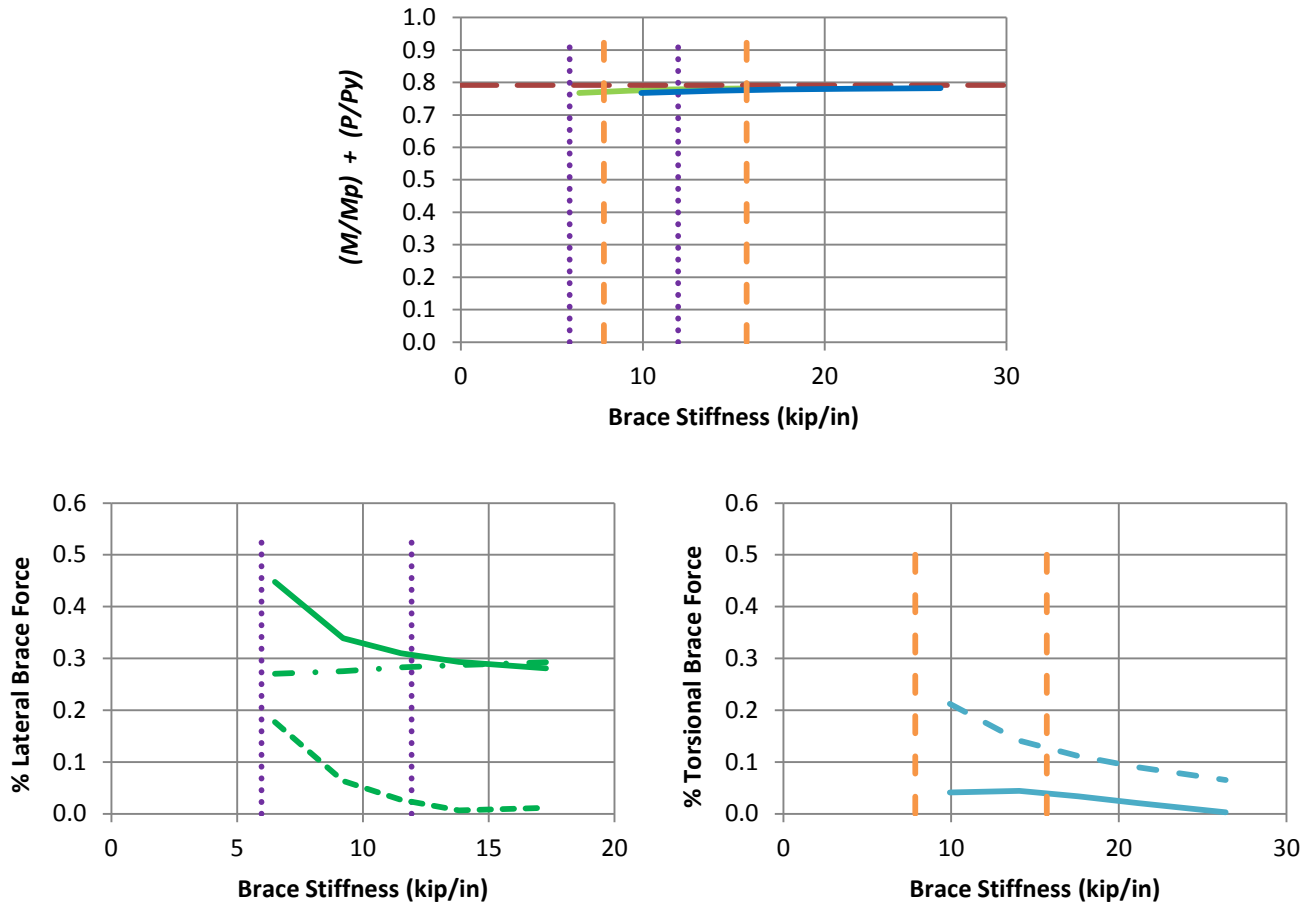
Fig. 7.9. Knuckle curves and brace force vs. brace stiffness plots for combined shear panel (relative) lateral and torsional bracing cases with $n = 2$ and constant axial load and Moment Gradient 1 loading with lateral brace on the flange in flexural compression, $L_b = 5$ ft.



g) BC_MG1p_CRTB_n2_Lb5_FFR0

- Rigidly-braced strength
- Test simulation results corresponding to torsional brace
- Test simulation results corresponding to lateral brace
- 1x and 0.5x lateral bracing stiffness from Eq. 6-7
- - - 1x and 0.5x torsional bracing stiffness from Eq. 6-8
- Left end panel shear force
- - - Right end panel shear force
- . - Middle panel shear force
- Torsional brace force 1
- Torsional brace force 2

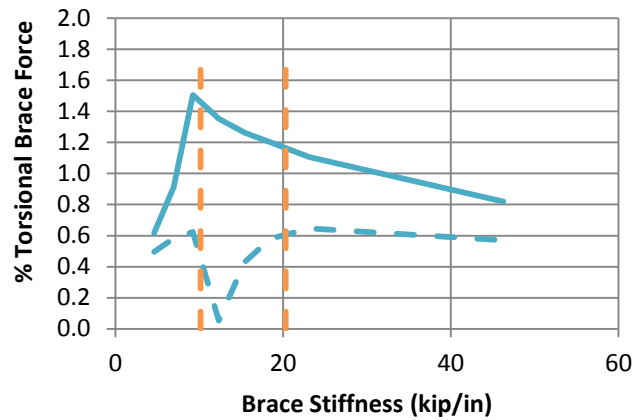
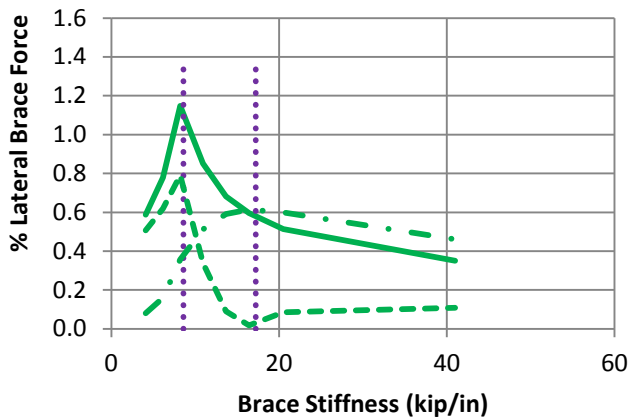
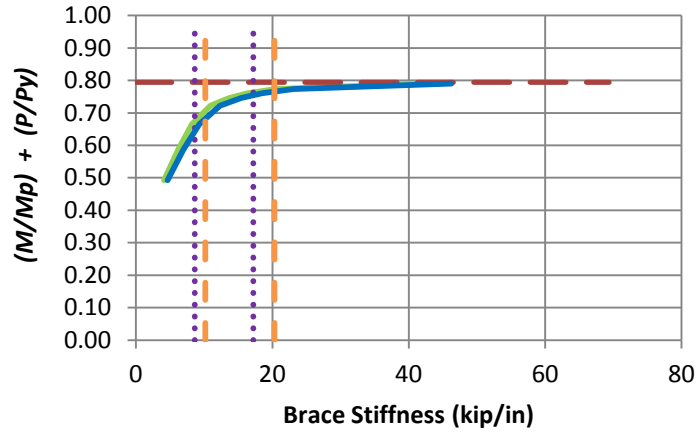
Fig. 7.9. (continued) Knuckle curves and brace force vs. brace stiffness plots for combined shear panel (relative) lateral and torsional bracing cases with $n = 2$ and constant axial load and Moment Gradient 1 loading with lateral brace on the flange in flexural compression, $L_b = 5$ ft.



h) BC_MG1p_CRTB_n2_Lb5_FFR0.5

- Rigidly-braced strength
- Test simulation results corresponding to torsional brace
- Test simulation results corresponding to lateral brace
- 1x and 0.5x lateral bracing stiffness from Eq. 6-7
- 1x and 0.5x torsional bracing stiffness from Eq. 6-8
- Left end panel shear force
- Right end panel shear force
- Middle panel shear force
- Torsional brace force 1
- Torsional brace force 2

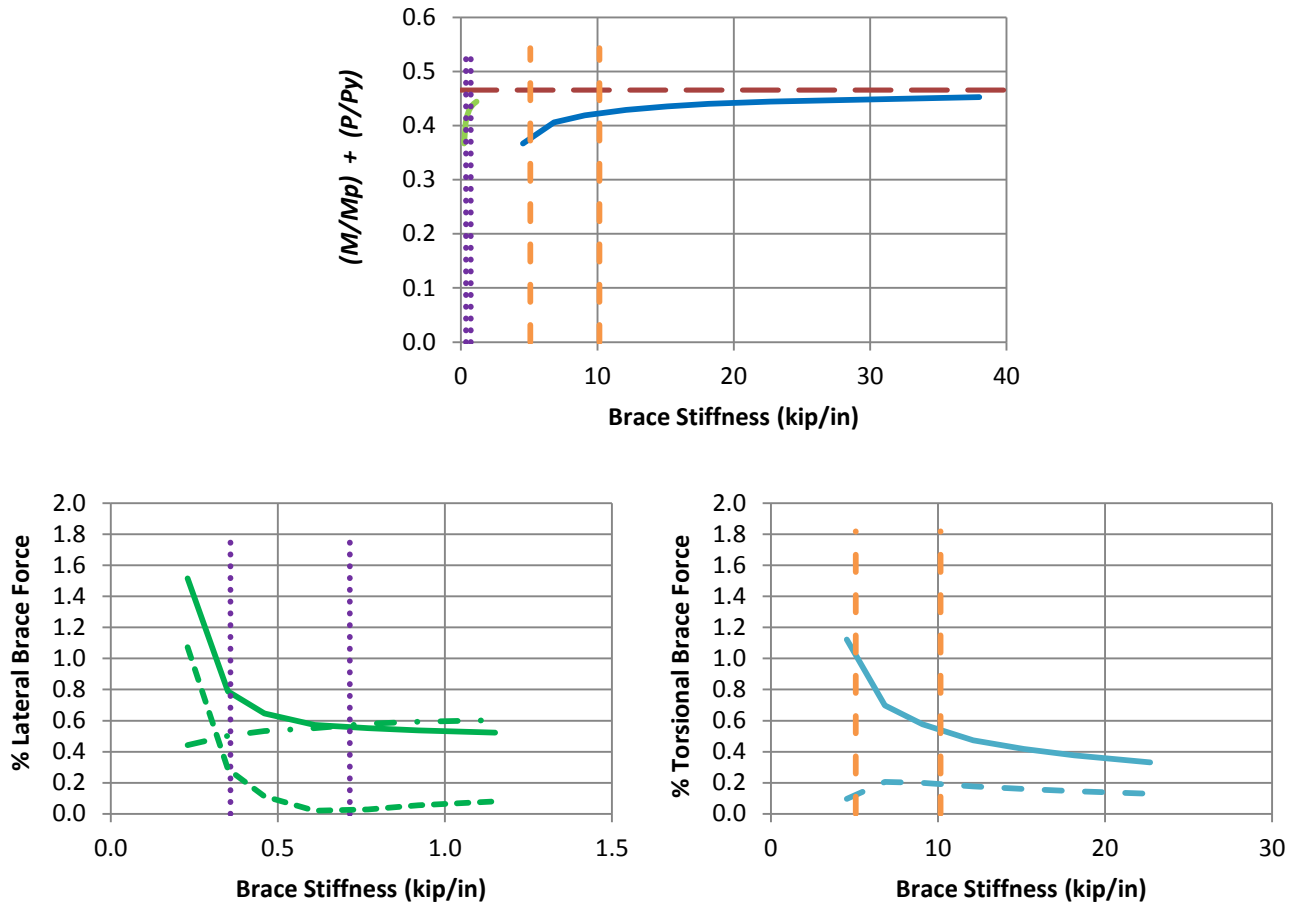
Fig. 7.9. (continued) Knuckle curves and brace force vs. brace stiffness plots for combined shear panel (relative) lateral and torsional bracing cases with $n = 2$ and constant axial load and Moment Gradient 1 loading with lateral brace on the flange in flexural compression, $L_b = 5\text{ft}$.



i) BC_MG1p_CRTB_n2_Lb5_FFR1

- Rigidly-braced strength
- Test simulation results corresponding to torsional brace
- Test simulation results corresponding to lateral brace
- 1x and 0.5x lateral bracing stiffness from Eq. 6-7
- - - 1x and 0.5x torsional bracing stiffness from Eq. 6-8
- Left end panel shear force
- - - Right end panel shear force
- . - Middle panel shear force
- Torsional brace force 1
- - - Torsional brace force 2

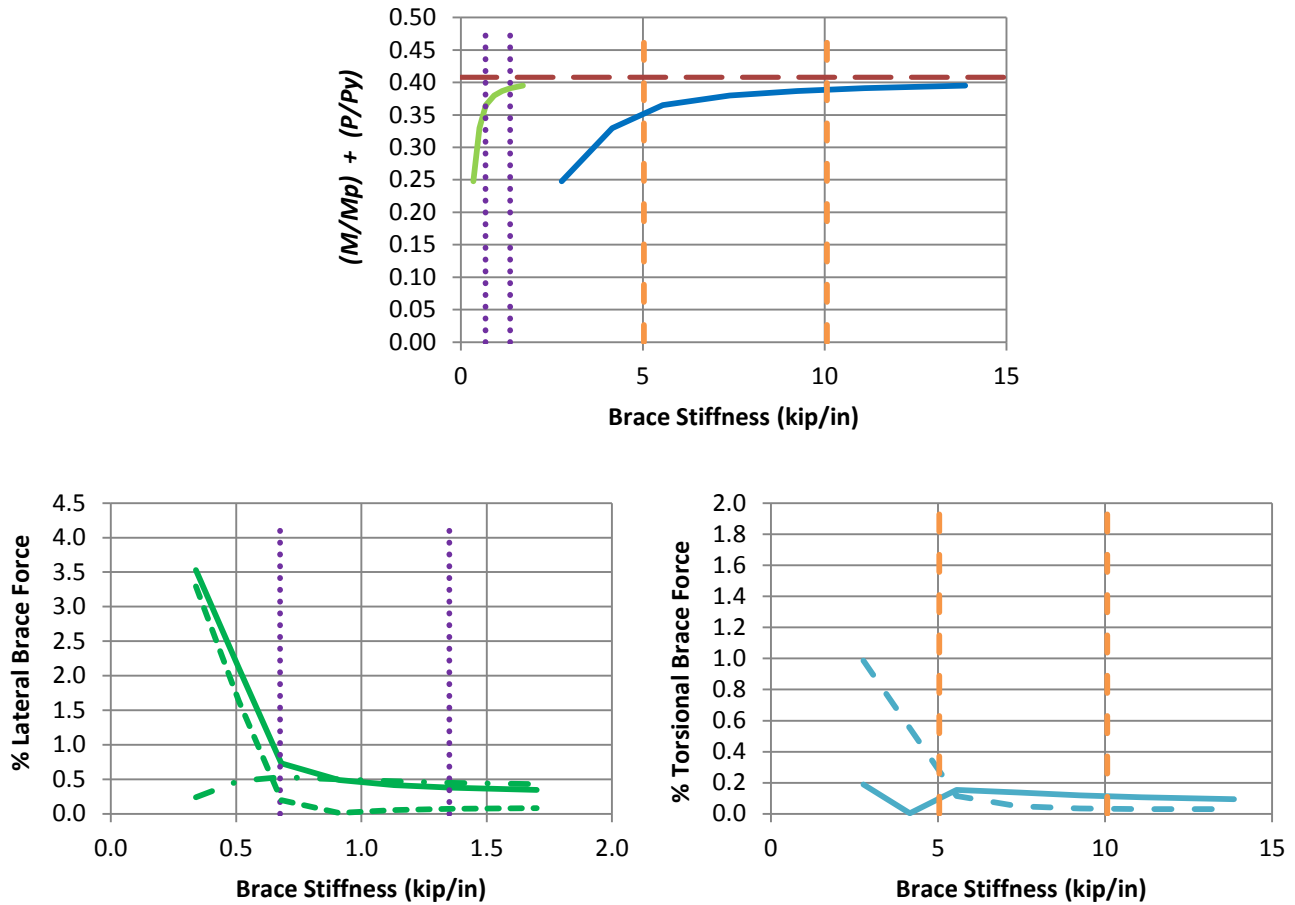
Fig. 7.9. (continued) Knuckle curves and brace force vs. brace stiffness plots for combined shear panel (relative) lateral and torsional bracing cases with $n = 2$ and constant axial load and Moment Gradient 1 loading with lateral brace on the flange in flexural compression, $L_b = 5$ ft.



a) BC_MG1p_CRTB_n2_Lb15_FFR-0.5

- Rigidly-braced strength
- Test simulation results corresponding to torsional brace
- Test simulation results corresponding to lateral brace
- 1x and 0.5x lateral bracing stiffness from Eq. 6-7
- - - 1x and 0.5x torsional bracing stiffness from Eq. 6-8
- Left end panel shear force
- - - Right end panel shear force
- . - Middle panel shear force
- Torsional brace force 1
- - - Torsional brace force 2

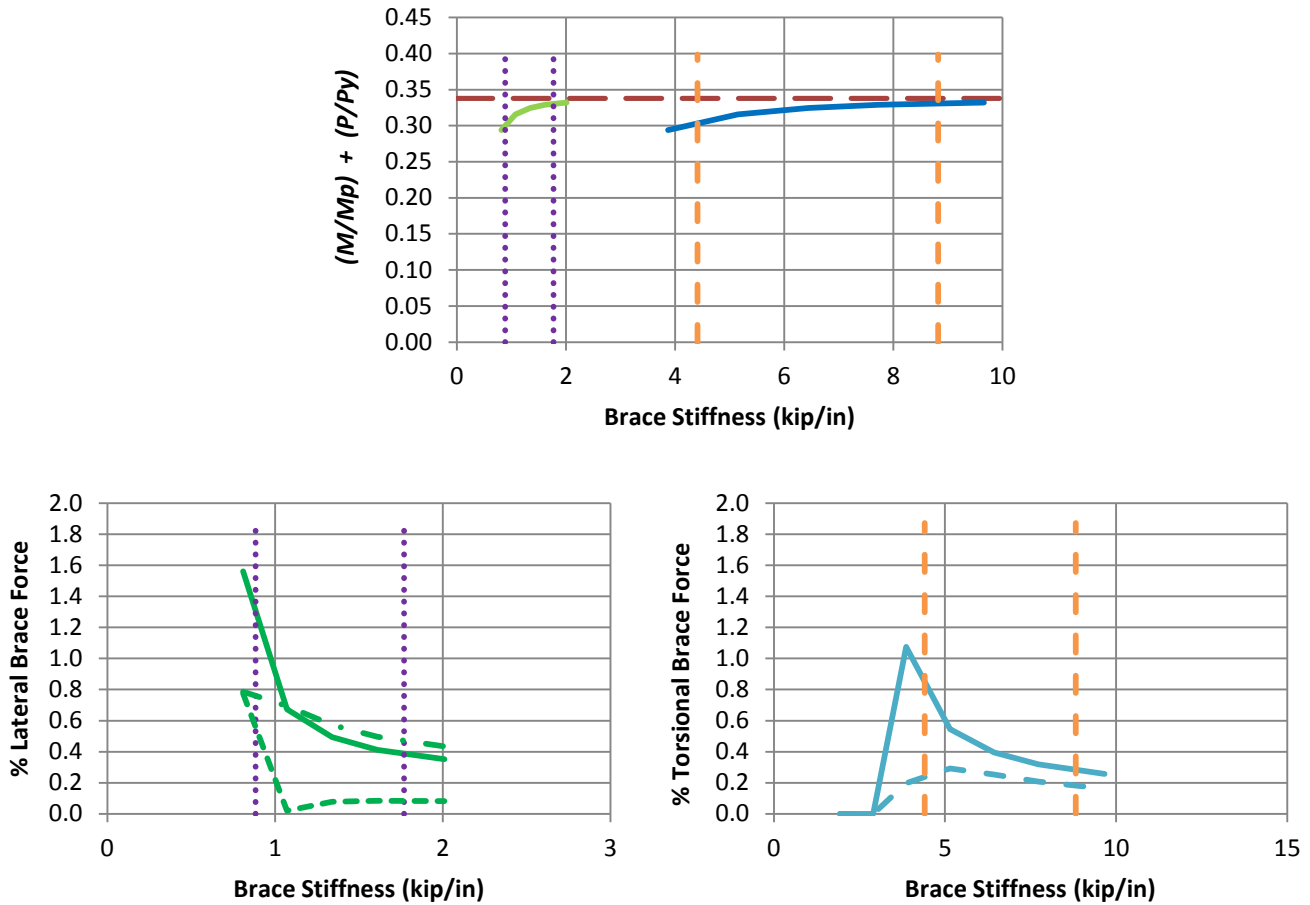
Fig. 7.10. Knuckle curves and brace force vs. brace stiffness plots for combined shear panel (relative) lateral and torsional bracing cases with $n = 2$ and constant axial load and Moment Gradient 1 loading with lateral brace on the flange in flexural compression, $L_b = 15$ ft.



b) BC_MG1p_CRTB_n2_Lb15_FFR0

- Rigidly-braced strength
- Test simulation results corresponding to torsional brace
- Test simulation results corresponding to lateral brace
- 1x and 0.5x lateral bracing stiffness from Eq. 6-7
- - - 1x and 0.5x torsional bracing stiffness from Eq. 6-8
- Left end panel shear force
- - - Right end panel shear force
- . - Middle panel shear force
- Torsional brace force 1
- Torsional brace force 2

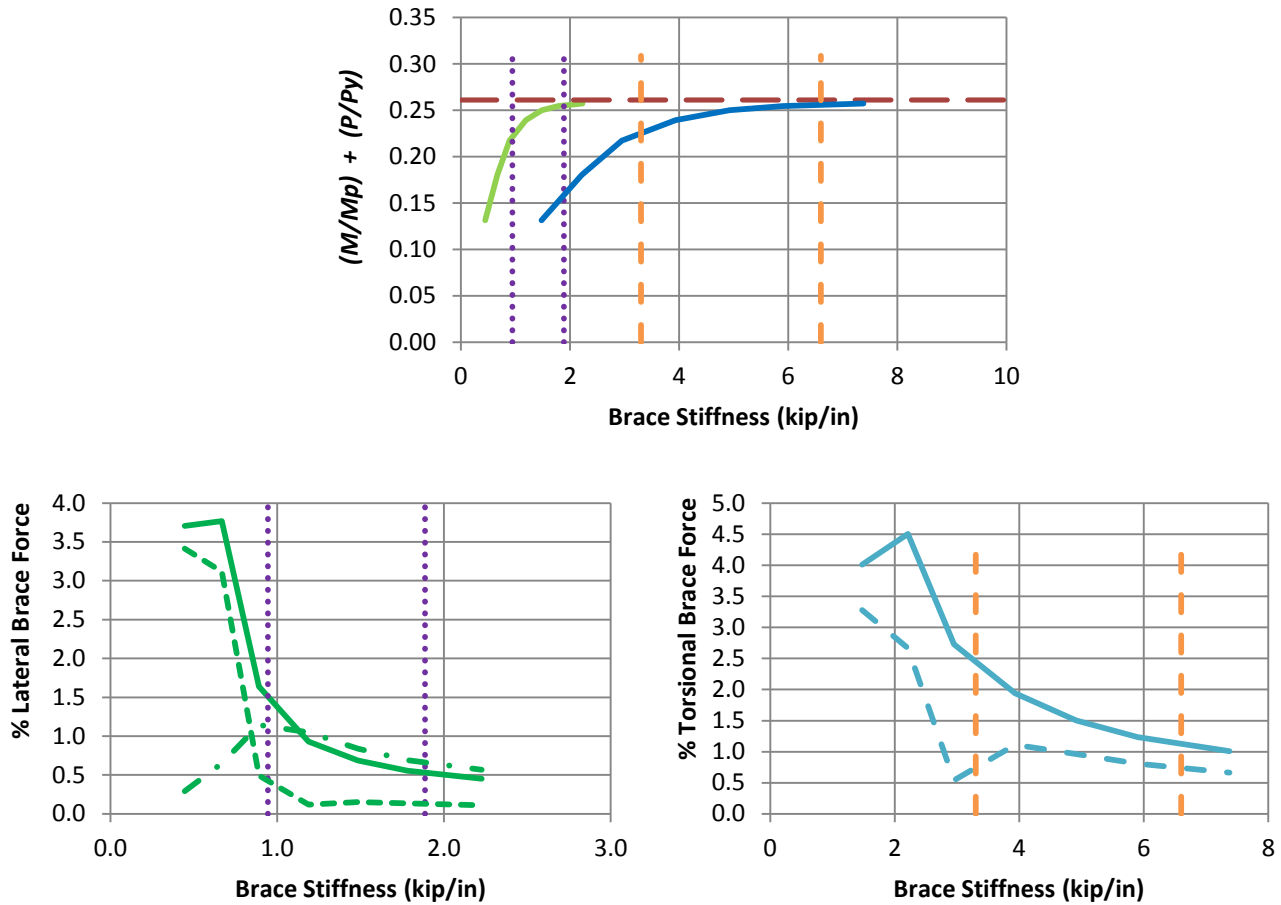
Fig. 7.10. (continued) Knuckle curves and brace force vs. brace stiffness plots for combined shear panel (relative) lateral and torsional bracing cases with $n = 2$ and constant axial load and Moment Gradient 1 loading with lateral brace on the flange in flexural compression, $L_b = 15$ ft.



c) BC_MG1p_CRTB_n2_Lb15_FFR0.5

- Rigidly-braced strength
- Test simulation results corresponding to torsional brace
- Test simulation results corresponding to lateral brace
- 1x and 0.5x lateral bracing stiffness from Eq. 6-7
- - - 1x and 0.5x torsional bracing stiffness from Eq. 6-8
- Left end panel shear force
- - - Right end panel shear force
- . - Middle panel shear force
- Torsional brace force 1
- Torsional brace force 2

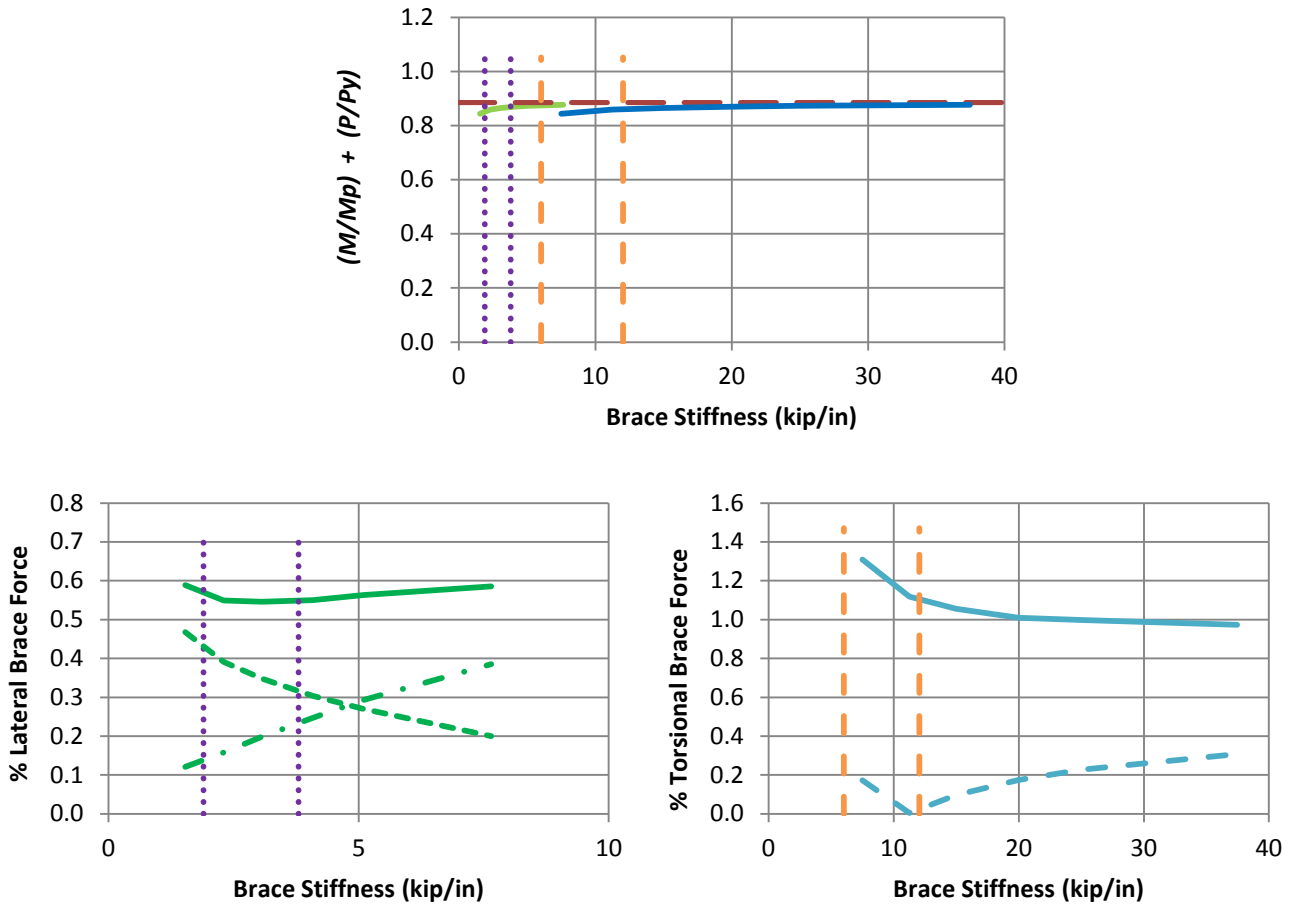
Fig. 7.10. (continued) Knuckle curves and brace force vs. brace stiffness plots for combined shear panel (relative) lateral and torsional bracing cases with $n = 2$ and constant axial load and Moment Gradient 1 loading with lateral brace on the flange in flexural compression, $L_b = 15$ ft.



d) BC_MG1p_CRTB_n2_Lb15_FFR1

- Rigidly-braced strength
- Test simulation results corresponding to torsional brace
- Test simulation results corresponding to lateral brace
- 1x and 0.5x lateral bracing stiffness from Eq. 6-7
- - - 1x and 0.5x torsional bracing stiffness from Eq. 6-8
- Left end panel shear force
- - - Right end panel shear force
- . - Middle panel shear force
- Torsional brace force 1
- Torsional brace force 2

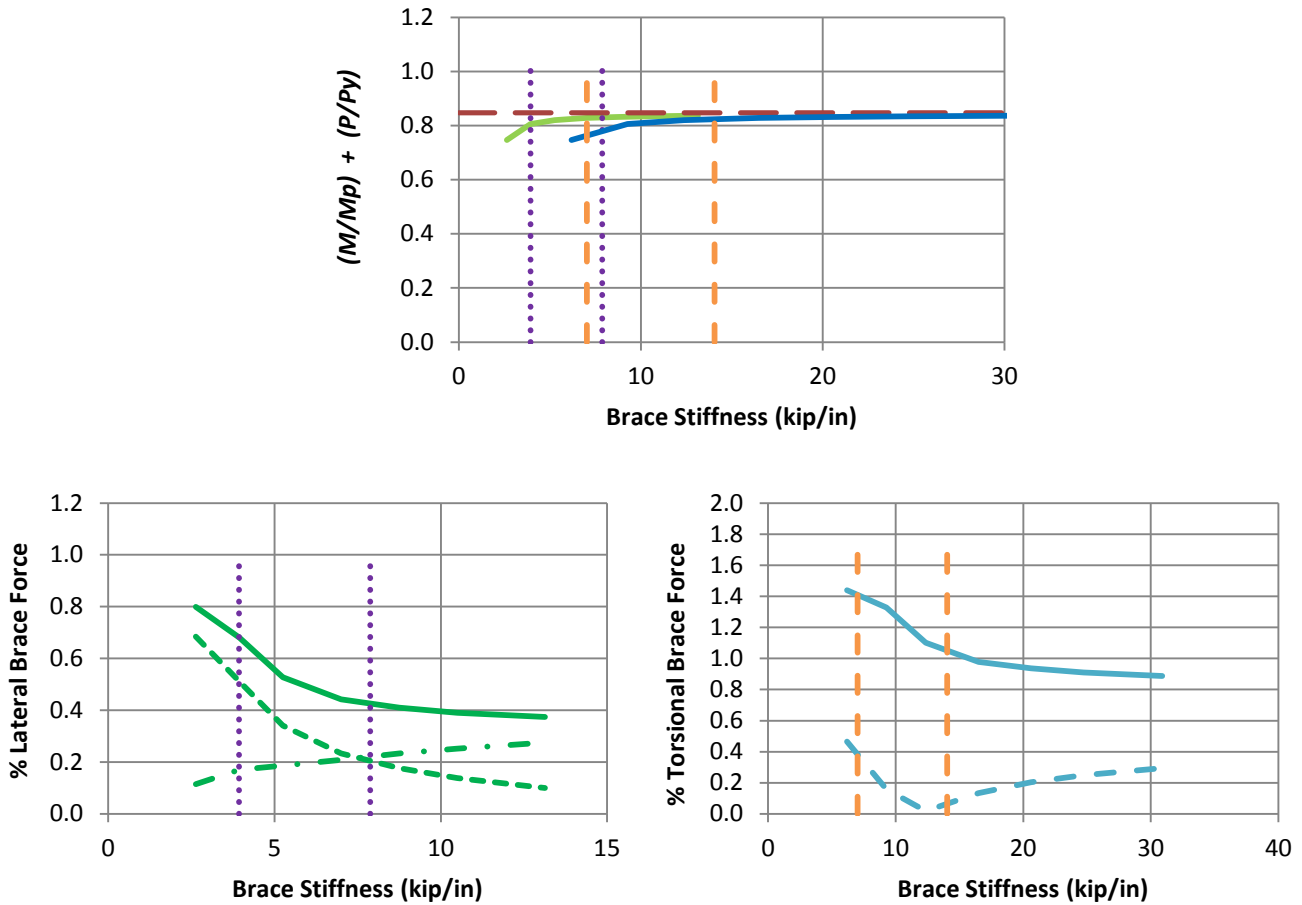
Fig. 7.10. (continued) Knuckle curves and brace force vs. brace stiffness plots for combined shear panel (relative) lateral and torsional bracing cases with $n = 2$ and constant axial load and Moment Gradient 1 loading with lateral brace on the flange in flexural compression, $L_b = 15$ ft.



a) BC_MG1n_CRTB_n2_Lb5_FFR-0.5

- Rigidly-braced strength
- Test simulation results corresponding to torsional brace
- Test simulation results corresponding to lateral brace
- 1x and 0.5x lateral bracing stiffness from Eq. 6-7
- - - 1x and 0.5x torsional bracing stiffness from Eq. 6-8
- Left end panel shear force
- - - Right end panel shear force
- . - Middle panel shear force
- Torsional brace force 1
- - - Torsional brace force 2

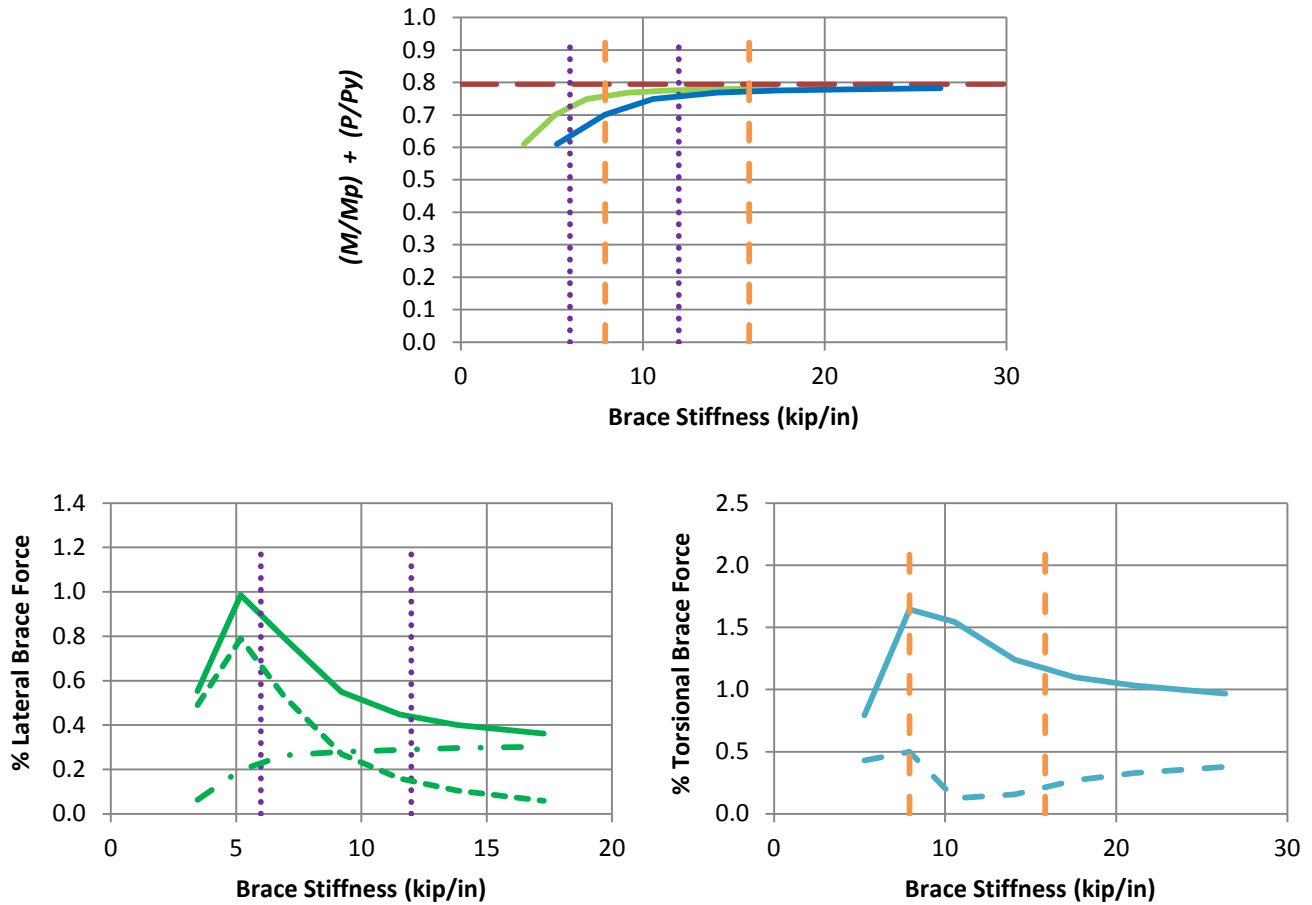
Fig. 7.11. Knuckle curves and brace force vs. brace stiffness plots for combined shear panel (relative) lateral and torsional bracing cases with $n = 2$ and constant axial load and Moment Gradient 1 loading with lateral brace on the flange in flexural tension, $L_b = 5$ ft.



b) BC_MG1n_CRTB_n2_Lb5_FFR0

- Rigidly-braced strength
- Test simulation results corresponding to torsional brace
- Test simulation results corresponding to lateral brace
- 1x and 0.5x lateral bracing stiffness from Eq. 6-7
- - - 1x and 0.5x torsional bracing stiffness from Eq. 6-8
- Left end panel shear force
- - - Right end panel shear force
- . - Middle panel shear force
- Torsional brace force 1
- - - Torsional brace force 2

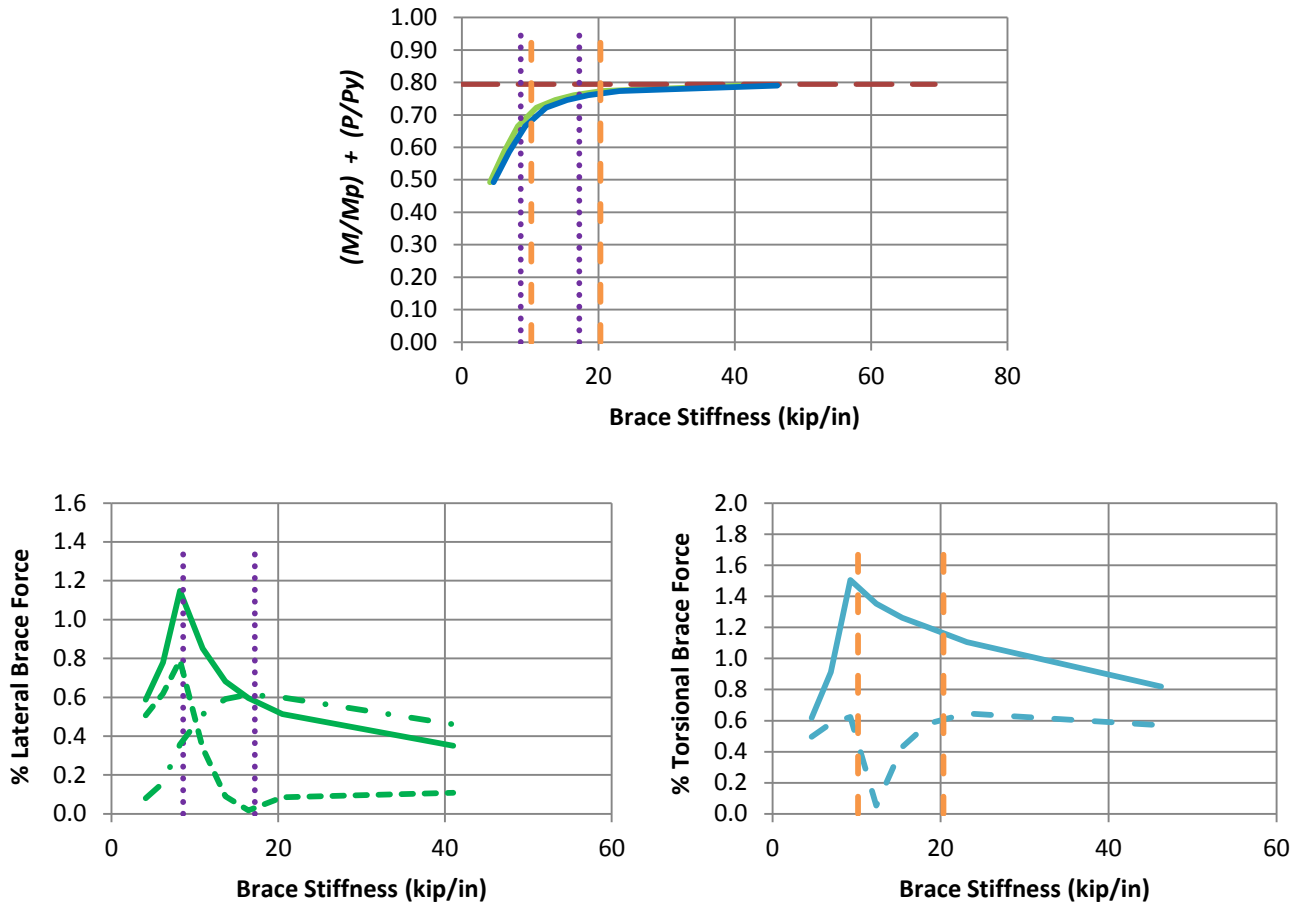
Fig. 7.11. (continued) Knuckle curves and brace force vs. brace stiffness plots for combined shear panel (relative) lateral and torsional bracing cases with $n = 2$ and constant axial load and Moment Gradient 1 loading with lateral brace on the flange in flexural tension, $L_b = 5\text{ft}$.



c) BC_MG1n_CRTB_n2_Lb5_FFR0.5

- Rigidly-braced strength
- Test simulation results corresponding to torsional brace
- Test simulation results corresponding to lateral brace
- 1x and 0.5x lateral bracing stiffness from Eq. 6-7
- - - 1x and 0.5x torsional bracing stiffness from Eq. 6-8
- Left end panel shear force
- - - Right end panel shear force
- . - Middle panel shear force
- Torsional brace force 1
- - - Torsional brace force 2

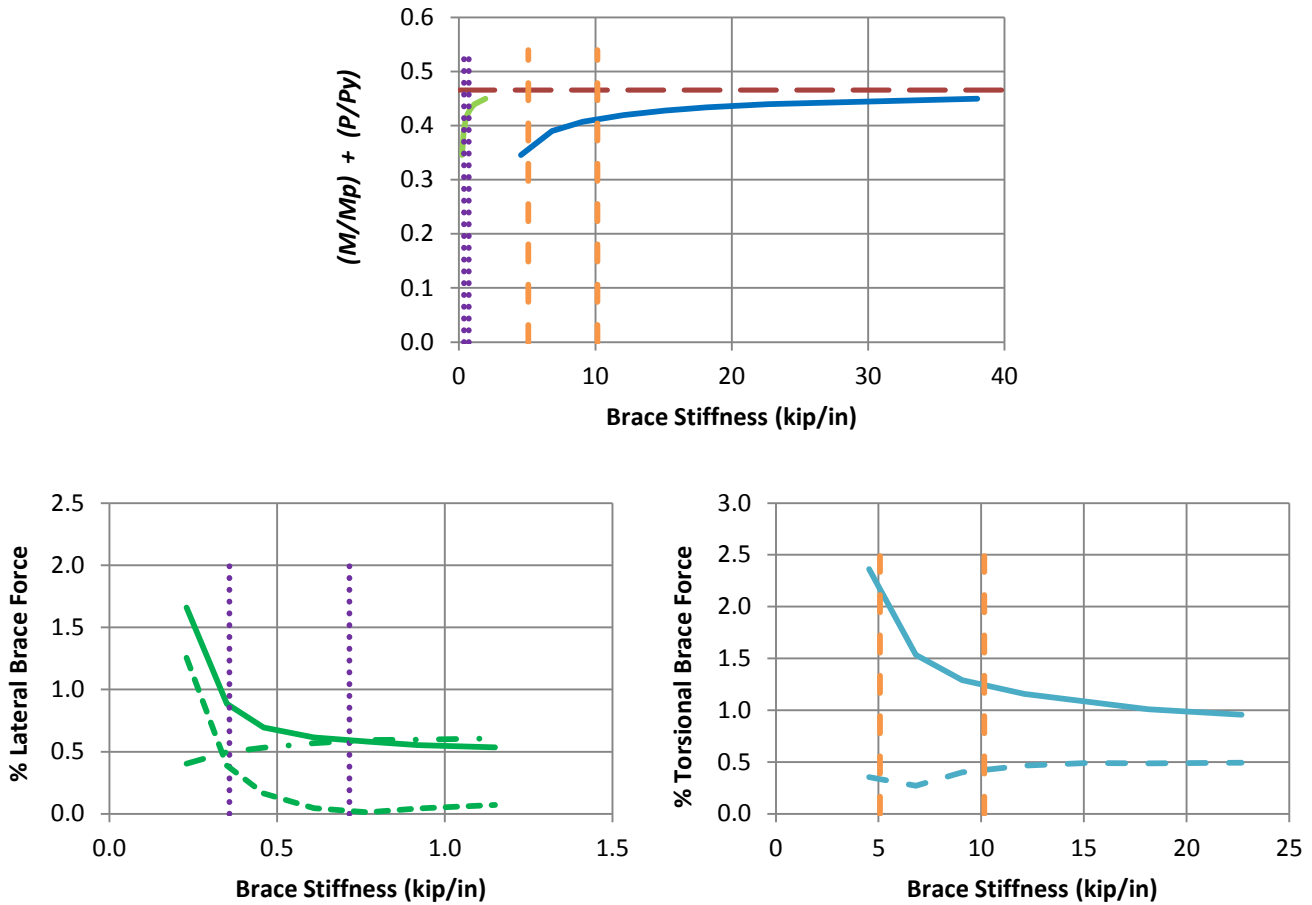
Fig. 7.11. (continued) Knuckle curves and brace force vs. brace stiffness plots for combined shear panel (relative) lateral and torsional bracing cases with $n = 2$ and constant axial load and Moment Gradient 1 loading with lateral brace on the flange in flexural tension, $L_b = 5$ ft.



d) BC_MG1n_CRTB_n2_Lb5_FFR1

- Rigidly-braced strength
- Test simulation results corresponding to torsional brace
- Test simulation results corresponding to lateral brace
- 1x and 0.5x lateral bracing stiffness from Eq. 6-7
- - - 1x and 0.5x torsional bracing stiffness from Eq. 6-8
- Left end panel shear force
- - - Right end panel shear force
- . - Middle panel shear force
- Torsional brace force 1
- - - Torsional brace force 2

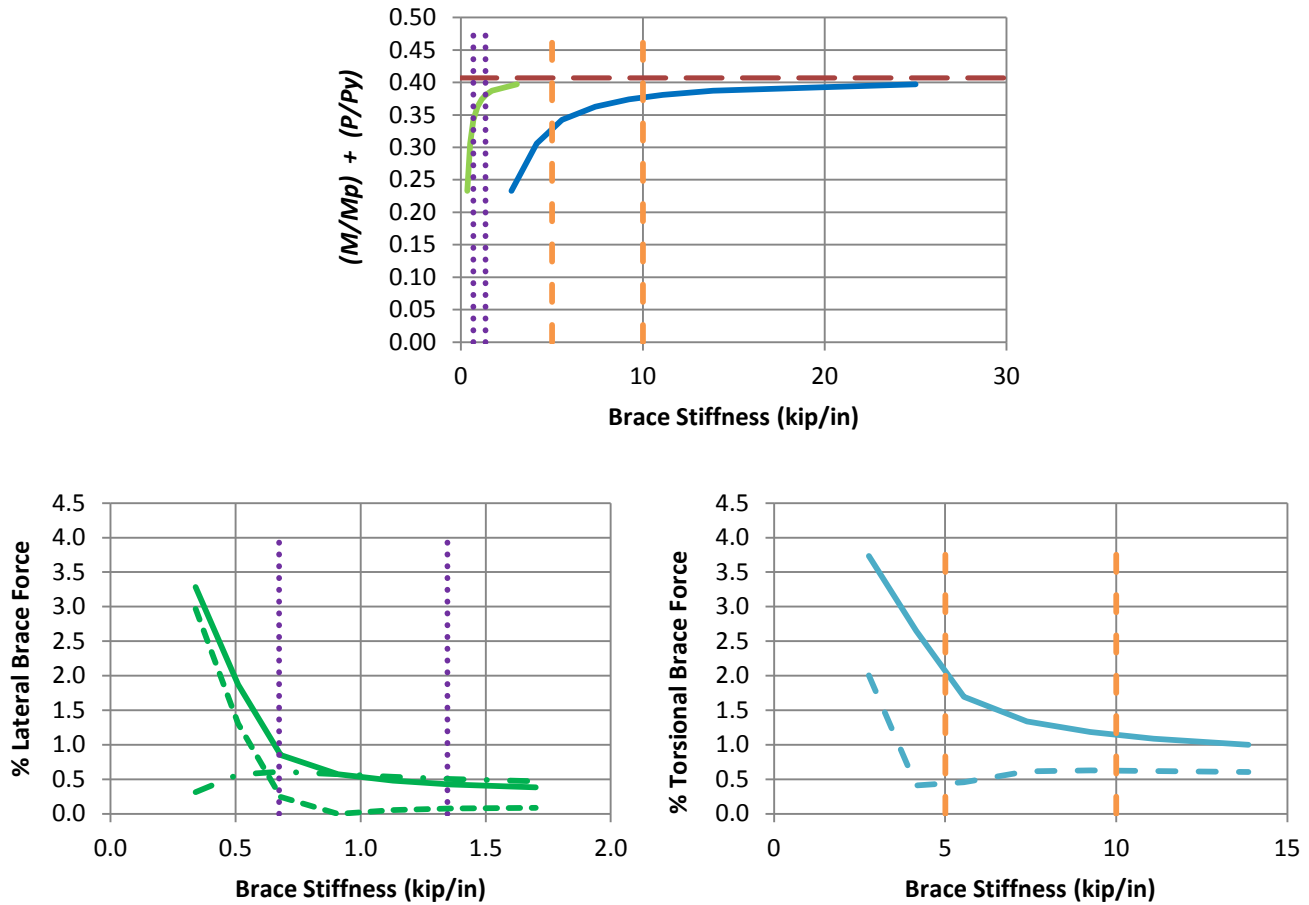
Fig. 7.11. (continued) Knuckle curves and brace force vs. brace stiffness plots for combined shear panel (relative) lateral and torsional bracing cases with $n = 2$ and constant axial load and Moment Gradient 1 loading with lateral brace on the flange in flexural tension, $L_b = 5\text{ft}$.



a) BC_MG1n_CRTB_n2_Lb15_FFR-0.5

- Rigidly-braced strength
- Test simulation results corresponding to torsional brace
- Test simulation results corresponding to lateral brace
- 1x and 0.5x lateral bracing stiffness from Eq. 6-7
- 1x and 0.5x torsional bracing stiffness from Eq. 6-8
- Left end panel shear force
- Right end panel shear force
- Middle panel shear force
- Torsional brace force 1
- Torsional brace force 2

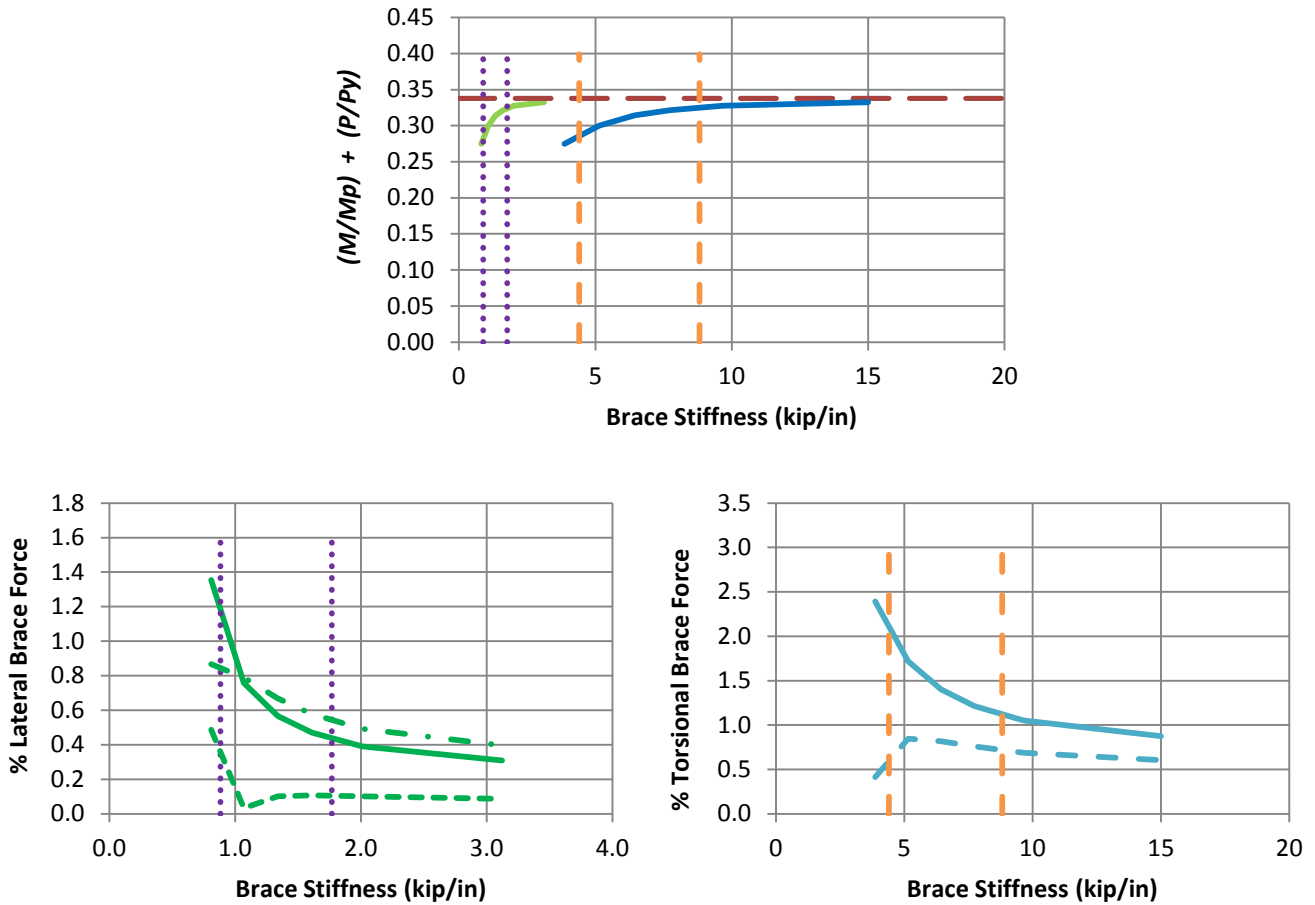
Fig. 7.12. Knuckle curves and brace force vs. brace stiffness plots for combined shear panel (relative) lateral and torsional bracing cases with $n = 2$ and constant axial load and Moment Gradient 1 loading with lateral brace on the flange in flexural tension, $L_b = 15$ ft.



b) BC_MG1n_CRTB_n2_Lb15_FFR0

- Rigidly-braced strength
- Test simulation results corresponding to torsional brace
- Test simulation results corresponding to lateral brace
- 1x and 0.5x lateral bracing stiffness from Eq. 6-7
- 1x and 0.5x torsional bracing stiffness from Eq. 6-8
- Left end panel shear force
- Right end panel shear force
- Middle panel shear force
- Torsional brace force 1
- Torsional brace force 2

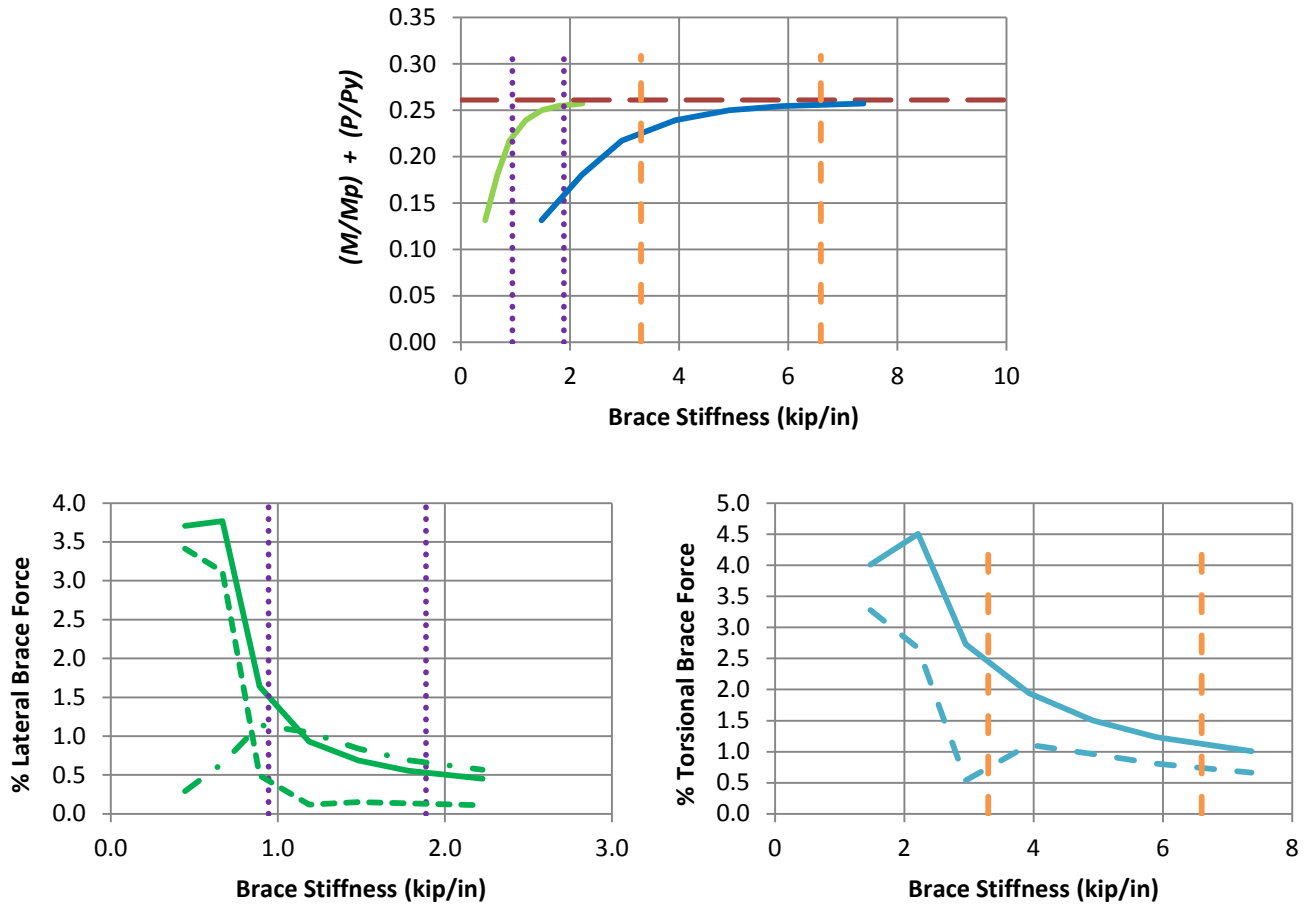
Fig. 7.12. (continued) Knuckle curves and brace force vs. brace stiffness plots for combined shear panel (relative) lateral and torsional bracing cases with $n = 2$ and constant axial load and Moment Gradient 1 loading with lateral brace on the flange in flexural tension, $L_b = 15$ ft.



c) BC_MG1n_CRTB_n2_Lb15_FFR0.5

- Rigidly-braced strength
- Test simulation results corresponding to torsional brace
- Test simulation results corresponding to lateral brace
- 1x and 0.5x lateral bracing stiffness from Eq. 6-7
- - - 1x and 0.5x torsional bracing stiffness from Eq. 6-8
- Left end panel shear force
- - - Right end panel shear force
- . - Middle panel shear force
- Torsional brace force 1
- - - Torsional brace force 2

Fig. 7.12. (continued) Knuckle curves and brace force vs. brace stiffness plots for combined shear panel (relative) lateral and torsional bracing cases with $n = 2$ and constant axial load and Moment Gradient 1 loading with lateral brace on the flange in flexural tension, $L_b = 15$ ft.



d) BC_MG1n_CRTB_n2_Lb15_FFR1

- Rigidly-braced strength
- Test simulation results corresponding to torsional brace
- Test simulation results corresponding to lateral brace
- 1x and 0.5x lateral bracing stiffness from Eq. 6-7
- - - 1x and 0.5x torsional bracing stiffness from Eq. 6-8
- Left end panel shear force
- - - Right end panel shear force
- . - Middle panel shear force
- Torsional brace force 1
- - - Torsional brace force 2

Fig. 7.12. (continued) Knuckle curves and brace force vs. brace stiffness plots for combined shear panel (relative) lateral and torsional bracing cases with $n = 2$ and constant axial load and Moment Gradient 1 loading with lateral brace on the flange in flexural tension, $L_b = 15$ ft.

Table 7.2. Comparison of simulation results in Figs. 7.5 through 7.12 with Eq. 6-7.

Case (a)	Lateral bracing Stiffness corresponding to 96% of simulation rigidly-braced strength (kip/in) (b)	Required lateral Bracing stiffness from Eq. 6-7 kip/in (c)	Col. (b) / Col. (c) (d)
BC_MG1p_CNTB_n1_Lb5_FFR-0.5	1.4	7.70	0.19
BC_MG1p_CNTB_n1_Lb5_FFR0	3.21	15.76	0.21
BC_MG1p_CNTB_n1_Lb5_FFR0.5	7.09	24.76	0.29
BC_MG1p_CNTB_n1_Lb5_FFR1	26.91	33.84	0.80
BC_MG1p_CNTB_n1_Lb15_FFR-0.5	1.82	1.46	1.26
BC_MG1p_CNTB_n1_Lb15_FFR0	2.1	2.70	0.78
BC_MG1p_CNTB_n1_Lb15_FFR0.5	2.17	3.48	0.63
BC_MG1p_CNTB_n1_Lb15_FFR1	2.37	3.68	0.65
BC_MG1n_CNTB_n1_Lb5_FFR-0.5	2.1	7.66	0.28
BC_MG1n_CNTB_n1_Lb5_FFR0	6.5	15.86	0.41
BC_MG1n_CNTB_n1_Lb5_FFR0.5	14	24.00	0.59
BC_MG1n_CNTB_n1_Lb5_FFR1	26.91	33.84	0.80
BC_MG1n_CNTB_n1_Lb15_FFR-0.5	2.16	1.46	1.49
BC_MG1n_CNTB_n1_Lb15_FFR0	2.59	2.70	0.96
BC_MG1n_CNTB_n1_Lb15_FFR0.5	2.59	3.48	0.75
BC_MG1n_CNTB_n1_Lb15_FFR1	2.37	3.68	0.65
BC_MG1p_CRTB_n2_Lb5_FFR-0.5	1.11	3.78	0.29
BC_MG1p_CRTB_n2_Lb5_FFR0	2.57	7.84	0.33

Table 7.2.(continued) Comparison of simulation results in Figs. 7.5 through 7.12 with Eq. 6-7.

Case (a)	Lateral bracing stiffness corresponding to 96% of simulation rigidly- braced strength (kip/in) (b)	Required lateral bracing stiffness from Eq. 6-7 (kip/in) (c)	Col. (b) / Col. (c) (d)
BC_MG1p_CRTB_n2_Lb5_FFR0.5	6.11	11.94	0.51
BC_MG1p_CRTB_n2_Lb5_FFR1	16.75	17.20	0.98
BC_MG1p_CRTB_n2_Lb15_FFR-0.5	1.4	0.72	1.96
BC_MG1p_CRTB_n2_Lb15_FFR0	1.41	1.36	1.04
BC_MG1p_CRTB_n2_Lb15_FFR0.5	1.33	1.76	0.76
BC_MG1p_CRTB_n2_Lb15_FFR1	1.53	1.88	0.81
BC_MG1n_CRTB_n2_Lb5_FFR-0.5	1.86	3.80	0.49
BC_MG1n_CRTB_n2_Lb5_FFR0	4.6	7.88	0.59
BC_MG1n_CRTB_n2_Lb5_FFR0.5	8.5	11.98	0.71
BC_MG1n_CRTB_n2_Lb5_FFR1	16.75	17.20	0.98
BC_MG1n_CRTB_n2_Lb15_FFR-0.5	1.74	0.72	2.44
BC_MG1n_CRTB_n2_Lb15_FFR0	2.16	1.34	1.61
BC_MG1n_CRTB_n2_Lb15_FFR0.5	1.8	1.76	1.02
BC_MG1n_CRTB_n2_Lb15_FFR1	1.53	1.88	0.81

Table 7.3. Comparison of simulation results in Figs. 7.5 through 7.12 with Eq. 6-8.

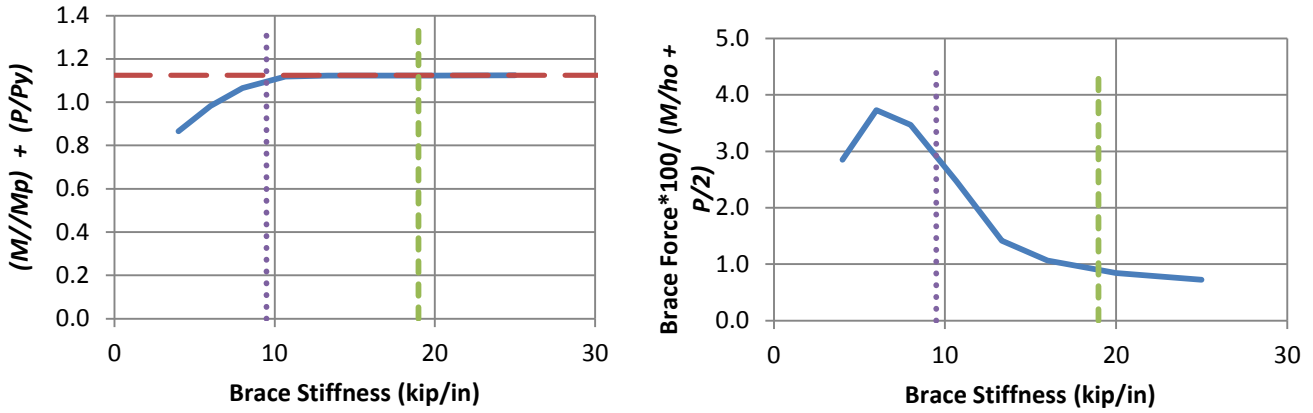
Case (a)	Torsional bracing Stiffness corresponding to 96% of simulation rigidly-braced strength (kip/in) (b)	Required torsional Bracing stiffness from Eq. 6-8 kip/in (c)	Col. (b) / Col. (c) (d)
BC_MG1p_CNTB_n1_Lb5_FFR-0.5	4.23	14.70	0.29
BC_MG1p_CNTB_n1_Lb5_FFR0	5.02	17.52	0.29
BC_MG1p_CNTB_n1_Lb5_FFR0.5	7.21	21.94	0.33
BC_MG1p_CNTB_n1_Lb5_FFR1	20.19	26.20	0.77
BC_MG1p_CNTB_n1_Lb15_FFR-0.5	24.03	13.48	1.79
BC_MG1p_CNTB_n1_Lb15_FFR0	11.48	13.34	0.86
BC_MG1p_CNTB_n1_Lb15_FFR0.5	6.94	11.46	0.61
BC_MG1p_CNTB_n1_Lb15_FFR1	5.2	8.36	0.62
BC_MG1n_CNTB_n1_Lb5_FFR-0.5	6.83	14.56	0.47
BC_MG1n_CNTB_n1_Lb5_FFR0	10.16	17.72	0.57
BC_MG1n_CNTB_n1_Lb5_FFR0.5	14.24	20.64	0.69
BC_MG1n_CNTB_n1_Lb5_FFR1	20.19	26.20	0.77
BC_MG1n_CNTB_n1_Lb15_FFR-0.5	28.55	13.46	2.12
BC_MG1n_CNTB_n1_Lb15_FFR0	14.16	13.34	1.06
BC_MG1n_CNTB_n1_Lb15_FFR0.5	8.3	11.46	0.73
BC_MG1n_CNTB_n1_Lb15_FFR1	5.2	8.36	0.62
BC_MG1p_CRTB_n2_Lb5_FFR-0.5	5.42	11.98	0.46
BC_MG1p_CRTB_n2_Lb5_FFR0	6.05	13.94	0.44

Table 7.3.(continued) Comparison of simulation results in Figs. 7.5 through 7.12 with Eq. 6-8.

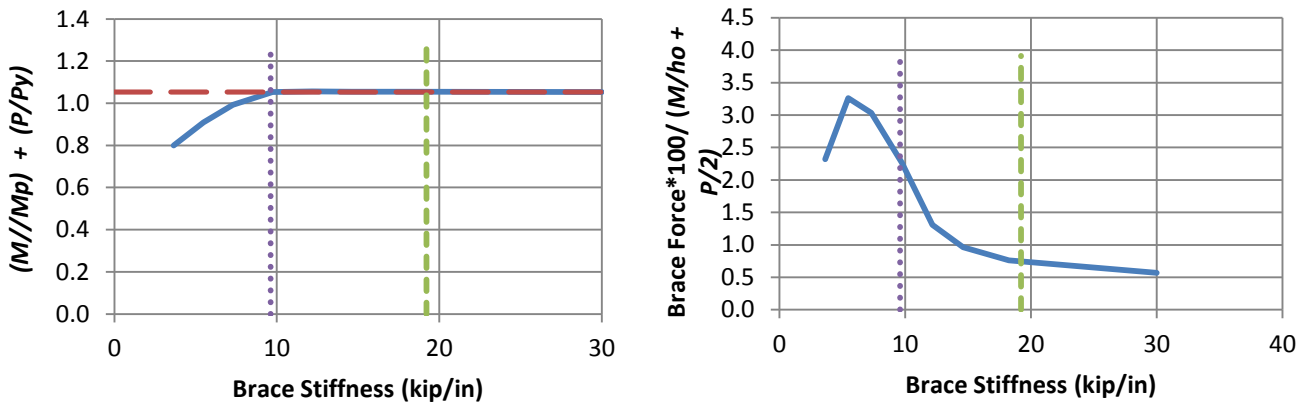
Case (a)	Lateral bracing stiffness corresponding to 96% of simulation rigidly- braced strength (kip/in) (b)	Required lateral bracing stiffness from Eq. 6-8 (kip/in) (c)	Col. (b) / Col. (c) (d)
BC_MG1p_CRTB_n2_Lb5_FFR0.5	9.33	15.72	0.60
BC_MG1p_CRTB_n2_Lb5_FFR1	18.9	20.32	0.93
BC_MG1p_CRTB_n2_Lb15_FFR-0.5	27.68	10.16	2.73
BC_MG1p_CRTB_n2_Lb15_FFR0	11.48	10.06	1.14
BC_MG1p_CRTB_n2_Lb15_FFR0.5	6.4	8.82	0.73
BC_MG1p_CRTB_n2_Lb15_FFR1	5.08	6.60	0.77
BC_MG1n_CRTB_n2_Lb5_FFR-0.5	9.11	12.04	0.76
BC_MG1n_CRTB_n2_Lb5_FFR0	10.84	14.06	0.77
BC_MG1n_CRTB_n2_Lb5_FFR0.5	12.99	15.84	0.82
BC_MG1n_CRTB_n2_Lb5_FFR1	18.9	20.32	0.93
BC_MG1n_CRTB_n2_Lb15_FFR-0.5	34.42	10.14	3.39
BC_MG1n_CRTB_n2_Lb15_FFR0	17.62	10.00	1.76
BC_MG1n_CRTB_n2_Lb15_FFR0.5	8.65	8.82	0.98
BC_MG1n_CRTB_n2_Lb15_FFR1	5.08	6.60	0.77

7.3.2 Beam-Columns with Moment Gradient 2 Loading

Results for beam-columns with Moment Gradient 2 loading and lateral bracing only are shown in Figs. 7.13 and 7.14. Table 7.4 compares the results from these figures. From Col. (d) of Table 7.4 it can be observed that the bracing stiffness calculated by Eq. 6-3 provides a conservative estimate of the bracing stiffness requirement. From Figs. 7.13 and 7.14, it can be observed that the bracing strength calculated by Eq. 6-4 is accurate to slightly conservative.



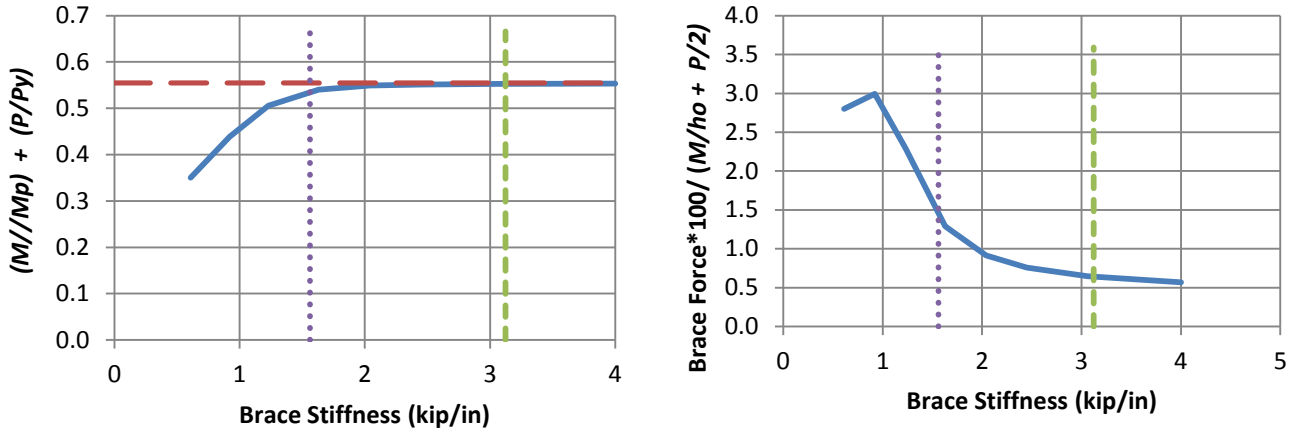
a) BC_MG2p_NB_n1_Lb5_FFR-0.5



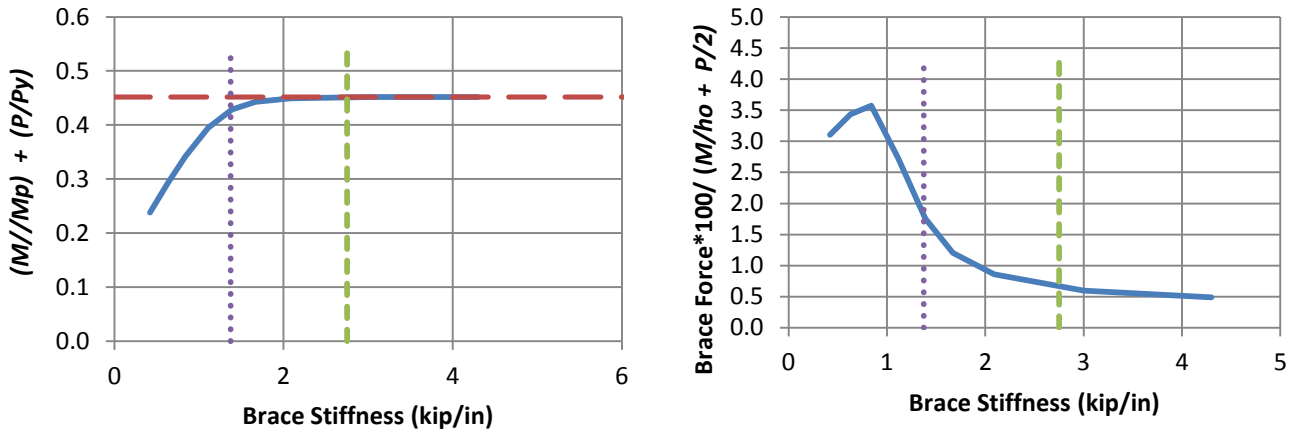
b) BC_MG2p_NB_n1_Lb5_FFR0

- Test simulation results
- - Rigidly-braced strength
- ⋯ 0.5 times bracing stiffness from Eq. 6-3
- - Bracing stiffness from Eq. 6-3

Fig. 7.13. Knuckle curves and brace force vs. brace stiffness plots for point (nodal) lateral bracing cases with $n = 1$ and constant axial load and Moment Gradient 2 loading, $L_b = 5$ ft.



a) BC_MG2p_NB_n1_Lb15_FFR-0.5



b) BC_MG2p_NB_n1_Lb15_FFR0

- Test simulation results
- - Rigidly-braced strength
- ⋯ 0.5 times bracing stiffness from Eq. 6-3
- - Bracing stiffness from Eq. 6-3

Fig. 7.14. Knuckle curves and brace force vs. brace stiffness plots for point (nodal) lateral bracing cases with $n = 1$ and constant axial load and Moment Gradient 2 loading, $L_b = 15$ ft.

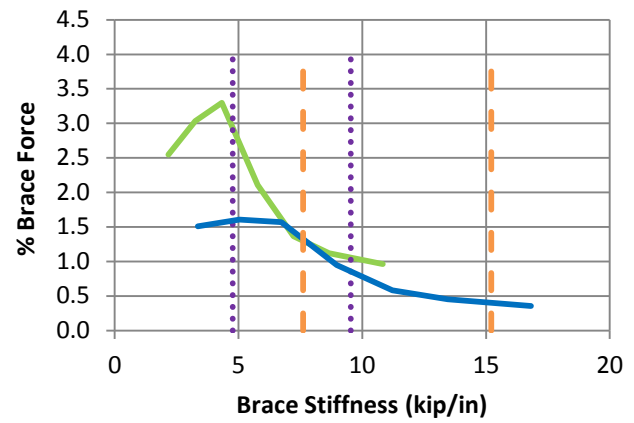
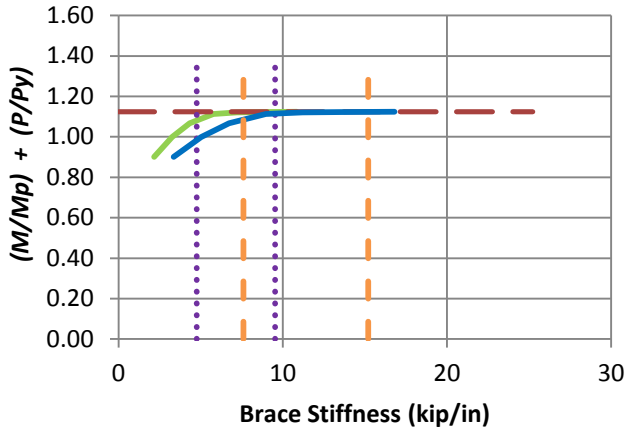
Table 7.4. Comparison of simulation results in Figs. 7.13 and 7.14 with Eq. 6-3.

Case (a)	Stiffness corresponding to 96% of simulation rigidly-braced strength (kip/in) (b)	Required bracing stiffness from Eq. 6-3 kip/in (c)	Col. (b) / Col. (c) (d)
BC_MG2p_NB_n1_Lb5_FFR-0.5	8.72	18.96	0.46
BC_MG2p_NB_n1_Lb5_FFR0	8.07	19.22	0.42
BC_MG2p_NB_n1_Lb15_FFR-0.5	1.54	3.12	0.50
BC_MG2p_NB_n1_Lb15_FFR0	1.49	2.74	0.54

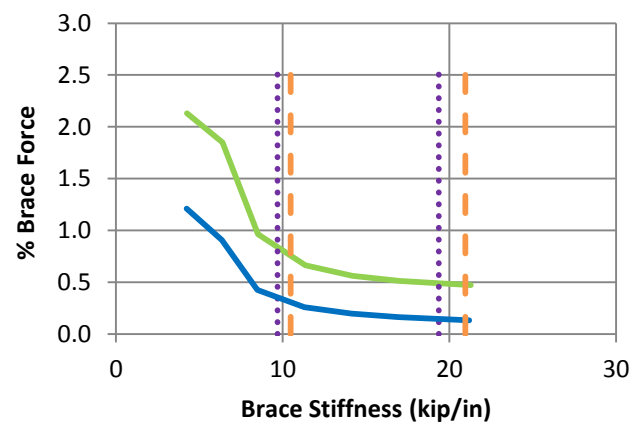
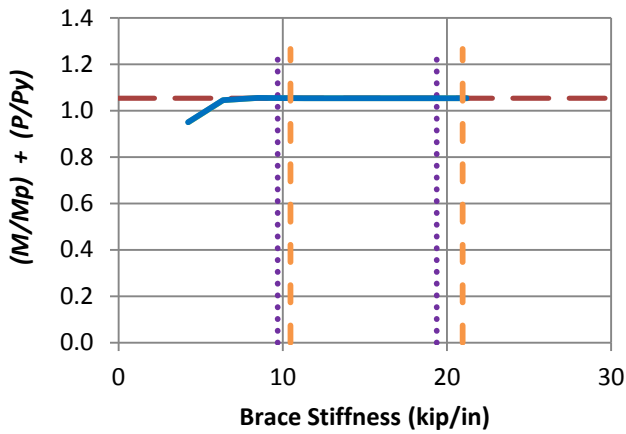
Combined point (nodal) lateral and torsional bracing

Results for beam-columns with Moment Gradient 2 loading, and combined lateral and torsional bracing are shown in Figs. 7.15 through 7.18. The lateral brace force in these figures is expressed as percentage with respect to P . The torsional brace force in Figs. 7.15 through 7.18 is expressed as percentage with respect to $M/h_o+P/2$.

Tables 7.5 and 7.6 compare the results in Figs. 7.15 through 7.18. From Col. (d) of these tables, it can be observed that the bracing stiffness calculated by Eqs. 6-7 and 6-8 is sufficient to develop 96 % of the minimum rigidly-braced member strength for all combined bracing cases.



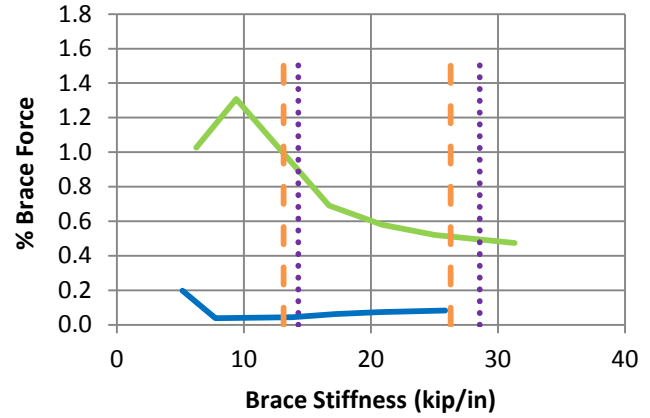
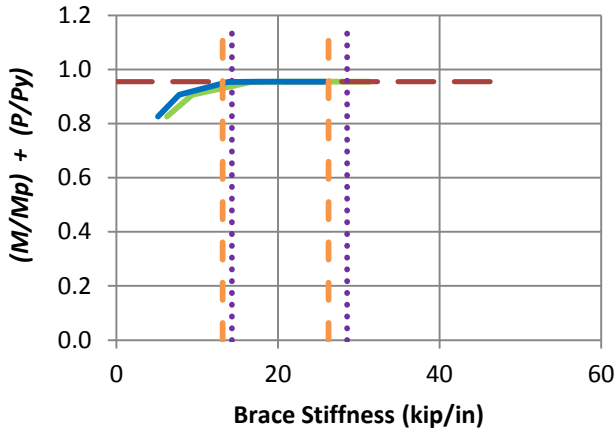
a) BC_MG2p_CNTB_n1_Lb5_FFR-0.5



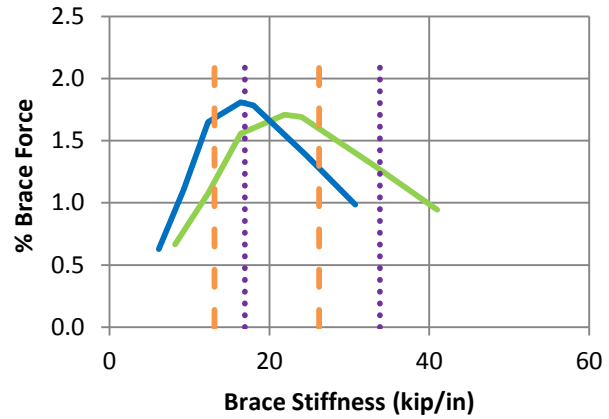
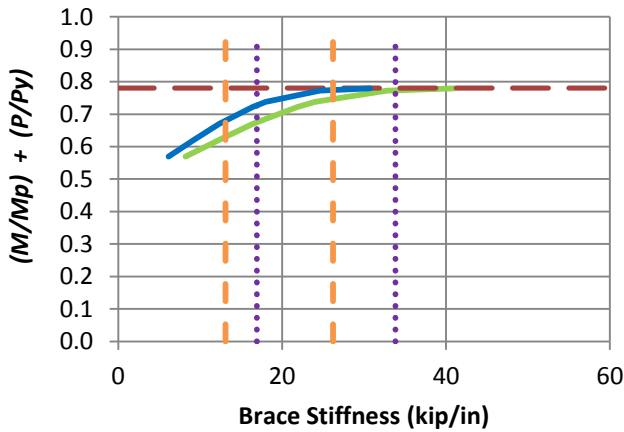
b) BC_MG2p_CNTB_n1_Lb5_FFR0

- Rigidly-braced strength
- Test simulation results corresponding to torsional brace
- Test simulation results corresponding to lateral brace
- 1x and 0.5x lateral bracing stiffness from Eq. 6-7
- 1x and 0.5x torsional bracing stiffness from Eq. 6-8

Fig. 7.15. Knuckle curves and brace force vs. brace stiffness plots for combined point (nodal) lateral and torsional bracing cases with $n = 1$ and constant axial load and Moment Gradient 2 loading with lateral brace on the flange in flexural compression, $L_b = 5$ ft.



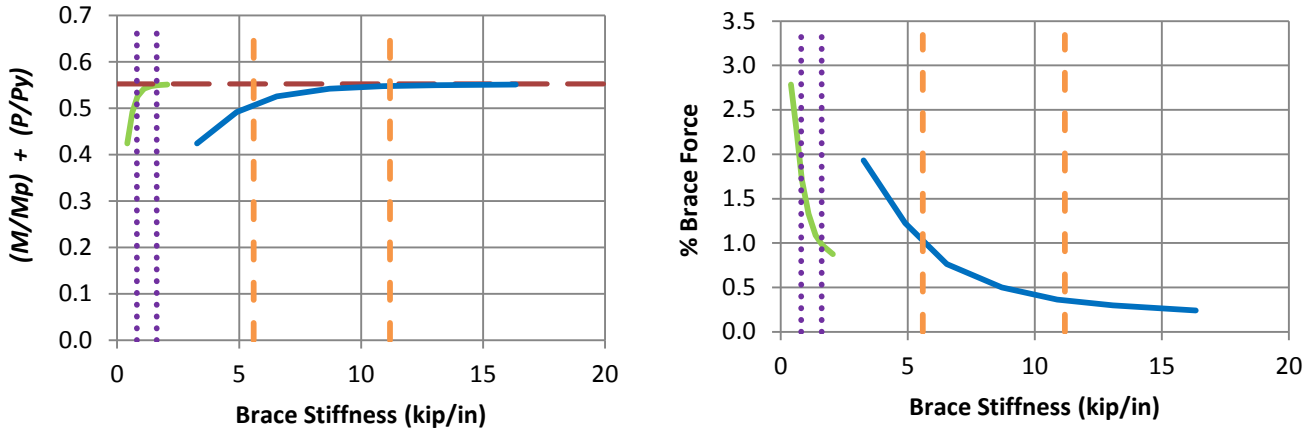
c) BC_MG2p_CNTB_n1_Lb5_FFR0.5



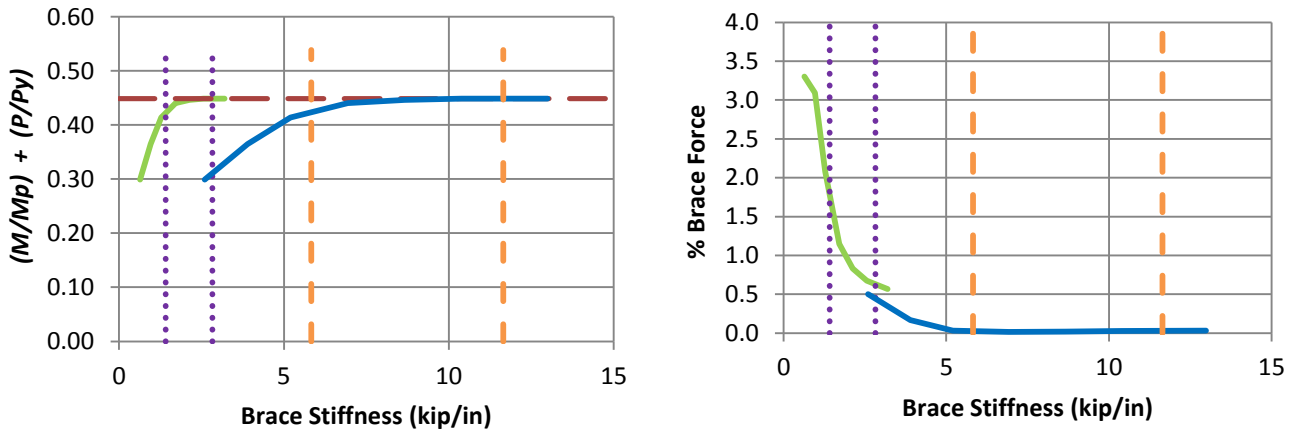
d) BC_MG2p_CNTB_n1_Lb5_FFR1

- Rigidly-braced strength
- Test simulation results corresponding to torsional brace
- Test simulation results corresponding to lateral brace
- 1x and 0.5x lateral bracing stiffness from Eq. 6-7
- 1x and 0.5x torsional bracing stiffness from Eq. 6-8

Fig. 7.15. (continued) Knuckle curves and brace force vs. brace stiffness plots for combined point (nodal) lateral and torsional bracing cases with $n = 1$ and constant axial load and Moment Gradient 2 loading with lateral brace on the flange in flexural compression, $L_b = 5$ ft.



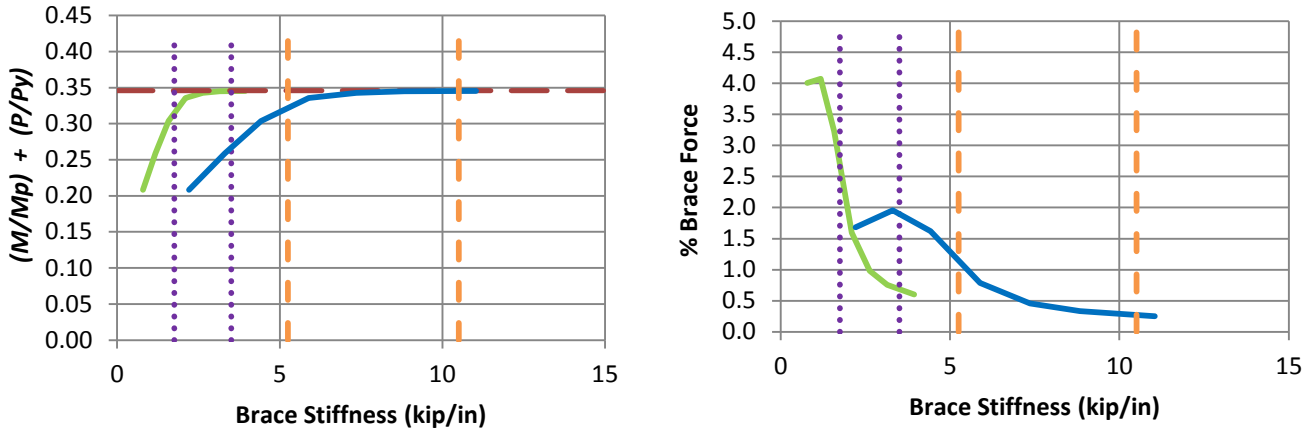
a) BC_MG2p_CNTB_n1_Lb15_FFR-0.5



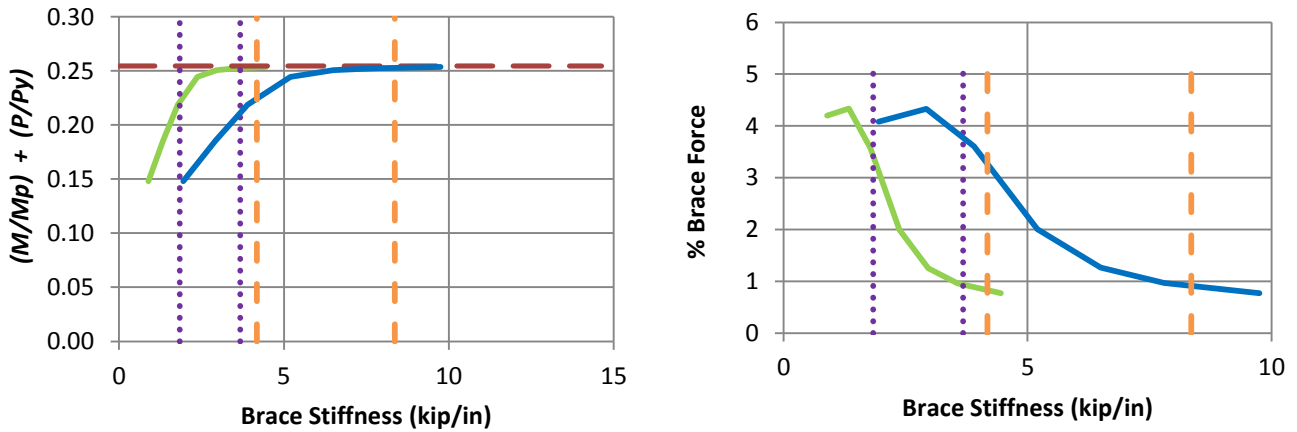
b) BC_MG2p_CNTB_n1_Lb15_FFR0

- Rigidly-braced strength
- Test simulation results corresponding to torsional brace
- Test simulation results corresponding to lateral brace
- 1x and 0.5x lateral bracing stiffness from Eq. 6-7
- 1x and 0.5x torsional bracing stiffness from Eq. 6-8

Fig. 7.16. Knuckle curves and brace force vs. brace stiffness plots for combined point (nodal) lateral and torsional bracing cases with $n = 1$ and constant axial load and Moment Gradient 2 loading with lateral brace on the flange in flexural compression, $L_b = 15$ ft.



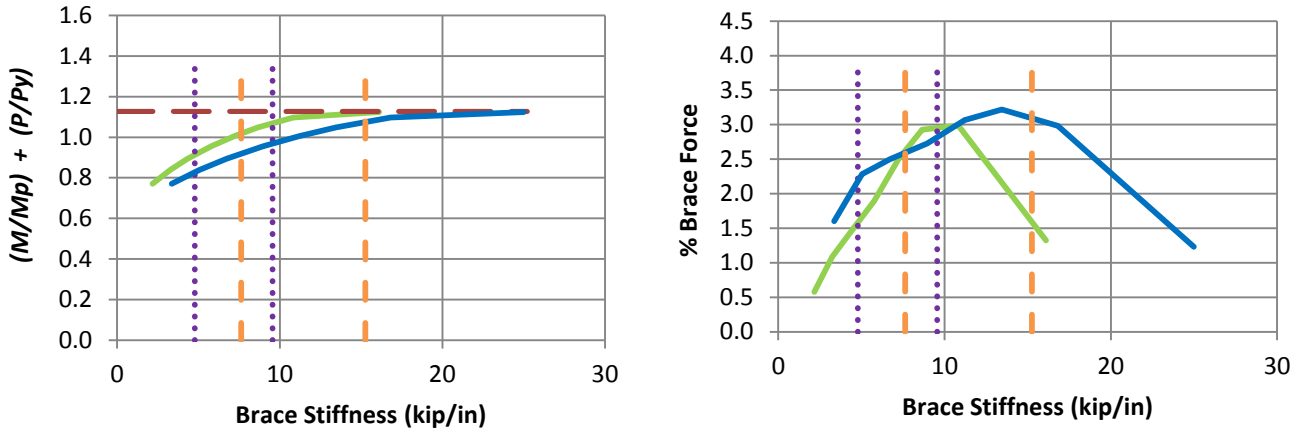
c) BC_MG2p_CNTB_n1_Lb15_FFR0.5



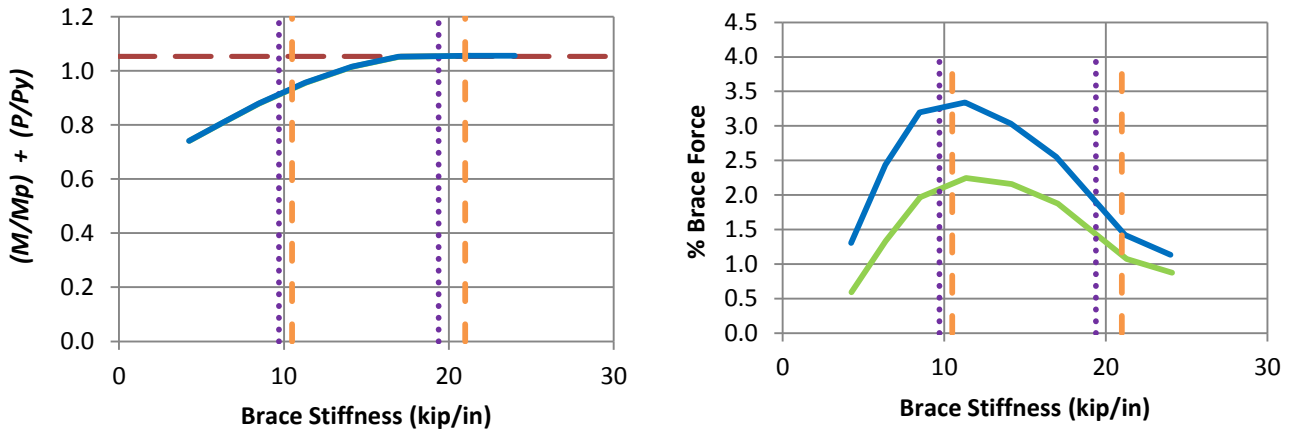
d) BC_MG2p_CNTB_n1_Lb15_FFR1

- Rigidly-braced strength
- Test simulation results corresponding to torsional brace
- Test simulation results corresponding to lateral brace
- ⋯ 1x and 0.5x lateral bracing stiffness from Eq. 6-7
- 1x and 0.5x torsional bracing stiffness from Eq. 6-8

Fig. 7.16. (continued) Knuckle curves and brace force vs. brace stiffness plots for combined point (nodal) lateral and torsional bracing cases with $n = 1$ and constant axial load and Moment Gradient 2 loading with lateral brace on the flange in flexural compression, $L_b = 15$ ft.



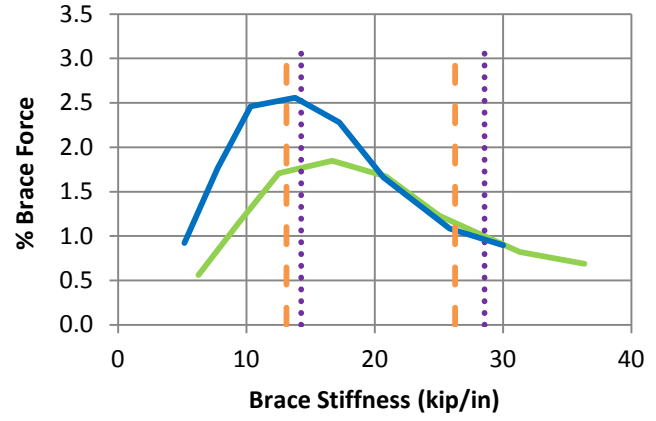
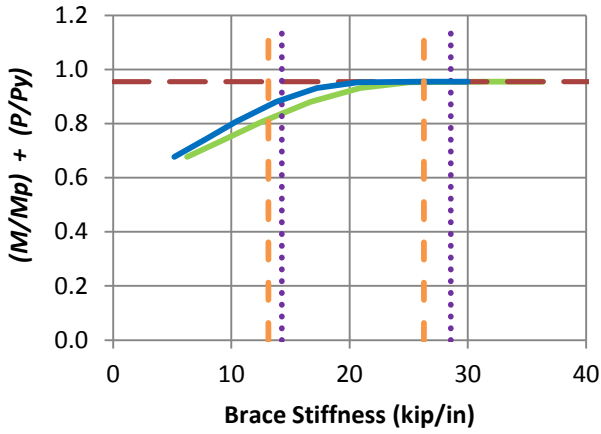
a) BC_MG2n_CNTB_n1_Lb5_FFR-0.5



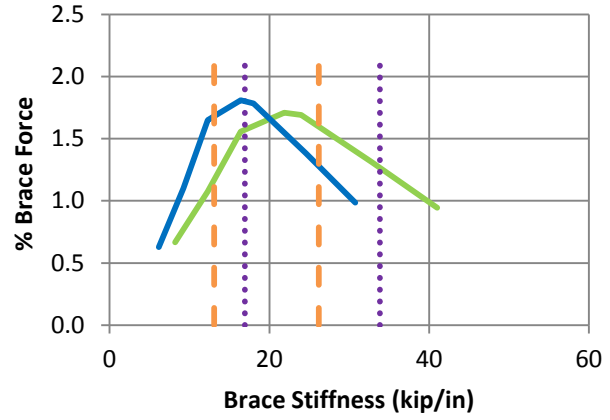
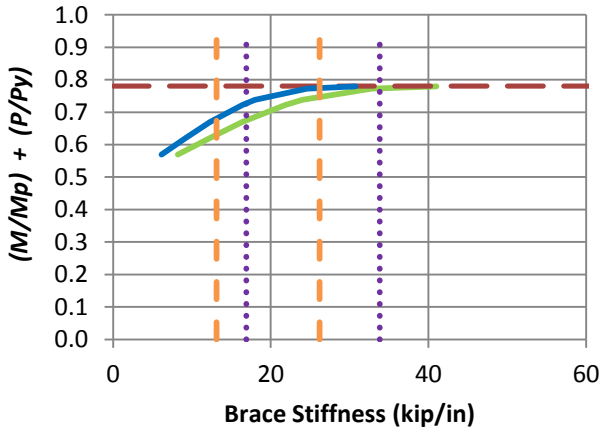
b) BC_MG2n_CNTB_n1_Lb5_FFR0

- Rigidly-braced strength
- Test simulation results corresponding to torsional brace
- Test simulation results corresponding to lateral brace
- ⋯ 1x and 0.5x lateral bracing stiffness from Eq. 6-7
- 1x and 0.5x torsional bracing stiffness from Eq. 6-8

Fig. 7.17. Knuckle curves and brace force vs. brace stiffness plots for combined point (nodal) lateral and torsional bracing cases with $n = 1$ and constant axial load and Moment Gradient 2 loading with lateral brace on the flange in flexural tension, $L_b = 5$ ft.



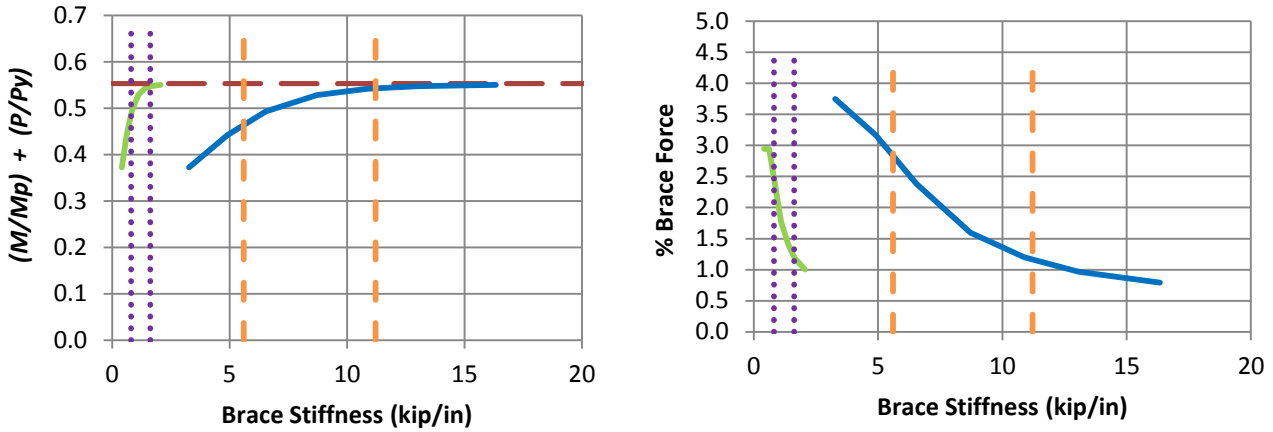
c) BC_MG2n_CNTB_n1_Lb5_FFR0.5



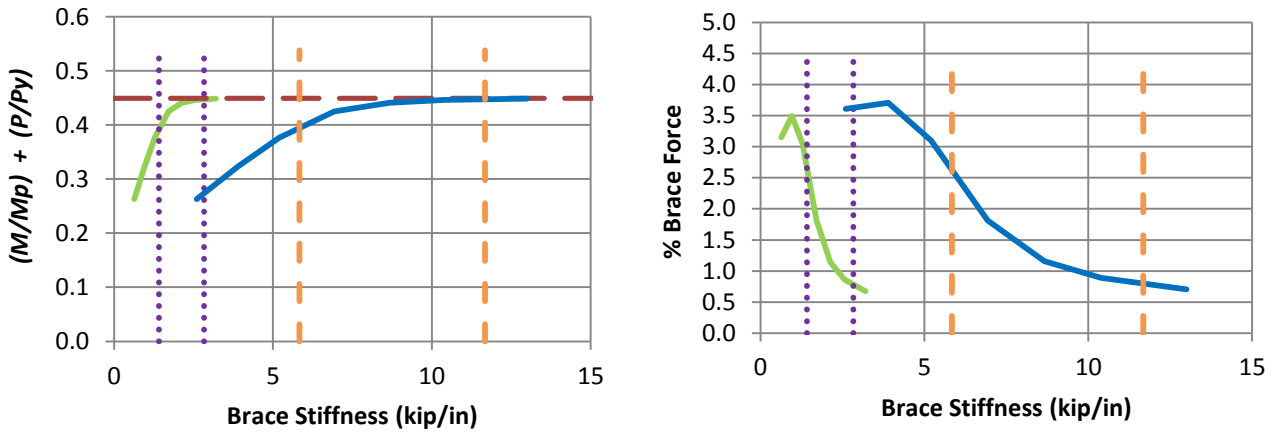
d) BC_MG2n_CNTB_n1_Lb5_FFR1

- Rigidly-braced strength
- Test simulation results corresponding to torsional brace
- Test simulation results corresponding to lateral brace
- 1x and 0.5x lateral bracing stiffness from Eq. 6-7
- - - 1x and 0.5x torsional bracing stiffness from Eq. 6-8

Fig. 7.17. (continued) Knuckle curves and brace force vs. brace stiffness plots for combined point (nodal) lateral and torsional bracing cases with $n = 1$ and constant axial load and Moment Gradient 2 loading with lateral brace on the flange in flexural tension, $L_b = 5$ ft.



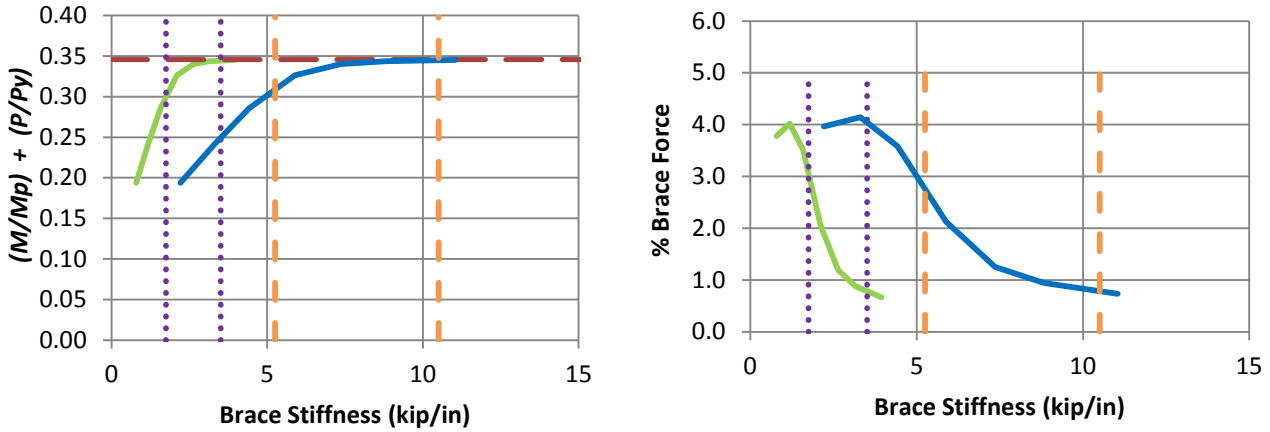
a) BC_MG2n_CNTB_n1_Lb15_FFR-0.5



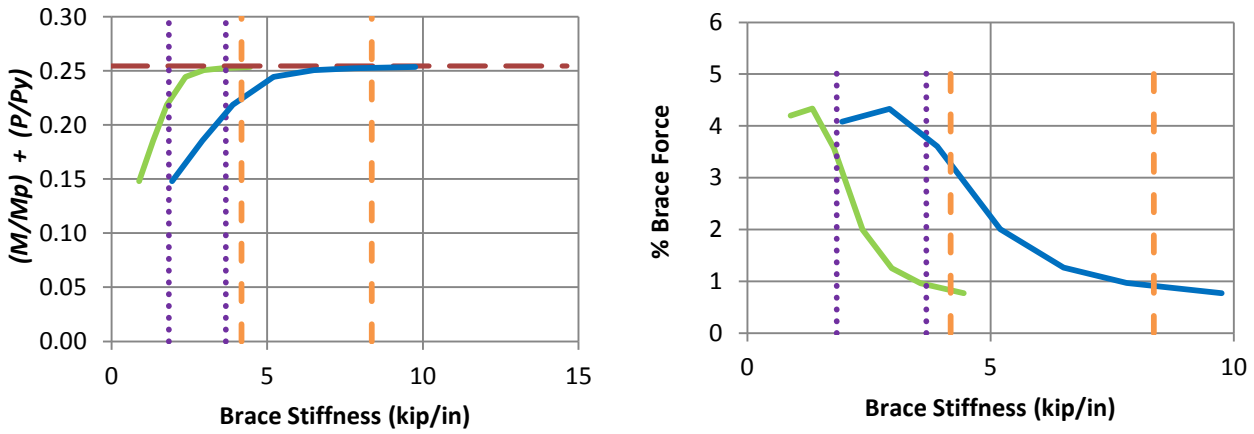
b) BC_MG2n_CNTB_n1_Lb15_FFR0

- Rigidly-braced strength
- Test simulation results corresponding to torsional brace
- Test simulation results corresponding to lateral brace
- 1x and 0.5x lateral bracing stiffness from Eq. 6-7
- 1x and 0.5x torsional bracing stiffness from Eq. 6-8

Fig. 7.18. Knuckle curves and brace force vs. brace stiffness plots for combined point (nodal) lateral and torsional bracing cases with $n = 1$ and constant axial load and Moment Gradient 2 loading with lateral brace on the flange in flexural tension, $L_b = 15$ ft.



c) BC_MG2n_CNTB_n1_Lb15_FFR0.5



d) BC_MG2n_CNTB_n1_Lb15_FFR1

- Rigidly-braced strength
- Test simulation results corresponding to torsional brace
- Test simulation results corresponding to lateral brace
- 1x and 0.5x lateral bracing stiffness from Eq. 6-7
- 1x and 0.5x torsional bracing stiffness from Eq. 6-8

Fig. 7.18. (continued) Knuckle curves and brace force vs. brace stiffness plots for combined point (nodal) lateral and torsional bracing cases with $n = 1$ and constant axial load and Moment Gradient 2 loading with lateral brace on the flange in flexural tension, $L_b = 15$ ft.

Table 7.5. Comparison of simulation results in Figs. 7.15 through 7.18 with Eq. 6-7.

Case (a)	Lateral bracing stiffness corresponding to 96% of simulation rigidly-braced strength (kip/in) (b)	Required lateral bracing stiffness from Eq. 6-7 kip/in (c)	Col. (b) / Col. (c) (d)
BC_MG2p_CNTB_n1_Lb5_FFR-0.5	4.71	9.54	0.50
BC_MG2p_CNTB_n1_Lb5_FFR0	5.61	19.36	0.29
BC_MG2p_CNTB_n1_Lb5_FFR0.5	10.98	28.56	0.39
BC_MG2p_CNTB_n1_Lb5_FFR1	26.91	33.82	0.80
BC_MG2p_CNTB_n1_Lb15_FFR-0.5	0.92	1.62	0.57
BC_MG2p_CNTB_n1_Lb15_FFR0	1.56	2.82	0.55
BC_MG2p_CNTB_n1_Lb15_FFR0.5	2.04	3.50	0.58
BC_MG2p_CNTB_n1_Lb15_FFR1	2.37	3.68	0.65
BC_MG2n_CNTB_n1_Lb5_FFR-0.5	10.15	9.56	1.06
BC_MG2n_CNTB_n1_Lb5_FFR0	14.02	19.38	0.73
BC_MG2n_CNTB_n1_Lb5_FFR0.5	19.67	28.56	0.69
BC_MG2n_CNTB_n1_Lb5_FFR1	26.91	33.82	0.80
BC_MG2n_CNTB_n1_Lb15_FFR-0.5	1.16	1.62	0.72
BC_MG2n_CNTB_n1_Lb15_FFR0	1.88	2.82	0.67
BC_MG2n_CNTB_n1_Lb15_FFR0.5	2.31	3.50	0.66
BC_MG2n_CNTB_n1_Lb15_FFR1	2.37	3.68	0.65

Table 7.6. Comparison of simulation results in Figs. 7.15 through 7.18 with Eq. 6-8.

Case (a)	Torsional bracing stiffness corresponding to 96% of simulation rigidly-braced strength (kip/in) (b)	Required torsional bracing stiffness from Eq. 6-8 kip/in (c)	Col. (b) / Col. (c) (d)
BC_MG2p_CNTB_n1_Lb5_FFR-0.5	7.33	15.20	0.48
BC_MG2p_CNTB_n1_Lb5_FFR0	5.58	20.96	0.27
BC_MG2p_CNTB_n1_Lb5_FFR0.5	9.07	26.28	0.35
BC_MG2p_CNTB_n1_Lb5_FFR1	20.19	26.20	0.77
BC_MG2p_CNTB_n1_Lb15_FFR-0.5	7.23	11.20	0.65
BC_MG2p_CNTB_n1_Lb15_FFR0	6.32	11.66	0.54
BC_MG2p_CNTB_n1_Lb15_FFR0.5	5.73	10.50	0.55
BC_MG2p_CNTB_n1_Lb15_FFR1	5.2	8.36	0.62
BC_MG2n_CNTB_n1_Lb5_FFR-0.5	15.75	15.26	1.03
BC_MG2n_CNTB_n1_Lb5_FFR0	13.96	21.00	0.67
BC_MG2n_CNTB_n1_Lb5_FFR0.5	16.24	26.28	0.62
BC_MG2n_CNTB_n1_Lb5_FFR1	20.19	26.20	0.77
BC_MG2n_CNTB_n1_Lb15_FFR-0.5	9.2	11.22	0.82
BC_MG2n_CNTB_n1_Lb15_FFR0	7.62	11.68	0.66
BC_MG2n_CNTB_n1_Lb15_FFR0.5	6.47	10.50	0.62
BC_MG2n_CNTB_n1_Lb15_FFR1	5.2	8.36	0.62

CHAPTER 8: SUMMARY OF RECOMMENDATIONS

Based on the results from this research, the following recommendations are made for improving the AISC Appendix 6 (AISC 2010) provisions.

- a) For combined lateral and torsional bracing systems for beams, the following bracing stiffness requirements are suggested:

When the lateral bracing is on the flange in compression (i.e., positive bending), the provided lateral and torsional bracing stiffness's should satisfy the requirement

$$\frac{\beta_T}{\beta_{To}} + \frac{\beta_L}{\beta_{Lo}} \geq 1.0 \quad (4-3)$$

where:

β_L = Provided lateral bracing stiffness

β_T = Provided torsional bracing stiffness

β_{Lo} = Base required lateral bracing stiffness for ideal full bracing per the AISC 360-10 Appendix 6 (AISC 2010) rules, including the refinements specified in the Appendix 6 Commentary.

β_{To} = Base required torsional bracing stiffness for ideal full bracing per the AISC 360-10 Appendix 6 (AISC 2010) rules, including the refinements specified in the Appendix 6 Commentary.

When the lateral bracing is on the flange in tension (i.e., negative bending), the provided lateral and torsional bracing stiffness's should satisfy the above interaction Eq. 4-3 and, in addition, the required torsional brace stiffness shall be greater than or equal to

the smaller of β_{To} , or h_o^2 times the point (nodal) lateral bracing stiffness requirement as per AISC, obtained from Eq. C-A-6-5 in the Appendix 6 (AISC 2010) Commentary.

b) For beam-column members the following bracing requirements are suggested:

For beam-columns with lateral bracing only, the bracing requirements can be obtained from Eqs. 6-3 through 6-6.

- When the effective flange force ratio $(P_{ft}/P_{fc}) \leq 0$,

$$\text{Required lateral bracing stiffness} = 2 \left[\frac{N_i \left(\frac{P}{2} \right)}{L_b} + \frac{N_i C_t \left(\frac{M}{h_o} \right)}{L_b} \right] \quad (6-3)$$

$$\text{Required strength} = 1\% \text{ of } \left[\frac{P}{2} + C_t \left(\frac{M}{h_o} \right) \right] \text{ for Point (nodal) lateral brace} \quad (6-4a)$$

$$= 0.5\% \text{ of } \left[\frac{P}{2} + C_t \left(\frac{M}{h_o} \right) \right] \text{ for Shear panel (relative) lateral brace} \quad (6-4b)$$

- When the effective flange force ratio $(P_{ft}/P_{fc}) > 0$,

$$\text{Required lateral bracing stiffness} = 2 \left[\frac{N_i (2.5P)}{L_b} + \frac{N_i C_t \left(\frac{M}{h_o} \right)}{L_b} \right] \quad (6-5)$$

$$\text{Required strength} = 1\% \text{ of } \left[2.5P + C_t \left(\frac{M}{h_o} \right) \right] \text{ for Point (nodal) lateral brace} \quad (6-6a)$$

$$= 0.5\% \text{ of } \left[2.5P + C_t \left(\frac{M}{h_o} \right) \right] \text{ for Shear panel (relative) lateral brace} \quad (6-6b)$$

where:

$N_i = 1$ for shear panel (relative) lateral bracing

$= (4-2/n)$ for Point (nodal) lateral bracing

$C_t = 1$ for centroidal loading

$= 1+(1.2/n)$ for top-flange loading

$n =$ number of intermediate braces

$L_b =$ unbraced length

$C_d =$ double curvature factor, which accounts for the potential larger demands on the lateral bracing in unbraced lengths containing inflection points

$= 1+(M_S/M_L)^2$ when an inflection point occurs within one of the unbraced lengths adjacent to the brace being considered

$= 1.0$ when neither of the unbraced lengths adjacent to the brace contains an inflection point, or when an inflection point exists within one of these lengths, but is closer to the adjacent brace location

$M_S =$ smallest moment within the two unbraced lengths adjacent to the brace under consideration

$M_L =$ largest moment within the two unbraced lengths adjacent to the brace under consideration

For beam-columns with combined lateral and torsional bracing the recommendation is made to design the lateral brace for a load equal to the axial load (P) and the torsional brace for a load equal to $(M/h_o + P/2)$. Thus, the bracing requirements for beam-columns with combined lateral and torsional bracing can be obtained from Eqs. 6-7 through 6-10

$$\text{Required lateral bracing stiffness} = \frac{2N_i P}{L_b} \quad (6-7)$$

$$\text{Required torsional bracing stiffness} = 10h_o^2 \left[\left[\frac{\left(\frac{M}{C_b h_o} + \frac{P}{2} \right)}{P_{e,eff}} \right] \right] \left[\left[\frac{\left(\frac{M}{C_b h_o} + \frac{P}{2} \right)}{L_b} \right] \right] \left[\frac{n_T + 1}{n_T} \right] C_{iT} \quad (6-8)$$

$$\text{Required lateral bracing strength} = 1\% \text{ of } P \quad (6-9)$$

$$\text{Required torsional bracing strength} = 2\% \text{ of } (M + Ph_o/2) \quad (6-10)$$

where:

n_T = number of intermediate torsional brace points

L_b = unbraced length

C_b = Lateral-torsional buckling modification factor

$C_{iT} = 1.2$ when the transverse loading is applied at the flange level in a way that

is detrimental to the member stability (this occurs when the transverse

loading is applied at the flange level and is directed towards the member

shear center from its point of application), assuming that substantial

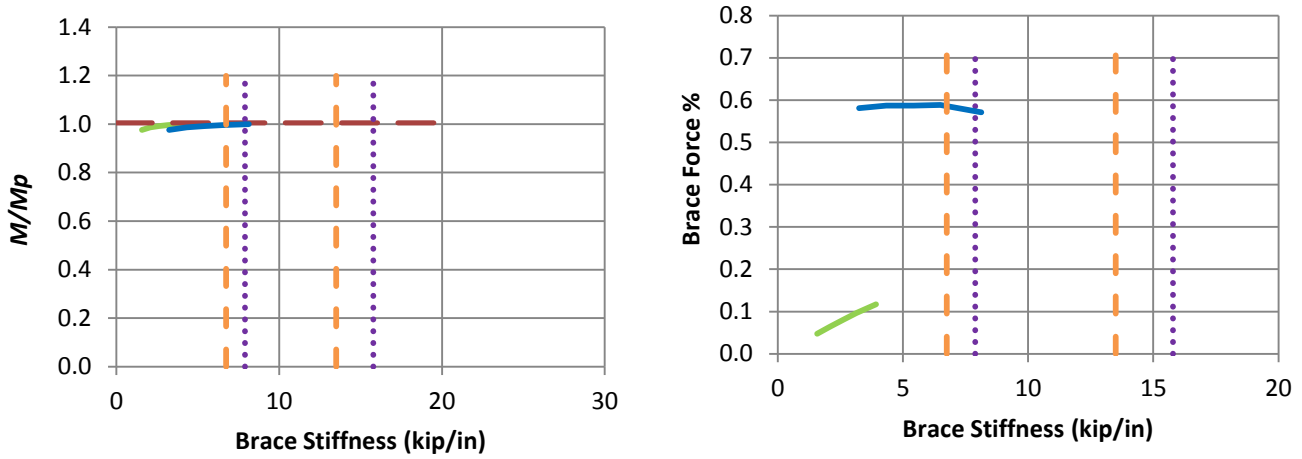
tipping restraint does not exist at the transverse loading points.

= 1 otherwise

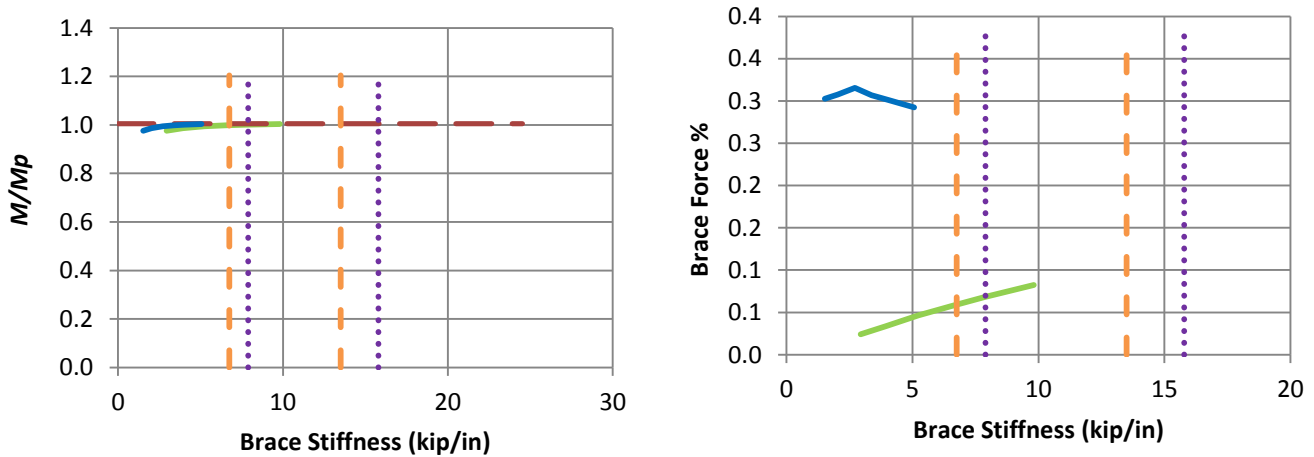
$$P_{e,eff} = \frac{\pi^2 E \left(\frac{I_y}{2} \right)}{L_b^2} = \text{effective flange buckling load}$$

APPENDIX A

The knuckle curves and brace force versus brace stiffness plots corresponding to every point on the interaction plots shown in Figs. 4.4, 4.5, 4.9 and 5.3 are shown below in Figs. A.1 through A.16.



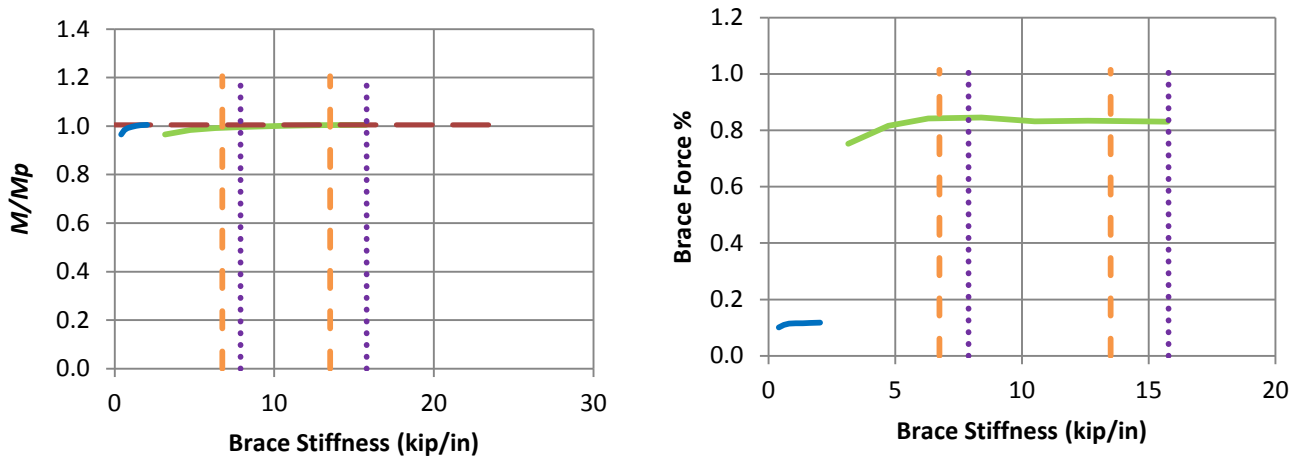
e) B_MG1p_CNTB_n1_Lb5_TLBSR4



f) B_MG1p_CNTB_n1_Lb5_TLBSR1

- Rigid bracing strength
- Test simulation results corresponding to torsional brace
- Test simulation results corresponding to lateral brace
- 1x and 0.5x lateral bracing stiffness from Eq. C-A-6-5, AISC 360-10, with $C_b P_f$ taken equal to M_{max}/h_o
- - - 1x and 0.5x torsional bracing stiffness equal to (β_{Tbr} / h_o^2) , where β_{Tbr} is given in Eq. 4-1

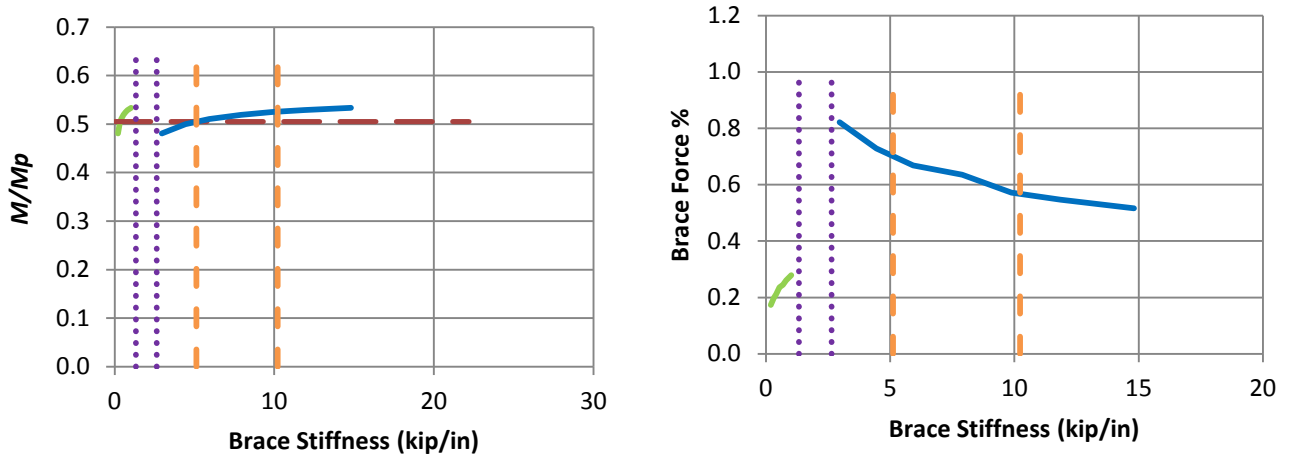
Fig. A.1. Knuckle curves and brace force vs. brace stiffness plots for point (nodal) lateral bracing cases with $n = 1$ and Moment Gradient 1 loading with lateral brace on the flange in compression, $L_b = 5$ ft.



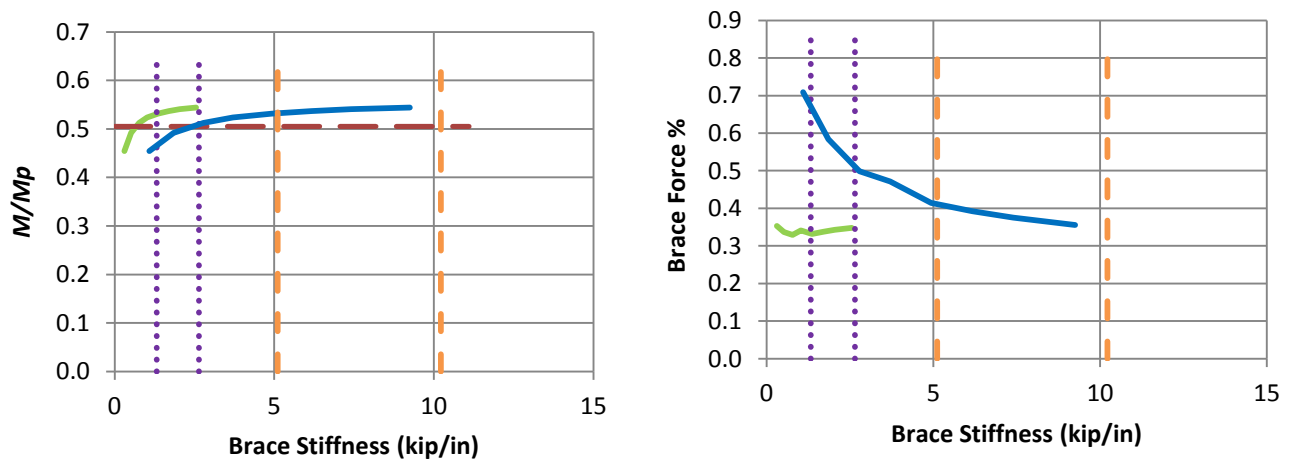
g) B_MG1p_CNTB_n1_Lb5_TLBSR0.25

- Rigid bracing strength
- Test simulation results corresponding to torsional brace
- Test simulation results corresponding to lateral brace
- 1x and 0.5x lateral bracing stiffness from Eq. C-A-6-5, AISC 360-10, with $C_b P_f$ taken equal to M_{max}/h_o
- 1x and 0.5x torsional bracing stiffness equal to (β_{Tbr} / h_o^2) , where β_{Tbr} is given in Eq. 4-1

Fig. A.1. (continued) Knuckle curves and brace force vs. brace stiffness plots for point (nodal) lateral bracing cases with $n = 1$ and Moment Gradient 1 loading with lateral brace on the flange in compression, $L_b = 5$ ft.



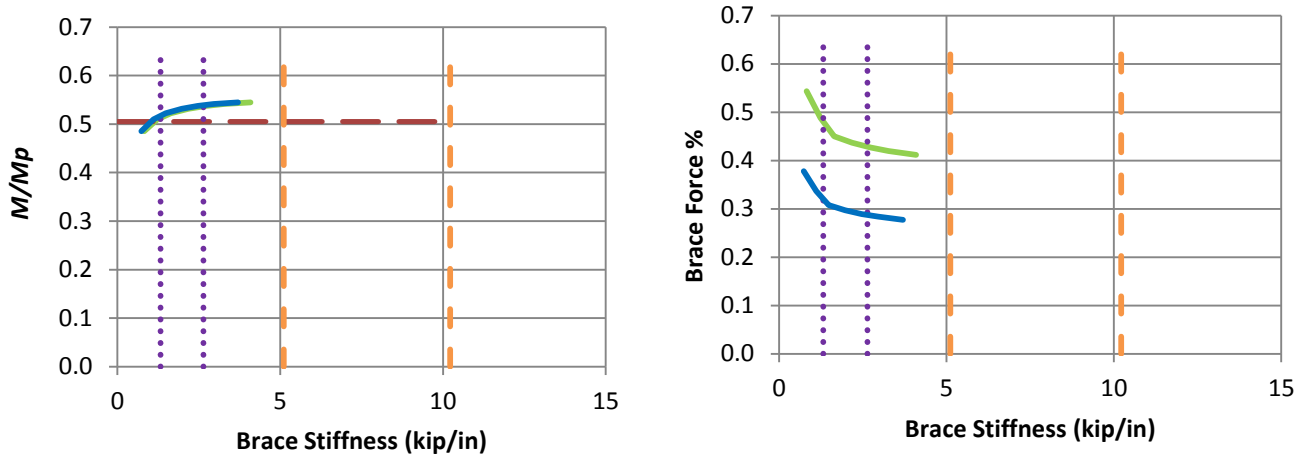
a) B_MG1p_CNTB_n1_Lb15_TLBSR4



b) B_MG1p_CNTB_n1_Lb15_TLBSR1

- Rigid bracing strength
- Test simulation results corresponding to torsional brace
- Test simulation results corresponding to lateral brace
- 1x and 0.5x lateral bracing stiffness from Eq. C-A-6-5, AISC 360-10, with $C_b P_f$ taken equal to M_{max}/h_o
- 1x and 0.5x torsional bracing stiffness equal to (β_{Tbr} / h_o^2) , where β_{Tbr} is given in Eq. 4-1

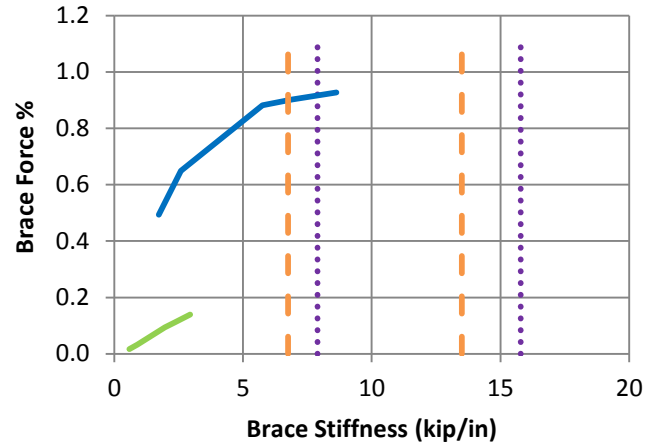
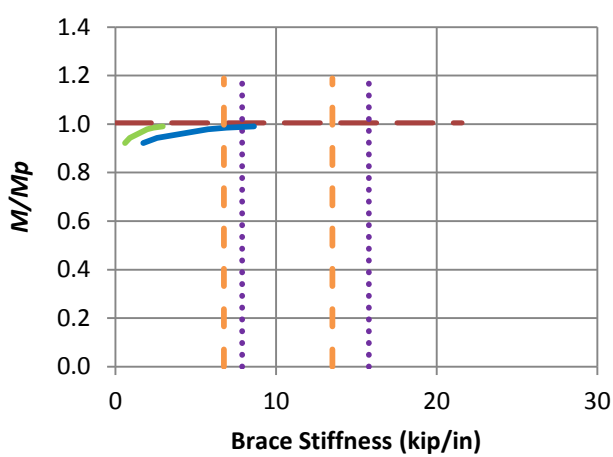
Fig. A.2. Knuckle curves and brace force vs. brace stiffness plots for point (nodal) lateral bracing cases with $n = 1$ and Moment Gradient 1 loading with lateral brace on the flange in compression, $L_b = 15$ ft.



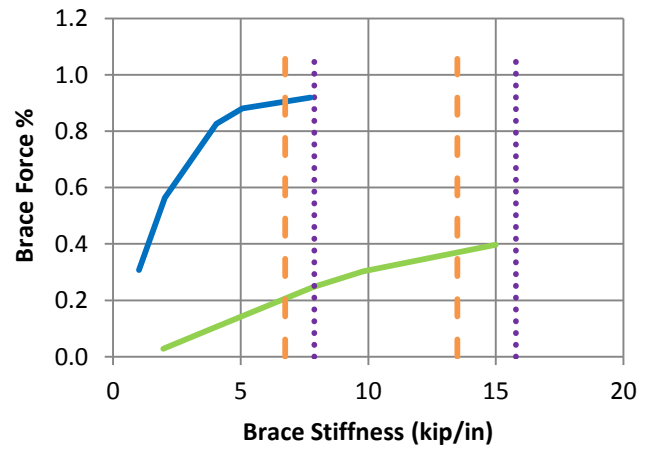
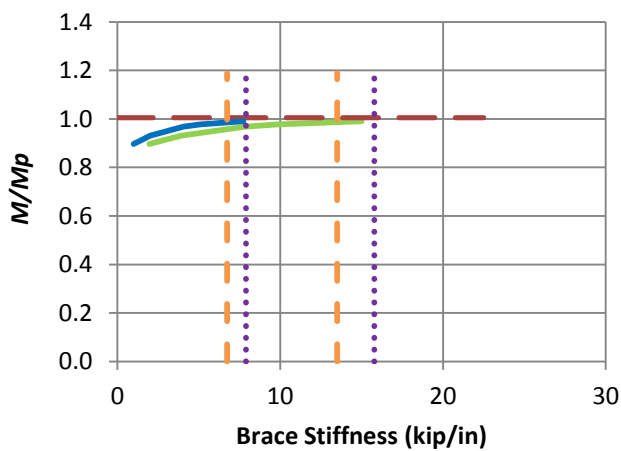
c) B_MG1p_CNTB_n1_Lb15_TLBSR0.25

- Rigid bracing strength
- Test simulation results corresponding to torsional brace
- Test simulation results corresponding to lateral brace
- 1x and 0.5x lateral bracing stiffness from Eq. C-A-6-5, AISC 360-10, with $C_b P_f$ taken equal to M_{max}/h_o
- 1x and 0.5x torsional bracing stiffness equal to (β_{Tbr} / h_o^2) , where β_{Tbr} is given in Eq. 4-1

Fig. A.2. (continued) Knuckle curves and brace force vs. brace stiffness plots for point (nodal) lateral bracing cases with $n = 1$ and Moment Gradient 1 loading with lateral brace on the flange in compression, $L_b = 15$ ft.



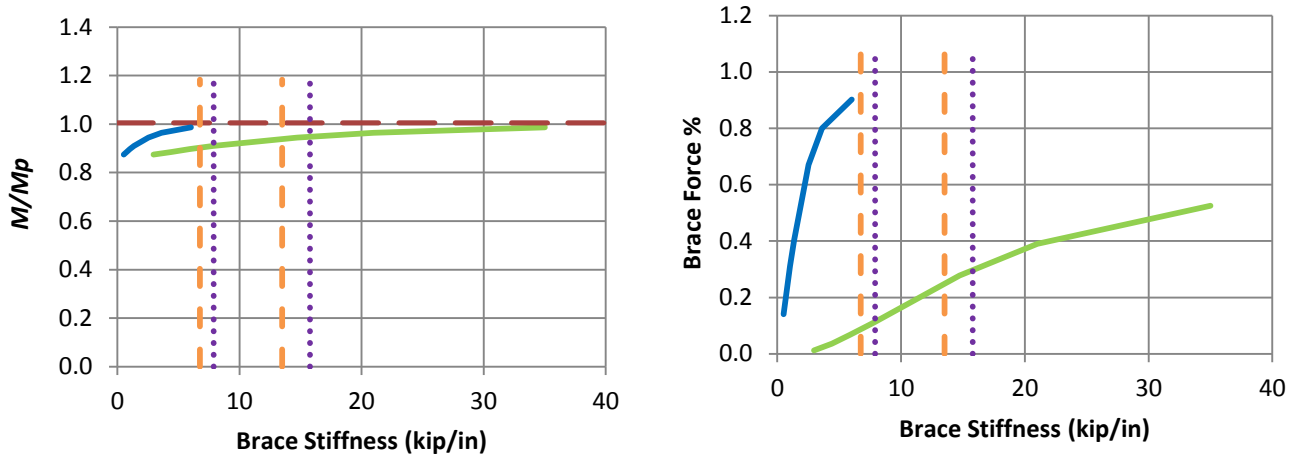
a) B_MG1n_CNTB_n1_Lb5_TLBSR5.67



b) B_MG1n_CNTB_n1_Lb5_TLBSR1

- Rigid bracing strength
- Test simulation results corresponding to torsional brace
- Test simulation results corresponding to lateral brace
- 1x and 0.5x lateral bracing stiffness from Eq. C-A-6-5, AISC 360-10, with $C_b P_f$ taken equal to M_{max}/h_o
- 1x and 0.5x torsional bracing stiffness equal to (β_{Tbr} / h_o^2) , where β_{Tbr} is given in Eq. 4-1

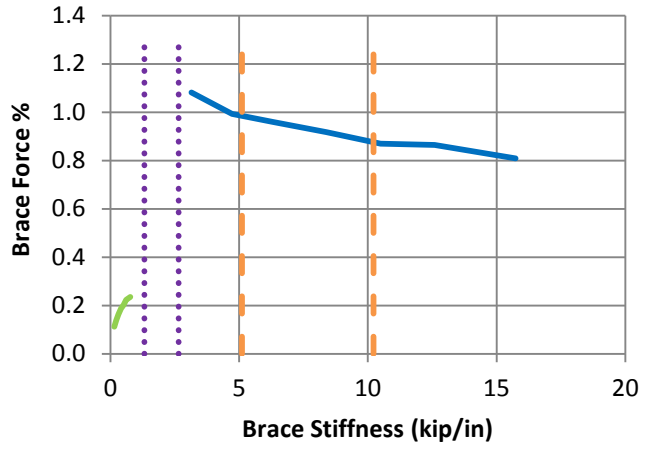
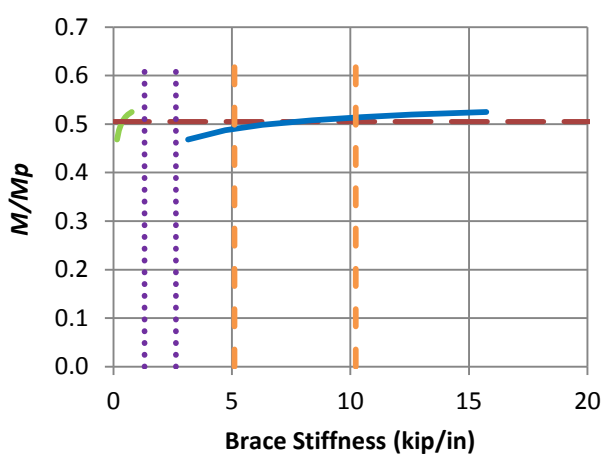
Fig. A.3. Knuckle curves and brace force vs. brace stiffness plots for point (nodal) lateral bracing cases with $n = 1$ and Moment Gradient 1 loading with lateral brace on the flange in tension, $L_b = 5$ ft.



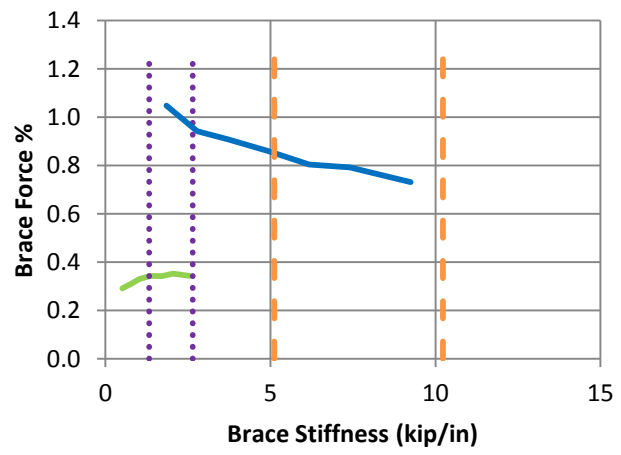
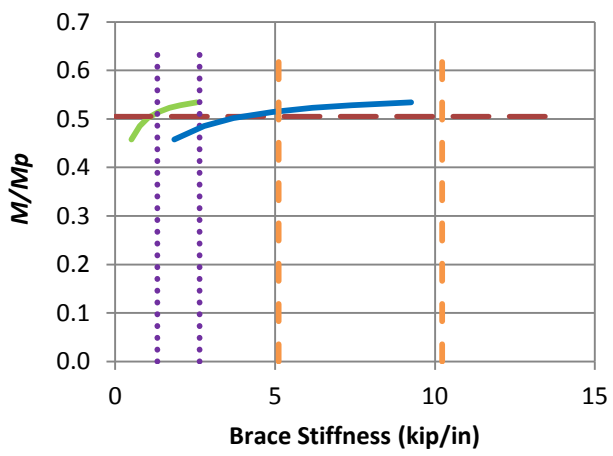
c) B_MG1n_CNTB_n1_Lb5_TLBSR0.33

- Rigid bracing strength
- Test simulation results corresponding to torsional brace
- Test simulation results corresponding to lateral brace
- 1x and 0.5x lateral bracing stiffness from Eq. C-A-6-5, AISC 360-10, with $C_b P_f$ taken equal to M_{max}/h_o
- 1x and 0.5x torsional bracing stiffness equal to (β_{Tbr} / h_o^2) , where β_{Tbr} is given in Eq. 4-1

Fig. A.3. (continued) Knuckle curves and brace force vs. brace stiffness plots for point (nodal) lateral bracing cases with $n = 1$ and Moment Gradient 1 loading with lateral brace on the flange in tension, $L_b = 5$ ft.



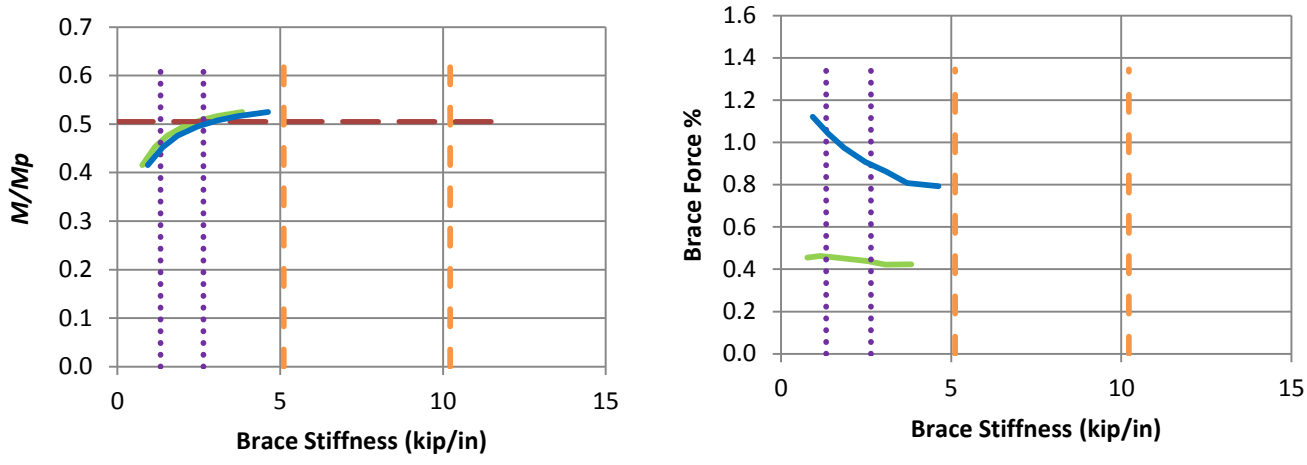
a) B_MG1n_CNTB_n1_Lb15_TLBSR5.67



b) B_MG1n_CNTB_n1_Lb15_TLBSR1

- Rigid bracing strength
- Test simulation results corresponding to torsional brace
- Test simulation results corresponding to lateral brace
- 1x and 0.5x lateral bracing stiffness from Eq. C-A-6-5, AISC 360-10, with $C_b P_f$ taken equal to M_{max}/h_o
- 1x and 0.5x torsional bracing stiffness equal to (β_{Tbr} / h_o^2) , where β_{Tbr} is given in Eq. 4-1

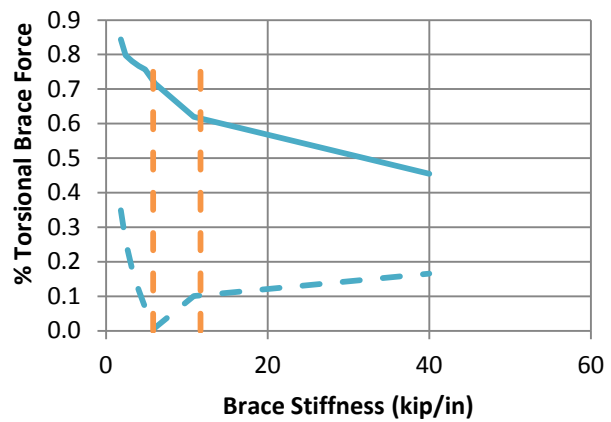
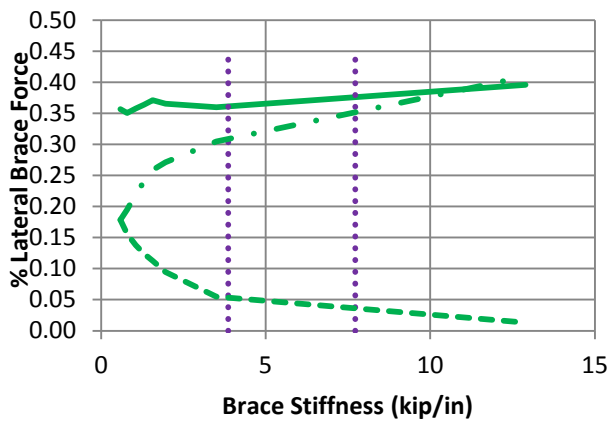
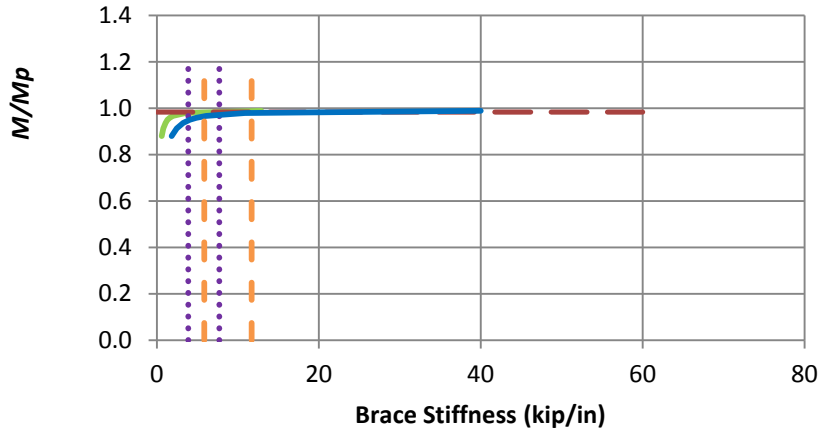
Fig. A.4. Knuckle curves and brace force vs. brace stiffness plots for point (nodal) lateral bracing cases with $n = 1$ and Moment Gradient 1 loading with lateral brace on the flange in tension, $L_b = 15$ ft.



c) B_MG1n_CNTB_n1_Lb15_TLBSR0.33

- Rigid bracing strength
- Test simulation results corresponding to torsional brace
- Test simulation results corresponding to lateral brace
- 1x and 0.5x lateral bracing stiffness from Eq. C-A-6-5, AISC 360-10, with $C_b P_f$ taken equal to M_{max}/h_o
- 1x and 0.5x torsional bracing stiffness equal to (β_{Tbr} / h_o^2) , where β_{Tbr} is given in Eq. 4-1

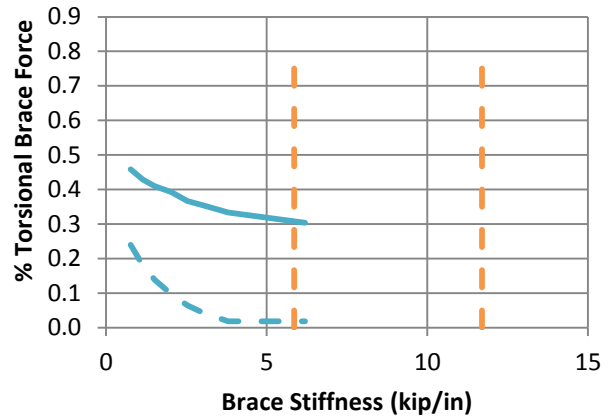
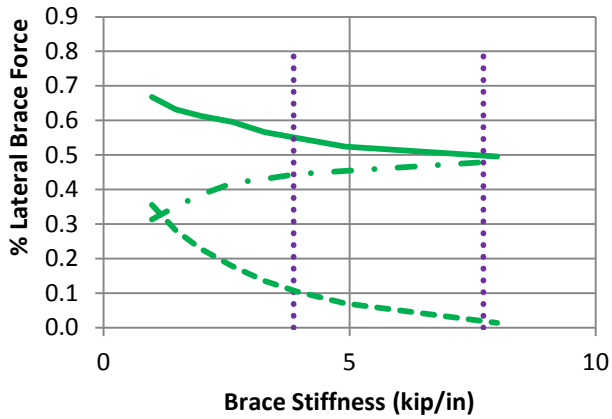
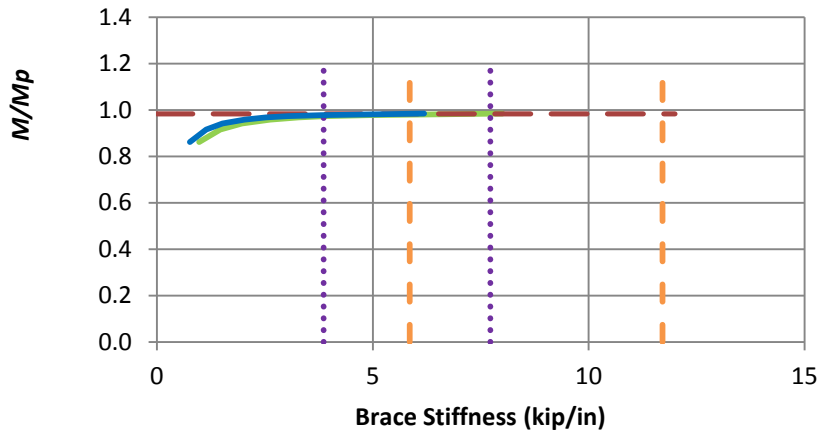
Fig. A.4. (continued) Knuckle curves and brace force vs. brace stiffness plots for point (nodal) lateral bracing cases with $n = 1$ and Moment Gradient 1 loading with lateral brace on the flange in tension, $L_b = 15$ ft.



j) B_MG1p_CRTB_n2_Lb5_TLBSR4

- Rigid bracing strength
- Test simulation results corresponding to torsional brace
- Test simulation results corresponding to lateral brace
- 1x and 0.5x lateral bracing stiffness from Eq. C-A-6-5, AISC 360-10, with $C_b P_f$ taken equal to M_{max}/h_o
- 1x and 0.5x torsional bracing stiffness equal to (β_{Tbr} / h_o^2) , where β_{Tbr} is given in Eq. 4-1
- Left end panel shear force
- Right end panel shear force
- Middle panel shear force
- Torsional brace force 1
- Torsional brace force 2

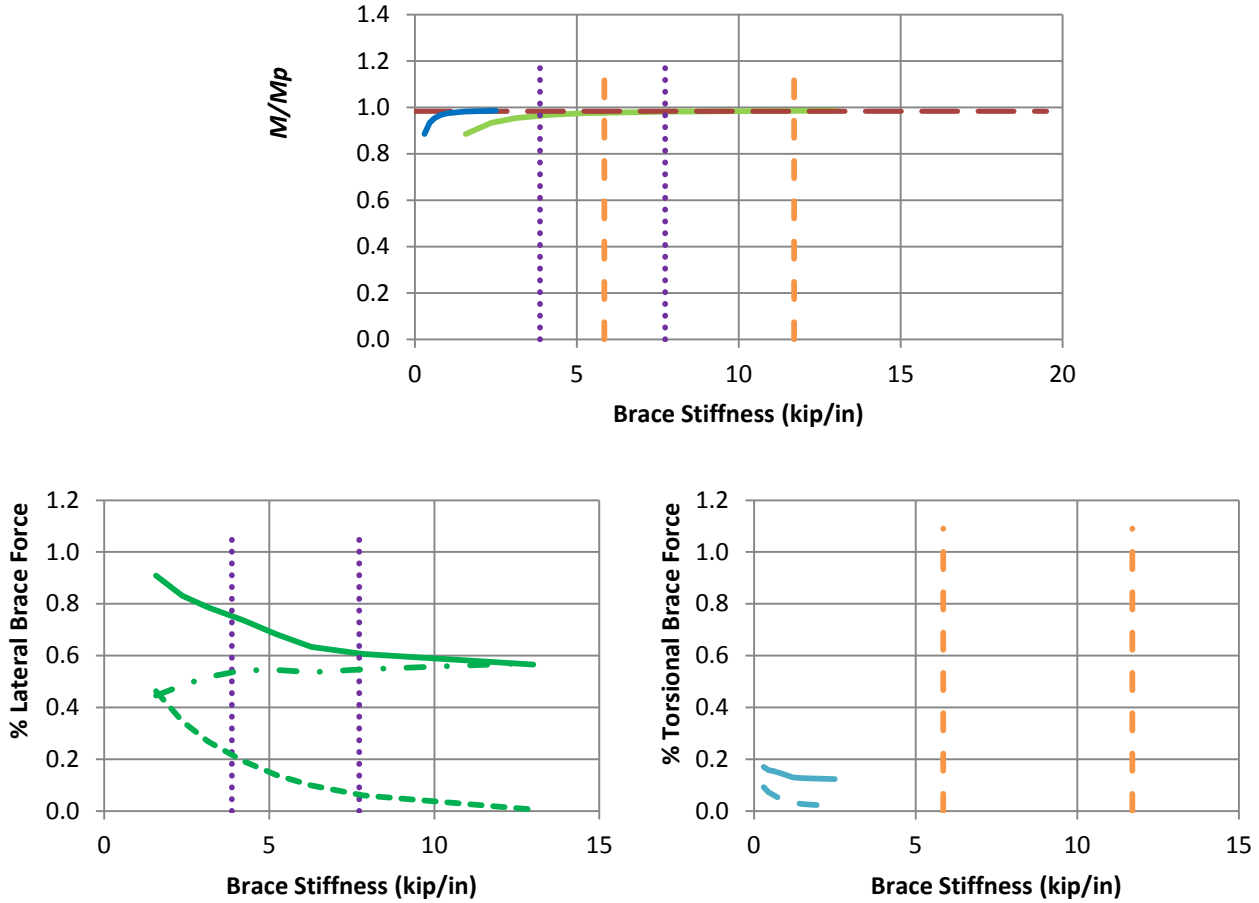
Fig. A.5. Knuckle curves and brace force vs. brace stiffness plots for shear panel (relative) lateral bracing cases with $n = 2$ and Moment Gradient 1 loading with lateral brace on the flange in compression, $L_b = 5\text{ft}$.



k) B_MG1p_CRTB_n2_Lb5_TLBSR1

- Rigid bracing strength
- Test simulation results corresponding to torsional brace
- Test simulation results corresponding to lateral brace
- 1x and 0.5x lateral bracing stiffness from Eq. C-A-6-5, AISC 360-10, with $C_b P_f$ taken equal to M_{max}/h_o
- - - 1x and 0.5x torsional bracing stiffness equal to (β_{Tbr} / h_o^2) , where β_{Tbr} is given in Eq. 4-1
- Left end panel shear force
- - - Right end panel shear force
- . - Middle panel shear force
- Torsional brace force 1
- - - Torsional brace force 2

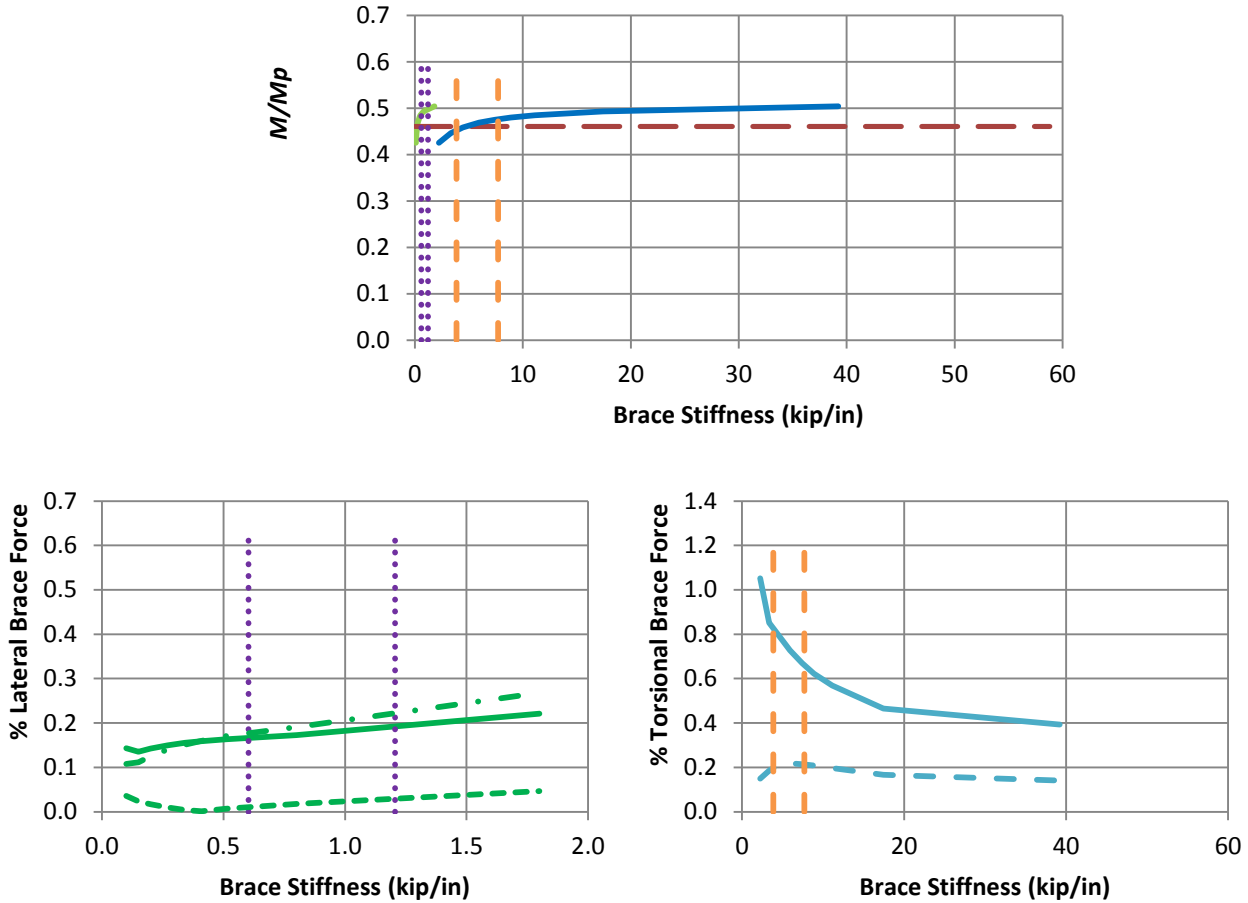
Fig. A.5. (continued) Knuckle curves and brace force vs. brace stiffness plots for shear panel (relative) lateral bracing cases with $n = 2$ and Moment Gradient 1 loading with lateral brace on the flange in compression, $L_b = 5$ ft.



1) B_MG1p_CRTB_n2_Lb5_TLBSR0.25

- Rigid bracing strength
- Test simulation results corresponding to torsional brace
- Test simulation results corresponding to lateral brace
- 1x and 0.5x lateral bracing stiffness from Eq. C-A-6-5, AISC 360-10, with $C_b P_f$ taken equal to M_{max}/h_o
- 1x and 0.5x torsional bracing stiffness equal to (β_{Tbr} / h_o^2) , where β_{Tbr} is given in Eq. 4-1
- Left end panel shear force
- Right end panel shear force
- . - Middle panel shear force
- Torsional brace force 1
- Torsional brace force 2

Fig. A.5. (continued) Knuckle curves and brace force vs. brace stiffness plots for shear panel (relative) lateral bracing cases with $n = 2$ and Moment Gradient 1 loading with lateral brace on the flange in compression, $L_b = 5$ ft.

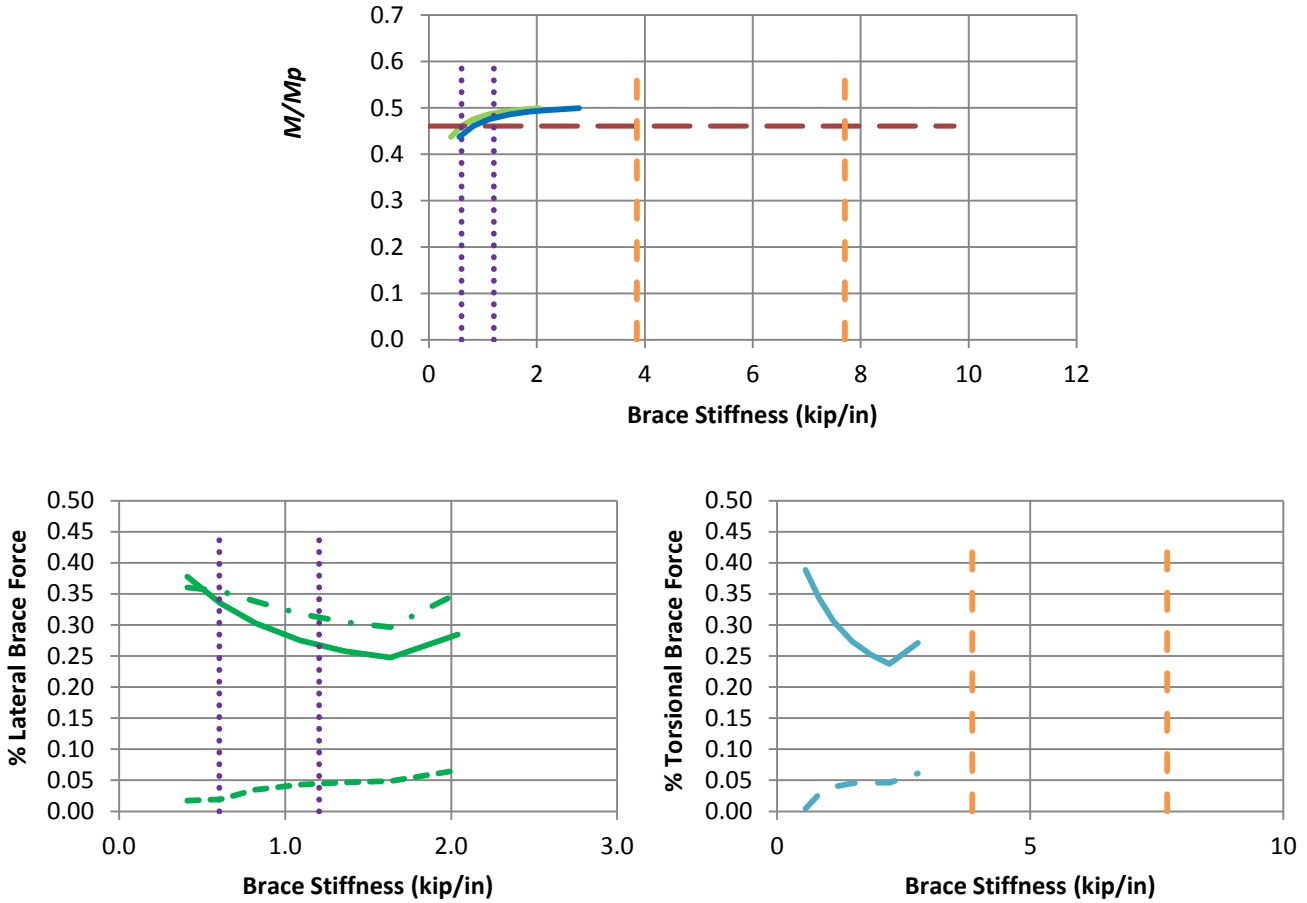


a) B_MG1p_CRTB_n2_Lb15_TLBSR4

- Rigid bracing strength
- Test simulation results corresponding to torsional brace
- Test simulation results corresponding to lateral brace
- 1x and 0.5x lateral bracing stiffness from Eq. C-A-6-5, AISC 360-10, with $C_b P_f$ taken equal to M_{max}/h_o
- 1x and 0.5x torsional bracing stiffness equal to (β_{Tbr} / h_o^2) , where β_{Tbr} is given in Eq. 4-1
- Left end panel shear force
- Right end panel shear force
- Middle panel shear force

- . - Middle panel shear force
- — Torsional brace force 1
- — Torsional brace force 2

Fig. A.6. (continued) Knuckle curves and brace force vs. brace stiffness plots for shear panel (relative) lateral bracing cases with $n = 2$ and Moment Gradient 1 loading with lateral brace on the flange in compression, $L_b = 15$ ft.

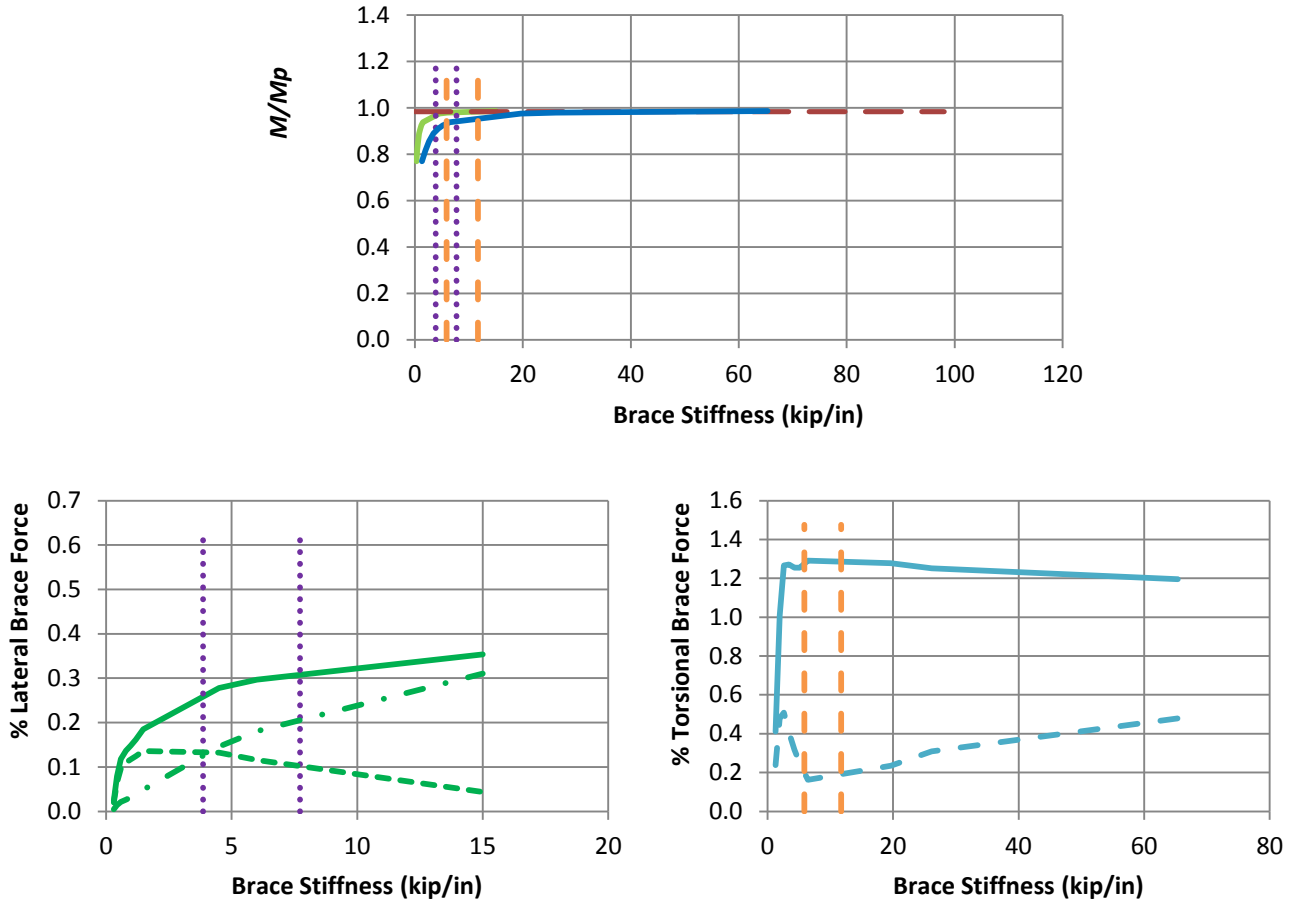


c) B_MG1p_CRTB_n2_Lb15_TLBSR0.25

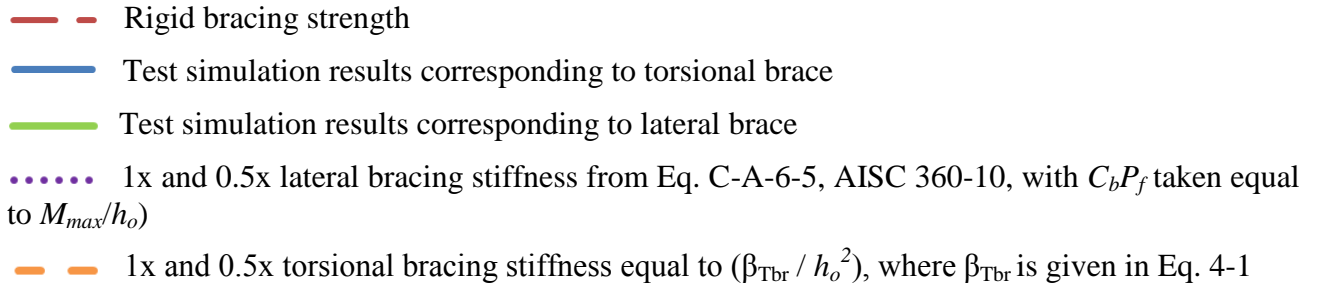
- - Rigid bracing strength
- — Test simulation results corresponding to torsional brace
- — Test simulation results corresponding to lateral brace
- 1x and 0.5x lateral bracing stiffness from Eq. C-A-6-5, AISC 360-10, with $C_b P_f$ taken equal to M_{max}/h_o
- - 1x and 0.5x torsional bracing stiffness equal to (β_{Tbr} / h_o^2) , where β_{Tbr} is given in Eq. 4-1



Fig. A.6. (continued) Knuckle curves and brace force vs. brace stiffness plots for shear panel (relative) lateral bracing cases with $n = 2$ and Moment Gradient 1 loading with lateral brace on the flange in compression, $L_b = 15$ ft.

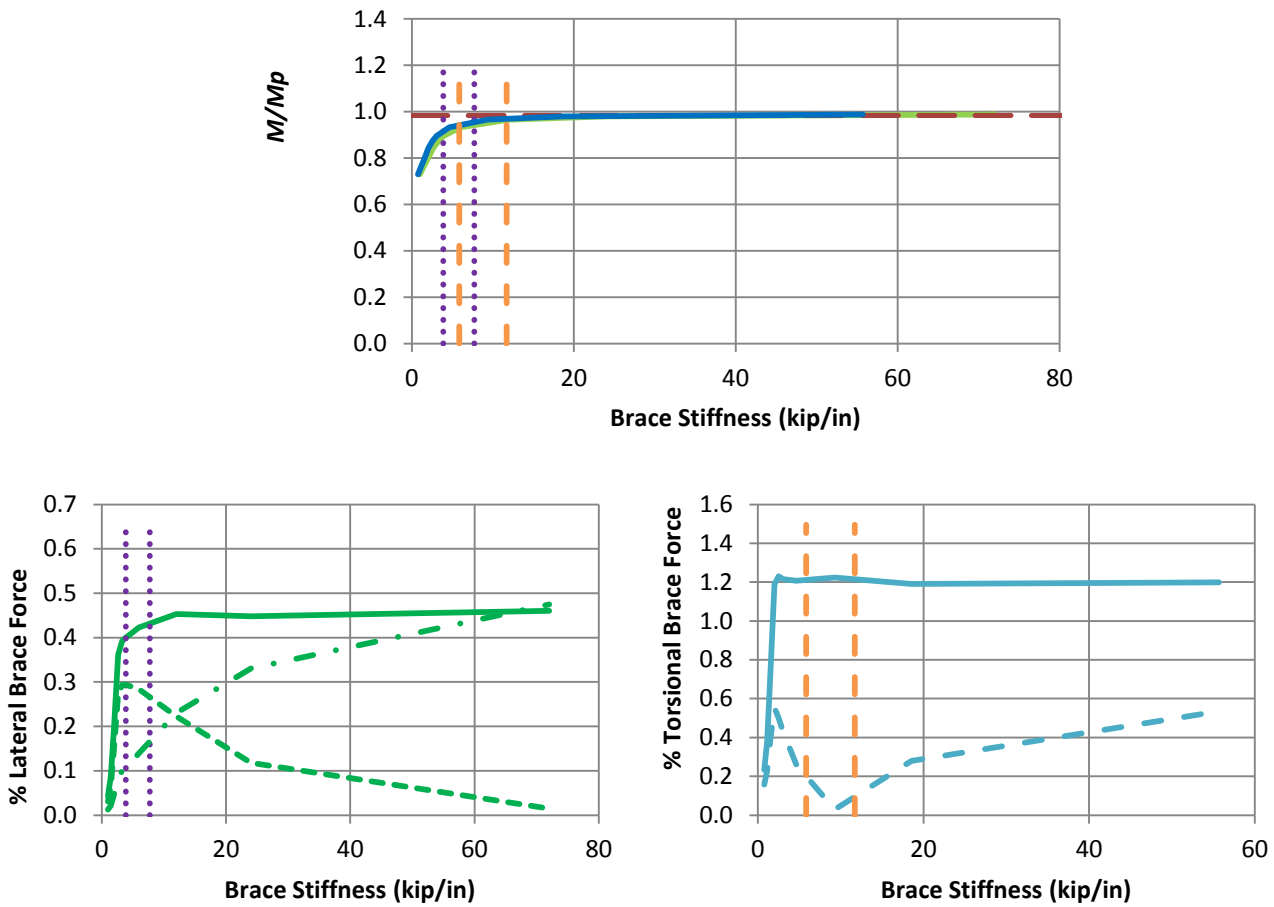


a) B_MG1n_CRTB_n2_Lb5_TLBSR5.67



- Left end panel shear force
- · - Middle panel shear force
- Torsional brace force 1
- - - Right end panel shear force
- - - Torsional brace force 2

Fig. A.7. Knuckle curves and brace force vs. brace stiffness plots for shear panel (relative) lateral bracing cases with $n = 2$ and Moment Gradient 1 loading with lateral brace on the flange in tension, $L_b = 5ft$.

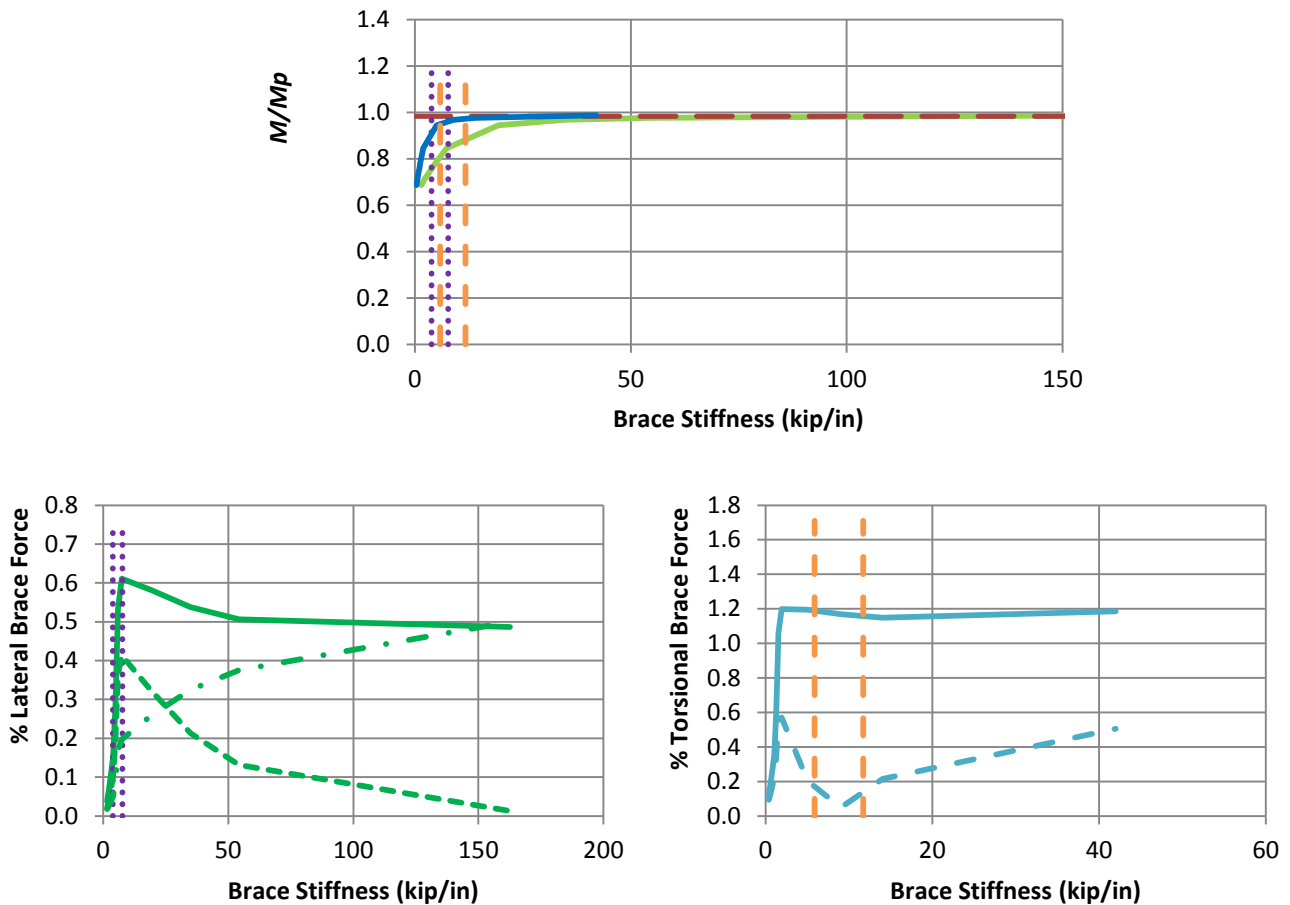


b) B_MG1n_CRTB_n2_Lb5_TLBSR1

- - - Rigid bracing strength
- Test simulation results corresponding to torsional brace
- Test simulation results corresponding to lateral brace
- · · · · 1x and 0.5x lateral bracing stiffness from Eq. C-A-6-5, AISC 360-10, with $C_b P_f$ taken equal to M_{max}/h_o

- 1x and 0.5x torsional bracing stiffness equal to (β_{Tbr} / h_o^2) , where β_{Tbr} is given in Eq. 4-1
- Left end panel shear force
- Right end panel shear force
- Middle panel shear force
- Torsional brace force 1
- Torsional brace force 2

Fig. A.7. (continued) Knuckle curves and brace force vs. brace stiffness plots for shear panel (relative) lateral bracing cases with $n = 2$ and Moment Gradient 1 loading with lateral brace on the flange in tension, $L_b = 5$ ft.

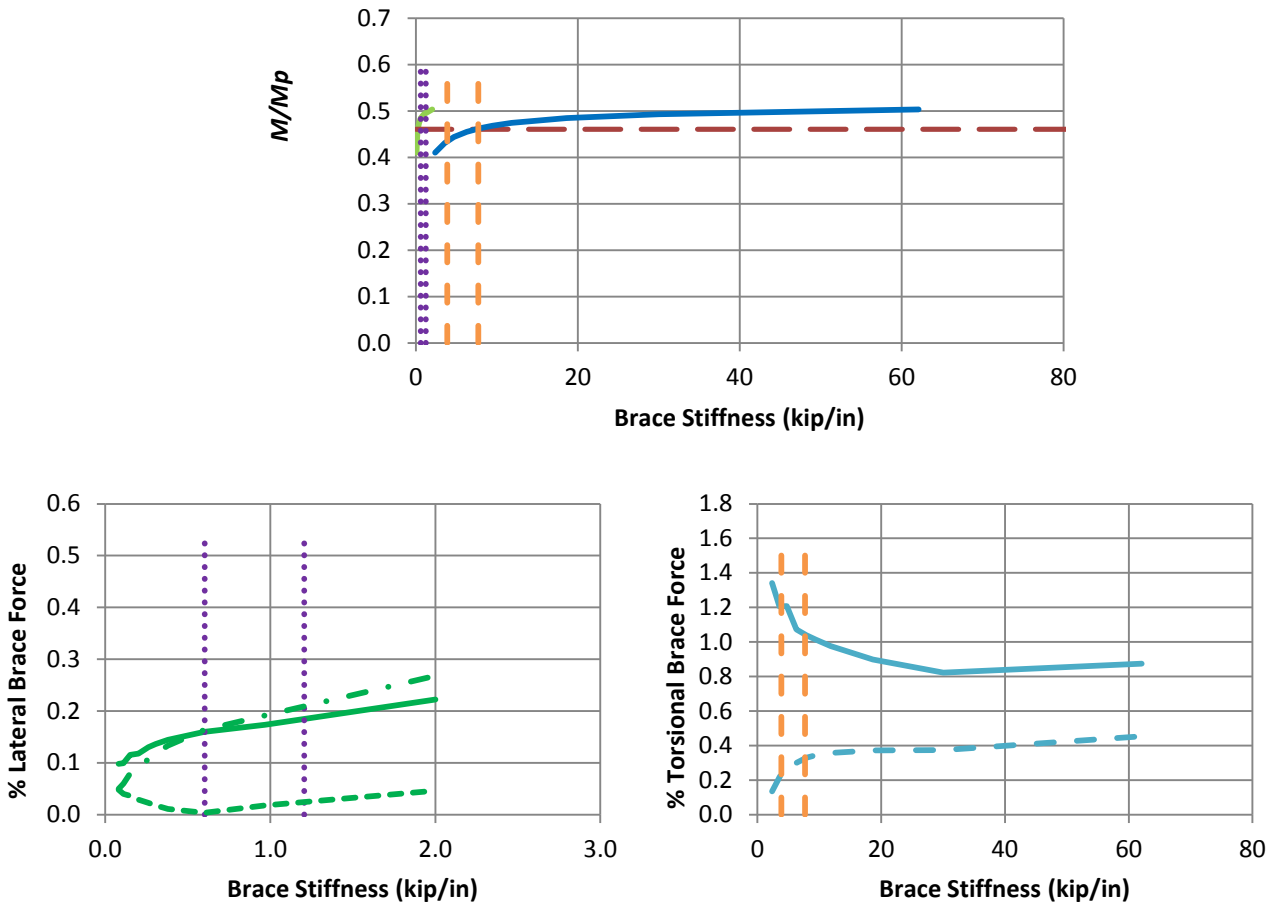


c) B_MG1n_CRTB_n2_Lb5_TLBSR0.33

- Rigid bracing strength
- Test simulation results corresponding to torsional brace
- Test simulation results corresponding to lateral brace

- 1x and 0.5x lateral bracing stiffness from Eq. C-A-6-5, AISC 360-10, with $C_b P_f$ taken equal to M_{max}/h_o
- 1x and 0.5x torsional bracing stiffness equal to (β_{Tbr} / h_o^2) , where β_{Tbr} is given in Eq. 4-1
- Left end panel shear force
- Right end panel shear force
- . - Middle panel shear force
- Torsional brace force 1
- Torsional brace force 2

Fig. A.7. (continued) Knuckle curves and brace force vs. brace stiffness plots for shear panel (relative) lateral bracing cases with $n = 2$ and Moment Gradient 1 loading with lateral brace on the flange in tension, $L_b = 5$ ft.

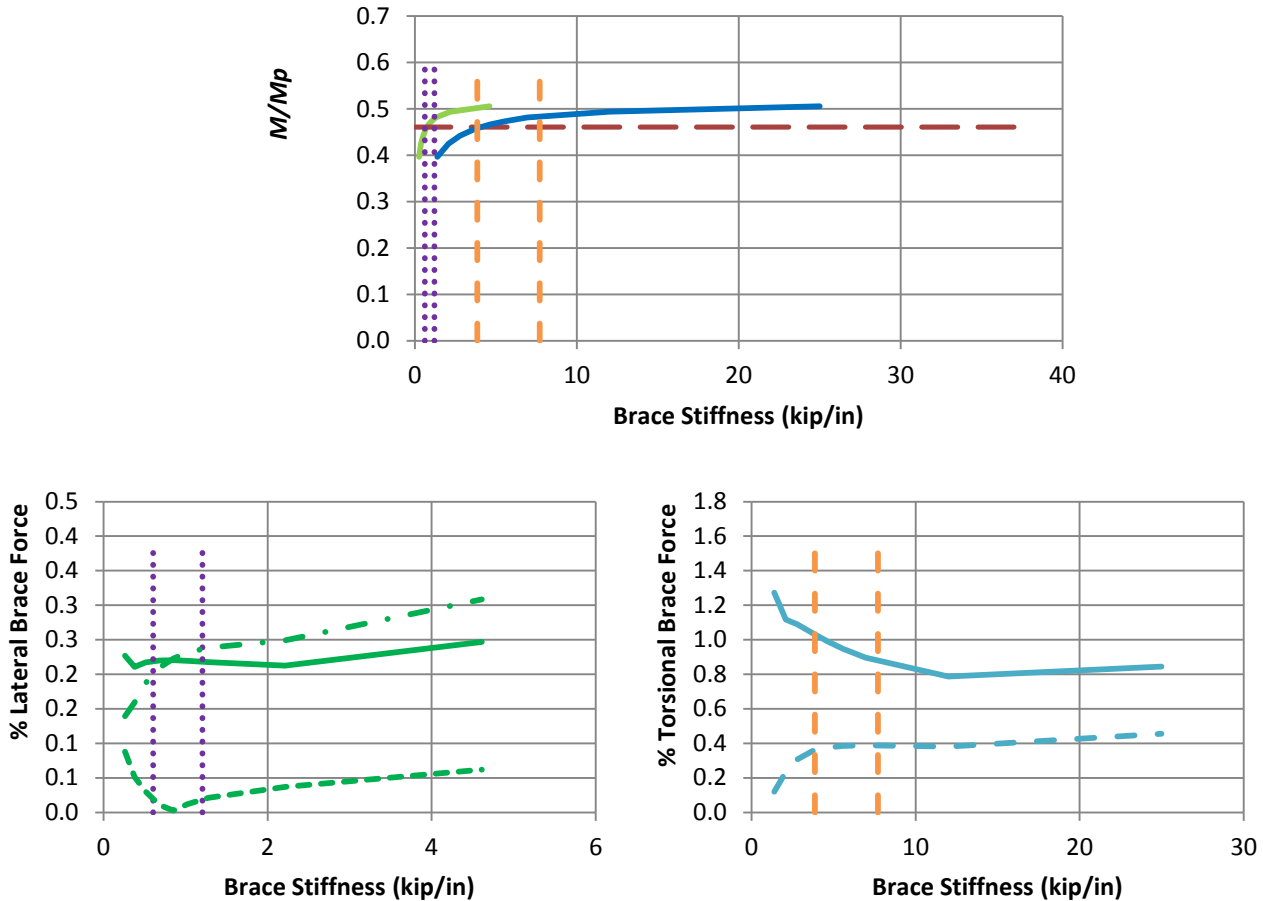


a) B_MG1n_CRTB_n2_Lb15_TLBSR5.67

- Rigid bracing strength
- Test simulation results corresponding to torsional brace

- Test simulation results corresponding to lateral brace
- ⋯ 1x and 0.5x lateral bracing stiffness from Eq. C-A-6-5, AISC 360-10, with $C_b P_f$ taken equal to M_{max}/h_o
- - 1x and 0.5x torsional bracing stiffness equal to (β_{Tbr} / h_o^2) , where β_{Tbr} is given in Eq. 4-1
- Left end panel shear force
- - - Right end panel shear force
- · - Middle panel shear force
- Torsional brace force 1
- - - Torsional brace force 2

Fig. A.8. Knuckle curves and brace force vs. brace stiffness plots for shear panel (relative) lateral bracing cases with $n = 2$ and Moment Gradient 1 loading with lateral brace on the flange in tension, $L_b = 15$ ft.

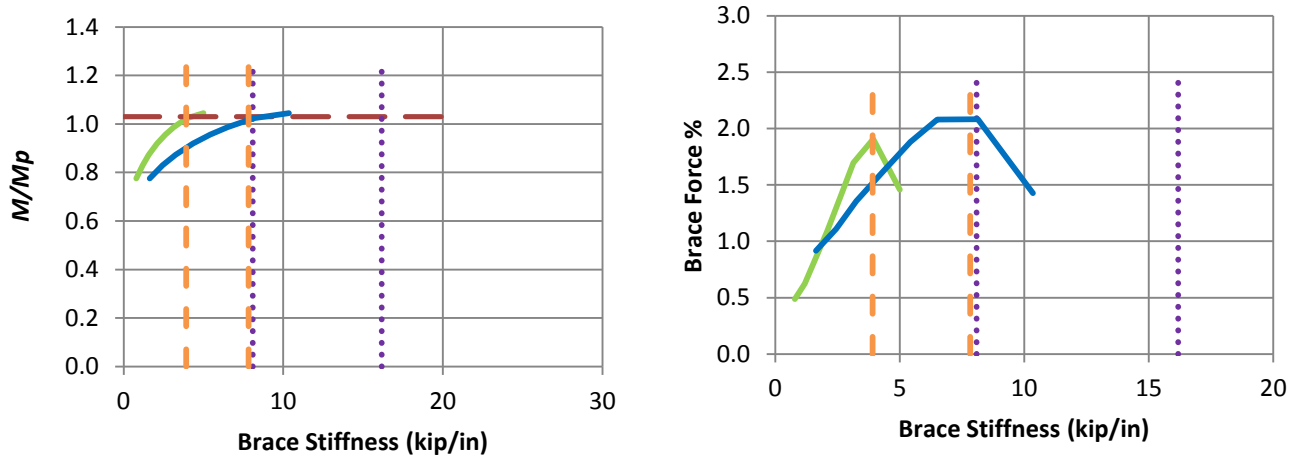


b) B_MG1n_CRTB_n2_Lb15_TLBSR1

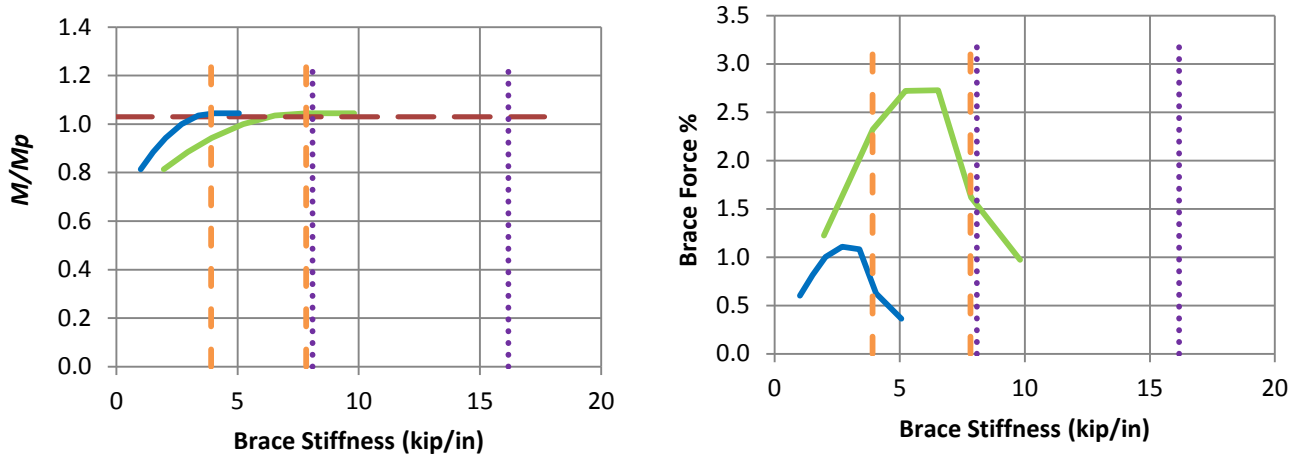
- - Rigid bracing strength

- Rigid bracing strength
- Test simulation results corresponding to torsional brace
- Test simulation results corresponding to lateral brace
- 1x and 0.5x lateral bracing stiffness from Eq. C-A-6-5, AISC 360-10, with $C_b P_f$ taken equal to M_{max}/h_o
- 1x and 0.5x torsional bracing stiffness equal to (β_{Tbr} / h_o^2) , where β_{Tbr} is given in Eq. 4-1
- Left end panel shear force
- Right end panel shear force
- Middle panel shear force
- Torsional brace force 1
- Torsional brace force 2

Fig. A.8. (continued) Knuckle curves and brace force vs. brace stiffness plots for shear panel (relative) lateral bracing cases with $n = 2$ and Moment Gradient 1 loading with lateral brace on the flange in tension, $L_b = 15$ ft.



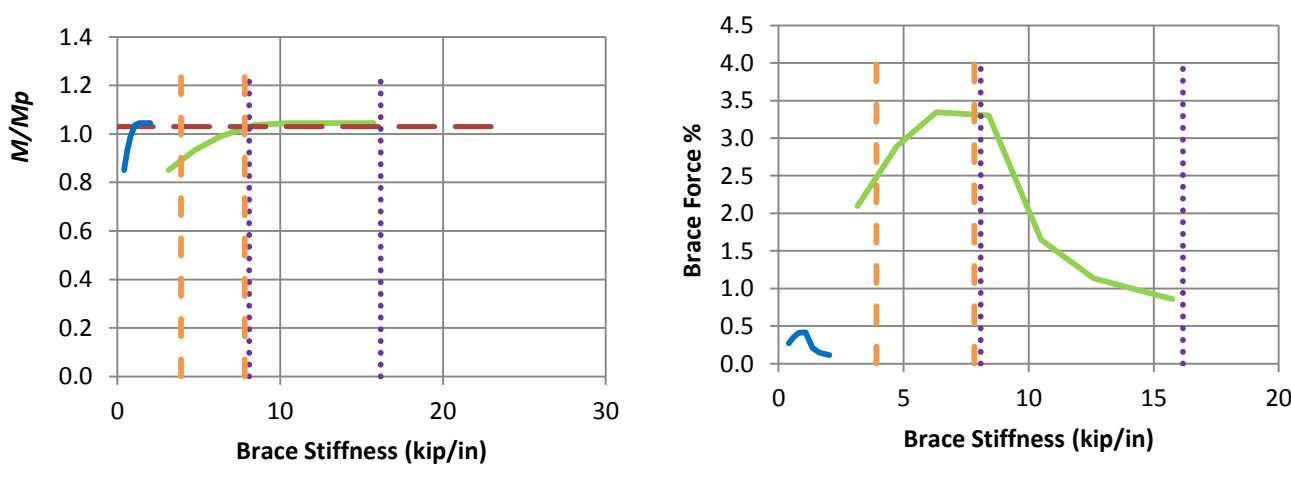
a) B_MG2pc_CNTB_n1_Lb5_TLBSR4



b) B_MG2pc_CNTB_n1_Lb5_TLBSR1

- Rigid bracing strength
- Test simulation results corresponding to torsional brace
- Test simulation results corresponding to lateral brace
- 1x and 0.5x lateral bracing stiffness from Eq. C-A-6-5, AISC 360-10, with $C_b P_f$ taken equal to M_{max}/h_o
- 1x and 0.5x torsional bracing stiffness equal to (β_{Tbr} / h_o^2) , where β_{Tbr} is given in Eq. 4-1

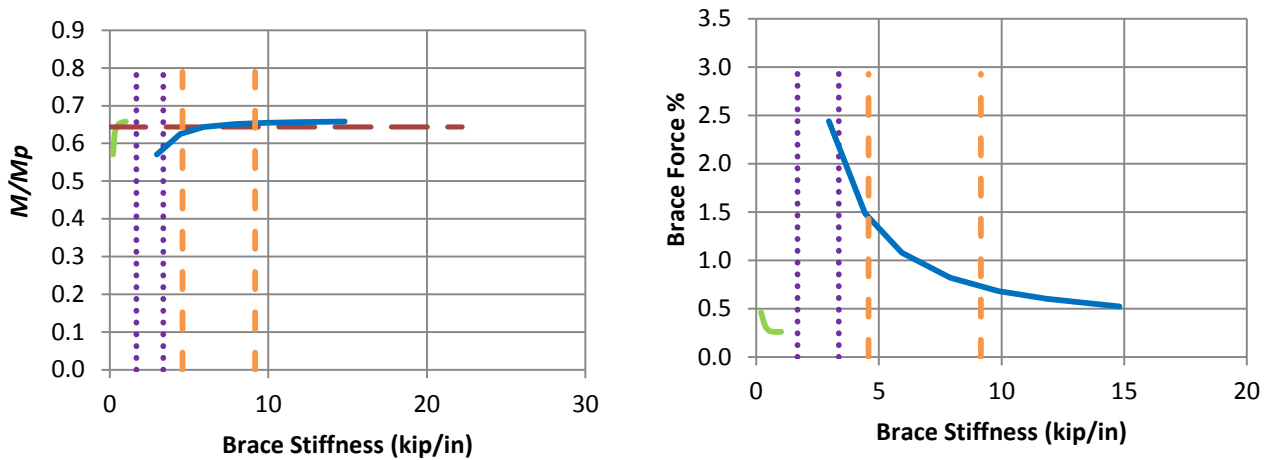
Fig. A.9. Knuckle curves and brace force vs. brace stiffness plots for point (nodal) lateral bracing cases with $n = 1$, Moment Gradient 2 loading, intermediate transverse load applied at centroid of the mid-span cross-section with lateral brace on the flange in compression, $L_b = 5$ ft.



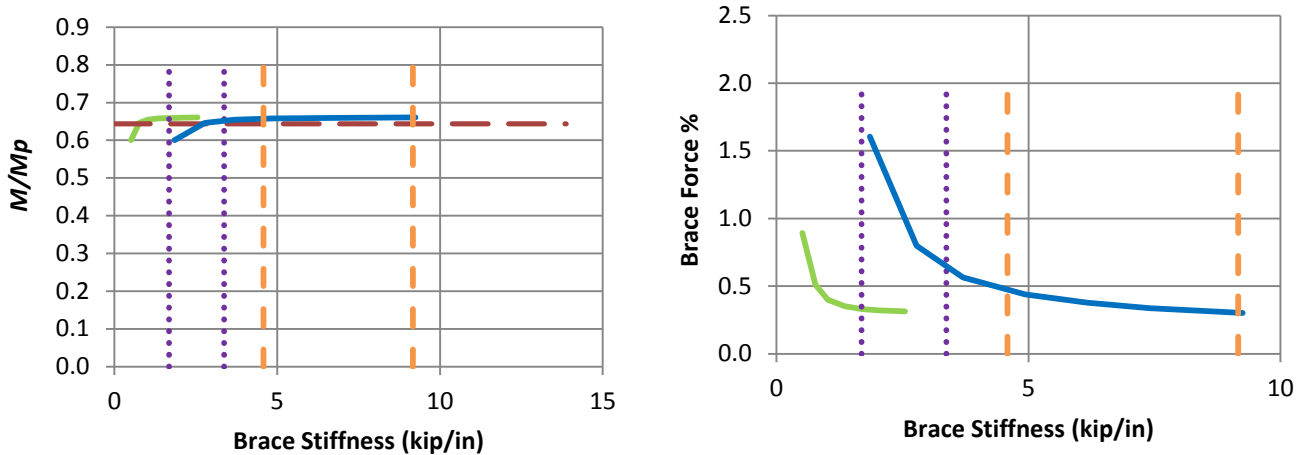
c) B_MG2pc_CNTB_n1_Lb5_TLBSR0.25

- Rigid bracing strength
- Test simulation results corresponding to torsional brace
- Test simulation results corresponding to lateral brace
- 1x and 0.5x lateral bracing stiffness from Eq. C-A-6-5, AISC 360-10, with $C_b P_f$ taken equal to M_{max}/h_o
- 1x and 0.5x torsional bracing stiffness equal to (β_{Tbr} / h_o^2) , where β_{Tbr} is given in Eq. 4-1

Fig. A.9. (continued) Knuckle curves and brace force vs. brace stiffness plots for point (nodal) lateral bracing cases with $n = 1$, Moment Gradient 2 loading, intermediate transverse load applied at centroid of the mid-span cross-section with lateral brace on the flange in compression, $L_b = 5$ ft.



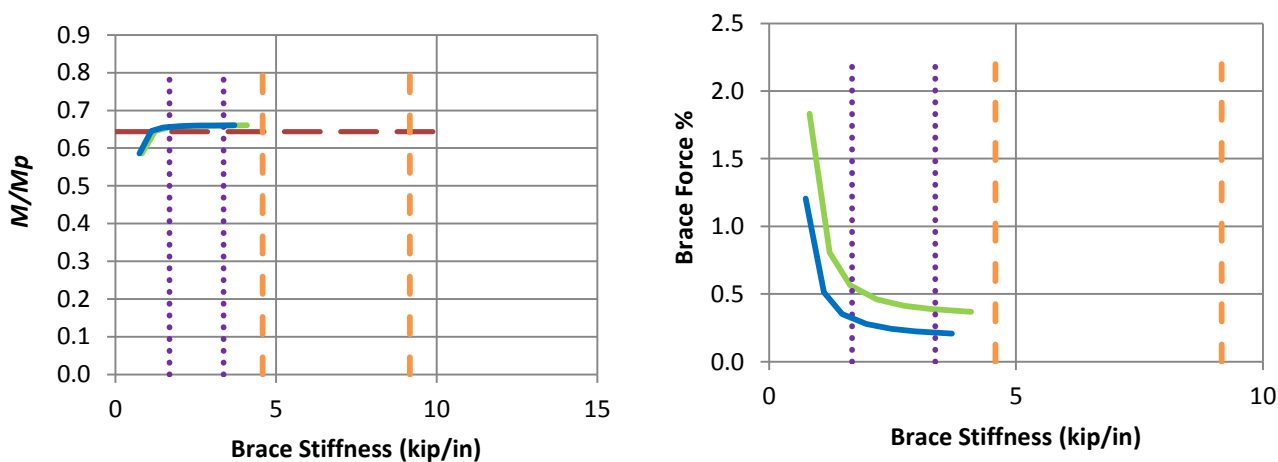
a) B_MG2pc_CNTB_n1_Lb15_TLBSR4



b) B_MG2pc_CNTB_n1_Lb15_TLBSR1

- Rigid bracing strength
- Test simulation results corresponding to torsional brace
- Test simulation results corresponding to lateral brace
- 1x and 0.5x lateral bracing stiffness from Eq. C-A-6-5, AISC 360-10, with $C_b P_f$ taken equal to M_{max}/h_o
- - - 1x and 0.5x torsional bracing stiffness equal to (β_{Tbr} / h_o^2) , where β_{Tbr} is given in Eq. 4-1

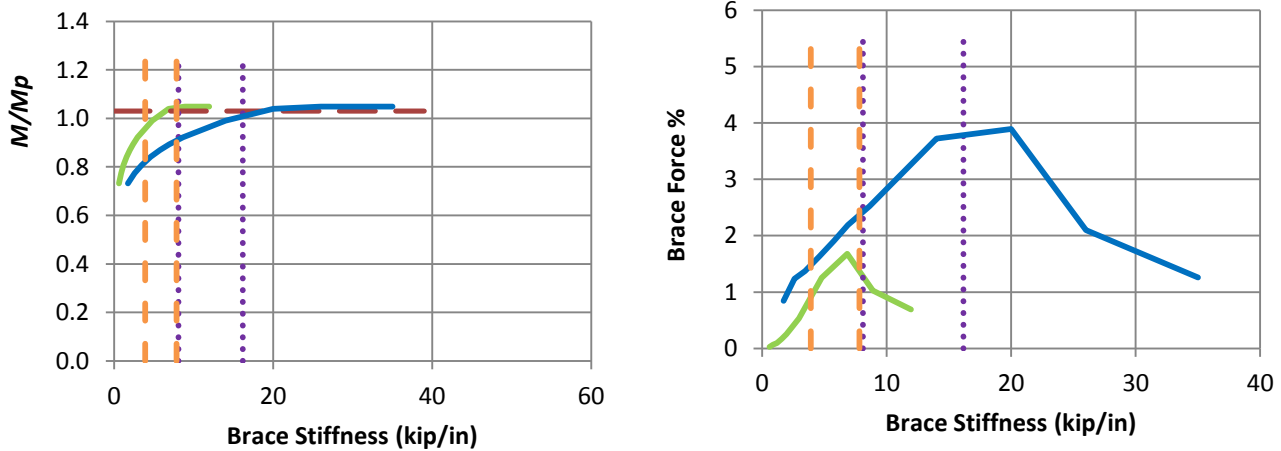
Fig. A.10. Knuckle curves and brace force vs. brace stiffness plots for point (nodal) lateral bracing cases with $n = 1$, Moment Gradient 2 loading, intermediate transverse load applied at centroid of the mid-span cross-section with lateral brace on the flange in compression, $L_b = 15$ ft.



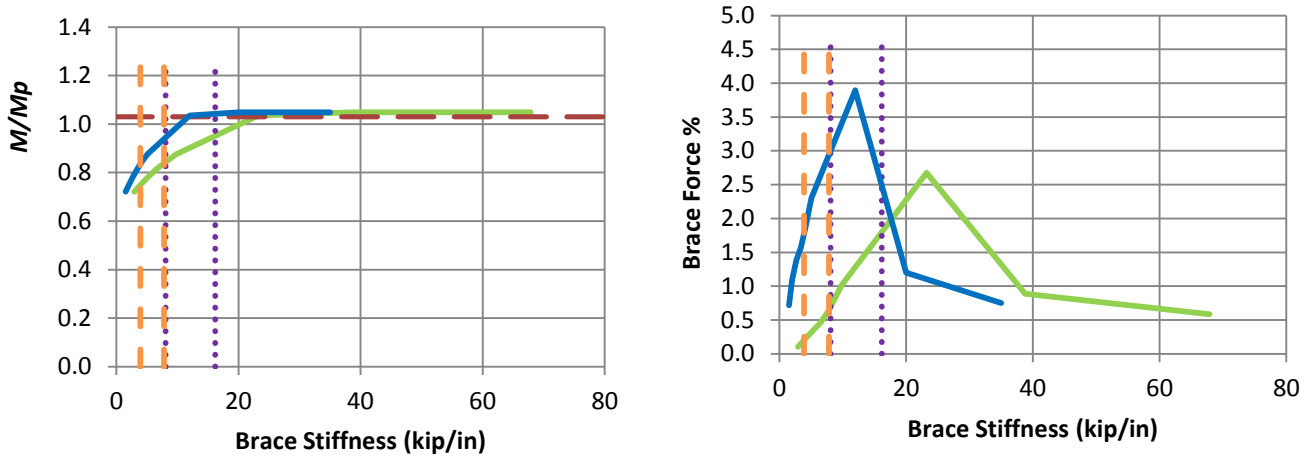
c) B_MG2pc_CNTB_n1_Lb15_TLBSR0.25

- Rigid bracing strength
- Test simulation results corresponding to torsional brace
- Test simulation results corresponding to lateral brace
- 1x and 0.5x lateral bracing stiffness from Eq. C-A-6-5, AISC 360-10, with $C_b P_f$ taken equal to M_{max}/h_o
- 1x and 0.5x torsional bracing stiffness equal to (β_{Tbr} / h_o^2) , where β_{Tbr} is given in Eq. 4-1

Fig. A.10. (continued) Knuckle curves and brace force vs. brace stiffness plots for point (nodal) lateral bracing cases with $n = 1$, Moment Gradient 2 loading, intermediate transverse load applied at centroid of the mid-span cross-section with lateral brace on the flange in compression, $L_b = 15$ ft.



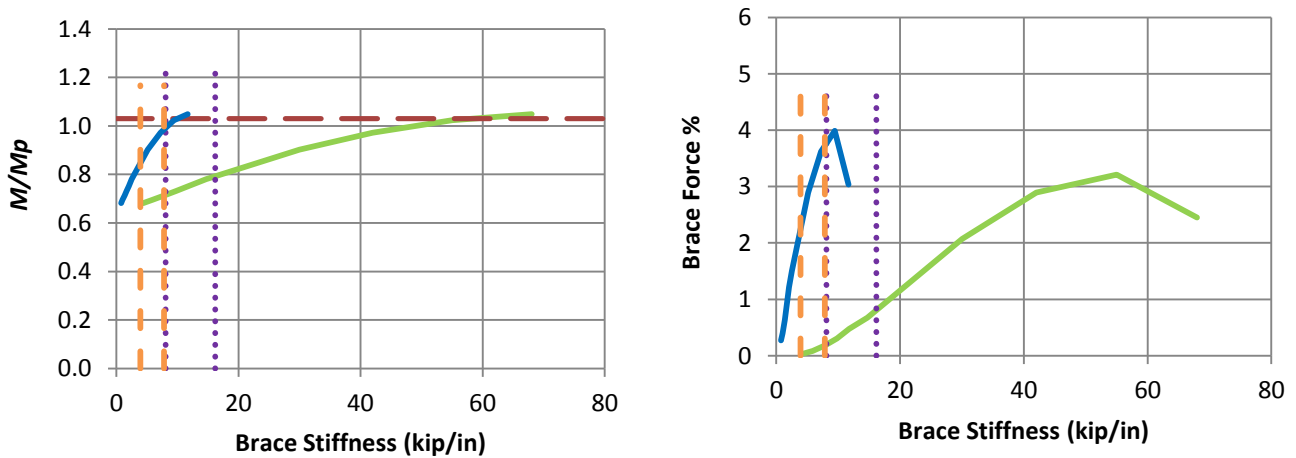
a) B_MG2nc_CNTB_n1_Lb5_TLBSR5.67



b) B_MG2nc_CNTB_n1_Lb5_TLBSR1

- Rigid bracing strength
- Test simulation results corresponding to torsional brace
- Test simulation results corresponding to lateral brace
- ⋯ 1x and 0.5x lateral bracing stiffness from Eq. C-A-6-5, AISC 360-10, with $C_b P_f$ taken equal to M_{max}/h_o
- - 1x and 0.5x torsional bracing stiffness equal to (β_{Tbr} / h_o^2) , where β_{Tbr} is given in Eq. 4-1

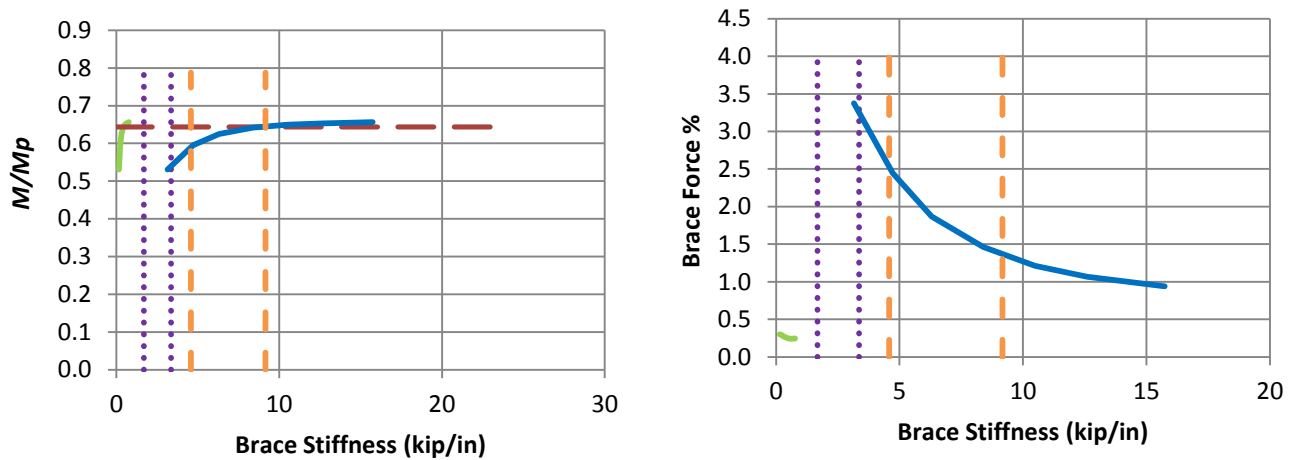
Fig. A.11. Knuckle curves and brace force vs. brace stiffness plots for point (nodal) lateral bracing cases with $n = 1$, Moment Gradient 2 loading, intermediate transverse load applied at centroid of the mid-span cross-section with lateral brace on the flange in tension, $L_b = 5$ ft.



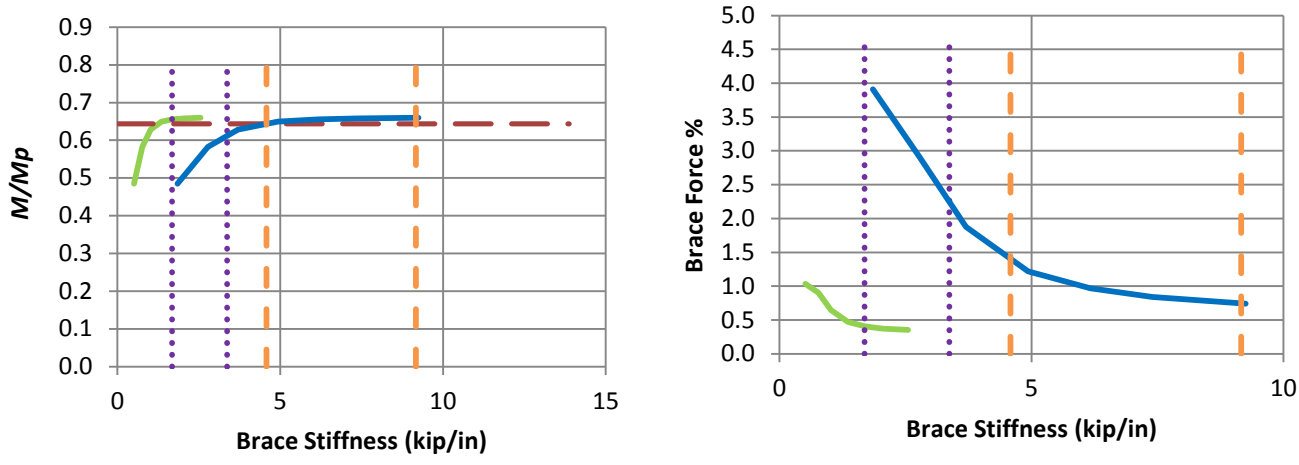
c) B_MG2nc_CNTB_n1_Lb5_TLBSR0.33

- Rigid bracing strength
- Test simulation results corresponding to torsional brace
- Test simulation results corresponding to lateral brace
- ⋯ 1x and 0.5x lateral bracing stiffness from Eq. C-A-6-5, AISC 360-10, with $C_b P_f$ taken equal to M_{max}/h_o
- 1x and 0.5x torsional bracing stiffness equal to (β_{Tbr} / h_o^2) , where β_{Tbr} is given in Eq. 4-1

Fig. A.11. (continued) Knuckle curves and brace force vs. brace stiffness plots for point (nodal) lateral bracing cases with $n = 1$, Moment Gradient 2 loading, intermediate transverse load applied at centroid of the mid-span cross-section with lateral brace on the flange in tension, $L_b = 5$ ft.



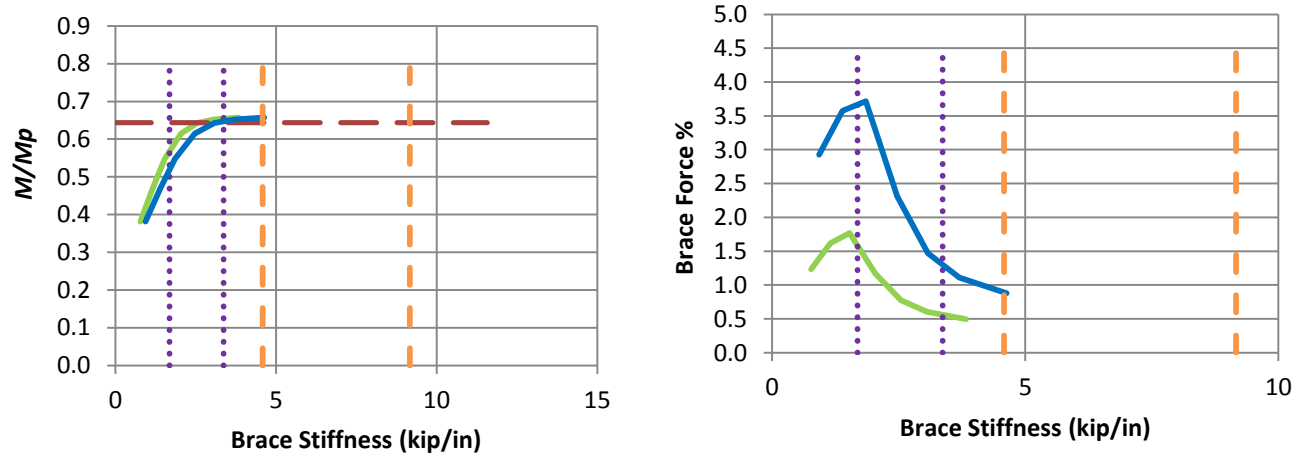
a) B_MG2nc_CNTB_n1_Lb15_TLBSR5.67



b) B_MG2nc_CNTB_n1_Lb15_TLBSR1

- Rigid bracing strength
- Test simulation results corresponding to torsional brace
- Test simulation results corresponding to lateral brace
- 1x and 0.5x lateral bracing stiffness from Eq. C-A-6-5, AISC 360-10, with $C_b P_f$ taken equal to M_{max}/h_o
- - - 1x and 0.5x torsional bracing stiffness equal to (β_{Tbr} / h_o^2) , where β_{Tbr} is given in Eq. 4-1

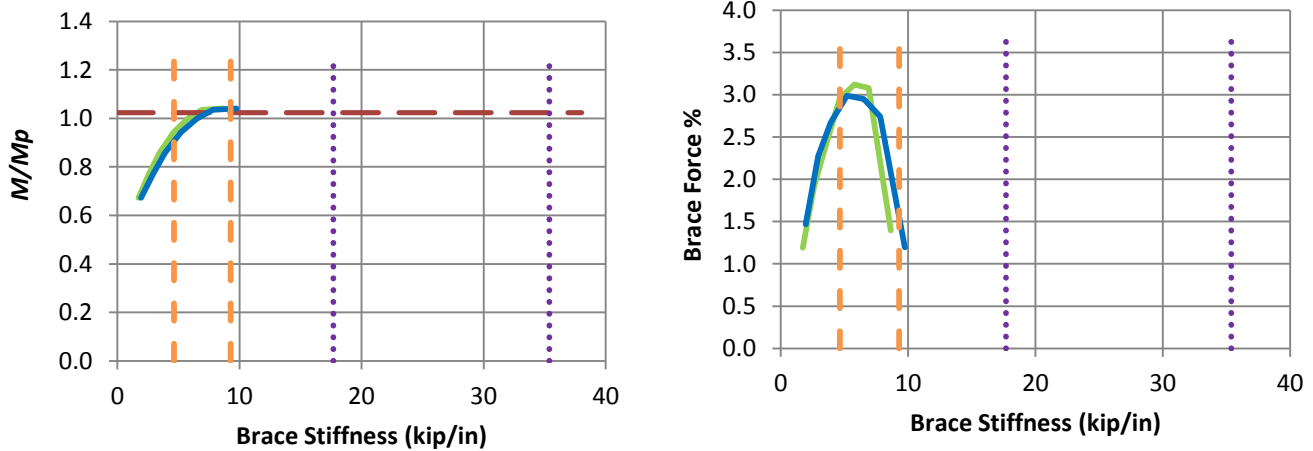
Fig. A.12. Knuckle curves and brace force vs. brace stiffness plots for point (nodal) lateral bracing cases with $n = 1$, Moment Gradient 2 loading, intermediate transverse load applied at centroid of the mid-span cross-section with lateral brace on the flange in tension, $L_b = 15$ ft.



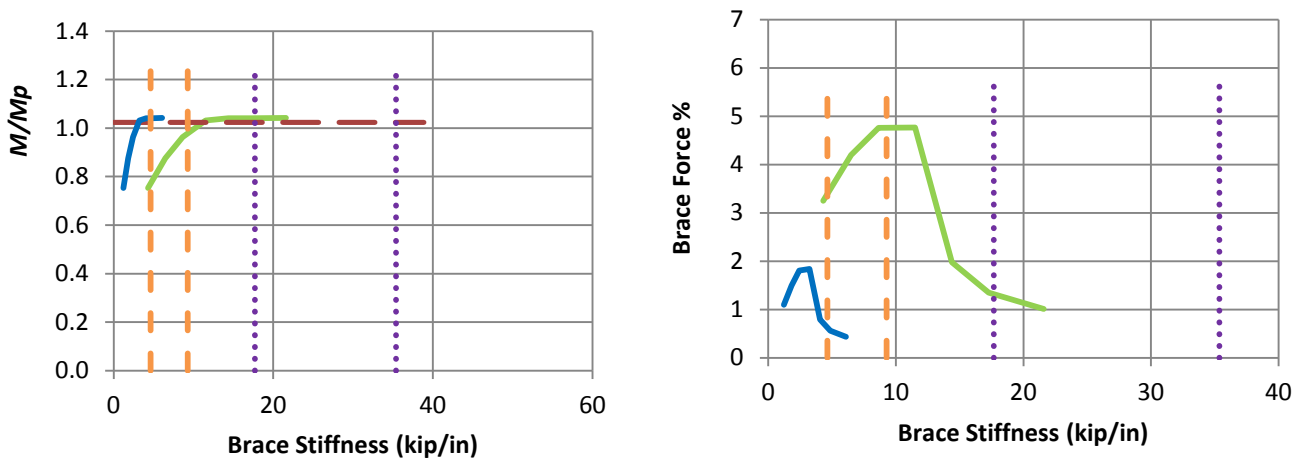
c) B_MG2nc_CNTB_n1_Lb15_TLBSR0.33

- Rigid bracing strength
- Test simulation results corresponding to torsional brace
- Test simulation results corresponding to lateral brace
- 1x and 0.5x lateral bracing stiffness from Eq. C-A-6-5, AISC 360-10, with $C_b P_f$ taken equal to M_{max}/h_o
- 1x and 0.5x torsional bracing stiffness equal to (β_{Tbr} / h_o^2) , where β_{Tbr} is given in Eq. 4-1

Fig. A.12. (continued) Knuckle curves and brace force vs. brace stiffness plots for point (nodal) lateral bracing cases with $n = 1$, Moment Gradient 2 loading, intermediate transverse load applied at centroid of the mid-span cross-section with lateral brace on the flange in tension, $L_b = 15$ ft.



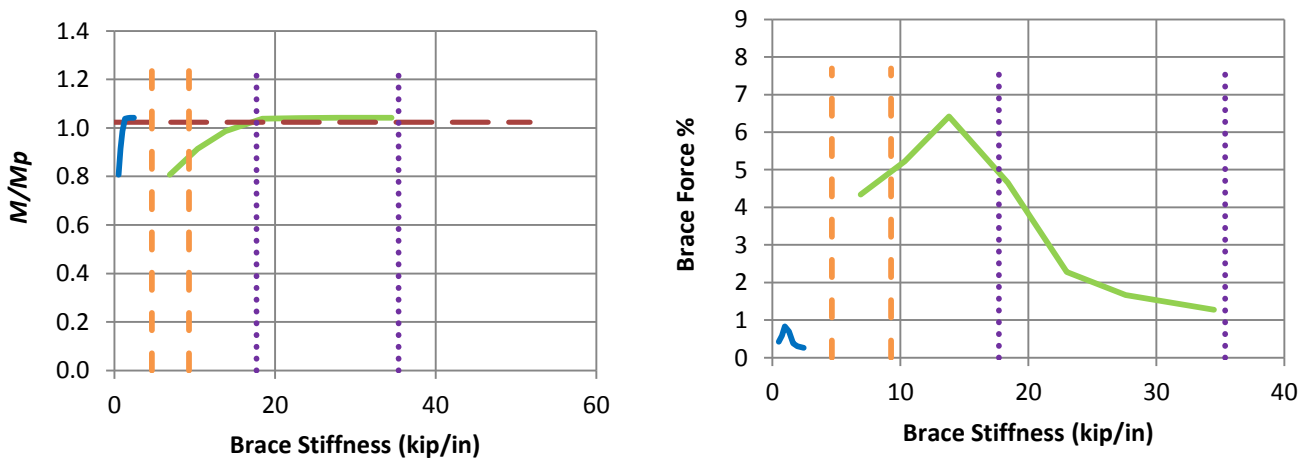
a) B_MG2pt_CNTB_n1_Lb5_TLBSR4



b) B_MG2pt_CNTB_n1_Lb5_TLBSR1

- Rigid bracing strength
- Test simulation results corresponding to torsional brace
- Test simulation results corresponding to lateral brace
- 1x and 0.5x lateral bracing stiffness from Eq. C-A-6-5, AISC 360-10, with $C_b P_f$ taken equal to M_{max}/h_o
- 1x and 0.5x torsional bracing stiffness equal to (β_{Tbr} / h_o^2) , where β_{Tbr} is given in Eq. 4-1

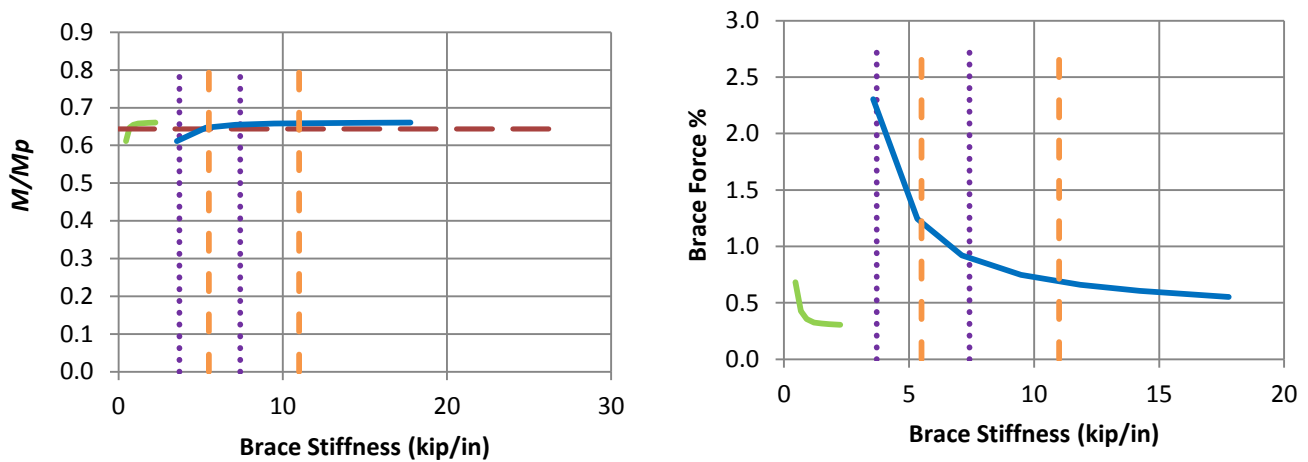
Fig. A.13. Knuckle curves and brace force vs. brace stiffness plots for point (nodal) lateral bracing cases with $n = 1$, Moment Gradient 2 loading, intermediate transverse load applied at top flange of the mid-span cross-section with lateral brace on the flange in compression, $L_b = 5$ ft.



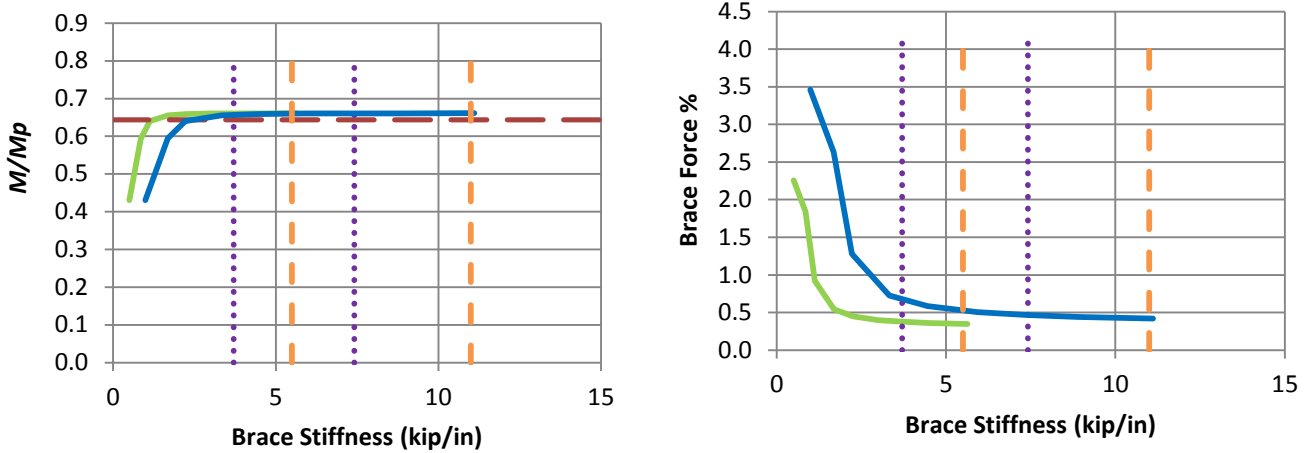
c) B_MG2pt_CNTB_n1_Lb5_TLBSR0.25

- Rigid bracing strength
- Test simulation results corresponding to torsional brace
- Test simulation results corresponding to lateral brace
- ⋯ 1x and 0.5x lateral bracing stiffness from Eq. C-A-6-5, AISC 360-10, with $C_b P_f$ taken equal to M_{max}/h_o
- 1x and 0.5x torsional bracing stiffness equal to (β_{Tbr} / h_o^2) , where β_{Tbr} is given in Eq. 4-1

Fig. A.13. (continued) Knuckle curves and brace force vs. brace stiffness plots for point (nodal) lateral bracing cases with $n = 1$, Moment Gradient 2 loading, intermediate transverse load applied at top flange of the mid-span cross-section with lateral brace on the flange in compression, $L_b = 5$ ft.



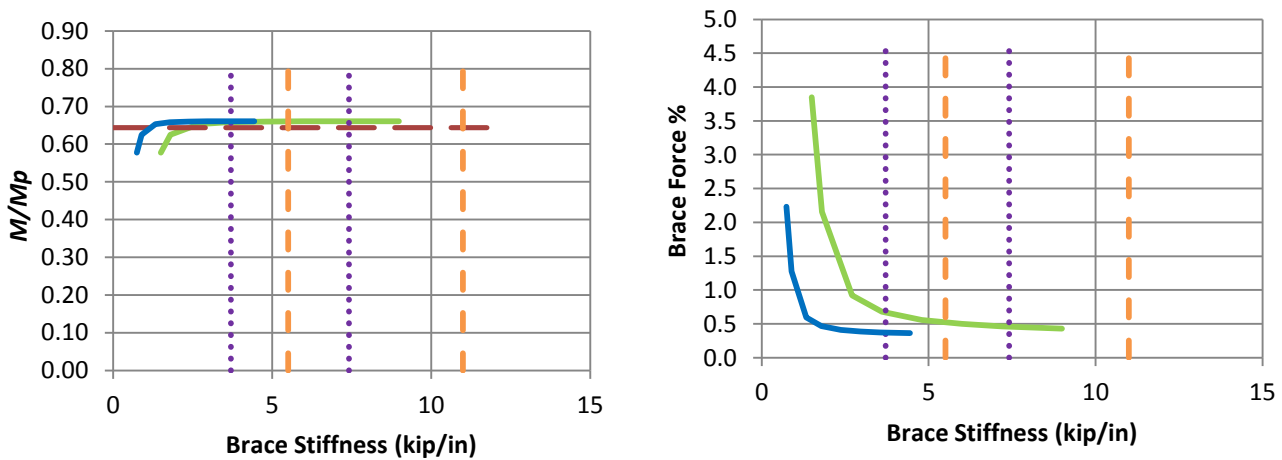
a) B_MG2pt_CNTB_n1_Lb15_TLBSR4



b) B_MG2pt_CNTB_n1_Lb15_TLBSR1

- Rigid bracing strength
- Test simulation results corresponding to torsional brace
- Test simulation results corresponding to lateral brace
- ⋯ 1x and 0.5x lateral bracing stiffness from Eq. C-A-6-5, AISC 360-10, with $C_b P_f$ taken equal to M_{max}/h_o
- 1x and 0.5x torsional bracing stiffness equal to (β_{Tbr} / h_o^2) , where β_{Tbr} is given in Eq. 4-1

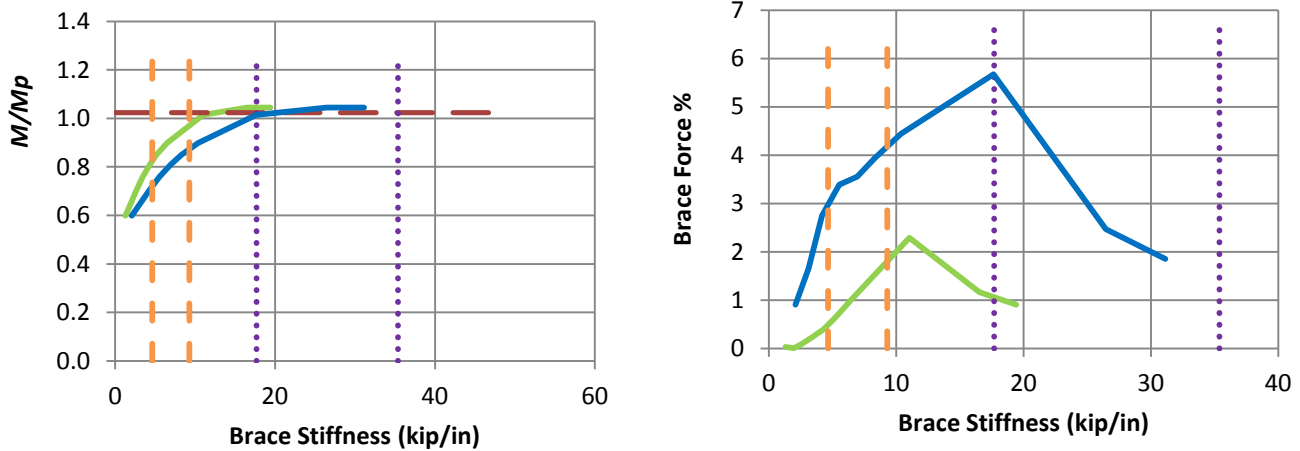
Fig. A.14. Knuckle curves and brace force vs. brace stiffness plots for point (nodal) lateral bracing cases with $n = 1$, Moment Gradient 2 loading, intermediate transverse load applied at top flange of the mid-span cross-section with lateral brace on the flange in compression, $L_b = 15$ ft.



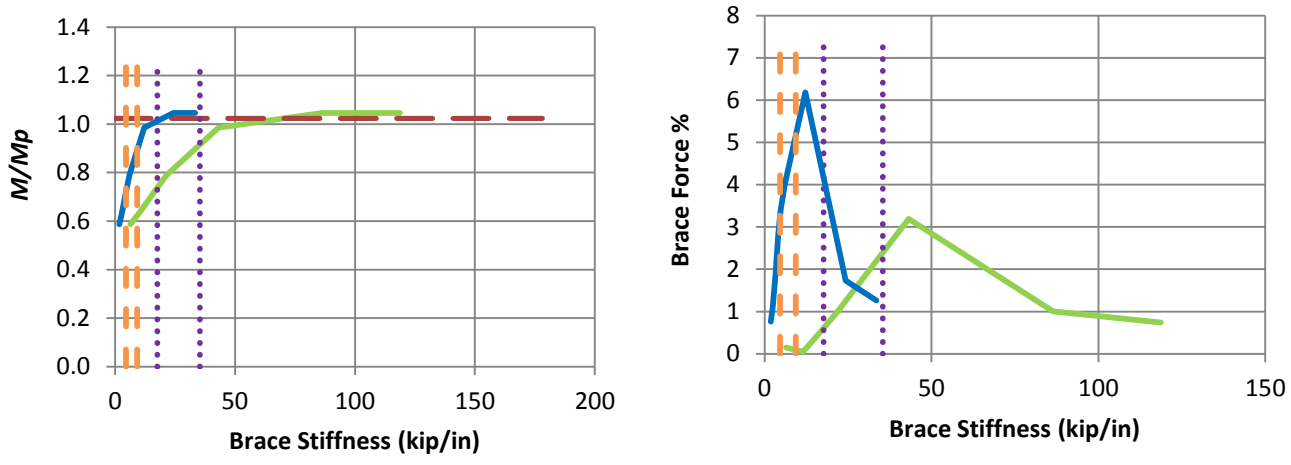
c) B_MG2pt_CNTB_n1_Lb15_TLBSR0.25

- Rigid bracing strength
- Test simulation results corresponding to torsional brace
- Test simulation results corresponding to lateral brace
- 1x and 0.5x lateral bracing stiffness from Eq. C-A-6-5, AISC 360-10, with $C_b P_f$ taken equal to M_{max}/h_o
- 1x and 0.5x torsional bracing stiffness equal to (β_{Tbr} / h_o^2) , where β_{Tbr} is given in Eq. 4-1

Fig. A.14. (continued) Knuckle curves and brace force vs. brace stiffness plots for point (nodal) lateral bracing cases with $n = 1$, Moment Gradient 2 loading, intermediate transverse load applied at top flange of the mid-span cross-section with lateral brace on the flange in compression, $L_b = 15$ ft.



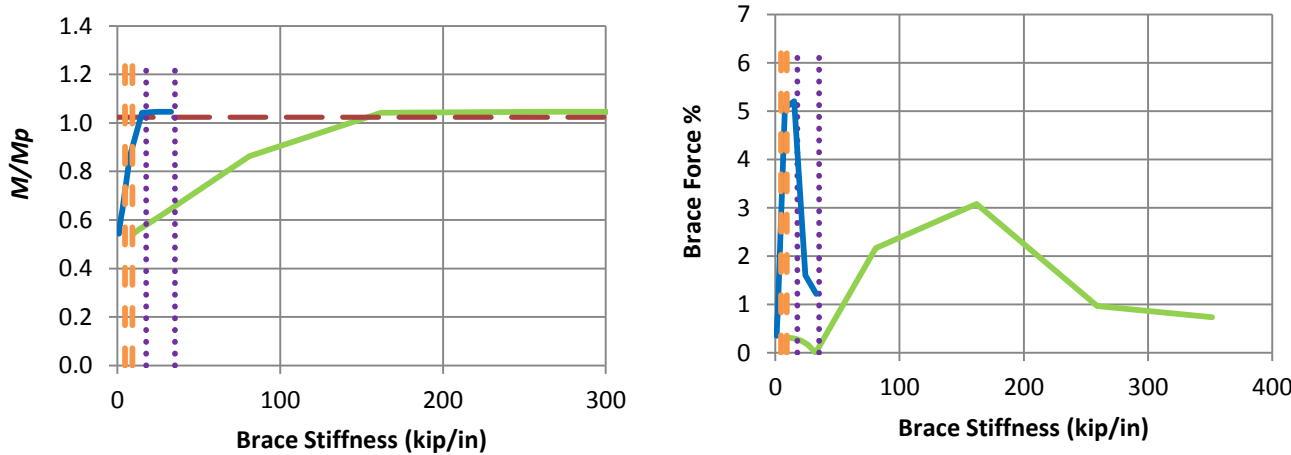
a) B_MG2nt_CNTB_n1_Lb5_TLBSR5.67



b) B_MG2nt_CNTB_n1_Lb5_TLBSR1

- Rigid bracing strength
- Test simulation results corresponding to torsional brace
- Test simulation results corresponding to lateral brace
- 1x and 0.5x lateral bracing stiffness from Eq. C-A-6-5, AISC 360-10, with $C_b P_f$ taken equal to M_{max}/h_o
- 1x and 0.5x torsional bracing stiffness equal to (β_{Tbr} / h_o^2) , where β_{Tbr} is given in Eq. 4-1

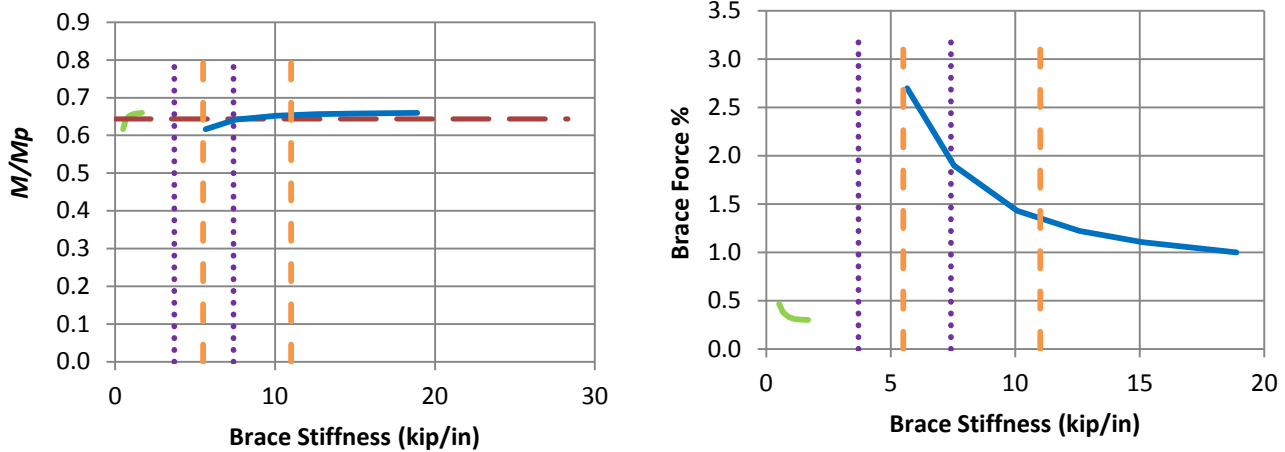
Fig. A.15. Knuckle curves and brace force vs. brace stiffness plots for point (nodal) lateral bracing cases with $n = 1$, Moment Gradient 2 loading, intermediate transverse load applied at top flange of the mid-span cross-section with lateral brace on the flange in tension, $L_b = 5$ ft.



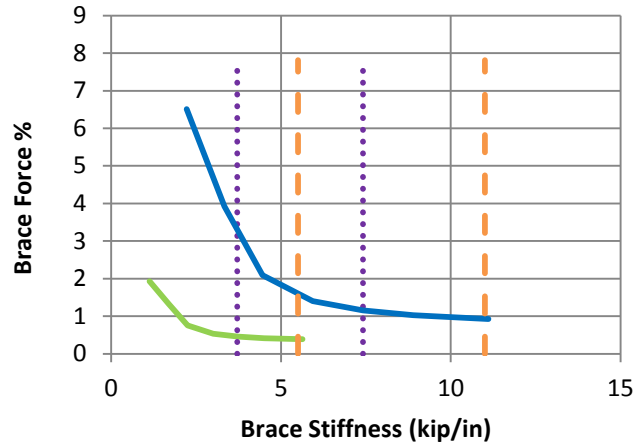
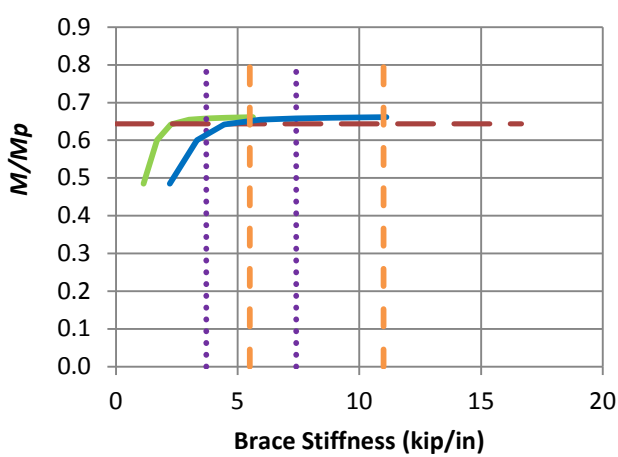
c) B_MG2nt_CNTB_n1_Lb5_TLBSR0.33

- — Rigid bracing strength
- Test simulation results corresponding to torsional brace
- Test simulation results corresponding to lateral brace
- ⋯⋯⋯ 1x and 0.5x lateral bracing stiffness from Eq. C-A-6-5, AISC 360-10, with $C_b P_f$ taken equal to M_{max}/h_o
- — 1x and 0.5x torsional bracing stiffness equal to (β_{Tbr} / h_o^2) , where β_{Tbr} is given in Eq. 4-1

Fig. A.15. (continued) Knuckle curves and brace force vs. brace stiffness plots for point (nodal) lateral bracing cases with $n = 1$, Moment Gradient 2 loading, intermediate transverse load applied at top flange of the mid-span cross-section with lateral brace on the flange in tension, $L_b = 5$ ft.



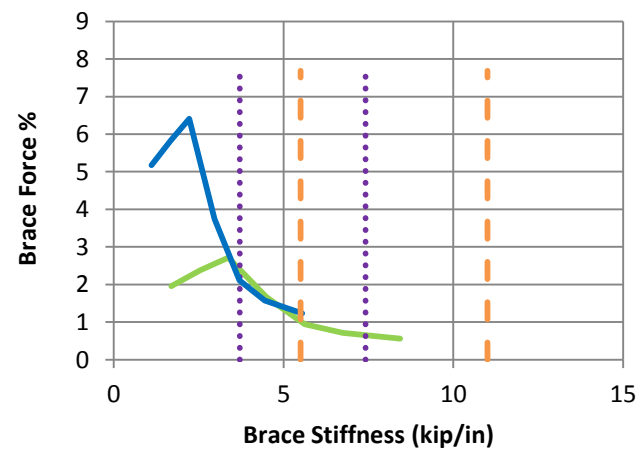
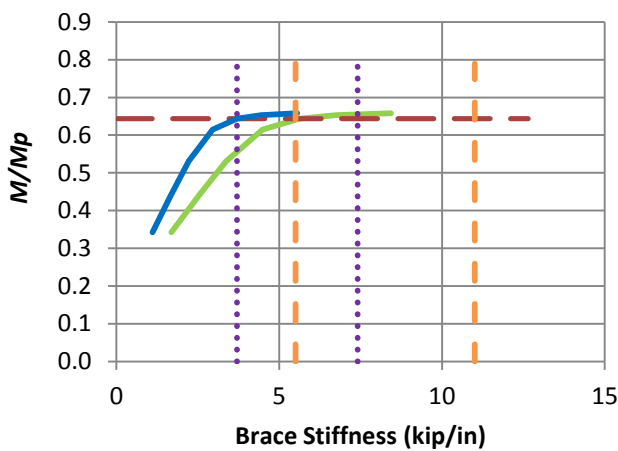
a) B_MG2nt_CNTB_n1_Lb15_TLBSR5.67



b) B_MG2nt_CNTB_n1_Lb15_TLBSR1

- Rigid bracing strength
- Test simulation results corresponding to torsional brace
- Test simulation results corresponding to lateral brace
- ⋯ 1x and 0.5x lateral bracing stiffness from Eq. C-A-6-5, AISC 360-10, with $C_b P_f$ taken equal to M_{max}/h_o
- - 1x and 0.5x torsional bracing stiffness equal to (β_{Tbr} / h_o^2) , where β_{Tbr} is given in Eq. 4-1

Fig. A.16. Knuckle curves and brace force vs. brace stiffness plots for point (nodal) lateral bracing cases with $n = 1$, Moment Gradient 2 loading, intermediate transverse load applied at top flange of the mid-span cross-section with lateral brace on the flange in tension, $L_b = 15$ ft.



c) B_MG2nt_CNTB_n1_Lb15_TLBSR0.33

- Rigid bracing strength
- Test simulation results corresponding to torsional brace
- Test simulation results corresponding to lateral brace
- 1x and 0.5x lateral bracing stiffness from Eq. C-A-6-5, AISC 360-10, with $C_b P_f$ taken equal to M_{max}/h_o
- 1x and 0.5x torsional bracing stiffness equal to (β_{Tbr} / h_o^2) , where β_{Tbr} is given in Eq. 4-1

Fig. A.16. (continued) Knuckle curves and brace force vs. brace stiffness plots for point (nodal) lateral bracing cases with $n = 1$, Moment Gradient 2 loading, intermediate transverse load applied at top flange of the mid-span cross-section with lateral brace on the flange in tension, $L_b = 15\text{ft}$.

REFERENCES

AISC (2010). “Code of Standard Practice for Steel Buildings and Bridges”, AISC 303-05 *American Institute of Steel Construction*, Chicago, IL.

AISC (2010). “Specification for Structural Steel Buildings”, *American Institute of Steel Construction*, Chicago, IL. ANSI/AISC 360-10. (2010b).

Bishop C.D. (2013). “Flange Bracing Requirements for Metal Building Systems” Doctoral Dissertation, Georgia Institute of Technology, Atlanta, GA.

CEN (2005). Eurocode 3: Design of Steel Structures, Part 1-1: General Rules and rules for buildings, EN 1993-1-1:2005: E, Incorporating Corrigendum February 2006, European Committee for Standardization, Brussels, Belgium, 91 pp.

Galambos, T.V. and Ketter, R. (1959). “Columns under Combined Bending and Thrust,” *Journal of the Engineering Mechanics Division*, ASCE, 85(EM2), 135-152.

Griffis, L., and White, D.W. “Stability Design of Steel Buildings”, *AISC Design Guide 28*. (2014)

Helwig, T.A. and Yura, J.A. (1999). “Torsional Bracing of Columns,” *Journal of the Structural Engineering*, American Society of Civil Engineers, 125(5), 547-555.

Nethercot, D.A and Trahair, N.S. (1976). “Lateral Buckling Approximations for Elastic Beams,” *The Structural Engineer*, 54(6), 197-204.

Prado E.P. and White, D.W. (2014). “Assessment of Basic Steel I-Section Beam Bracing Requirements by Test Simulation,” Research Report, Georgia Institute of Technology, Atlanta, GA.

Simulia (2013). ABAQUS, *Software and Analysis User’s Manual*, Version 6.13.

Stanway, G.S., Chapman, J.C., and Dowling, P.J. (1992a). “A simply supported imperfect column with a transverse elastic restraint at any position. Part 1: design models.” *Proc. Instn. Civ. Engrs., Strucs. and Bldgs.*, 94(2), 217-218.

Stanway, G.S., Chapman, J.C., and Dowling, P.J. (1992b). "A simply supported imperfect column with a transverse elastic restraint at any position. Part 1: behavior." *Proc. Instn. Civ. Engrs., Strucs. and Bldgs.*, 94(2), 205-216.

Taylor, A.C. and Ojalvo, M. (1966). "Torsional Restraint of Lateral Buckling," *Journal of Structural Division*, ASCE, ST2, 115-129.

Timoshenko, S. and Gere, J. (1963). "Theory of Elastic Stability". *New York: McGraw-Hill*.

Tran, D.Q. (2009). "Towards Improved Flange Bracing Requirements for Metal Building Frame Systems" Masters thesis, Georgia Institute of Technology, Atlanta, GA.

Wang, L., and Helwig, T.A. "Critical Imperfections for Beam Bracing Systems," *ASCE Journal of Structural Division*, 131(6), 993-940. (2005).

White, D.W., Sharma, A., Kim, Y.D. and Bishop, C.D. (2011). "Flange Stability Bracing Behavior in Metal Building Frame Systems," Final Research Report to Metal Building Manufacturers Association, Structural Engineering, Mechanics and Materials Report No. 11-74, *School of Civil and Environmental Engineering*, Georgia Institute of Technology, Atlanta, GA, 361 PP.

Yura, J.A., (1995), "Bracing for Stability – State-of-the-Art," Is Your Structure Suitably Braced? 1995 Conference, Structural Stability Research Council.

Yura, J.A., Philips, B., Raju, S., and Webb, S., (1992), "Bracing of Steel Beams in Bridges," Research Report 1239-4F, Center for Transportation Research, Univ. of Texas, October, 80 pp.

Yura, J.A., (1993), "Fundamentals of Beam Bracing," Is Your Structure Suitably Braced? 1993 Conference, Milwaukee, Wisconsin, Structural Stability Research Council, Bethlehem, PA, Pp. 1-40.